



Prevalence of Eating Disorders among Medical Students in Ipoh, Perak, Malaysia

Najwa Syafawati Binti Rasman¹, Nur Aimi Kay Mohd Rashid Kay¹, Shaker Uddin Ahmed^{1*} and Mohammad Kabir Ahmed²

¹Medicine Based Department, Faculty of Medicine, Universiti Kuala Lumpur, Malaysia.

²Preclinical Department of Biochemistry, Faculty of Medicine, Universiti Kuala Lumpur, Malaysia.

Received: 21 Nov 2017

Revised: 11 Dec 2017

Accepted: 27 Dec 2017

*Address for correspondence

Shaker Uddin Ahmed

Medicine Based Department,
Faculty of Medicine, Universiti Kuala Lumpur,
Malaysia.

E.mail: shaker@unikl.edu.my



This is an Open Access Journal / article distributed under the terms of the **Creative Commons Attribution License** (CC BY-NC-ND 3.0) which permits unrestricted use, distribution, and reproduction in any medium, provided the original work is properly cited. All rights reserved.

ABSTRACT

This study is to assess the chance of having eating disorders (ED) among medical students. This is important as medical students are a high-risk population for EDs. We hope that this study can be used to improve the life of medical students and help solving their problems. By using Epi Info version 7.1.4.0 software, the sample size was calculated to be 233 participants with 95% confident level. The aim of this study is to determine the prevalence of eating disorders among medical students in Ipoh, Perak. Particular objectives is to determine the prevalence of eating disorders according to genders, age group, years of studying and ethnicity and to relate the socio-demographic status of the respondents students of medical courses.

This cross sectional study was conducted from 5th December 2016 until 20th January 2017. The study population involved medical students currently studying in Ipoh from aged between 18 to 26 years. The survey was distributed online among medical students studying in Ipoh. Sample size was calculated using Epi Info version 7.1.4.0 software which is 211 respondents at 95% confidence level. The survey was carried out using the questionnaire as the tool which was prepared in English and distributed to the selected participants after getting their consent for participating in this study. Analysis was done in SPSS 17 using appropriate statistical test, $p < 0.05$ was considered as significant.

A total of 285 questionnaires were retrieved and only 279 survey forms were completed. The response rate was 100% while the completion rate was 97.9%. Among 279 respondents, SCOFF detected 42.7% (119) as positive with 80.7% were females and 19.3% were males. The prevalence of eating disorders was found to be high among medical students in Ipoh with majority of them are females and Indians.

13024



**Shaker Uddin Ahmed et al.**

Therefore, strategies to detect eating disorders earlier should be implemented so we can treat it earlier as eating disorders can affect negatively the performance of students and future doctors. It also suggests the need for further research to identify the causes and to facilitate planning of prevention activities.

Keywords: Medical student, Eating disorder, prevalence.

INTRODUCTION

Eating disorders is a group of conditions characterized by abnormal eating habit and is the most common psychiatric problems that affect particularly young women [1]. According to National Association of Anorexia Nervosa and Associated Disorders, at least 30 million people of all ages and genders suffer from an ED in the United State. [2] In Malaysia, there is no concrete study or systematic research done on the prevalence of EDs. However the estimated figure is 1% of the population having anorexia nervosa, while 3% suffer from bulimia nervosa [2]. According to a survey done by the Malaysian Psychiatric Association (MPA), for every 10 to 20 females with eating disorders, there would be one male with a similar problem, but males are less likely to present for such disorders. These disorders—which include anorexia nervosa, bulimia nervosa, and the six different eating disorders that fall under the category eating disorder not otherwise specified—generally occur during adolescence and early adulthood, often endure throughout life, and can have a devastating impact on patients themselves and their families [3]. Moreover, eating disorders often co-existed with other psychiatric disorders and disturbances, including depression, anxiety, obsessionality, substance abuse disorders, and marked impairments in social functioning. Serious cardiovascular and neurological complications as well as impaired physical development are some of the medical morbidities associated with eating disorders, and in particular with anorexia nervosa. Within the context of anorexia nervosa, the mortality rate is 5% per decade, making it one of the leading contributors to excess mortality of any of the psychiatric disorders [3]. Anorexia nervosa occurs 10 to 20 times more often in females than in males. Estimates of bulimia nervosa range from 1 to 4 percent of young women. Bulimia nervosa is more common in women than in men [4].

In Malaysia, there is no concrete study or systematic research done on the prevalence of eating disorders, however the estimated figure is 1% of the population having anorexia nervosa, while 3% suffer from bulimia nervosa, which would translate to between 250,000 to 900,000 sufferers. According to a survey by the Malaysian Psychiatric Association (MPA), for every 10 to 20 females with eating disorders, there would be one male with a similar problem, but males are less likely to come forward for such disorders. Bulimia nervosa occurs slightly within the young adult population [5]. A study done in 2016 found that there are partial associations between academic burnout and eating disorder among Monash University Malaysia students [6]. Medical students, residents/fellows, and EC physicians were more likely to be burned out compared with the population control samples according to a study done in United States [7]. Despite eating disorders are categorized as mental health disorders, they can affect physical health causing multiple medical complication which can be fatal. By diagnosing and detecting the eating disorders earlier, the better the prognosis and recovery will be. Therefore, we planned to conduct a cross-descriptive study to assess the prevalence of possible eating disorders among medical students in Ipoh. Additionally, there are only a few studies done in Malaysia regarding prevalence of possible eating disorders among medical students. Based on studies done, it showed that medical students are more prone to develop eating disorders especially due to academic burnout. Therefore, we are going to explore more about the prevalence of eating disorders among medical students in medical schools in Ipoh. It will benefit us to study regarding this topic as to help in early diagnosis of eating disorders and its prevention among medical students who will be doctors in the future. Hopefully, this study will be used to assist in organizing an efficient strategy among medical students to reduce the complications and fatality of eating disorders thus improving their performance as future doctors. Therefore, the aim of this study is to determine the prevalence of eating disorders among medical students in Ipoh, Perak, emphasizing on eating disorder by levels of medical education the students are attending and according to age, gender and ethnicity they belong to. Therefore, it will be beneficial for us to explore about that in order to help in diagnosis of EDs as medical



**Shaker Uddin Ahmed et al.**

students also tend to deny that they have abnormal eating habits. Hopefully, the purpose of this study will help the future doctors regarding the lethal of EDs and its consequences.

METHODS AND MATERIALS**Subjects of Study**

The study was a descriptive cross-sectional study among medical students in Ipoh region. The study was done in all medical schools in Ipoh which are Quest International University Perak (QIUP) and UniKL Royal College of Medicine Perak (RCMP) Main Campus. The current total medical students in UniKL RCMP are 604 people while in QIUP are 371 students. The total study population is 975 students. Only the students who are of the age between 18 years old and 33 years old and currently enrolled in Bachelor of Medicine and Surgery (MBBS) course in Ipoh are included in this study with their consent.

Sampling and Sample Size

A non-probability quota sampling method was used for data collection. The questionnaire was distributed to the participants after getting their consent for participating in this study. The sample size required was calculated using Epi Info version 7.1.4.0 software. The population size was 975. Based on the research done by Akhtar Amin Memon, the prevalence or expected frequency of respondents that have high risk of eating disorders are 22.75% and 17% according to SCOFF questionnaire. [7] Using all of this information, the sample size is calculated to be 211 with confidence level 95% and confidence limits 5%. With the addition of 10% dropout, 233 participants were approached for the study. This study was performed within 7 weeks starting from 5th December 2016 until 20th January 2017.

Questionnaire Development

The questionnaires we developed are based on SCOFF questionnaire by John F. Morgan. [9], [10]The SCOFF questionnaire utilizes an acronym (Sick, Control, One stone, Fat, Food) in a simple five question test devised for use by non-professionals to assess the possible presence of an eating disorder and was devised by Morgan et al. in 1999. [9].

Data Analysis

Data was collected according to the SCOFF questionnaire. The self-administered questionnaire was distributed online to the medical students of Quest International University Perak and Universiti Kuala Lumpur Royal College of Medicine Perak for response. It was distributed using Google Forms application. The forms were then collected.

After the completion of the questionnaires, the forms were checked for completeness, and prepared for analysis. All the data were compiled into a computerized database using Microsoft Office Excel 2007 and analyzed using the SPSS version 17.

The data were analyzed primarily to find out socio-demographic characteristics of the respondents in this study. An analysis of the scoring of SCOFF questionnaire was done based on genders, age group, ethnicity and levels of enrollment in medical course.



**Shaker Uddin Ahmed et al.****Ethical Consideration**

This questionnaire was distributed to the participants after briefing the participants regarding our study. On top of the questionnaires, a consent form is provided with signature or fingerprint as prove of the students' permissions to participate in the study voluntarily. All responses from the participants were kept confidential, and they were allowed to refuse participation in this study. No unique identifiers were collected.

RESULTS

A total of 285 questionnaires were retrieved and only 279 survey forms were completed. The response rate was 100% while the completion rate was 97.9%. The socio-demographic characteristics of the respondents were summarized in Table 1.

Prevalence of Possible Eating Disorders among Medical Students in Ipoh

SCOFF questionnaire detected 119 people (42.7%) out of 279 people with possible eating disorders.

The table above showed that there is a difference between the median and mean for all questionnaires. This showed that the data is not normally distributed.

SCOFF Findings

Out of 119 respondents that scored 2 or above, 23 (19.3%) were males while 96 (80.7%) were females [$p = 0.092$], not significant. Majority of positive SCOFF finding was 70 (58.8%) from age group of 21-23 years [$p = 0.972$], not significant. The respondents who are positive in results from Year 1 were the highest of 31 (26.1%) while the least from Year 4, 17 (14.3%) [$p = 0.538$], not significant. The number of positive Indian respondents were the highest 50 (42.0%) then Malay, 48 (40.3%), Chinese, 15 (12.6%), and other ethnicity, 6 (5.0%) [$p = 0.278$], not significant.

DISCUSSION

This study shows that there is a high prevalence of eating disorders among medical students in Ipoh 119 people (42.7%) detected by SCOFF questionnaire. This is much higher when compared to a study done by Akhtar Amin Memon et al, in which only 17% detected by SCOFF questionnaire having high-risk of possible eating disorders [8]. This means that eating disorders are on rise among Malaysian population especially students of medical colleges. According to this study the females are more likely to have eating disorders compared to males. SCOFF questionnaire reported of 96 (80.7%) females compared to 23 (19.3%) males have eating disorders. This is consistent with the finding of previous studies [7] [10].

This study significantly supporting the findings [9] [10] that both anorexia nervosa and bulimia nervosa are more commonly seen in girls and women with estimation of female-to-male ratio range from 6 : 1 to 10 : 1. Ethnicity, self-esteem, and ethnic identity play significant roles in ED risks (11,12) Asian Americans continue to take a diet similar to traditional Asian diets while native Americans prefer a diet based primarily on beans, rice, and corn tortillas, seasoned with chilli peppers and accompanied by beef, pork and chicken and small amounts of dairy products [13]. Religious beliefs may also influence on dietary choices.

This study showed that individuals with normal BMI values, 25.9% still suffered from EDs as diagnosed by SCOFF, 43.9% (61/139, Table 7) of normal individuals were suffering from EDs. In addition, this study reveals that overweight individuals are more likely to have EDs in relation to underweight individuals. According to SCOFF,





Shaker Uddin Ahmed *et al.*

47.1% (32/68) of the overweight while 27.5% (11/40) of underweight individuals scored above the cutoff score thus were likely to have EDs. There is a significant finding in which we found that Indian respondents, followed by Malay and Chinese respondents are more likely to have eating disorders. This is supported by a past study which found that Chinese women had smaller actual-ideal body weight discrepancy scores than both Malay and Indian women, [14]. Based on a study done among 187 Malay (15), and 80 Chinese college students attending a Malaysian medical college (16). Anorexia nervosa can cause multiple fatal medical complications such as electrocardiographic changes which may also result from potassium loss and partial diabetes insipidus. Studies have shown a range of mortality rates from 5 to 18 percent. Such a high mortality rate showed how dangerous eating disorders particularly anorexia nervosa is.

In conclusion, a significant number of medical students in Ipoh are at high risk of development of eating disorders, females being more prone than males. It suggests the need for further research to identify the causes and to facilitate planning of prevention activities. Therefore, strategies to reduce prevalence of eating disorders among medical students should be implemented such as detecting eating disorders earlier before complications begin.

ACKNOWLEDGEMENTS

All MBBS students from UniKL RCMP and QIUP for their willingness to take part in this project by answering the questionnaire. Without them, this study would not be successful.

REFERENCES

- Hudson, J. I., Hiripi, E., Pope, H. G., & Kessler, R. C. (2007). The prevalence and correlates of eating disorders in the national comorbidity survey replication. *Biol Psychiatry*, 61(3), 348–358.
- Caren A, (2016) The rise of eating disorders among young Malaysians. *Monthly Index of Medical Specialities (MIMS) Malaysia*.
- Carta M, Preti A, Moro M, Aguglia E, Balestrieri M, Caraci F et al. Eating disorders as a public health issue: Prevalence and attributable impairment of quality of life in an Italian community sample. *International Review of Psychiatry*. 2014 ;26(4):486-492.
- Sadock B, Sadock V, Ruiz P. Kaplan & Sadock's synopsis of psychiatry. 11th ed. Wolters Kluwer; 2015. 1499 p.
- Andexer D. The rise of eating disorders among young Malaysians. *MIMS News*. 2017 January [2017].
- Kristanto T, Chen W, Thoo Y. Academic burnout and eating disorder among students in Monash University Malaysia. *Eating Behaviors* January 2017;22:96-100.
- Andexer D. The rise of eating disorders among young Malaysians. *MIMS News*. 2017
- Memon A, Adil S, Siddiqui E, Naeem S, Ali S, Mehmood K. Eating disorders in medical students of Karachi, Pakistan-a cross-sectional study. *BMC Research Notes*. 2012
- Morgan J, Reid F, Lacey J. The SCOFF questionnaire: assessment of a new screening tool for eating disorders. *BMJ*. 1999 319(7223):1467-1468.
- EAT-26 Self-Test: Permission. *Eat-26.com*. 2016
- Herzog D, Eddy K. Eating Disorders: What Are the Risks?. *Journal of the American Academy of Child & Adolescent Psychiatry* 2009 48(8):782-783.
- Grabe S, Ward L, Hyde J. The role of the media in body image concerns among women: A meta-analysis of experimental and correlational studies. *Psychological Bulletin* 2008
- Swami V. Female Physical Attractiveness and Body Image Disorders in Malaysia. *Malaysian Journal of Psychiatry*. 2006;14(1).
- Swami V, Tovée M, Harris A. An examination of ethnic differences in actual-ideal weight discrepancy and its correlates in a sample of Malaysian women. *International Journal of Culture and Mental Health* 2013 6(2):96-107.





Shaker Uddin Ahmed et al.

15. Edman JYates A. Eating attitudes among college students in Malaysia: an ethnic and gender comparison. European Eating Disorders Review 2004;12(3):190-196.
16. Smith K. The Effect of Eating Disorders on Work Performance. UCHC Graduate School Masters Theses 2003 - 2010 :157.

Table 1: Socio- demographic Characteristics of Respondents

Characteristics	Frequency	Percentage (%)
College		
Unikl RCMP	121	43.4
QIUP	158	56.6
Gender		
Male	69	24.7
Female	210	75.3
Age group (Years)		
18-20	65	23.3
21-23	163	58.4
24-26	51	18.3
<i>Mean: 21.86 Median: 22 Standard deviation: 1.656</i>		
Ethnicity		
Malay	131	47.0
Chinese	30	10.8
Indian	104	37.3
Others	14	5.0
Year of Study		
One (1)	66	23.7
Two (2)	58	20.8
Three (3)	57	20.4
Four (4)	50	17.9
Five (5)	48	17.2
Body Mass Index (BMI)		
Underweight (<18.5 kg/m ²)	40	14.3
Normal (18.5-22.9 kg/m ²)	139	49.8
Overweight (23-27.4 kg/ m ²)	68	24.4
Obese (≥27.5 kg/m ²)	32	11.5
<i>Mean: 22.47 Standard deviation: 4.46</i>		

Table 2: Descriptive analysis of questionnaires

Scores	SCOFF
Mean	1.36
Median	1.00
Standard deviation	1.239
Range	5





Shaker Uddin Ahmed et al.

Table 3: SCOFF results in relation to Gender, Age group, Year of Study, Ethnicity and BMI ratios
 Thus, this showed that females are more likely to have EDs compared to males and Indians are more likely to have EDs compared to other races. Respondents from age group of 21-23 years old and Year 1 medical students are more likely to have EDs compared to others.

Variables		SCOFF Score		Total (n=279)	P-values
		Positive (n=119)	Negative (n=160)		
Gender	Male	23 (33.3%)	46 (66.7%)	69 (100%)	0.092
	Female	96 (45.7%)	114 (54.3%)	214 (100%)	
Age group	18-20 years old	28 (43.1%)	37 (56.9%)	65 (100%)	0.972
	21-23 years old	70 (42.9%)	93 (57.1%)	163 (100%)	
	24-26 years old	21 (41.2%)	30 (58.8%)	51 (100%)	
Year of study	1	31 (47.0%)	35 (53.0%)	66 (100%)	0.538
	2	27 (46.6%)	31 (53.4%)	58 (100%)	
	3	26 (45.6%)	31 (54.4%)	57 (100%)	
	4	17 (34.0%)	33 (66.0%)	50 (100%)	
	5	18 (37.5%)	30 (62.5%)	48 (100%)	
Ethnicity	Malay	48 (36.6%)	83 (63.4%)	131 (100%)	0.278
	Chinese	15 (50.0%)	15 (50.0%)	30 (100%)	
	Indians	50 (48.1%)	54 (51.9%)	104 (100%)	
	Others	6 (42.9%)	8 (57.1%)	14 (100%)	
BMI	Underweight	11 (27.5%)	29 (72.5%)	40 (100%)	0.202
	Normal	61 (43.9%)	78 (56.1%)	139 (100%)	
	Overweight	32 (47.1%)	36 (52.9%)	68 (100%)	
	Obese	15 (46.9%)	17 (53.1%)	32 (100%)	

Table 4: Response of the Respondents towards the SCOFF Questions 117 respondents (41.9%) worry that they have lost control over how much they eat while 108 respondents (38.7%) would say the food dominates their lives. However, only 26 respondents (9.3%) had recently lost more than one stone (6.35kg) in a 3-month period while 30 (10.8%) respondents make themselves sick because they feel uncomfortably full.

Questions	Frequency (%) of responses	
	Yes	No
Do you make yourself sick because you feel uncomfortably full?	30 (10.8%)	249 (89.2%)
Do you worry that you have lost control over how much you eat?	117 (41.9%)	162 (58.1%)
Have you recently lost more than one stone (14 lb, 6.35kg) in a 3-month period?	26 (9.3%)	253 (90.7%)
Do you believe yourself to be fat when others say you are too thin?	99 (35.5%)	180 (64.5%)
Would you say that food dominates your life?	108 (38.7%)	171 (61.3%)





Shaker Uddin Ahmed et al.

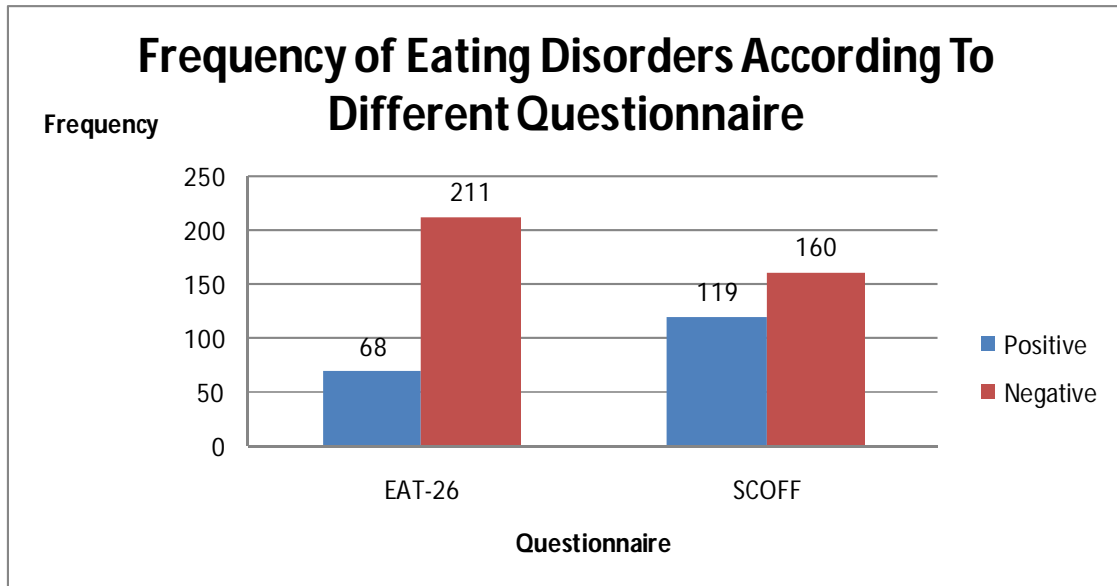


Figure 1: Frequency of possible eating disorders according to different questionnaires

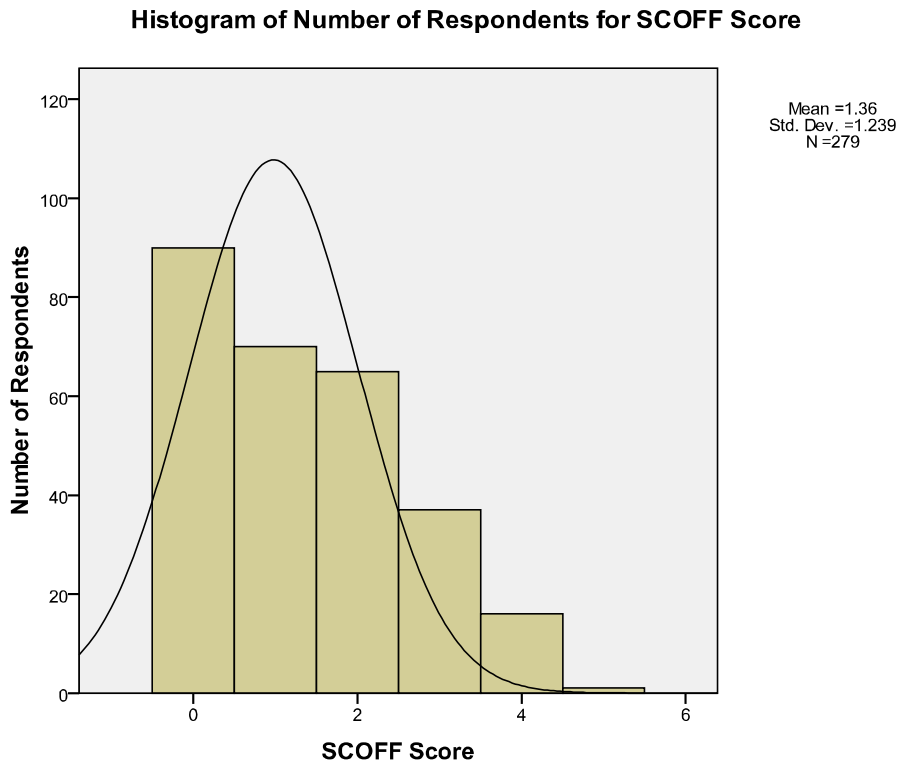


Figure 2: Number of respondents for SCOFF score





Optical Fiber Sensor Based on Local Surface Plasmon Resonance to Measured Refractive Index

Hammad R.Humud^{1*}, Abdulhadi Kadhim² and Reham Salah²

¹Department of Physics, College of Science, University of Baghdad, Iraq.

²Laser Engineering Department, University of Technology, Baghdad, Iraq.

Received: 28 Nov 2017

Revised: 21 Dec 2017

Accepted: 03 Jan 2018

*Address for correspondence

Hammad R.Humud

Department of Physics,

College of Science, University of Baghdad,

Baghdad, Iraq,

E.mail: dr.hammad6000@yahoo.com



This is an Open Access Journal / article distributed under the terms of the **Creative Commons Attribution License** (CC BY-NC-ND 3.0) which permits unrestricted use, distribution, and reproduction in any medium, provided the original work is properly cited. All rights reserved.

ABSTRACT

This work reports the implementation of an optical fiber sensor to measure the refractive index in different media based on localized surface plasmon resonance (LSPR), where the photo deposition technique was used to immobilize silver nanoparticles on the optical fiber end. This technique has a simple instrumentation, involves laser light via an optical fiber and silver nanoparticles suspended in an aqueous medium. The optical sensor was assembled using a tungsten lamp as white light, an optical spectrum analyzer OSA, and multi-mode optical fiber with silver nanoparticles. The response of this sensor is such that the LSPR peak wavelength is linearly shifted to longer wavelengths as the refractive index is increased, showing a sensitivity of 150.77 nm/RIU.

Keywords: localized surface plasmon resonance; photo deposition; fiber optic sensor; refractive index; silver nanoparticles.

INTRODUCTION

During the last few years, the optical fiber sensors based on Localized surface plasmon resonance (LSPR) have drawn major attention because of their main features in high sensitivity, fast response, and the detection is free label [1,2]. The optical fiber sensors based LSPR used in different technical fields such as chemical, medical, biological, biomedical applications, and environmental industries. They have been used to measure various physical properties, such as temperature, chemical changes and refractive index (RI). The surface Plasmon are coherent oscillations of free electrons at the boundaries between metal and dielectric which are often classified into two categories: (1) propagating surface Plasmon resonance (SPR), (2) (LSPR). Propagating surface Plasmons are evanescent electromagnetic waves,





Hammad Humud et al.

which are propagating along of a flat metal-dielectric interface and they arise from oscillation of the conduction electrons. Propagating surface plasmons can be excited on the metallic films which have many approaches such as the Otto [3], Kretschman [4], prism coupler, optical waveguides coupler [5], optical fiber coupler [6], and diffraction gratings [7]. Whereas localized surface Plasmon are non-propagating excitations of the conduction electrons of metal nanoparticles. When the oscillation frequency of the conduction electrons within the metal nanoparticles coincides with the light frequency, the resonance condition is obtained giving rise to large extinction coefficients. LSPR is a phenomenon relied on a localized electromagnetic field around noble metal surfaces, which are sensitive to the surrounding refractive indices. The LSPR peak wavelength and its width depend strongly on the composition, size, shape, dielectric environment, and separation distance of the nanoparticles [8,9]. Traditional SPR sensors are manufactured in the base of the Kretschmann configuration where a thin noble metal film is coated on a prism. On the other hand, the LSPR sensors are normally fabricated with noble metal nanoparticles which are deposited on a substrate such as optical fiber. LSPR sensors have additional features such as compact size, electromagnetic immunity, and portability [10]. To fabricate an optical fiber sensor based on LSPR, there are some methods to immobilize nanoparticles on the optical fiber, such as photo deposition technique [11], electron-beam lithography [12–14], self-assembly of polyelectrolyte [15,16], and self-assembly [17–19]. Both types of SPR can induce a strong enhancement of electromagnetic field in the near-field region (resonance amplification), leading to a extensive application in surface-enhanced Raman scattering (SERS) [20], fluorescence enhancement [21], refractive index (RI) measurement [22] and biomolecular interaction detection [23]. This work construct of an optical fiber sensor to measure the refractive index in different media based on LSPR phenomenon using silver nanoparticles these nanoparticles were immobilized on the optical fiber end by the photodeposition technique.

THEORY

The dependence of LSPR peak wavelength with the dielectric function of the surrounding environment can be proven by means the Drude model [24,25]

$$\epsilon_r = 1 - \frac{\epsilon_p^2}{\omega^2 + \gamma^2} \quad (1)$$

Where ϵ_r denotes the real part of the complex dielectric function (ϵ) of the plasmonic material, ω is the angular frequency of the radiation, ω_p is the plasma frequency and γ is the damping parameter of the bulk metal. In the visible and near-infrared regions $\gamma \ll \omega_p$, so that, the above expression becomes.

$$\epsilon_r = 1 - \frac{\omega_p^2}{\omega^2} \quad (2)$$

The polarizability α of a small spherical nanoparticle with a much smaller size than the wavelength of the light is given by

$$\alpha = 3\epsilon_0 V \frac{\epsilon - \epsilon_m}{\epsilon + 2\epsilon_m} \quad (3)$$

where V is the nanoparticle volume, ϵ_0 is the free space permittivity, and ϵ_m is the dielectric constant of the surrounding medium. The plasmon resonance occurs when polarizability attains a maximum, that is, when Equation (3) diverges. Accordingly, the resonance condition is $\epsilon_r = -2\epsilon_m$. Using the Equation (2) and the resonance condition, J. Gabriel and Alfonso get the frequency of the LSPR peak which is denoted by ω_{\max} and it is given as follows [26]:





Hammad Humud *et al.*

$$\omega_{\max} = \frac{\omega_p}{\sqrt{2\varepsilon_m + 1}} \quad (4)$$

Considering that $\varepsilon_m = n_2^2$ and $\lambda = 2\pi c/\omega$, Equation (4) becomes

$$\lambda_{\max} = \lambda_p + \sqrt{2n_m^2 + 1} \quad (5)$$

where λ_{\max} is the LSPR peak wavelength and λ_p is the wavelength corresponding to the plasma frequency of the bulk metal. Therefore, it is important to note that there exists a linear relationship between LSPR peak wavelength and the refractive index of the surrounding medium. The sensitivity S of a LSPR sensor expressed in nanometers per refractive index unit (nm/RIU) is defined as the change in the LSPR peak wavelength maximum per unit change in the refractive index of the medium and it can be calculated by

$$S = \frac{\Delta\lambda}{\Delta n} \quad (6)$$

EXPERIMENTAL WORK

Photo Deposition of Silver Nanoparticles on the Optical Fiber End

The photo deposition technique was used to immobilize silver nanoparticles on the optical fiber end using laser diode. The laser works in continuous-mode, wavelength 532 nm and output power 100mW. The silver nanoparticles with average particles size 40 nm suspended in ethanol. The diameter of the used multi-mode optical fiber core and its cladding were $\sim 50\mu\text{m}$ and $\sim 125\mu\text{m}$ respectively. The first optical fiber end used to couple to the laser where the coupling performed by using micro lens-SMA adapter coupled with SMA fiber optics adapter and this configuration connected to laser diode by homemade micro connector. The second optical fiber end was cleaved and cleaned. Then placed into the ethanol silver nanoparticle suspension, the suspension was prepared by mixing 30 cc of ethanol and 27 mg of Ag powder and then homogenized using an ultrasonic bath for 15 minutes. The suspension container was a cylindrical cell of 1.5 cm in diameter and 30 cm height. The container was filled to $\sim 90\%$ of its capacity. The typical distance from solution free surface to fiber end was approximately 2cm and the distance from the optical fiber end to the container bottom was about 28cm as shown in Fig.1. Laser diode source was turned on to deposit the silver nanoparticles on optical fiber end. With this method it is possible to choose the maximum size of nanoparticles adhered on the optical fiber end by means of the laser power. Furthermore, the nanoparticles amount depends on the time of the optical fiber submerged into the colloidal and the laser power. It is important to notice that if the laser is not turned on, there are not nanoparticles adhered on the optical fiber end. The silver nanoparticles begin to adhere to the optical fiber end when the laser diode is turned on and the nanoparticles amount adhered on the fiber-optical end is related to the immersion time of the fiber into the colloidal solution.

Measurement Setup

The optical sensor system consists of a tungsten lamp as a white light source and optical spectrum analyzer (THORLABS) to measure the transmission spectra. The optical fiber end was immersed into the different media under study, and the absorption spectrum was recorded according to Figure 2. To get the reference spectrum, the optical fiber end without nanoparticles was put into the suspension container without liquid and the transmission spectrum was recorded. To obtain the calibration curve, the end of the optical fiber sensor was immersed into different media: air ($n = 1.00$), distilled water ($n = 1.33$), hexane ($n = 1.37$), benzene ($n = 1.501$) and aniline ($n = 1.586$).





and the transmitted spectrum were recorded, and then the relation between the refractive indexes versus the LSPR peak position was plotted.

RESULTS AND DISCUSSION

Figure 3 shows Scanning Electron Microscope (SEM) images of optical fiber end before and after deposit the silver nanoparticles. The deposition was performed for one hour. Figure 3(a) shows the optical fiber end, core and clad after cutting and cleaving, Figure 3(b) shows SEM image for the fiber optics end after immersed into silver acetone collide for one hours, it is clear that no particles deposited into the optical fiber end. Figure 3(c) shows the fiber optics end after an hour of immersion in the collide with the laser diode is on. From the figure notice that the smaller nanoparticles are deposited on the fiber clad and large particles are deposited around the core as shown in Figures 3(d).

The concentration of the deposited silver nanoparticles was examined by energy dispersive X-ray (EDX) examination and the results are shown in Figures 4. (a and b). From Figure 4. (a) it can be seen the composition of optical fiber end consist of silicon material only which had maximum peak and there is no silver nanoparticles was found that was because laser diode was off. Fig.4 (b) shows the optical fiber end after immersed in the silver acetone collide for one hour where the laser diode turn on. From the figure observed that the fiber optics end coated by silver nanoparticles. This is evidenced by the silver peak, which was seen in the Figures 4 (b) and did not exist in the Figure 4(a). The calculated silver nanoparticles concentration was 5.21. This was good evidence that the optical fiber end coated by the silver nanoparticles.

The experimental results indicate that deposition of nanoparticles on core of the optical fiber is achieved when the laser diode was turned on.

Figure 5 shows the LSPR absorption peaks position for the silver nanoparticles where its concentration was 5.21% as a function of refractive index changes. The change in the refractive index was done by placing the optical fiber sensor based on LSPR in four different medium having different refractive index. These media are air, distilled water, hexane, benzene and aniline.

From Figure 5 it can be seen that, there is 89nm change in the LSPR peak wavelength position when the sensor medium was changed from air to aniline and there is change 44nm in the LSPR peak wavelength position when the sensor medium was changed from air (400nm) to water (444nm). This peak position is moved to red when the refractive index of the liquid medium is increase. The sensor has peak position at 451nm when it was immersed in Hexane and it has peak at 476nm when it was immersed in benzene.

Figure 6 shows the LSPR peak wavelength as a function of the refractive index for the four medium. From this figure it can see that the LSPR peak position of the sensor changes with change of refractive index. This change is a linear change where the LSPR peak position is linearly changed to longer wavelengths as the refractive index was increase. From the obtained data in Fig 6 the sensor sensitivity is calculate and equal to $S=150.77\text{nm/RI}$.

CONCLUSIONS

It has been implemented and characterized an optical fiber sensor based on LSPR using silver nanoparticles. Novel technique known photo deposition has used to immobilize the silver nanoparticles on the optical fiber end. This technology with fiber optics made the system simple lightweight and low cost. The sensor based on the LSPR idea and the photo deposition on the end of the optical fiber, giving the sensor high flexibility to use in different applications with little modification.





REFERENCES

- Holmaj, Sinclair S. Yee, Günter Gauglitz, Sensors and Actuators B: Chemical, vol. 54, no.1-2, (1999), 3–15.
- Xudong Fan, Ian M. White, Siyka I. Shopova, Hongying Zhu, Jonathan D. Suter, Yuze Sun, Anal. Chim., vol.620, (2008), 8–26.
- Otto A., Zeitschrift für Physik A Hadrons and Nuclei, vol. 216, no. 4, (1968), 398–410.
- Matsubara K., Kawata S., and Minami S., Applied Optics, vol. 27, no.6, (1988), 1160–1163.
- Harris R. D. and Wilkinson J. S., Sensors and Actuators B: Chemical, vol. 29, no. 1–3, (1995), 261–267.
- Webb D. J., Photonic Sensors, vol. 1, no. 2, (2011), 140–151.
- Ritchie R. H., Arakawa E. T., Cowan J. J., and Ham R. N., Phys. Rev. Lett., vol. 21, no. 22, 1530–1533, (1968).
- Mayer, K.M.; Hafner, J.H., Chem. Rev., (2011) 3828–3857.
- Huanjun Chen, Xiaoshan Kou, Zhi Yang, Weihai Ni, and Jianfang Wang, Langmuir, vol.24, (2008), 5233–5237.
- Gupta D.B., Verma R.K. Journal of Sensor, vol. 2009, (2009), 1–12.
- Ortega-Mendoza J. G., Chávez F., Zaca-Morán P., Felipe C., Pérez-Sánchez G. F., Beltrán-Pérez G., Goiz O., and Ramos-García, Opt. Express, vol. 21, no. 5, (2013), 6509–6518.
- Yongbin Lin, Yang Zou, Robert G. Lindquist Biomed, Opt. Express, vol.2, no.3, (2011), 478–484.
- Yongbin Lin, Yang Zou, Yuanyao Mo, Junpeng Guo, Robert G. Lindquist, Sensors vol.10, (2010), 9397–9406.
- Sanders M, Lin Y, Wei J, Bono T, Lindquist RG, Biosens. Bioelectron, vol.61, (2014), 95–101.
- Ye W., F.-Q. Bu, Y.-J. Gu, P. Xu, X.-H. Ning, S.-P. Xu, B. Zhao, W.-Q. Xu, Chem. J. Chin. Univ., vol.29, (2008), 1539–1543.
- Shao Y., Xu S., X. Zheng, Y. Wang, W. Xu., Sensors, vol.10, (2010), 3585–3596.
- Jeong, H., Erdene N., S.-K. Lee, D.-H. Jeong, J.-H. Park, Opt. Eng., vol.50, (2011).
- J.L. Tang, S.F. Cheng, W.-T. Hsu, T.-Y. Chiang, L.-K. Chau, Sens. Actuators B Chem, vol.119, (2006), 105–109.
- Hsing-Ying Lin, Chen-Han Huang, Gia-Ling Cheng, Nan-Kuang Chen, Hsiang-Chen Chui, Opt. Express, vol.20, no.19, (2012), 21693–21701.
- Chen C. Y., E. Burstein, Phys. Rev. Lett., vol. 45, no. 15, (1980), 1287–1291.
- Sokolov K., G. Chumanov, and T. M. Cotton, Anal. Chem., vol. 70, no. 18, (1998), 3898–3905.
- Zeng J., D. Liang, and Z. X. Cao, Proc. SPIE, vol. 5855, (2005), 667–670.
- Karlsson R. and A. Fält, Journal of Immunological Methods, vol. 200, no. 1–3, (1998), 121–133.
- Cennamo N., D'Agostino G., Dona A., Dacarro G., Pallavicini P., Pesavento M., Zeni L., Sensors vol.13, (2013), 14676–14686.
- Hong Y., Huh Y.-M., Yoon D.S., Yang J., J. Nano Mat., vol.2012, (2012), 1–13 [26] Gabriel Ortega-Mendoza J., Alfonso Padilla-Vivanco, Carina Toxqui-Quitl Plácido Zaca-Morán, David Villegas-Hernández, Fernando Chávez, Sensor, vol.2014, (2014), 18701-18710.

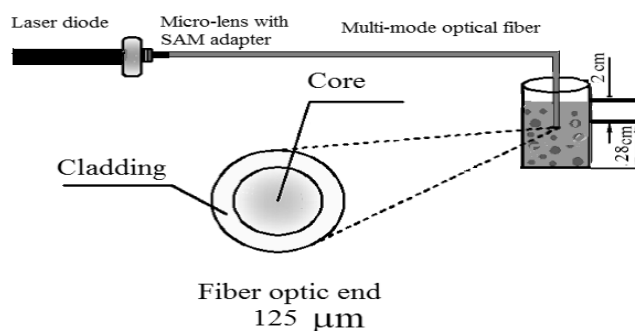


Fig. 1: Experimental setup for depositing silver nanoparticles onto optical fiber end



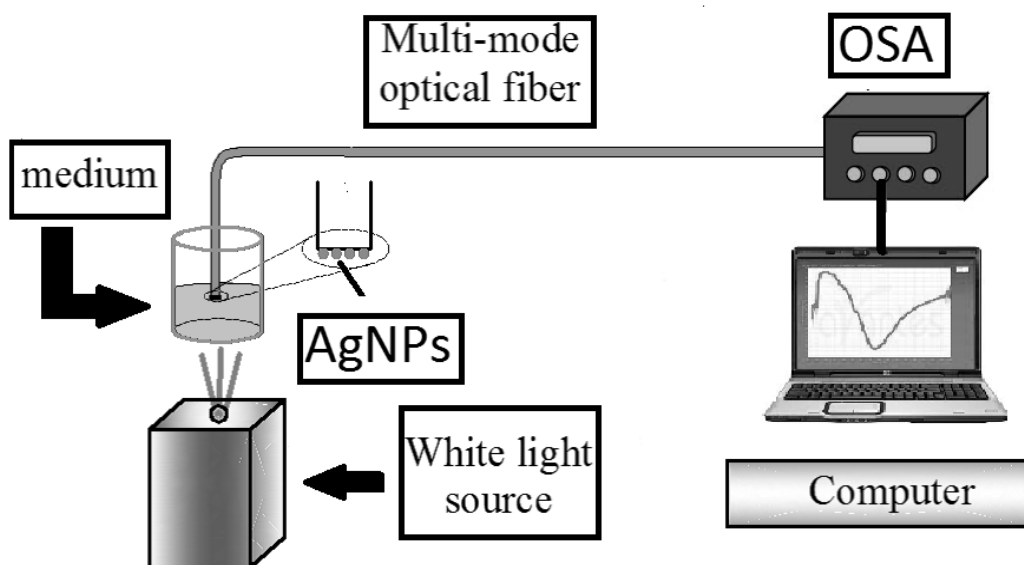


Fig.2: Experimental setup for measuring the refractive index of different liquidmedium.

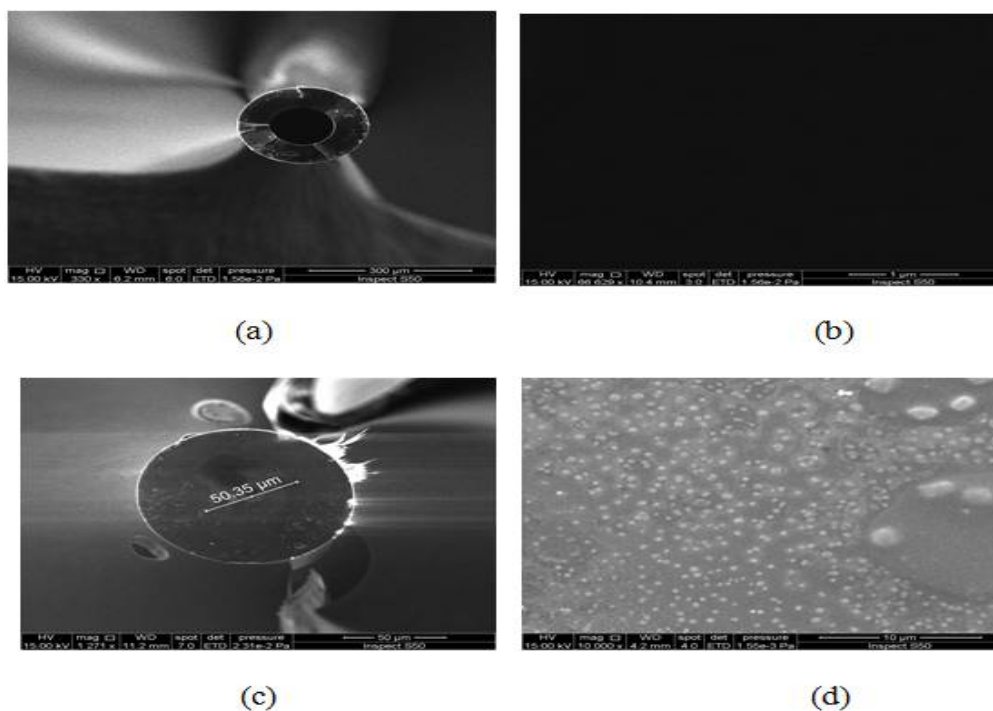


Fig. 3: imagesof the optical fiber end obtained with SEM,a) Optical fiber end after cut,b) closer view of the optical fiber corewhen optical fiber was immersed into solution for up to one hour with laser light off, c) laser was turned on for one hour and power = 100mW,d)closer view of the optical fiber corewhen laser was turned on for one hour.





Hammad Humud et al.

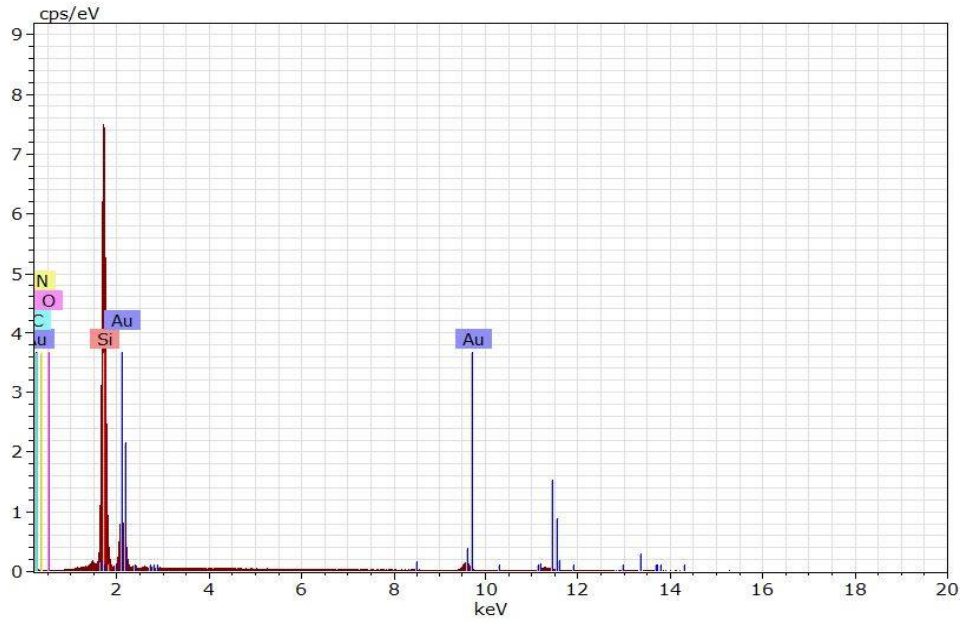


Fig. 4 (a):Optical fiber end with out deposition

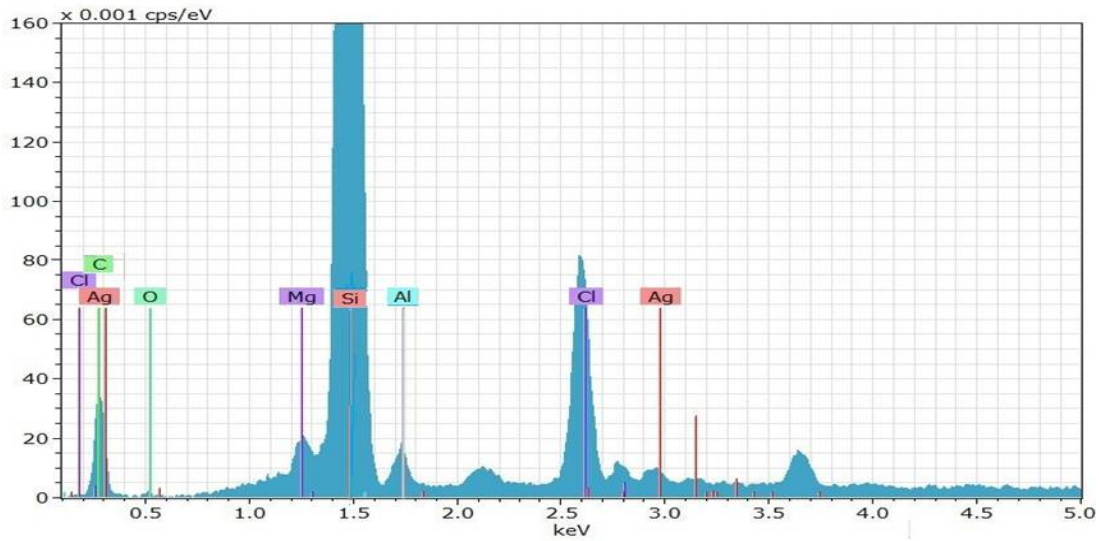


Fig. 4: (b) Optical fiber end when it was deposited with silver nanoparticles for an hour





Hammad Humud et al.

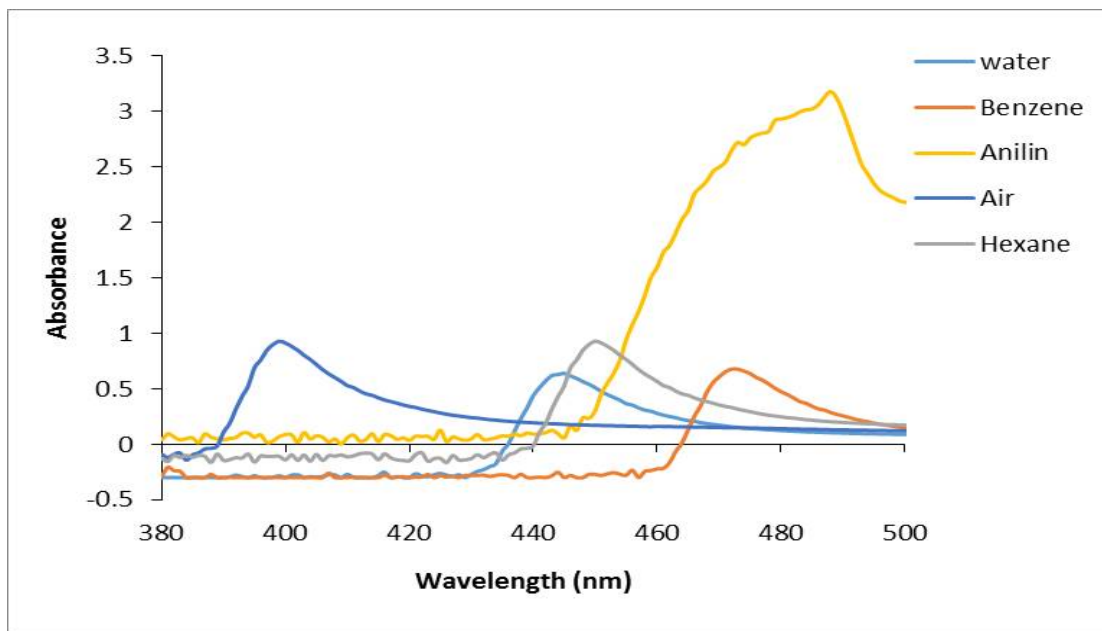


Fig. 5:The LSPR peaks position for silver nanoparticles concentration 5.21% as a function of refractive index changes.

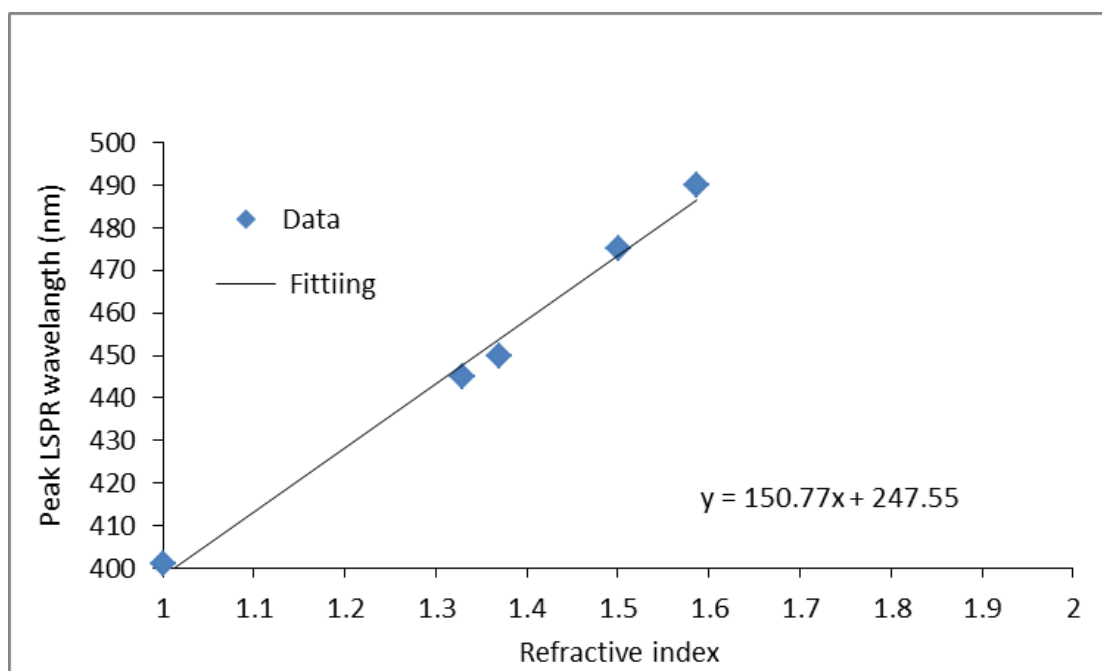


Fig. 6:LSPR peak position vires refractive index for the optical fiber sensor based on LSPR using silver nanoparticles.





RESEARCH ARTICLE

Evaluation of Bio-efficacy of Acetamiprid 20% SP against Brown Plant Hopper, *Nilaparvata lugens* (Stal.) in Rice

H.G. Umashankar^{1*}, M.P. Rajanna² and B.S. Chetana³

¹Jr. Entomologist, AICRP on Rice, Zonal Agricultural Research Station, VC Farm Mandya-571405, Karnataka, India.

²Prof. & Scheme Head, AICRP on Rice, Zonal Agricultural Research Station, VC Farm Mandya-571405., Karnataka, India.

³Asst. Prof. AICRP on Rice, Zonal Agricultural Research Station, VC Farm Mandya-571405., Karnataka, India.

Received: 27 Nov 2017

Revised: 21 Dec 2017

Accepted: 03 Jan 2018

*Address for correspondence

H.G. Umashankar

Jr. Entomologist, AICRP on Rice,
Zonal Agricultural Research Station,
VC Farm Mandya-571405, Karnataka, India.
E.mail: umashankarhg21@gmail.com



This is an Open Access Journal / article distributed under the terms of the **Creative Commons Attribution License** (CC BY-NC-ND 3.0) which permits unrestricted use, distribution, and reproduction in any medium, provided the original work is properly cited. All rights reserved.

ABSTRACT

The field evaluation was carried out in Zonal Agricultural Research Station, V.C. Farm, Mandya during Kharif 2016 to assess the efficacy of insecticides against brown plant hopper. The study revealed that application of test product Acetamiprid 20% SP at lower dosage @ 10 and 20 g.ai./ha gave effective control of brown planthopper and with increase in yield. Similarly, Acetamiprid 20% SP had no phytotoxic effect on rice crop. The study indicated that the test product Acetamiprid 20% SP at lower dosage @ 10 and 20 g.ai./ha is equally effective compared to market product of acetamiprid 20% SP @ 10 and 20 g.ai./ha. The results on the effect of different doses of Acetamiprid 20% SP on spiders and mirids revealed that application of Acetamiprid 20% SP at different doses had no adverse effect on the spiders and mirid bugs at 10 days after first and second application as the natural enemies build up was not affected.

Keywords: Acetamiprid 20% SP, Bio-efficacy, Brown planthopper, natural enemies and spiders.

INTRODUCTION

Rice, *Oryza sativa* a cereal crop, belongs to the family Gramineae. It is staple food for more than half of human population. Rice constitutes 52 per cent of total food grain production and 55 per cent of total cereal production in India [1]. About 100 insects were recorded as pests on rice crop, of them 20 are designated as major pests [2]. Among

13040



**Umashankar et al.**

them brown planthoppers constitute one of the most important pest causing substantial yield losses. Use of insecticides forms one of the most effective management tools and an important component of Integrated Pest Management (IPM) besides biological and cultural means. Insecticide proves to be the only option where we can rely for emergency management of insect pest reaching on or beyond ETL. The indiscriminate use of broad spectrum chemicals also reduce the biodiversity of natural enemies, reduce the natural control and induce outbreak of secondary pests and contaminate eco-system [3] result in resurgence of brown planthopper. But still chemical control forms the first line of defense [4]. As, the resistance to existing insecticides is an on-going problem that requires the development of new insect control tools [5] so there is a need to evaluate the new groups, new formulations of insecticides and their combinations for their target and non target effects. Therefore the present investigation was carried out to evaluate bio-efficacy of Acetamiprid 20% SP molecule against BPH infesting rice.

MATERIALS AND METHODS

The present study was conducted in the Zonal Agricultural Research Station, V.C. Farm, Mandya during Kharif 2016. The paddy crop (Variety- CTH-1) was raised as per recommended practices and experimental plot size was 2.5X2.5 m². The insecticides tested at recommended concentration (Table 1). An untreated control without any insecticide was included in trail for comparison. Spraying were given by using a hand compression knapsack high volume sprayer during morning hours. The required spray fluid per each plot is one litre. The plot in each treatment was sprayed with respective insecticides ensuring uniform coverage of insecticide. The treatments are imposed as and when the pest reaches ETL. The data on population of BPH on 10 randomly selected hills from each plot were recorded at one day before the application of treatments and 1,2,3,5,7 and 10 days after spray. The natural enemy numbers (spiders & mirid bugs) was recorded on plants before application and on 10th day after application. The grain yield was recorded plot wise and presented as quintals/ha. The data subjected to [6]. The data on the population of planthoppers are transformed into square root values.

RESULTS AND DISCUSION

Bio Efficacy of Acetamiprid 20% SP on BPH

The data on bio efficacy of Acetamiprid 20% SP on brown planthopper (BPH) are presented in Table 2. Among the treatments, one day before application the population of BPH varied between 231.66 to 213.07 per 10 hills at one day before spray. The BPH population was found significantly varying among the treatments on one, three, five, seven and ten days after the application of insecticides. One day after spray least number of 202.3 BPH per 10 hills were recorded in plots treated with Acetamiprid 20% SP@ 40 g.a.i. per ha and was on par with Acetamiprid 20% SP @ 10 and 20 g. a.i. per ha and Acetamiprid 20% SP (Market product) @ 20 and 10 g ai/ha. Similar trend was observed at three, five, seven and ten days after spray. The cumulative mean of different days observation did not indicate much variation among different dosages of the test product acetamiprid 20% SP and market product of acetamiprid at different dosages. However, the lower dosages of test product acetamiprid @ 10 and 20 g.a.i./ha recorded on par population of BPH in comparison with the same dosages of market product of acetamiprid at one, three, five seven and ten days after first and second application thus, indicating the on par efficacy of acetamiprid test product with market product. Present findings are also experimentally corroborated by earlier workers. Acetamiprid 20SP was superior in minimizing the population of BPH in rice [7].

Effect of Acetamiprid 20% SP on Natural Enemies of Brown Planthopper

The results on the effect of different doses of Acetamiprid 20% SP on spiders and mirids are presented in Table 4. The results revealed application of Acetamiprid 20% SP at different doses had no adverse effect on the spiders and mirid bugs at 10 days after application as the natural enemies build up was not affected.





Umashankar et al.

Grain Yield

Grain yield of rice increased with the application of insecticides compared to untreated control (Table. 2). Application of test product Acetamiprid 20% SP at lower dosages viz., 10 and 20 g.ai./ha recorded on par grain yield (49.25 and 51.56 q/ha) compared to market product of acetamiprid 20% SP @ 10 and 20 g.a.i/ha (47.59 and 50.60 q/ha). This indicates that the test product acetamiprid is equally effective compared to market product of acetamiprid 20%SP. These results are in agreement with previous studies where acetamiprid recorded the highest yield ((4763 kg ha-1)) [8] compared to untreated control.

CONCLUSION

The overall results on incidence of brown plant hopper and grain yield revealed that test product Acetamiprid 20% SP at lower dosage @ 10 and 20 g.ai./ha is equally effective compared to market product of acetamiprid 20% SP @ 10 and 20 g.ai./ha.

REFERENCES

1. R. C. Sexena, R. K. Singh. Rice research in India and the asian perspective, Asian Biotech Dev. Rev, Neem Foundation, Gurgaon, India. Formerly with IRRI, Philippines. 2003, 81-96.
2. M. D. Pathak, G. S. Dhaliwal, Trends and strategies for rice insect problems in Tropical Asia. IRRI Res. Pap.Ser. 1981, 64, 5-6.
3. S. P. Singh, Bio-intensive approach helpful. The Hindu Survey of Indian Agriculture. 2000, 159-163.
4. I. C. Pasalu, N. V. Krishnaiah, G. Katti, N. R. G. Varma, IPM in Rice. IPM Mitra. 2002, 45 - 55.
5. Whalon, M.E, M. Mota-Sanchez R. M. Hollingworth, Analysis of global pesticide resistance in arthropods.Global Pesticide Resistance in Arthropods. Michigan State University, USA. 2008, 5-31.
6. D. B. Duncan, A significance test for differences between ranked treatment means in an analysis of variance. The. Vir. J. Sci. 1951, 2, 171-189.
7. R. K. Murali Baskaran, K. Suresh, D. S. Rajavel, N. Palanisamy, Field efficacy of pymetrozine 50 WG against rice brown planthopper, Nilaparvata lugens (Homoptera: Delphacidae). Pestology. 2009, 33, 20-21.
8. M. Hegde, J. P. Nidagundi, Effect of newer chemicals on planthoppers and the mirid predators in rice.Karnataka J. Agric. Sci. 2009, 22, 511-513.

Table 1. Treatment details:

SI.No	Treatment	Dosage	
		g a.i./ha	(Kg/ha)
T ₁	Acetamiprid 20% SP	10	50
T ₂	Acetamiprid 20% SP	20	100 (X)
T ₃	Acetamiprid 20% SP	30	150
T ₄	Acetamiprid 20% SP	40	200 (2X)
T ₅	Acetamiprid 20% SP (Market sample)	10	50
T ₆	Acetamiprid 20% SP (Market sample)	20	100





Umashankar et al.

Table 2. Efficacy of Acetamiprid 20 % SP on the Population of Brown Plant Hopper

Treatments	Dosage (ga.i./ha)	Number of BPH/10 hills						Mean
		1 DBS	1 DAS	3 DAS	5 DAS	7 DAS	10 DAS	
T1	10	219.12	209.17	178.65	118.47	78.32	36.42	124.2
		-14.13	-13.74	-12.7	-10.25	-8.4	-5.78	
T2	20	213.07	206.45	176.42	109.1	63.68	29.28	116.98
		-14.01	-13.69	-12.61	-9.78	-7.46	-5.3	
T3	30	225.1	205.71	147.12	98	50	20.76	104.31
		-14.32	-13.66	-11.55	-9.31	-6.69	-4.36	
T4	40	222.12	202.23	131.21	92.42	48.13	17.26	98.25
		-14.34	-13.7	-11.12	-9.12	-6.66	-4.33	
T5	10	225.18	207.56	181.25	129	83.09	43	128.78
		-14.43	-13.66	-12.85	-10.84	-8.58	-6.45	
T6	20	231.66	208.16	177.54	121.13	68.24	30.12	121.03
		-14.51	-13.82	-12.68	-10.64	-7.67	-5.46	
T7	-	229.54	234.17	239.42	248	221.71	242.42	237.14
		-14.75	-15.64	-15.84	-16.1	-14.15	-15.42	
SEm±			0.4	0.4	0.4	0.4	0.4	
CD at 5%		NS	1.03	1.59	1	0.96	1.91	

Table 3. Efficacy of Acetamiprid 20% SP insecticide molecules against grain yield

Treatments	Dosage (g a.i./ha)	Grain Yield (Q/ha)	% increase in yield over control
T1: Acetamiprid 20% SP	10	49.25	38.34
T2: Acetamiprid 20% SP	20	51.56	44.83
T3: Acetamiprid 20% SP	30	51.68	45.17
T4: Acetamiprid 20% SP	40	52.29	46.88
T5: Acetamiprid 20% SP (Market sample)	10	47.59	33.68
T6: Acetamiprid 20% SP (Market sample)	20	50.60	42.13
T7: Control	-	35.60	
SEm±		5.69	
CD at 5%		1.59	





Umashankar et al.

Table 4. Efficacy of Acetamiprid 20% SP insecticide molecules against non target organism

Treatment	Number of spiders/10hills				Number of mirid bugs/10hills			
	1 DBS	First Spray	Second Spray	Mean	1 DBS	First Spray	Second Spray	Mean
		10 DAS	10 DAS			10 DAS	10 DAS	
T1	7.33 (2.89)	6.99 (2.83)	6.99 (2.83)	7.10	13.33 (3.79)	12.99 (3.74)	12.99 (3.74)	13.10
T2	7.33 (2.89)	6.66 (2.77)	6.66 (2.77)	6.88	12.99 (3.74)	12.33 (3.65)	12.66 (3.70)	12.66
T3	6.99 (2.83)	6.33 (2.71)	6.33 (2.71)	6.55	13.33 (3.79)	12.99 (3.74)	12.99 (3.74)	13.10
T4	6.99 (2.83)	5.99 (2.64)	6.66 (2.77)	6.55	12.99 (3.74)	12.33 (3.65)	12.33 (3.65)	12.55
T5	7.33 (2.89)	6.99 (2.83)	6.99 (2.83)	7.10	13.33 (3.79)	12.99 (3.74)	12.99 (3.74)	13.10
T6	7.33 (2.89)	6.66 (2.77)	6.33 (2.71)	6.77	13.66 (3.83)	13.33 (3.79)	12.99 (3.74)	13.33
T7	6.99 (2.83)	7.33 (2.89)	7.33 (2.89)	7.22	13.33 (3.79)	12.99 (3.74)	12.99 (3.74)	13.10
SEm±	0.4	0.4	0.39		0.4	0.38	0.39	
CD at 5%	NS	1.56	0.35		NS	1.56	0.35	





Characterization of the Anthropometric Indices in 3–18 years old Down's Syndrome Children in Ipoh Malaysia

Tahamida Yesmin^{1*}, Sabaridah Binti Ismail², MarMarWai³, Padmini V⁴, Sandheep Sugathan⁵, Myo Than⁶

¹Senior Lecturer, Department of Anatomy, Faculty of Medicine, University Kuala Lumpur, Royal College of Medicine Perak, Ipoh, Malaysia.

²Senior Lecturer, Department of Public Health, Faculty of Medicine, University Kuala Lumpur, Royal College of Medicine Perak, Ipoh, Malaysia.

³Senior Lecturer, Department of Anatomy, Faculty of Medicine, University Kuala Lumpur, Royal College of Medicine Perak, Ipoh, Malaysia.

⁴Professor, Department of Paediatric Faculty of Medicine, University Kuala Lumpur, Royal College of Medicine Perak, Ipoh, Malaysia.

⁵Senior Lecturer, Department of Public Health, Faculty of Medicine, University Kuala Lumpur, Royal College of Medicine Perak, Ipoh, Malaysia.

⁶Professor, Department of Anatomy, Faculty of Medicine, University Kuala Lumpur, Royal College of Medicine Perak, Ipoh, Malaysia.

Received: 21 Nov 2017

Revised: 03 Dec 2017

Accepted: 28 Dec 2017

* Address for correspondence

Tahamida yesmin

Senior Lecturer, Department of Anatomy,
Faculty of Medicine, University Kuala Lumpur,
Royal College of Medicine Perak, Ipoh, Malaysia.
E.mail: tahamida.yesmin@yahoo.com



This is an Open Access Journal / article distributed under the terms of the **Creative Commons Attribution License** (CC BY-NC-ND 3.0) which permits unrestricted use, distribution, and reproduction in any medium, provided the original work is properly cited. All rights reserved.

ABSTRACT

Anthropometry provides a simple and non-invasive method of quantitative assessment of changes in the surface anatomy of head, face, hand and foot in individuals with Down syndrome. The evaluation of measurements of DS children in Malaysia to other country DS children eliminated the population specific variations. The purpose of the present study was to identify the type of different indices which contribute specific character of individuals with Down syndrome of children of Malaysian origin. The present cross sectional descriptive type of study was done different rehabilitation centre in Ipoh Malaysia on Down's syndrome children age 3-18 years. To measure the parameters digital slide caliper and spreading caliper were used. The indices calculated according to the formula and the result obtained were analyzed statistically using the t-test and a subset of four indices namely facial index, cephalic index, hand index and foot index which accurately classify with DS. Comparison of facial, cephalic, hand and foot index between male and female were statistically nonsignificant. Both male and female cephalic index type were Hyperbrachycephalic but for facial index type Hypereuryprosopic for female and Euryprosopic for

13045





Tahamida Yesmin et al.

male. Foot index Mesopod type for both sex. Brachycheir was the commonest type of hand index for male downs syndrome children.

Keywords: Indices, sex, Downs's syndrome.

INTRODUCTION

Down syndrome (DS) is an autosomal chromosome disorder associated with trisomy 21 [10]. It is one of the commonest disorders in Malaysia. Few decades ago the frequency was approximately 20% but in the last 2 decades the reported frequency has increased to approximately 50% [9]. According to the Kiwanis Down syndrome foundation in Malaysia (2012) the incidence of Down syndrome is 1: 660 live births [8]. DS has indicated by marked abnormalities in the craniofacial morphology, the highest percentage of mild-moderate disproportion was found in the face (79.3%) [5]. The typical facial appearances in down Children are round face. Epicanthic fold, protruding tongue, small ears, flat occiput [7]. About 45% of people with Down Syndrome have the Single Palmar Crease; Compare that to 1% of the general population [3] Deficient growth rate throughout the growing period is another sign of Down's syndrome children which is more marked in infancy and again at adolescence [4] therefore short stature and obesity occurring during adolescence with broad, short hands, feet and digits, a short curved fifth finger with single flexion crease are typical presentation in DS children [2]. Anthropometry provides a simple and non-invasive method of quantitative assessment of changes in the surface anatomy of head, face, hand and foot in individuals with Down syndrome. A precise diagnosis makes available all the accumulated knowledge and experience of that condition and generally provides a better estimate of risk of recurrence [6]. The evaluation of measurements from DS children in other country with DS children in Malaysia from the same ethnic background eliminated the population specific variations. The purpose of the present study was to identify the type of different indices which contribute to the craniofacial, hand and foot stigmata of individuals' with Down syndrome of children of Malaysian origin.

MATERIALS AND METHODS

Forty four Down syndrome children (25 boys and 19 girls) aged 3–18 years were chosen as a defined population to investigate the anthropometric craniofacial pattern profiles. Out of 25 male DS Malay 18, Indian 2 and Chinese 5 and in Female it were Malay 8, Indian 3 and Chinese 8 in number.

In a pretested study, detailed history and general physical examination of the subjects including anthropometric measurements meeting the objectives of the study were taken. The subjects were examined after informed written consent from their parents or guardians was obtained. Subjects were made sit on a wooden chair with head rest. A total of eight measurements per subject were performed by single observer in order to avoid inter observer bias. Measurements and range variations were recorded according to Saller and martin [12] by using digital sliding caliper and spreading caliper. Measurements were taken according to following distance.

- Maximum head length—distance from glabella (g) to opisthocranium (op).
- Maximum head breadth—distance between two eurya (eu).
- Breadth of bizygomatic arch—distance between two zygia (zy).
- Morphological facial height—distance from nasion (n) to gnathion (gn).
- Length of hand—distance between the midpoint of a line joining the two stylium (Sty) and dactylion (da) of the middle finger.
- Breadth of the hand— distance between metacarpal radiale (mr) and metacarpal ulnare (mu).
- Length of foot—distance directly from pterion (pte) to acropodion (ap).
- Breadth of the foot— distance between metatarsal tibiale (mtt) and metatarsal fibulare (mtf).





Tahamida Yesmin et al.

Craniofacial indices calculated were:

Cephalic index: $\frac{\text{Maximum head breadth}}{\text{Maximum head length}} \times 100$

Morphological facial index: $\frac{\text{Morphological facial height}}{\text{Breadth of bizygomatic arch}} \times 100$

Index of hand: $\frac{\text{Breadth of the hand}}{\text{Length of the hand}} \times 100$

Index of foot: $\frac{\text{Breadth of the foot}}{\text{Length of the foot}} \times 100$

STATISTICAL ANALYSIS

The data were analyzed by using the software SPSS 17 version. Independent sample t test and for descriptive statistics Shapiro Wilk test were done.

RESULTS AND DISCUSSION

The present study was aimed to establish various anthropometric variables that discriminate 44 Down syndrome children. Very limited study reports are available and may not be able to be extrapolated for use in our local population due to different mix of ethnicity. This study focused attention on the head, face, hand and foot type that are most frequently described in the Down syndrome literature [10].

According to table 1 in male Down syndrome facial and cephalic index range were 27.32-65.66 and 76.47-97.29 and mean \pm SD were 43.46 \pm 7.47 and 85.62 \pm 5.93 respectively. In female Down syndrome facial range was 25.07-54.14 and facial index was 41.32 \pm 6.49 but mean \pm SD cephalic index for female was 85.79 \pm 3.48. Comparison of facial index and cephalic index between male and female were statistically nonsignificant.

According to table 2 both male and female DS cephalic index were hyperbrachycephalic type (86.5-91.9). Second commonest type of cephalic index for female were brachycephalic but hyperbrachycephalic for male. Increased the cephalic index due to increase the breadth of the head than the length of the head. Asha et al (2012) done one study on Indian DS children age 1-18 years and cephalic index classified under brachycephalic group (cephalic index-88) [1]. Allanson JE et al (1993) also did same study on 199 individuals with DS patients ageing between 6 months to 61 years [2] which correlated with Asha et al study. Although Down's syndrome is a chromosomal aneuploidy but there can be some environmental and race can influence that causes change of cephalic index group.

In table 3 most female DS children classified in hypereuryprosopic group (<78.9) and in male DS were Euryprosopic group (79-83.9) that means male DS children facial index bigger than female DS. Indian DS children age (1-18 years) facial index classified under hypereuryprosopic (Asha et al 2012). Subjects with DS had faces that were significantly narrower, less deep and short [1] that is same as Malaysian Down's syndrome children. This similarity also indicated that all facial special features are common and it not influenced by any other racial or environmental factors.

According to table 4 in male and female Down syndrome hand index range were 39-58 and 41-80 and mean \pm SD were 48.68 \pm 4.16 and 51.13 \pm 10.32 respectively. In case of foot index range in male was 27.99-48 and in female was 24.97-





Tahamida Yesmin et al.

69.79. Mean±SD of foot index for male and female Down syndrome were 40.51±4.6 and 42.19±8.23. Comparison of hand index and foot index between male and female were statistically nonsignificant.

According to table 5 hyperbrachycheir (>50.0) was the commonest type of hand index for female DS but it was brachycheir (47-49.9) was the commonest and hyperbrachycheir was the second commonest for male DS which was similar Asha et al who did study on DS children in India and found DS children hand breadth was more than hand height. In the present study showed the similar result that indicated that DS have their own hand character which is controlled by gene, not controlled by race and sex.

In table 6 mesopod was the most common type of foot index for DS in Malaysia. Asha et al (2012) did study and found DS in India could be classified under Brachypod group, which was the second commonest classification for DS in Ipoh Malaysia.

On the basis of anthropometric measurement of three races (Malay, Indian and Chinese) of DS children origin in Malaysia, it is possible to conclude that DS have specific and recognizable anthropometric patterns. Facial index and hand index were same only little variation found on cephalic and foot index this may be due to environmental cause.

There were no sex differences in DS children.

Although there were limitations to get consent from patients and find the rehabilitation centre but obviously there is a need for large sample study to resolve some differences between different ethnic groups.

ACKNOWLEDGMENTS

I would like to take this opportunity to express my heartfelt thanks to Kiwanis Down syndrome foundation-Ipoh centre, Sekolah Semangat Maju Ipoh, Yayasan Sultan Idris Shah, Bagl Orang Cacat Perak Pusat Pemulihan Sultan Azian Shah. Sincere thanks to the authority of the UniKL for the support and cooperation by providing the grant of STRG.

REFERENCES

1. Asha KR, Lakshmi Prabha S, Nanjiah CM, Prashanth S. Craniofacial anthropometric analysis in Down syndrome. Indian J Pediatr. 2011 Sep;78(9):1091-5. doi: 10.1007/s12098-011-0377-1. Epub 2011 Feb 22.
2. Allanson JE, Hara P, Farkas LG, Nair RC. Anthropometric craniofacial pattern profiles in down syndrome. Am J Med Genet 1993; 47:748-52.
3. Ai Peng Tan Down Syndrome: Multimodality Imaging of Associated Congenital Anomalies and Acquired Diseases Med J Malaysia Vol 68 No 6 December 2013.
4. Cronk C, Crocker AC, Pueschel SM, Shea AM, Zackai E, Pickens G, Reed RB. Growth charts for children with Down syndrome: 1 month to 18 years of age.
5. Farkas LG¹, Katic MJ, Forrest CR Surface anatomy of the face in Down's syndrome: anthropometric proportion indices in the craniofacial regions. J Craniofac Surg. 2001 Nov;12(6):519-24; discussion 525-6. 988 Jan;81(1):102-10.
6. Ferrario VF, Dellavia C, Zanotti G, Sforza C Soft tissue facial anthropometry in Down syndrome subjects J Craniofac Surg. 2004 May;15(3):528-32.
7. Lissauer T, Clayden Graham, Genetics, Illustrated textbook of paediatrics, Sydney Toronto. Elsevier limited 2003. P.83-97.
8. Lydia Binti Zainal Abidin. Carers experience and Coping strategies with Down's syndrome children. Faculty of medicine and health science. University Malaysia Sarawak. 2010.





Tahamida Yesmin et al.

9. Fuad I. Abbag, Congenital heart diseases and other major anomalies in patients with Down syndrome. Saudi Med J 2006; Vol. 27 (2): 219-222
10. Ivana Bagi} and @eljkoVerzak Craniofacial Anthropometric Analysis in Down's syndrome. Patients Coll. Antropol. 27 Suppl. 2 (2003) 23–30 UDC 572.545:616-056.7
11. SingIP, Bhasin MK. Anthropometry. A laboratory manual of biological Anthropology. Delhi: Kamla Raj Enterprises Publishers; 2004. p 7-26.

Table 1: Range Variation of Cephalic Index

Type	Cephalic Index
1) Hyperdolichocephalic	<70.9
2) Dolichocephalic	72.0-76.9
3) Mesocephalic	77.0-81.9
4) Brachycephalic	82.0-86.4
5) Hyperbrachycephalic	86.5-91.9
6) ultrabrachycephalic	>91

Table 2: Range Variation of Facial Index

Type	Facial Index
1) Hypereuryprosopic	<78.9
2) Euryprosopic	79.0-83.9
3) Mesoprosopic	84.0-87.9
4) Leptoprosopic	88.0-92.4
5) Hyperleptoprosopic	>93.0

Table 3: Range Variation of Hand Index

Type	Hand Index
1) Hyperdolichocheir	<40.9
2) Dolichocheir	41.0-43.9
3) Mesocheir	44-46.9
4) Brachycheir	47-49.9
4) Hyperbrachycheir	>50.0
5) Hyperlepten	>57.0

Table 4: Range Variation of Foot Index

Type	Foot Index
1) Dolichopod	<37.9
2) Mesopod	38.0-40.9
3) Brachypod	>41.0





Tahamida Yesmin et al.

Table 5: Mean and SD of Cephalic index and Facial Index of Downs’s Syndrome Males and Females.

Sex	Cephalic index mean±SD	Cephalic index range	P value	Facial index mean±SD	Facial index range	P value
Male	85.62±5.93	76.47-97.29	>0.05	43.46±7.47	27.32-65.66	>0.05
Female	85.79±3.48	80.00-92.30-		41.32±6.49	25.07-54.14	

Table 6: Distributions of Cephalic Index in Downs’s Syndrome Males and Females.

Type	Cephalic Index	
	Female	Male
1)Hyperdolichocephalic	0	0
2) Dolichocephalic	0	1
3) Mesocephalic	3	6
4) Brachycephalic	4	5
5) Hyperbrachycephalic	10	7
6) ultrabrachycephalic	1	6

Table 7: Distributions of facial index in Downs’s syndrome males and females.

Type	Facial Index	
	Female	Male
1) Hypereuryprosopic	11	9
2) Euryprosopic	6	13
3) Mesoprosopic	1	1
4)Leptoprosopic	1	1
5)Hyperleptoprosopic	0	1

Table 8: Mean and SD of hand index and foot index of Downs’s syndrome males and females.

Sex	Hand index mean±SD	Hand index Range (mm)	P value	Foot index mean±SD	Foot index Range (mm)	P value
Male	48.68±4.16	39-58	>0.05	40.51±4.6	27.99-48	>0.05
Female	51.13±10.32	41-80		42.19±8.23	24.97-69.79	





Tahamida Yesmin et al.

Table 9: Distributions of hand index in Downs's syndrome males and females.

Type	Hand Index	
	Female	Male
1)Hyperdolichocheir	0	1
2) Dolichocheir	3	0
3) Mesocheir	5	3
4) Brachycheir	3	13
4)Hyperbrachycheir	6	6
5) Hyperlepten	2	2

Table 10: Distributions of foot index in Downs's syndrome males and females.

Type	Foot Index	
	Female	Male
1) Dolichopod	3	5
2) Mesopod	9	11
3) Brachypod	7	9





Free Radical Scavenging Activity of Gold Nanoparticles due to Ionizing Radiation Effect

Hammad R.Humud, Rasha Waleed AbdulHadi, Asia H.AI-Mashhadani* and Rana M.Yas

Department of Physics, College of Science, University of Baghdad, Iraq.

Received: 27 Nov 2017

Revised: 18 Dec 2017

Accepted: 04 Jan 2018

*Address for correspondence

Asia H.AI-Mashhadani

Department of Physics,
College of Science, University of Baghdad,
Baghdad, Iraq.

E.mail: assia19662006@yahoo.com



This is an Open Access Journal / article distributed under the terms of the **Creative Commons Attribution License** (CC BY-NC-ND 3.0) which permits unrestricted use, distribution, and reproduction in any medium, provided the original work is properly cited. All rights reserved.

ABSTRACT

In vitro free radical scavenging activity of synthesized gold nanoparticles (AuNPs) by electrical explosion wire (EEW) technique was investigated. In the present study, the synthesis of AuNPs in order to prevent free radical formation and inhibition in water samples due to ionizing radiation effect. UV-visible spectroscopy was used for quantification of AuNPs synthesis. Appearance of optical absorption peak around 526 nm was confirmed the presence of metallic AuNPs. The synthesized AuNPs were characterized with atomic force microscopy (AFM). The in vitro antioxidant properties of AuNPs have been evaluated and these nanoparticles were found to have higher antioxidant capacity and thus can be used as potential radical scavenger against deleterious damages caused by the free radicals..

Keywords: Free radical scavenging, gold nanoparticles, ionizing radiation, DPPH.

INTRODUCTION

Ionizing radiation is a form of energy travelling either as electromagnetic waves (x-rays and gamma rays) or particles (alpha, beta, neutrons etc). They transmit energy to materials they encounter. Faster or heavier particles deliver a harder punch [1]. Ionizing radiation causes damage to living system through a series of molecular events, such as Photoelectric, Compton and Auger effects, depending on the radiation energy. Since the predominant molecule in biological systems is water, it is usually the intermediary of the radical formation and propagation. The major radiation damage is due to the aqueous free radicals, generated by the action of radiation on water. A free radical is an electrically neutral atom with an unshared electron in the orbital position, where the radical is highly reactive [2]. When radiation interacts with target atoms, energy is deposited, resulting in ionization or excitation. The absorption of energy from ionizing radiation produces damage to molecules by direct and indirect actions. For direct action, damage occurs as a result of ionization of atoms on key molecules in the biologic system. This causes inactivation or functional alteration of the molecule. Indirect action involves the production of reactive free radicals whose toxic



**Asia Al-Mashhadani et al.**

damage on the molecule results in a biologic effect [3]. The presence of an unpaired electron results in certain common properties that are shared by most radicals. Many radicals are unstable and highly reactive. They can either donate an electron to or accept an electron from other molecules, therefore behaving as oxidants or reductants[4]. Free radicals attack important macromolecules leading to cell damage and homeostatic disruption. Targets of free radicals include all kinds of molecules in the body. Among them, lipids, nucleic acids, and proteins are the major targets [5]. This damage is often referred as oxidative stress [6] that is defined as an imbalance between production of free radicals and reactive metabolites, and their elimination by protective mechanisms, referred to as antioxidants, which is any molecule capable of stabilizing or deactivating free radicals before they attack cells [7]. An antioxidant may terminate the oxidative potentiality by scavenging the free radical which is generated during oxidation process. To date, large number of natural and synthetic antioxidants has been investigated to inhibit these oxidation reactions. Nowadays it is a growing interest in the development of nanotechnology, the science which deals with the creation, production, characterization and manipulation of materials at the nanoscale [8, 9]. Nano-sized materials, known as nanoparticles, possess unique and improved properties because of their larger surface area to volume ratio and are considered building blocks of nanotechnology to design materials with interesting properties. [10]

The synthesis of noble metal nanoparticles attracts an increasing interest due to their new and different characteristics as compared with those of macroscopic phase, that allow attractive applications in various fields such as antimicrobials, medicine, biotechnology, optics, microelectronics, catalysis, information storage and energy conversion[11]. Among all the known chemical and physical preparation methods, the exploding wire technique is one of the newest and simplest methods for producing metal nanoparticles [12, 13]. The explosion is achieved when a very high current density is applied to a thin metal wire, causing the wire to explode to very small fragments. This process involves wire heating and melting followed by wire evaporation, formation of a high-density core surrounded by low-density ionized corona, coronal compression, and fast expansion of the explosion products [14]. Recently, some progresses have been achieved in the evaluation of antioxidant activity of nano materials [15, 16]. Due to the physicochemical and optoelectronic properties of anisotropic Au nanoparticles, they find potent applications in catalysis [17-19], biosensing [20] and optics [21]. Au and other noble metal nanoparticles exhibit promising catalytic activities for radical scavenging reactions [22]. Among various metal nanoparticles, Au nanoparticles are well-suited for a wide range of biological applications because of its chemical inertness and resistance to surface oxidation [23, 24]. DPPH (2,2-diphenyl-1-picryl-hydrazyl-hydrate) free radical method is an antioxidant assay based on electron-transfer that produces a violet solution in ethanol. This free radical, stable at room temperature, is reduced in the presence of an antioxidant molecule, giving rise to colorless ethanol solution. The use of the DPPH assay provides an easy and rapid way to evaluate antioxidants by spectrophotometry, so it can be useful to assess various products at a time [25]. The DPPH method is rapid, simple, accurate and inexpensive assay for measuring the ability of different compounds to act as free radical scavengers or hydrogen donors, and to evaluate the antioxidant activity of foods and beverages [26].

EXPERIMENTAL DETAILS

Preparation of Gold Nanoparticles

Electrical explosion wire has become one of promising method for synthesis metal nanoparticles because of its simplicity, effectiveness and low cost. Synthesis of nanoparticles in liquid does not need vacuum system. In addition, nanoparticles can synthesize in water without impurities or in any arbitrary solution. In the explosion process, several parameters such as voltage, current pulse, material type and their wire dimension, and the medium in which the explosion is performed these effects the properties of product [27-28]. Gold nanoparticle was produced by electrical explosion wire in deionized water (DIW) as a medium of explosion. A thin gold wire (0.35 mm in diameter, 30 cm in length) was used. Fig.1 shows image of gold colloid, prepared by electrical explosion wire technique with different concentrations.





Determination of Free Radical Scavenging Activity

The free radical scavenging capacity of gold nanoparticles was assayed using the modified DPPH method as reported previously [29]. DPPH (2, 2-diphenyl-1-picrylhydrazyl) is a stable free radical and has been used as a model free radical compound to evaluate the effectiveness of antioxidant. Ethanolic solution of DPPH (0.1 mM) was prepared and incubated at ambient temperature. To prevent free radical formation, AuNPs added to the water samples before and after irradiation process. Different concentrations (0.0234-0.2681g/l) of AuNPs were added, in equal volume, to ethanolic DPPH solution and water sample. The mixture was shaken vigorously and allowed to stand for 30 min in the dark and the absorbance of all samples was monitored around 520 nm. DPPH solution without gold nanoparticles served as the control. The percentage inhibition of DPPH was calculated according to the formula:

$$\% \text{ Inhibition (I\%)} = [(A_c - A_s) / A_c] \times 100$$

Where A_c is the absorbance of irradiated water with DPPH radical samples as a control, and A_s is the absorbance of samples with different concentration of gold nanoparticle.

MATERIAL

DPPH were purchased from Sigma Aldrich by United Tetra Group for Medical and Scientific Supplies / Jordan. Water samples were irradiated by ^{137}Cs gamma source at a dose rate of 0.2 rad / hr.

The synthesized colloidal gold nanoparticles were used with a series of concentrations (0.0234, 0.0671, 0.2043, 0.2459, 0.2681 g/l) which were determined by atomic absorption method.

RESULTS AND DISCUSSION

Characterization of gold Nanoparticles

- Characterization of gold nanoparticles by UV-VIS Spectroscopy: The absorption spectrum of prepared AuNPs was investigated by UV-vis method in the wavelength range of 400–800 nm. Absorption spectrum of AuNPs showed Surface Plasmon Resonance (SPR) absorption peak centered around 526 nm for all samples. Fig.2 shows the absorbance of AuNPs with the increasing of concentration.
- Atomic Force Microscopy (AFM): The morphology and the size of the prepared AuNPs were determined by atomic force microscopy. Fig. 3 shows the AFM images together with histograms of the particles size distribution. It is observed that the particles are nanosized and approximately spherical in shape.

DPPH radical scavenging activity of AuNPs

DPPH is a stable nitrogen-centered free radical, the color of which changes from violet to yellow upon the reduction by either the process of hydrogen or electron donation. Substances which are able to perform this reaction can be considered as antioxidants and, therefore, radical scavengers [30].

In vitro antioxidant activity of AuNPs was investigated by DPPH assay. A series of AuNPs concentrations added to the water samples before and after irradiation in order to evaluate the capacity of AuNPs to prevent free radical formation due to the radiation effect and also inhibition the free radical. The results are summarized in Table (1). In its radical form, DPPH absorbs around 520 nm, and its absorbance decreases upon reduction with an antioxidant. Thus, the radical scavenging activity in the presence of a hydrogen-donating antioxidant can be monitored by a



**Asia AI-Mashhadani et al.**

decrease in the absorbance of DPPH solution as shown in Fig.4. Radical scavenging activities of all samples with AuNPs under study increased with increasing concentration exhibiting its dose dependant manner. Percent of inhibition for DPPH radical scavenging activity is presented in Fig.5. A perusal of the results shows that at concentration 0.2681g/l has maximum percent of inhibition (90.32%).For both cases (increasing of AuNPs before and after irradiation into the water samples) the behavior of absorbance and inhibition is asymmetric but the first has greater efficiency of scavenging free radicals. For the second case, DPPH absorption decreases with AuNPs concentration increasing (Fig.6); accordingly the percentage radical inhibition increases and has maximum value (86.31%) at concentration 0.2681g/l (Fig.7). These results indicate that AuNPs synthesized using EEW exhibit the ability to quench the DPPH radical. The results also suggest that AuNPs are more active and good antioxidants with DPPH free radical scavenging activity.

CONCLUSION

The current study revealed that gold nanoparticles can be synthesized in a simple and effective method that is the Electrical Explosion Wire (EEW), where the results confirmed the nanosize of the synthesized AuNPs.

The free radical scavenging property as measured by DPPH method showed that percentage of inhibition increases with increasing concentrations of synthesized gold nanoparticles. Thus the synthesized AuNPs could play the role of a neoadjuvant antioxidant offering effective protection from free radicals in a wide range of conditions. Therefore the antioxidant behavior of AuNPs makes them useful in therapy of many diseases caused by oxidative stress.

ACKNOWLEDGEMENTS

The authors would like to express their gratitude to Dr. Dawood M. Kadeer for providing the necessary facilities for carrying out the experiment.

REFERENCES

1. Radiation Protection Series Publication No. 18, 2012. IAEA, Radiation Biology, A Handbook for Teachers and Students, Vienna, IAEA-TCS-42, Printed by the IAEA in Austria, 2010.
2. C. K. K. Nair, D. K. Parida, and T. Nomura, "Radio protectors in radiotherapy", J Radiat Res. 42, 21–37, 2001.
3. E. J. Hall and A. J. Giaccia, "Radiobiology for the radiologist", Lippincott Williams and Wilkins, New York, 2006.
4. K. H. Cheesman and T. F. Salter, "An introduction to free radicals chemistry", Br Med Bull, 49, 481-493, 1993.
5. V. Lobo, A. Patil, A. Phatak, and N. Chandra, "Free radicals, antioxidants and functional foods: Impact on human health", Pharmacogn Rev. 4(8), 118–126, 2010.
6. G. Poli, G. Leonarduzzi and F. Biasi, "Oxidative stress and cell signaling", Curr Med Chem.11,1163–82, 2004.
7. E. A. Sisein, "Biochemistry of Free Radicals and Antioxidants", Sch. Acad. J. Biosci. 2(2), 110-118, 2014.
8. M. E. Barbinta Patrascu, A. Cojocariu, L. Tugulea, N. M. Badea, I. Lacatusu, A. Meghea, "Nanostructures with liposomes and carbon nanotubes", J Optoelectron Adv Mater 13(9), 1163-1158, 2011.
9. K.N. Thakkar, S.S. Mhatre, R.Y. Parikh, "Biological synthesis of metallic nanoparticles", Nanomed.Nanotechnol.Biol. Med. 6, 257, 2010.
10. I. R. Bunghez, M. E. Barbinta Patrascu, N. Badea, S. M. Doncea, A. Popescu, R. M. Ion, "Antioxidant silver nanoparticles green synthesized using ornamental plants", J Optoelectron Adv Mater, 14(11), 1016 – 1022, 2012.
11. M. Kalaiselvi, R. Subbaiya and MasilamaniSelvam, "Synthesis and characterization of silver nanoparticles from leaf extract of Partheniumhysterophorus and its anti-bacterial and antioxidant activity", Int.J.Curr.Microbiol.App.Sci, 2,6, 220-227, 2013.





Asia Al-Mashhadani et al.

12. P. Sen, J. Ghosh, Alqudami Abdullah, P. Kumar and Vandana, "Process and Apparatus for Producing Metal Nanoparticles", PCT International Appl. No. PCT/IN2004/000067, International Pub. No. WO 2004/112997, (2003) Indian Patent 840/Del/03, (2005) National Phase Entry in USA (filed).(2004)
13. P. Sen, J. Ghosh, Alqudami Abdullah, P. Kumar and Vandana, "Preparation of Cu, Ag,Fe and Al nanoparticles by the exploding wire technique", Indian Acad. Sci. (Chem. Sci.), 115 ,5 &6,, 499-508,2003.
14. Vandana and P. Sen,"Nanometrescales surface modification in a needle-plate explodingsystem", J. Phys.: Condense. Matter, 17, 5327-5334, 2005
15. M. S. Abdel-Aziz , M. S. Shaheen , A. A. El-Nekeety and M. A. Abdel-Wahhab , " Antioxidant and antibacterial activity of silver nanoparticles biosynthesized using *Chenopodium murale* leaf extract " , J Sau Chem Soc., 18: 356–363, 2014.
16. S. Arun, U. Saraswathi and Singaravelu," Investigation on the free radical scavenging activity of biogenic silver nanoparticle", Int J Pharm Bio Sci, 6(2), 439 – 445, 2015.
17. M. Chirea, , A. Freitas, B. S.Vasile, C.Ghitulica, C. M. Pereira and F. Silva, "Gold nanowire networks: synthesis, characterization, and catalytic activity", *Langmuir*, 27, 3906, 2011.
18. M. H. Rashid, T. K. Mandal,"Template less Synthesis of Polygonal Gold Nanoparticles: An Unsupported and Reusable Catalyst with Superior Activity", *Adv. Funct. Mater.* 18, 2261,2008.
19. R. Isono, T. Yoshimura, K. Esumi, "Preparation of Au/TiO₂ nanocomposites and their catalytic activity for DPPH radical scavenging reaction" *J. Colloid Interface Sci.*, 288, 177, 2005.
20. X.Wang, M. Zou, H. Huang, Y. Ren, , L. Li, X. Yang, N. Li," Gold nanoparticle enhanced fluorescence anisotropy for the assay of single nucleotide polymorphisms (SNPs) based on toehold-mediated strand-displacement reaction", *Biosens. ioelectron.*, 41, 569, 2013.
21. C. L. Nehl, H. Liao, J. H. Hafner,"Optical properties of star-shaped gold nanoparticles". *Nano Lett.*, 6, 683, 2006.
22. K. Esumi, N. Takei and T. Yoshimura, "Antioxidant- Potentiality of Gold–Chitosan Nanocomposites," *Colloids and Surfaces B: Biointerfaces*, 32, 2, 117-123, 2003.
23. P. Prema, S .Thangapandiyan " In-vitro antibacterial activity of gold nanoparticles capped with polysaccharide stabilizing agents", *Int J Pharm Pharm Sci.* 5, 310–314, 2013.
24. D. Pissuwan, C. H. Cortie, S. M.Valenzuela, M. B.Cortie,"Functionalized gold nanoparticles for controlling pathogenic bacteria",*Trends Biotechnol.*28, 207, . 2010.
25. Eugenio José Garcia, TatianeLuizaCadorinOldoni, Severino Matias de Alencar, Alessandra Reis, Alessandro D. Loguercio, Rosa Helena Miranda Grande, " Antioxidant activity by DPPH assay of potential solutions to be applied on bleached teeth", *Braz Dent J*, 23,1, 22-27,2012.
26. G. Marinova and V. Batchvarov,"Evaluation of the methods for determination of the free radical scavenging activity by DPPH", *Bulgarian Journal of Agricultural Science*, 17 (1), 11-24, 2011.
27. R.Das, B. k. Das, R. Shukla, T. Prabaharan and A. Shyam, "Analysis of electrical explosion of wire systems for the production of nanopowders", *Sadhana Indian Academy of Sciences*, 37, 5, 629, 2012.
28. L. H. Bac¹, G. S. Yun¹, J. S. Kim¹, H. S. Choi², and J. C. Kim, "Preparation and Stability of Gold Colloid byElectrical Explosion of Wire in Various Media", *J. Nanosci. Nanotechnol.*, 11, 2, 2011.
29. C. Dipankar, S. Murugan, "The green synthesis, characterization and evaluation of the biological activities of silver nanoparticles synthesized from *Iresine herbstii* leaf aqueous extracts", *ColloidsSurf B*, 98:112–119, 2012.
30. A. A. Dehpour, M.A. Ebrahimzadeh, S. F. Nabavi and S. M. Nabavi, "Antioxidant activity of methanol extract of *Ferula assafoetida* and its essential oil composition", *Grasas Aceites*, 60(4), 405-412, 2009.





Asia Al-Mashhadani et al.

Table 1: Values of DPPH Absorbance and Inhibition % with AuNPs Concentrations.

Water samples	Before irradiation		After irradiation	
	DPPH absorption	Inhibition %	DPPH absorption	Inhibition %
Non irradiated	0.401		0.469	
irradiated	0.496		0.526	
Au nanoparticles concentration g/l				
0.0234	0.326	33.66	0.407	22.62
0.0671	0.247	50.20	0.343	34.79
0.2043	0.174	64.91	0.195	62.93
0.2459	0.085	82.86	0.082	84.41
0.2681	0.048	90.32	0.072	86.31

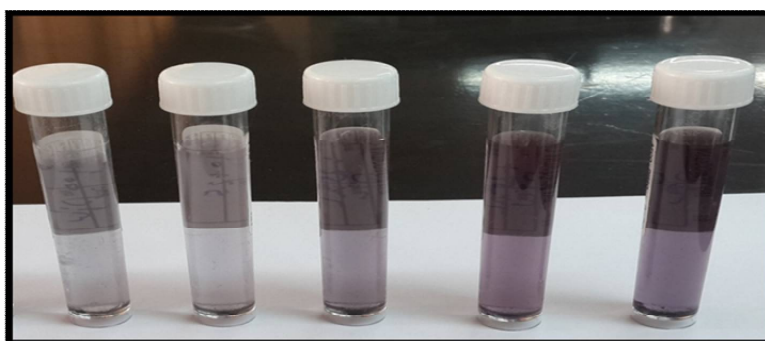


Fig.1: Image of Ag colloid prepared by EEW in DIW

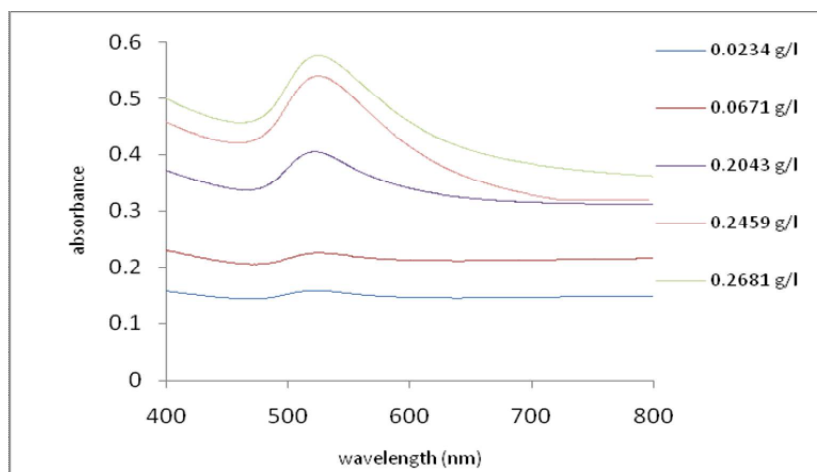


Fig. 2: Absorption of Synthesized AuNPs for Different Concentrations





Asia AI-Mashhadani et al.

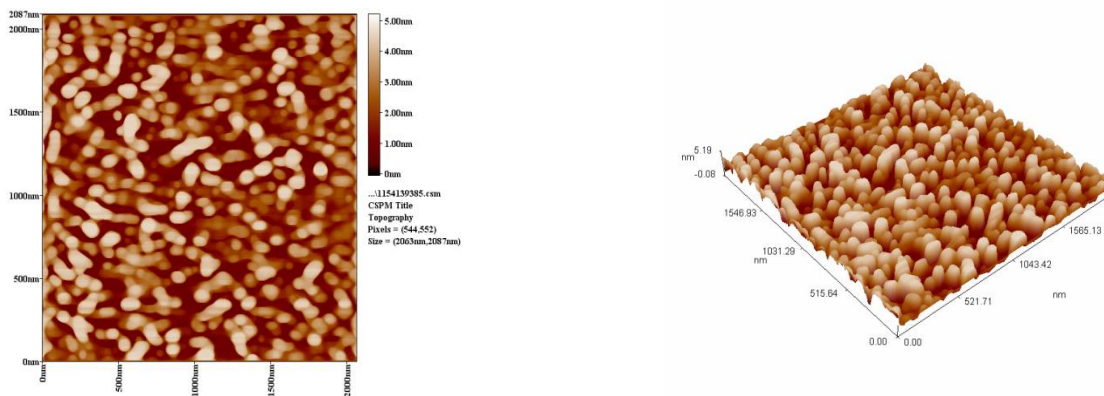
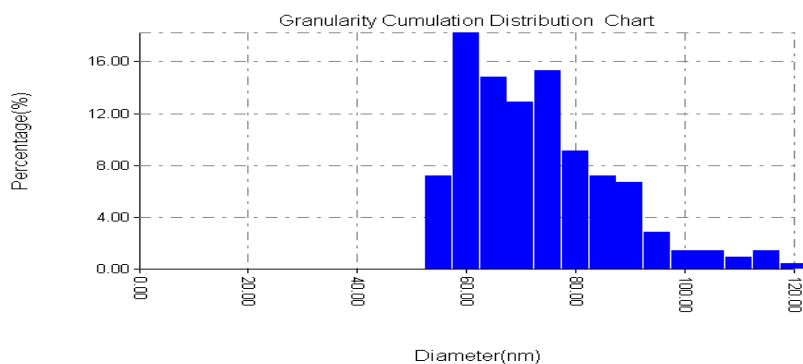


Fig.3: AFM Image (2D and 3D) and Distribution Chart of Synthesis AuNPs.

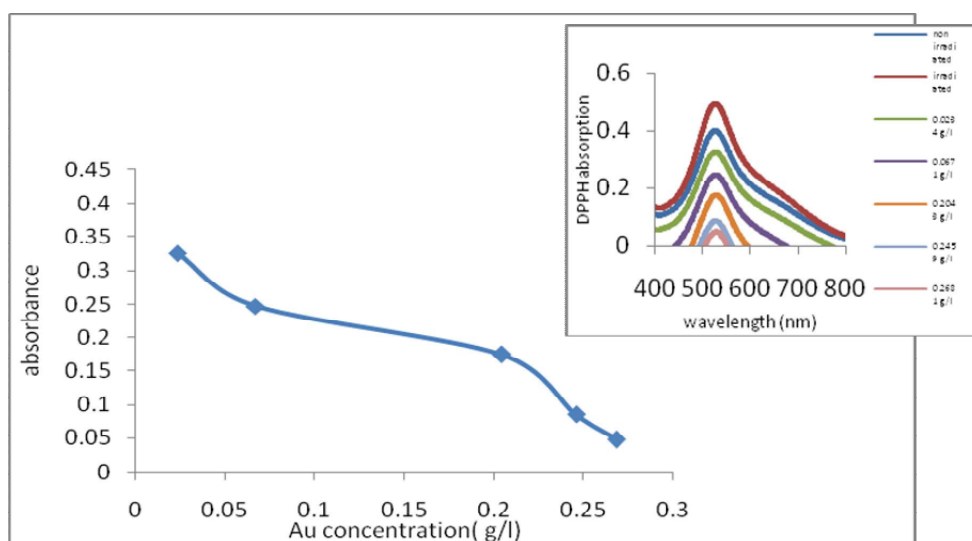


Fig. 4: The Absorbance of DPPH Around 520 nm with different Concentrations before Irradiation.





Asia Al-Mashhadani et al.

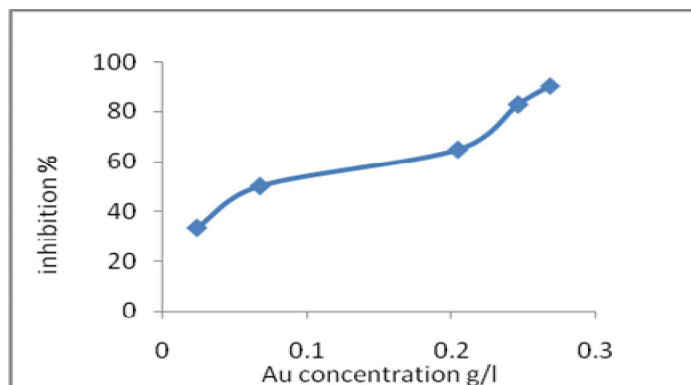


Fig. 5: Free Radical Inhibition% with different Concentration before Irradiation.

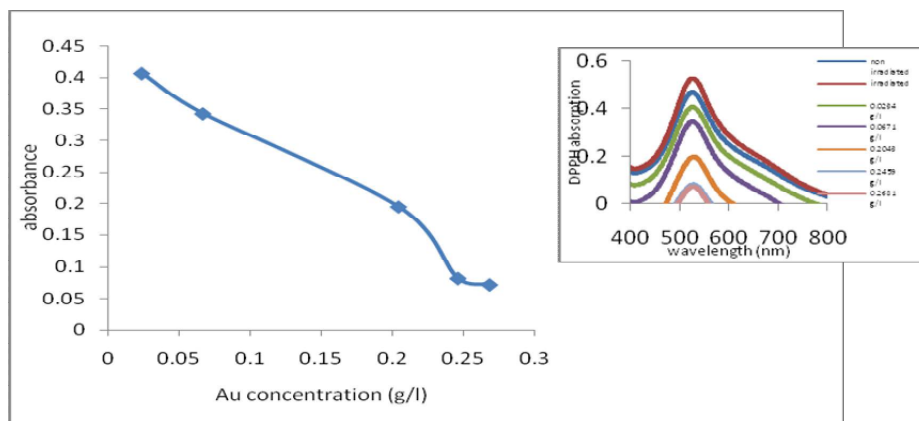


Fig.6: The Absorbance of DPPH around 520 nm with different Concentrations after Irradiation.

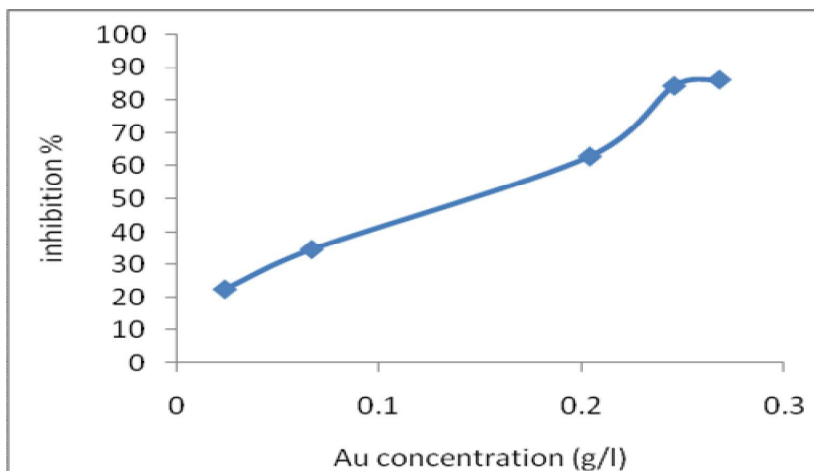


Fig.7: Free Radical Inhibition % with different Concentration after Irradiation.





Inhibition and Recovery of Aquatic Macrophyte *Lemna gibba* Exposed to a Combination Pesticide

Joshua Amarnath Duvvuru¹, Rajini Arjun^{2*}, Satyanarayan Sethi³ and Revathy Kasthuri⁴

¹Professor, Department of Chemical Engineering, Sathyabama Institute of Science and Technology, Chennai – 600119. Tamil Nadu, India.

²Scientist, International Institute of Biotechnology and Toxicology, Padapai- 601 301. Kancheepuram Dist., Tamil Nadu, India.

³Senior Scientist, Fish Culture Division, Central Institute of Brackishwater Aquaculture, CIBA, 75, Santhome High Road, R.A.Puram (ICAR), Chennai 600028. Tamil Nadu, India.

⁴Head, Associate Professor, Department of Advanced Zoology, Ethiraj College, University of Madras, Chennai 600008. Tamil Nadu, India.

Received: 21 Nov 2017

Revised: 13 Dec 2017

Accepted: 08 Jan 2018

* Address for correspondence

Rajini Arjun

Scientist,

International Institute of Biotechnology and Toxicology,

Padapai- 601 301, Kancheepuram Dist., Tamil Nadu, India

E.mail: rajitox@gmail.com



This is an Open Access Journal / article distributed under the terms of the **Creative Commons Attribution License** (CC BY-NC-ND 3.0) which permits unrestricted use, distribution, and reproduction in any medium, provided the original work is properly cited. All rights reserved.

ABSTRACT

Ecotoxicological effects of mixture pesticides are studied less on aquatic plants though they have an important role in environment. *Lemna* sp. is adopted for natural attenuation for both organic and inorganic pollutants and widely studied for their potential application in phytoremediation, waste water treatment facilities and constructed wetlands. The primary objective of this semi-static study is to quantify pesticide related growth inhibition effect to freshwater aquatic plant *Lemna gibba* during 7 days of exposure followed by a 7 days recovery period. It was exposed to Chlorpyrifos 50% + Cypermethrin 5% EC in 20X AAP growth medium. Ten fronds from pre-culture were exposed to a series of 3.1, 6.3, 12.5, 50 and 100 mg/L concentration. Inhibition and yield was found to be reversible during the recovery period in 3.1, 6.3, 12.5 mg/L except 50 and 100 mg/L. Morphological changes such as gibbosity, chlorosis, short roots, broken roots, small fronds and necrosis were observed in 50 and 100 mg/L. Growth rate inhibition and yield in the exposed concentrations was found to be dose dependent. Recovery of *Lemna gibba* exposed to 3.1, 6.3, 12.5 mg/L in medium without pesticide is attributed to its rapid growth rate and its ability to withstand the impact of the pesticide caused by the acute exposure. Phytostatic fronds in 50 and 100 mg/L did not grow during recovery period and it could be due to suppression of cellular activity. Yield $E_{yC_{50}}$ based on frond number and dry weight was 12.19 mg/L and 8.56 mg/L. Growth rate $E_{rC_{50}}$ based on frond number and dry weight was 47.69 mg/L and 14.79 mg/L. Agilent QQQ GC-MS/MS,

13060



**Rajini Arjun et al.**

Electron Impact Ionization mode was used for active content analysis. 13.4 µg/L stock solution of the pesticide was prepared in 20 X AAP growth medium and checked for stability. At 0 hour Chlorpyrifos and Cypermethrin recovery was 90.6%, 82.0% and at 48 hour it was 83.7%, 61.2%. There is no published data related to the mixture toxicity of Organophosphorus and Pyrethroid pesticide to macrophyte *Lemna gibba*. Pesticide mixtures can extirpate the macrophyte thereby affect the biodiversity of the ecosystem. This is the first study to report the combination pesticide toxicity effect to aquatic macrophyte; it contributes to fill the ecotoxicity data gap to determine the potential impact of the pesticide for environmental risk assessment.

Keywords: *Lemna*, Inhibition, Recovery, Growth rate, Combination Pesticide.

INTRODUCTION

Environmental degradation of pesticide mixtures in aquatic ecosystem is a global problem, environmentalist are concerned about the ecosystem health and it is been confronted as a serious issue. It's becoming a major ecological challenge with increasing development for safe disposal of industrial wastewater and drainage. *Lemna* is a free floating freshwater aquatic plant from duckweed family is commonly found in open ponds or shallow wetlands in India. It grows by vegetative reproduction which leads to rapid colonization in water. They are flowering plants and the flowers are tiny and hardly seen without a magnification glass[1]. *Lemna gibba* distribution in India is in Gujarat, Jammu and Kashmir, Punjab and West Bengal [2]. The *Lemna* genus now in the world is 14 and 7 in India [3]. National Wetland Plant List contains 7,937 species in wetland among them *Lemna gibba* is also present [4]. Duckweed utilizes nutrients in waste water to produce large amount of biomass and it grows on waste water consumes the nutrients, cleans the contaminated water, Hence, it is used in environmental studies and in bioremediation of polluted waters, also widely studied for their potential application in phytoremediation [5]. Besides from water treatment *Lemna* also reduces evaporation of water from the surface.

Ducks and water fowls feed on duckweed. It is used as animal feed and during aquaculture the water must not contain too much toxic pesticides run off from agricultural lands. In agriculture often large amounts of fertilizers are sprayed on the soil, a part of fertilizers, pesticides are washed out and contaminate surface and ground water. Duckweeds are considered as one the best feed resource in future for livestock's and fish. Lack of proper effluent treatment facilities and disposal system of wastewater, water bodies are getting polluted causing adverse effects on flora and fauna present in it because of presence of toxic and persistence chemicals [6]. Over time additional use of pesticide may lead to frequent residual detections with aquatic toxicity problems. Stream degradation is a major challenge for ecologists seeking to understand the interactions of stream ecosystems with their catchments [7]. Eventual need for monitoring, mitigation, or reevaluation of a pesticide or class of pesticides is always required. Effect of increased use of synthetic pyrethroids and organophosphate insecticides has replaced many pesticides, leading to subsequent toxicity in surface water and sediments. Chlorpyrifos is a hazardous insecticide and important pollutant of the environment. European Union Directive 2008/105/EC lists it as one of the priority water pollutants and the maximal allowable concentration of chlorpyrifos in water is 0.1µg active ingredient per Litre according to the directive [8]. Pesticides reach aquatic ecosystem by diffuse or point source. Diffuse sources are probably the most important since surface runoff, erosion, leaching and drainage becomes the major pathways for water pollution. Pesticide mixtures can extirpate the macrophyte thereby affect the biodiversity of the ecosystem. The first attempts to use wetland macrophyte for pesticide removal were carried out as early as the 1970's [9]. Cypermethrin usage gradually increased from 1997 as a result of increase in use toxicity concerns of pyrethroids was reevaluated in California¹⁰. Inhibition and recovery of aquatic macrophyte *Lemna gibba* exposed to the pesticide was studied based on OECD 2006, EPA's OCSPP 2012 guidelines [11][12]. Bioassays have gained importance in the last few years and the objective of this study is to observe the phytotoxicity of the pesticide.





Rajini Arjun et al.

MATERIALS AND METHODS

Chlorpyrifos 50% + Cypermethrin 5% EC was purchased from commercial market and *Lemna gibba* obtained from Department of Ecotoxicology, IIBAT. Preculture was inoculated in 20X AAP growth medium and maintained for seven days in growth cabinet with continuous illumination. Inhibition, recovery toxicity assay as per OECD and EPA guideline was conducted. Semi-static exposure was adopted and the test concentrations were prepared by serial dilutions from the freshly prepared pesticide stock and the medium was changed at the end of 48 hour. 160 mL of prepared test solution was transferred into sterile 500 mL glass beaker and 10 fronds were inoculated in each beaker under aseptic conditions. Three replicates per concentration along with six replicates for control were placed randomly and maintained in growth cabinet.

Range finding experiment was performed for 7 days and *Lemna* was exposed semi-statically to 0.00134, 0.0134, 0.134, 1.34 and 13.4 $\mu\text{g/L}$; concentrations, followed by a range of 1, 5, 50, 100 mg/L. Based on the range finding experiment *Lemna gibba* was exposed semi-statically for 7 days to concentrations of 3.1, 6.3, 12.5, 50 and 100 mg/L. pH, temperature and Light intensity (LUX) were analysed using instruments (Eutech pH Testr 30 and Lutron LUX meter LX-101). The number of fronds projecting beyond the edge of the parent frond and their appearance morphological changes and root growth were recorded on 3rd, 5th and 7th day during the experiment (Figure 1).

Dry weight was determined at test beginning from inoculum culture and at test termination from each replicate of the test concentrations and control by drying at 60°C in hot air oven for three days. The doubling time (Td) of frond number was calculated by $Td = \ln 2 / \mu$ (average specific growth). The average specific growth rate for exponentially growing culture (based on frond number and dry weight) were calculated using μ_{i-j} (average specific growth rate from time i to j) = $\ln(N_j) - \ln(N_i) / t$. Where, i is Day 0, j is Day 7 and t is time period from i to j. Percent inhibition in average specific growth rate % Ir = $((\mu_C - \mu_T) / \mu_C) \times 100$. μ_C and μ_T is mean value of average specific growth rate in control and treatment group. The concentration/effect relationship yield based on frond number and dry weight is calculated using Yield from the start of the test to the end of the test $Y_i - j = X_j - X_i$. Where, X_i and X_j is the biomass at time i hour beginning of the test and time j hour at end of the test. Percent reduction in yield % Iy = $[(b_C - b_T) / b_C] \times 100$. b_C and b_T is the final biomass minus starting biomass in the control group and treatment group. Statistical analysis was performed to determine the E_{yC50} (Day 7), E_{rC50} (Day 7) with their 95% confidence limits, NOEC and LOEC values based on frond number and dry weight using software ECOSTATS program version 2012.06.03 [13].

Stability of 13.4 $\mu\text{g/L}$ pesticide stock solution prepared in 20X-AAP medium was analysed using Agilent QQQ GC-MS/MS, Election Impact Ionization mode with Mass Hunter software, USA. Chlorpyrifos and Cypermethrin residues were separated using HP-5 MS fused silica capillary column (30 m length, 0.25 mm internal diameter and 0.25 μm film thickness). Carrier gas was Helium at 1.8 mL/min, Injector and source temperature was 310°C with a split ratio of 1:5. Column temperature was maintained at 70°C. Sample Injection volume was 3.0 μL . Chlorpyrifos and Cypermethrin had a retention time of 11.8 and 24.1 minutes. The residues extracted with 2 x 25 mL of dichloromethane and dichloromethane layer was evaporated by turbopap, the residues were reconstituted with 2 mL hexane was analyzed for active content.

RESULTS

Initial pH of control medium was 7.52 and test concentrations were in the range of 7.51-7.54. Final pH of control was 8.14 and test item concentrations were in the range of 8.26-8.42. During the study, temperature of the growth cabinet was recorded in the range of 23.4-24.2°C and the light intensity was recorded in the range of 6814-7841 LUX.

Ten Fronds were inoculated during the conduct of the experiment in all control and treatment beakers. No inhibition of *Lemna* in control or treatment concentrations of 0.00134, 0.0134, 0.134, 1.34 and 13.4 $\mu\text{g/L}$ was observed and the



**Rajini Arjun et al.**

average growth rate was in the range of 0.469 - 0.472. Hence it was tested with higher concentrations of 1, 5, 50, 100 mg/L and the average growth rate was in the range of 0.466-0.033. Therefore, in the main experiment *Lemna* was exposed to 3.1, 6.3, 12.5, 50 and 100 mg/L and the average growth rate was in the range of 0.472 - 0.061. No morphological changes were observed in fronds exposed to 0.00134, 0.0134, 0.134, 1.34, 13.4 µg/L, 1 mg/L and 5 mg/L. Morphological changes such as gibbosity, chlorosis, short roots, broken roots, small fronds and necrosis were observed in 50 and 100 mg/L (Figure 2).

Validity criteria of the experiment was met since the doubling time (Td) of frond number in the control was 1.96, corresponding to 27.2 fold increase in 7 days with an average growth rate of 0.472 per day. The variation of pH value of the control from test initiation to test end was 1.10 units which is within the limit of 1.5 units as stated in the guideline. The dry weight of *Lemna gibba* inoculum culture was recorded as 2.52 mg at test initiation and at test termination average of six replicates in control was 38.28 mg. The percent inhibition of yield and growth rate based on frond number and dry weight at Day 7 with different concentrations Chlorpyrifos 50% + Cypermethrin 5% EC are presented in Table 1 and statistical analysis Table 2. The statistical analysis was performed using ECOSTATS program version 2012.06.03 (SAS VERSION 9.3, SAS Institute Inc., Cary, NC, USA, 2002-2010) [13].

For the analytical verification, the limit of detection and quantification was 1 µg/L with 0.999 correlation co-efficient for chlorpyrifos and cypermethrin. Linearity range was 1 µg/L to 500 µg/L for chlorpyrifos and cypermethrin. The chlorpyrifos active content in 13.4 µg/L stock at 0 hour and 48 hour was 90.6% and 82.0% and cypermethrin at 0 hour and 48 hour was 83.7% and 61.2%.

DISCUSSION

Environmental degradation of pesticide mixtures in aquatic ecosystem is a global problem, environmentalist are concerned about the ecosystem health and it is been confronted as a serious issue. Agricultural catchments and aquatic ecosystems can experience a pulse exposure to pesticides. *Lemna gibba* is adopted for natural attenuation for both organic and inorganic pollutants and widely studied for their potential application in phytoremediation, waste water treatment facilities and constructed wetlands. Industrial fertilizer factory wastewater and sewage water was found adversely affecting growth of *Lemna minor* with longer periods of exposure it affects the physiological process, thus it leads to death of the plants. Non-target aquatic plants that are not extirpated due to the agricultural run-off or pesticide contaminated industrial waste water may recover if the exposed concentration is less. Pesticide contamination in higher concentrations could have deleterious effect in the aquatic flora. Widely used insecticides in Argentina are chlorpyrifos and cypermethrin and were detected in sediments, suspended particles and water. 226 µg/kg chlorpyrifos and 13.2 µg/kg cypermethrin in stream Brown, Horqueta stream contained 150 and 53 µg/kg chlorpyrifos and cypermethrin in runoff sediments has been reported [14]. Monitoring programs involving samples of water, sediment and aquatic fauna established in selected catchments to assess the validity of predicted migration potential of pesticides during the risk assessment process. Chlorpyrifos and cypermethrin pesticides rated as high risk have been detected in Australia and Philippines sites [15].

Information on the toxicity of herbicides and plant growth regulators to *Lemna* are available but not much work has been done on mixture pesticide. It has been reported that *Lemna minor* could phytotransform some persistent organic pollutants including organophosphorus pesticide Malathion. During the fruiting stage in soy plant increased populations of bugs pose a serious threat, to control synthetic pyrethroid cypermethrin and organophosphate chlorpyrifos is used extensively. In Argentina the National Secretary of Water Resources fixed the levels of water column quality for cypermethrin and chlorpyrifos <0.6 µg/L [16]. Pesticide residues were detected with chlorpyrifos and cypermethrin in all surface soil samples in Philippines which proves the indiscriminate usage of pyrethroid and organophosphate [17]. Growth Recovery of *Lemna gibba* and *Lemna minor* following a 7 day exposure to Diuron herbicide in which recovery has been observed for environmentally relevant concentrations which are considered



**Rajini Arjun et al.**

significant in ecological risk assessment [18]. Nevertheless, it is similar to the combination pesticide recovery though in exposed higher concentrations growth inhibition has been observed. Pesticide contamination has a great impact on the duckweed vegetation and it affects the biomass and yield. Chemical pesticides are largely used in different types of crops all over the world [19]. The onset of recovery of duckweeds is likely due to the reversibility in exposure effects. During the recovery phase except where the toxicity of the pesticide was sufficient to cause effect on the ability to recover within 7 days in all the other treated groups frond multiplication were observed to be normal.

CONCLUSION

The present research work infers that *Lemna gibba* exposure to the pesticide had effects on the macrophyte which is a significant component of biodiversity. While the plant is used effectively in phytoremediation the findings reveals that it can also be used effectively in pesticide bioremediation. This is the first study to report the combination pesticide toxicity effect to aquatic macrophyte; it contributes to fill the ecotoxicity data gap to determine the potential impact of the pesticide for environmental risk assessment.

ACKNOWLEDGEMENTS

The author is thankful to the staff's of Department of Ecotoxicology and Management of International Institute of Biotechnology and Toxicology, Padappai, TamilNadu, India (IIBAT), Padappai for providing research facilities.

CONFLICT OF INTEREST

Potential conflicts of interest none

REFERENCES

1. Klaus J Appenroth, K Sowjanya Sree. Duckweed—a future crop plant for India? 2014; <http://www.internationallemnaassociation.org/uploads/post.jagran>. Accessed on 22.10.2015.
2. Suman Halder, Potharaju Venu. The taxonomy and report of flowering in *Lemna* L. (*Lemnaceae*) in India. Current science. 2012; Vol. 102, No. 12: 1629-1632.
3. Suman Halder, Potharaju Venu. *Lemna landoltii* sp. (*Lemnaceae*) from India. Taiwan. 2013; 58(1): 12–14.
4. Lichvar RW, The National Wetland Plant List: 2013 wetland ratings. Phytoneuron 2013; 49: 1–241. ISSN 2153 733X.
5. Juliet Selvarani A, Padmavathy P, Srinivasan A, Jawahar P. Performance of Duckweed (*Lemna minor*) on different types of wastewater treatment. International Journal of Fisheries and Aquatic Studies. 2015; 2(4): 208-212.
6. Vivek Kumar Singh, Jaswant Singh. Toxicity of industrial wastewater to the aquatic plant *Lemna minor* L. Journal of Environmental Biology. April 2006; 27(2) 385-390.
7. Collins SL, Carpenter SR, Swinton SM, Orenstein DE, Childers DL, Gragson TL, Grimm NB, Grove JM, Harlan S L, Kaye J P. An integrated conceptual framework for long-term social–ecological research. Frontiers in Ecology and the Environment 2010; 9:351–357.
8. Sonja Gvozdenac, Dušanka Inđić and Slavica Vuković. Phytotoxicity of Chlorpyrifos to White Mustard (*Sinapis alba* L.) and Maize (*Zea mays* L.): Potential Indicators of Insecticide Presence in Water. Pestic. Phytomed. 2013; (Belgrade), 28(4), 265–271.
9. Jan Vymazal, Tereza Březinová . The use of constructed wetlands for removal of pesticides from agricultural runoff and drainage: A review. Environment International. 2015; 75 pp 11-20.





Rajini Arjun et al.

10. Kay Lynn Newhart. Summary of New Pesticide Active Ingredient Use Tracking For Field Monitoring In Surface Water. 2013; February 12, 2005-2010. Accessed on 15.08. 2015.
11. Organization for Economic Co-operation and Development. OECD Guidelines for the Testing of Chemicals. *Lemna sp.* Growth Inhibition Test. No. 221; 2006; Adopted: 23rd March. Accessed on 02.02.2015.
12. Aquatic Plant Toxicity Test Using *Lemna* spp. OCSPP 850.4400. <http://www.epa.gov/test-guidelines-pesticides-and-toxic-substances/series-850-ecological-effects-test-guidelines>. 2012; Accessed on 12.01.2015.
13. ECOSTATS program version 2012.06.03. SAS. Version 9.3, SAS Institute Inc., Cary, NC, USA (2002-2010).
14. Jergentz S, Hernan Mugni, Carlos Bonetto, Schulz R. Assessment of insecticide contamination in runoff and stream water of small agricultural streams in the main soybean area of Argentina. Zoological Institute, Technical University, Fasanenstrasse 3, D-38092 Braunschweig, Germany. Chemosphere. 2005; 61(6):817-26.
15. Rai Kookana, Ian Willett. Minimising the off-site impact of pesticides from agricultural systems - a risk based approach, Project ID LWR/2000/084. 2005; <http://aciarc.gov.au> Accessed on 29.10.2015.
16. Walter D. Di Marzio, Maria E Saenz, Jose L, Alberdi, Nicola Fortunato, Veronica Cappello, Clarisa Montivero, Gabriela Ambrini Environmental Impact Of Insecticides Applied On Biotech Soybean Crops In Relation To The Distance From Aquatic Ecosystems. Environmental Toxicology and Chemistry. 2010; Vol. 29, No. 9, pp. 1907–1917.
17. Robert T. Ngidlo. Impacts of Pesticides and Fertilizers on Soil, Tail Water and Groundwater in Three Vegetable Producing Areas in the Cordillera Region, Northern Philippines American Journal of Experimental Agriculture. 2013; 3(4): 780-793.
18. Mitchell Burns, Mark L. Hanson, Ryan S. Prosser, Angus N. Crossan, Ivan R. Kennedy Growth Recovery of *Lemna gibba* and *Lemna minor* Following a 7-Day Exposure to the Herbicide Diuron. Bull Environ Contam Toxicol. 2015; DOI 10.1007/s00128-015-1575-8.
19. Abraham Jayanthi, Mukherjee Prantik, Bose Deyashini, Dutta Ankita Utilization of monocrotophos by *Aspergillus sojae* strain JPDA1 isolated from sugarcane fields of Vellore district in India Research Journal of Pharmacy and Technology 2016, 9(12): 2155 - 2160 Article DOI : 10.5958/0974-36.

Tables 1: Inhibition of Growth rate of *Lemna gibba* on Different Concentrations of Pesticides.

Concentrations (mg/L)	Growth Inhibition rate based on Dry Weight Frond Number		Inhibition of Yield based on Frond Number Dry Weight	
	Ir (%)	Ir (%)	Iy (%)	Iy (%)
Control	-	-	-	-
3.10	2.01	0.99	3.35	5.70
6.30	13.52	14.76	40.08	32.94
12.50	38.23	21.55	52.89	69.21
50.00	77.01	42.45	78.29	93.88
100.00	98.99	87.07	97.97	99.80





Rajini Arjun et al.

Table 2 Yield and growth rate of Lemna gibba on different levels of pesticides.

Parameters	Concentration mg/L	95% LCL mg/L	95% UCL mg/L	NOEC mg/L	LOEC mg/L
Yield based on Frond Number*	E _y C ₅₀ 12.1873	8.91078	16.6685	3.1	6.3
Growth rate based on Frond Number**	E _r C ₅₀ 47.6909	38.8556	56.5263	3.1	6.3
Yield Based on Dry weight#	E _y C ₅₀ 8.56151	6.39780	11.4570	12.5	50
Growth rate Based on Dry weight ##	E _r C ₅₀ 14.7918	12.9576	16.6260	3.1	6.3

*Bruce & Versteeg Weighted model Fit by MARQUARDT for EC₅₀/Dunnnett for NOEC,

**OECD Model 2 Fit by MARQUARDT for EC₅₀/Dunnnett for NOEC, #Hormetic Logistic model Fit by MARQUARDT for EC₅₀/Dunn,s for NOEC (Non-parametric test), ##OECD Model 3 by MARQUARDT for EC₅₀/Dunnnett for NOEC (Parametric test) 19.0X.2016.00437.6.



Figure 1. Lemna gibba plant.

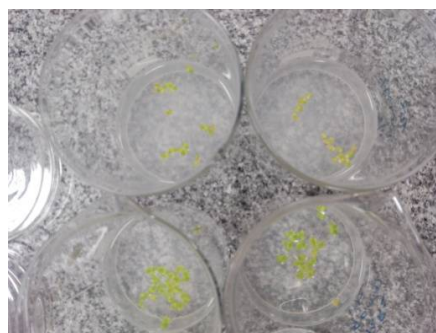


Figure 2. Morphological Changes in Lemna gibba plant





Gallium Nitride Nanocrystal Spectroscopic Properties using Diamondoids Structures

Bilal K. Al-Rawi

Department of Physics, College of Education for Pure Sciences, University of Anbar, Anbar, Iraq.

Received: 23 Nov 2017

Revised: 13 Dec 2017

Accepted: 03 Jan 2018

*Address for correspondence

Bilal K. Al-Rawi

Department of Physics,
College of Education for Pure Sciences,
University of Anbar, Anbar, Iraq.
E.mail: bilal_al_rawi@yahoo.com



This is an Open Access Journal / article distributed under the terms of the **Creative Commons Attribution License (CC BY-NC-ND 3.0)** which permits unrestricted use, distribution, and reproduction in any medium, provided the original work is properly cited. All rights reserved.

ABSTRACT

In the current work, we study the electronic structure, Fourier Transform Infrared (FTIR), and Raman spectra of GaN diamondoids as a function of particle size and shape, using density functional theory (DFT). We calculated the vibrational spectra of GaN and analyzed them with respect to mass, force constant, and intensity of vibration. Since the size and shape of diamondoids vary among the nanoparticles, we compared them using the tetrahedral angles and bond lengths.

The results show that the bond length strongly depends on the shape of the diamondoid molecules. The bond length was also found to increase as the number of cages increased. The total energy as well as the energy gap decrease as the size of nanocrystal clusters increases. These trends might persist at the level of bulk properties because surface effects are negligible in diamondoids.

Keywords: GaN, diamondoids structures, infrared spectroscopy, Raman spectra, nanocrystal cluster, DFT.

INTRODUCTION

GaN is a group III-nitride and a semiconductor [1]. It is a hard compound that exhibits two crystal structures: zinc-blende and wurtzite. In the zinc-blende structure, GaN has a wide band gap of 3.46 eV, which makes it useful for optoelectronic applications such as light-emitting diodes (LEDs) and other light emitting devices [2,3]. In addition, the nanocrystals of GaN are used in nanoscale electronics and biochemical sensing [4]. This is because these nanocrystals help us maneuver many physical properties that are required for electronic devices, such as energy gap and lattice constant. Similarly, the recently discovered higher diamondoids (octamantane) have generated excitement



**Bilal Al-Rawi**

for their potential as nanoscale devices. However, these devices are based on molecular electronics, in which diamondoids are isolated on metal surfaces. The properties of such systems are not yet fully understood [5].

THEORY

We investigated the properties of GaN diamondoids using ab-initio DFT. This method involves full geometrical optimization in accordance with the Hartree-Fock method (HF), which is one of the most accurate methods to simulate the electronic structure and study the optical properties of nanocrystals. Even though this method is computationally expensive, in terms of memory and time, it was feasible at our computational facility [6]. All the calculations of geometrical optimization were executed by combining ab-initio DFT with the generalized gradient approximation (GGA) proposed by Perdew, Burke, and Emzerhof (PBE), in the program Gauss View 5.0 according with Gaussian 09W [7].

To perform these calculations, the basis function 3-21G was chosen so that all the vibrational analyses could be performed at the same theoretical level. Using this program, the stable positions of atoms in the nanocrystal were determined and the vibrational frequencies and Raman lines of GaN nanocrystals were calculated [8].

Diamondoids are carbon nanostructures that have a perfect size and selectable shapes along with passivated hydrogen and sp³-hybridized. Being perfectly size-selectable, they are well suited to investigate the size-dependence of electronic structure, i.e., quantum confinement (QC) effects [9]. To study these effects, using the current method, GaN diamondoids were constructed from the size of a few molecules to the nano region (bottom-up method). At every intermediate size, we calculated the vibrational frequencies to understand their variation as a function of the size of GaN clusters [10].

RESULTS AND DISCUSSION

GaussView 5.0 and Gaussian 09W were used to optimize the geometries and calculate the vibrational spectra of GaN diamondoid nanocrystals (diamantane, tetramantane, hexamantane, and octamantane). The calculated frequency error that results from ab-initio calculations [11].

The present scale factor is one of the nearest scale factors of the unscaled data (very close to 1) and thus was used without modification for all spectra. The geometrical optimization method was used in the present work to obtain the electronic structure of GaN molecules, while the infrared spectrum is shown as a function of frequency (Figure 1). These include cage-like molecules such as diamantane Ga₇N₇H₂₀, tetramantane Ga₁₁N₁₁H₂₈, hexamantane Ga₁₃N₁₃H₃₀, octamantane Ga₂₀N₂₀H₄₂.

Bulk GaN is identified by its IR absorption at approximately 0–700 cm⁻¹ vibrational mode peak [12].

However, the highest intensity line in for GaN diamantane was seen at 706.45 cm⁻¹ while octamantane was seen at 1885.21 cm⁻¹. We noticed a shift in the intensity maxima toward the right side of the infrared vibrational frequencies. This includes the 997–2495 cm⁻¹ modes in the Ga-H and N-H vibrational regions. The region around the broad peak at 706 cm⁻¹ is indicative of Ga–N.

(Figure 2) shows the highest intensity line in the present calculation for GaN diamantane is at 1711.36 cm⁻¹, for tetramantane it is at 1788.96 cm⁻¹ and for hexamantane it is at 1799.79 cm⁻¹ while for octamantane it is at 2288.92 cm⁻¹. A shift in the intensity maxima at about 3500 cm⁻¹ of the Raman vibrational frequencies was noted. This includes the 1543–3489 cm⁻¹ modes in the Ga-H and N-H vibrational regions.





Bilal Al-Rawi

Equation (1) relates the frequency of vibration to the harmonic force constant and reduced mass [13]:

$$\nu = \frac{1}{2\pi} \sqrt{\frac{k}{\mu}} \quad (1)$$

The reduced mass μ of two particles of masses m_a and m_b is given by [14]:

$$\frac{1}{\mu} = \frac{1}{m_a} + \frac{1}{m_b} \quad (2)$$

Although the above equation is for diatomic molecules, it can also be used to explain the vibrational modes of other larger molecules.

Represents the reduced masses of GaN-diamondoid vibrations, the left parts of Ga-N vibrations are larger than the right parts of H vibrations and the right part is nearly equal to 1 shown in (Figure 3). The high reduced mass mode (HRMM) of octamantane is larger than of the other diamondoids.

(Figure 4) shows GaN-diamondoid force constants as a function of vibration frequency. As deduced from a part of the statistical difference between the numbers of vibration frequencies of all GaN-diamondoids, all shapes as shown (Figure 4) are nearly similar and begin from approximately 0 cm^{-1} of Ga-N vibrations and ends at less than 300 cm^{-1} , whereas right parts of H vibrations start at approximately 375 cm^{-1} and ends at nearly 2180 cm^{-1} .

The GaN diamondoid bond lengths generally increase as the number of cages increases with a remarkable dependence on the size of the diamondoid molecules. The experimental bulk of GaN bond lengths (19.5 nm) is inside this distribution range, as shown in (Figure 5).

(Figure 6) shows a comparison between the density of tetrahedral angles in GaN-diamantane and GaN-octamantane. In a piece of bulk far from the surface all tetrahedral angles should have the value 109.47° [15]. As we can see from (Figure 6A) the highest peak of GaN-diamantane is at 106° while that of GaN-octamantane in (Figure 6B) is at 110°. The tetrahedral angle of octamantane is much closer to the ideal value 109.47° than that of diamantane. This is due to the effect of surface reconstruction that has an effect on all the atoms in GaN-diamantane (all the atoms are bonded to surface hydrogen atoms) while it has an effect on some of the atoms in GaN-octamantane.

(Figure 7) shows the tetrahedral angle as a function of the number of cages for GaN. The variation of the tetrahedral angle between atoms starts from gallium hydrogenated surface layer (H-Ga-N angle) and reach the nitride hydrogenated surface layer (Ga-N-H angle) at the opposite face of the nanocrystal. The tetrahedral angles range from 109.47° is compared with the tetrahedral angle if an ideal diamond and zincblende structure. Tetrahedral angles approach the value of bulk as we go to higher diamondoids. This angle takes oscillatory values starting from gallium terminated surface and ending at the nitride terminated surface. The tetrahedral angle of octamantane is much closer to the ideal value 109.47° than that of diamantane.

This is due to the effect of surface reconstruction that has an effect on all the atoms in GaN-diamantane (all the atoms are bonded to surface hydrogen atoms), while it has an effect on some of the atoms in GaN-octamantane.

The dihedral angles should have one of the values -180°, -60°, 60° and 180° in bulk zincblende structure [16]. While this might be true for the angles -180° and 180° in GaN-diamantane in (Figure 8A) it is not completely true for the



**Bilal Al-Rawi**

angles -60° and 60° . For GaN-octamantane (Figure 8B) the situation improves for the angles -60° and 60° that become closer to its ideal value.

The comparison between the pulsed depolarization spectrum in GaN-diamantane and GaN-octamantane shown in Figure 9. GaN is used in a semiconductor for pulsed power applications, switching several megawatts of electrical power in several nanoseconds [17]. As a sensor material, GaN is able to work reliably in conditions where other materials may malfunction.

The energy gap reduces from 3.69 eV in GaN-diamantane to 3.39 eV in GaN-octamantane. This reduction is in compliance with the confinement effects that require size reduction of the energy gap as manifested in (Figure10). The value of energy gap for GaN-experimental is more similar to the bulk value at 3.46 eV.

(Figure11) shows the variation in the total energy with the varying number of GaN atoms. It shows that the total energy decreases with increasing the number of Ga and N atoms. On the scale shown in this figure, the size dependence of the energy is linear.

CONCLUSION

As concluding remarks, we can note that the present theory can adequately reproduce most of the experimental data of infrared vibrational frequencies. This includes the $997\text{--}2495\text{ cm}^{-1}$ modes in the Ga-H and N-H vibrational region. The region of Ga-N mode of vibration is between $0\text{--}700\text{ cm}^{-1}$. The present theory suggests different types of Ga-H and N-H vibrations, which include symmetric, antisymmetric, wagging, scissor, rocking, and twisting modes. It also reproduces the movement of the highest reduced mass of Ga-N of nanocrystals while growing in size.

REFERENCES

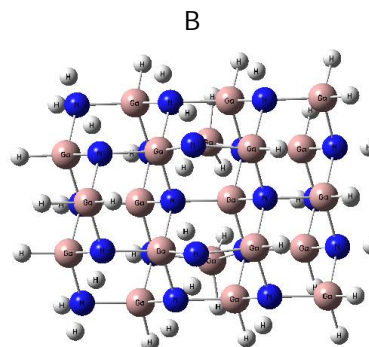
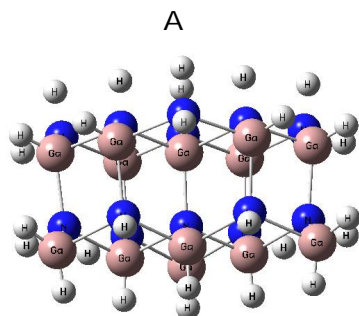
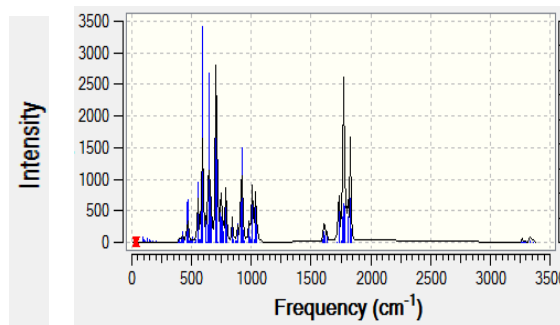
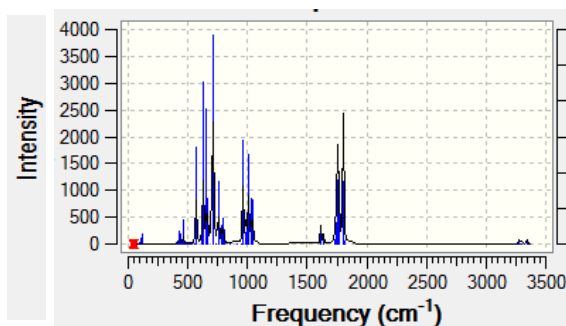
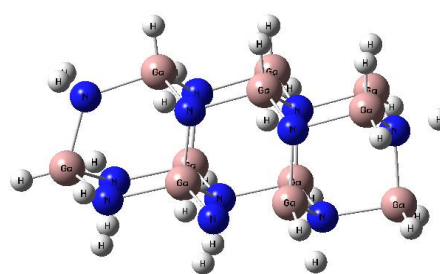
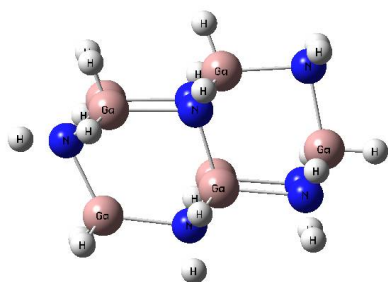
1. S. Strite and H. Morkoç, Journal of Vacuum Science & Technology B: Microelectronics and Nanometer Structures Processing, Measurement, and Phenomena, GaN, AlN, and InN: A review., 1992, Volume 10, Issue 4, 1237.
2. A. I. Hochbaum, R. Chen, R. Diaz Delgado, W. Liang, E. C. Garnett, M. Najarian, A. Majumdar and P. Yang, Enhanced thermoelectric performance of rough silicon nanowires, 2008, PubMed, Nature 451, 163.
3. J. Ristic, E. Calleja, S. Fernandez-Garrido, L. Cerutti, A. Trampert, U. Jahn and K. H. Ploog, J. Cryst, On the mechanisms of spontaneous growth of III-nitride nanocolumns by plasma-assisted molecular beam epitaxy Growth, Journal of Crystal Growth, ELSEVIER, 2008, Volume 310, Issue 18, Pages 4035-4045.
4. R. Koester, J. S. Hwang, C. Durand, D. Le Si Dang and J. Eymery, Self-assembled growth of catalyst-free GaN wires by metal-organic vapour phase epitaxy, PubMed, Nanotechnology 21, 2010, 015602.
5. J. B. Baxtera and E. S. Aydil, Dye-sensitized solar cells based on semiconductor morphologies with ZnO nanowires, Solar Energy Materials and Solar Cells, ELSEVIER, 2006, Volume.90, Issue5, Pages 607-622.
6. J. B. Foresman and A. E. Frisch, Exploring Chemistry with Electronic Structure Methods: A Guide to using Gaussian, Gaussian, 1996, 2nd edition, Gyan Books Pvt. Ltd.
7. M. J. Frisch, G. W. Trucks and H. B. Schlegel, Gaussian 03 Revision B-01, Gaussian, 2003, Inc, Pittsburgh, PA, USA.
8. N.N. Greenwood, Spectroscopic properties of inorganic and organometallic compounds, Royal Society of Chemistry, 1976, Volume 9.
9. Tobias Z. , Robert R. , Andre K. , Andrey A., Tetyana V. , Lesya V. , Pavel A., Peter R., Thomas M. ,1 and Torbjorn R. Exploring covalently bonded diamondoid particles with valence photoelectron spectroscopy, The Journal of Chemical Physics, 2013, Volume 139, Issue 8139.





Bilal Al-Rawi

10. Anil K. Kandalam, Ravindra Pandey, M. A. Blanco, Aurora Costales, J. M. Recio and John M. Newsam, First Principles Study of Polyatomic Clusters of AlN, GaN, and InN. 1. Structure, Stability, Vibrations, and Ionization, *J. Phys. Chem. B* 2000, 104, 2000, 4361-4367.
11. Yuyu Wang, Emmanouil Kioupakis, Xinghua Lu, Daniel Wegner, Ryan Yamachika, Jeremy E. Dahl, Robert M K Carlson, Steven G. Louie, Michael F. Crommie, Spatially resolved electronic and vibronic properties of single diamondoids molecules, *nature materials*, 2008, volume 7 , pp.38-42.
12. T. Azuhata, T. Sota, K. Suzuki, S. Nakamura [*J. of Physics: Condensed Matter*, (UK) 1995, Volume7, p. L129-33].
13. Thornton, Stephen T.; Marion, Jerry B. *Classical Dynamics of Particles and Systems* (5th ed.), 2003, Brooks Cole.
14. J.R. Forshaw, A.G. Smith, *Dynamics and Relativity*, Wiley, 2009.
15. Nasir H N, Abdulsattar M A, Abduljalil H M, Electronic Structure of Hydrogenated and Surface Modified GaAs Nanocrystals: Ab Initio Calculations, *Adv. Condens. Matter*, 2012, Phys., 348-354.
16. Alice Qinhua Zhou, Corey S. O'Hern, Lynne Regan, The Power of Hard-Sphere Models: Explaining Side-Chain Dihedral Angle Distributions of Thr and Val, *Biophysical journal*, 2012, Volume 102, Issue 10, p2345-2352.
17. Aldo Mele, Anna Giardini, Tonia M. Di Palma, Chiara Flamini, Hideo Okabe and Roberto Teghil. Preparation of the group III nitride thin films AlN, GaN, InN by direct and reactive pulsed laser ablation, *International Journal Of Photoenergy*, 2001, Vol.3, p111-121.





Bilal Al-Rawi

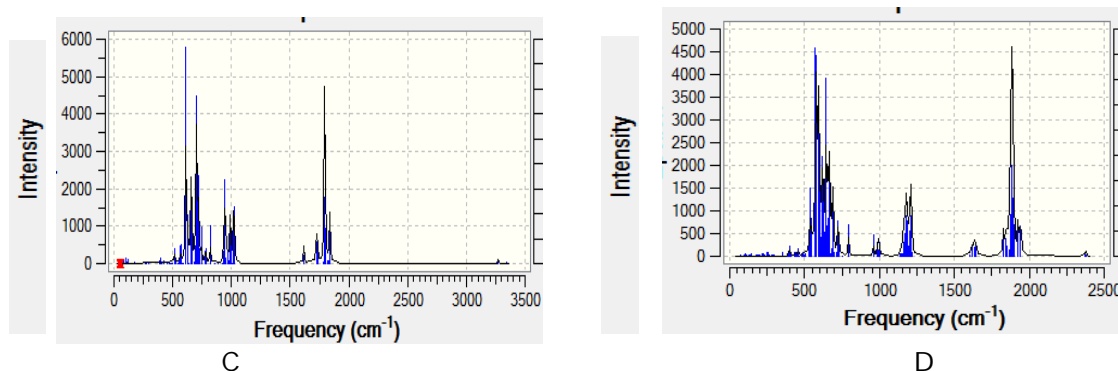


Figure 1: Shape of Geometrically Optimized and IR Spectra of GaN-Diamondoids as a Function of Frequency of :A- Diamantanediamantane $Ga_7N_7H_{20}$ B- Tetramantane $Ga_{11}N_{11}H_{28}$ C- Hexamantane $Ga_{13}N_{13}H_{30}$ D- Octamantane $Ga_{20}N_{20}H_{42}$.

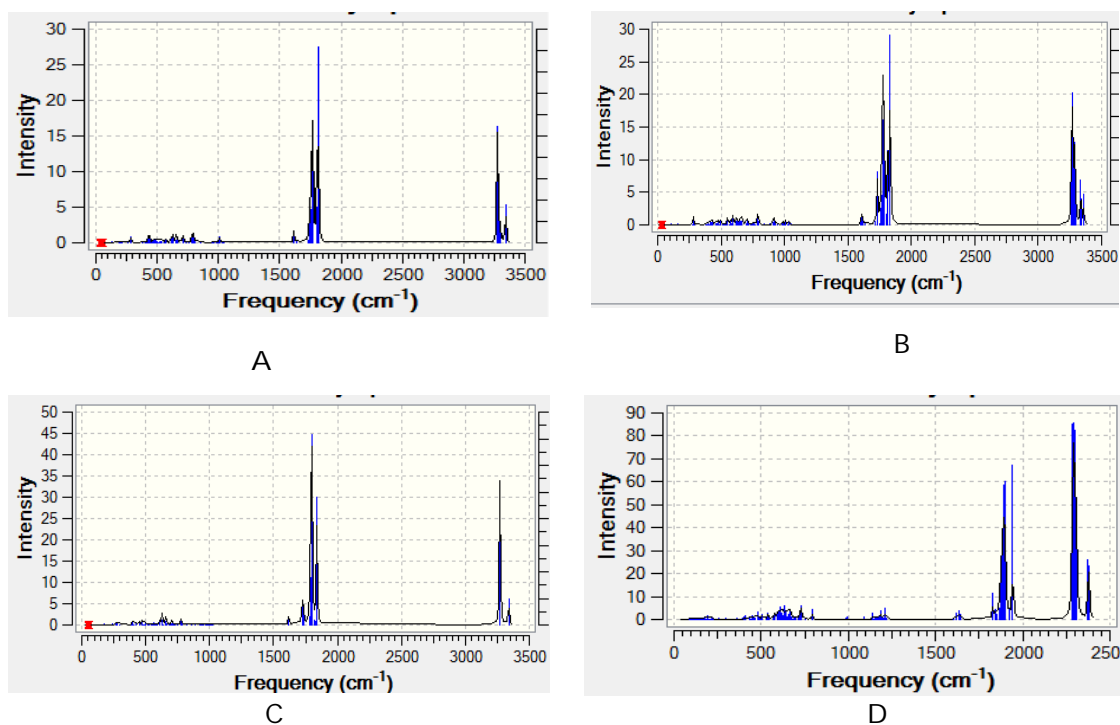


Figure 2: Raman Intensities of GaN-Diamondoids of Infrared Spectrum as a Function of Frequency of A- Diamantanediamantane $Ga_7N_7H_{20}$ B- Tetramantane $Ga_{11}N_{11}H_{28}$ C- Hexamantane $Ga_{13}N_{13}H_{30}$ D- Octamantane $Ga_{20}N_{20}H_{42}$.





Bilal Al-Rawi

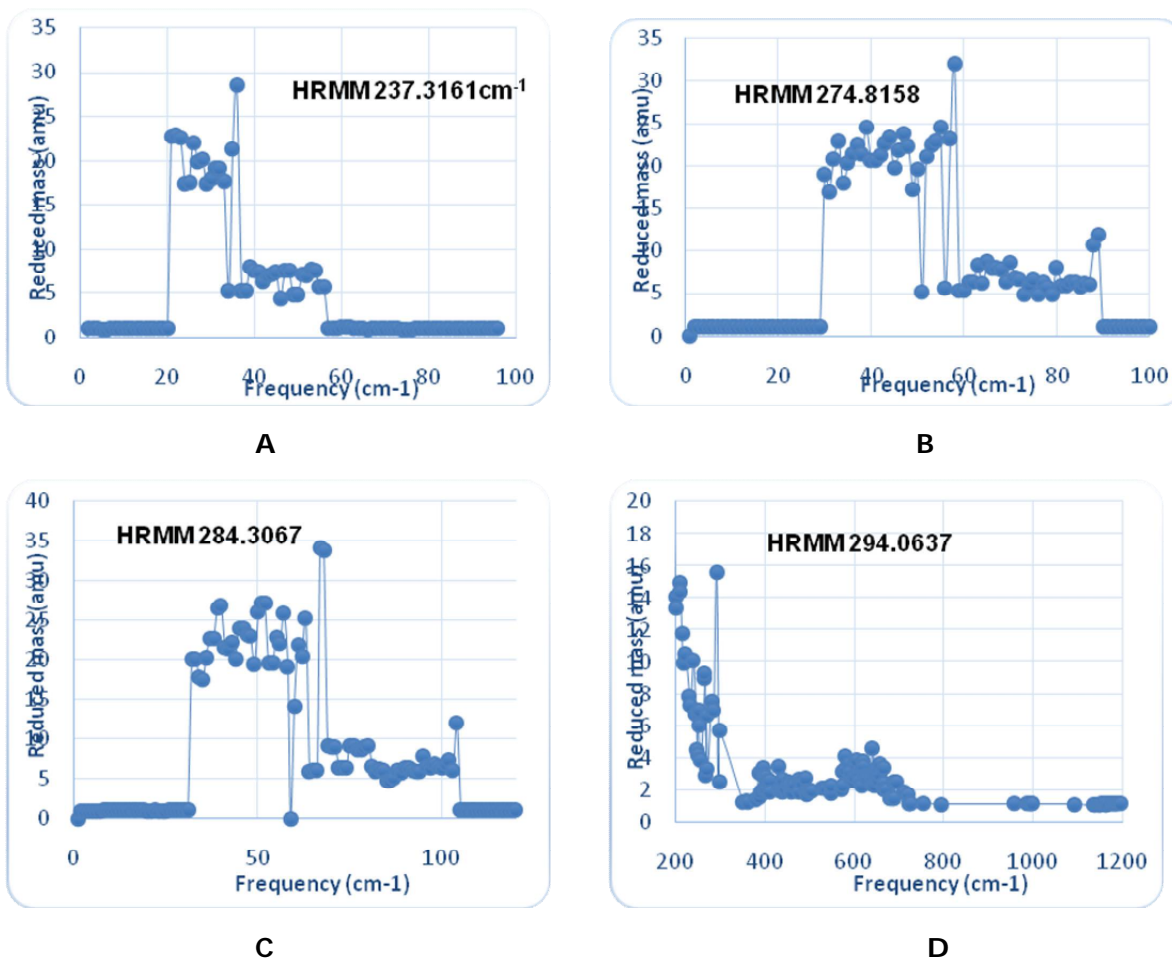
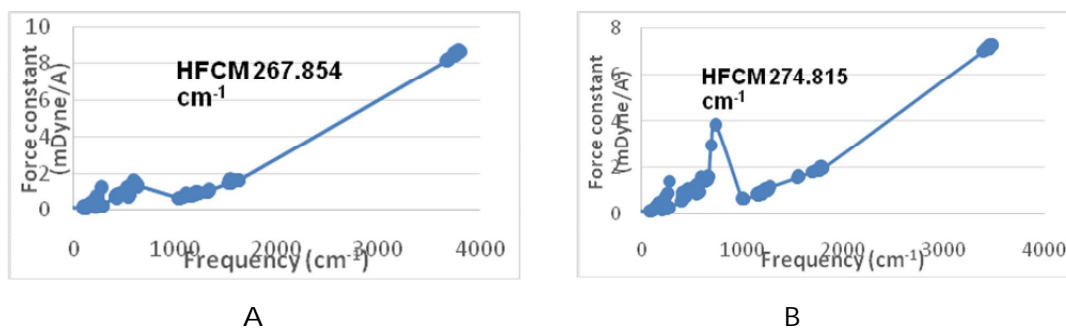


Figure 3: GaN-Diamondoids reduced mass as a function of vibration frequency of A. Diamantanediamantane Ga₇N₇H₂₀ B- Tetramantane Ga₁₁N₁₁H₂₈ C- Hexamantane Ga₁₃N₁₃H₃₀ D- Octamantane Ga₂₀N₂₀H₄₂.





Bilal Al-Rawi

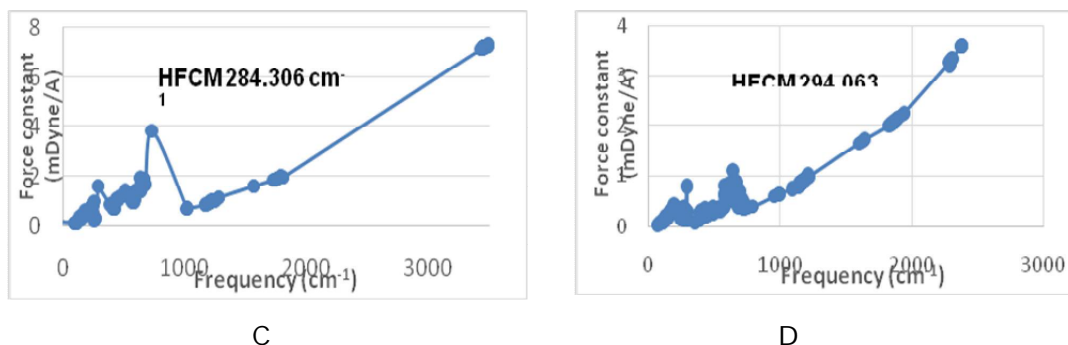


Figure 4: Force Constant of GaN- Diamondoids as a function of frequency of A. Diamantanediamantane $Ga_7N_7H_{20}$ B- Tetramantane $Ga_{11}N_{11}H_{28}$ C- Hexamantane $Ga_{13}N_{13}H_{30}$ D- Octamantane $Ga_{20}N_{20}H_{42}$

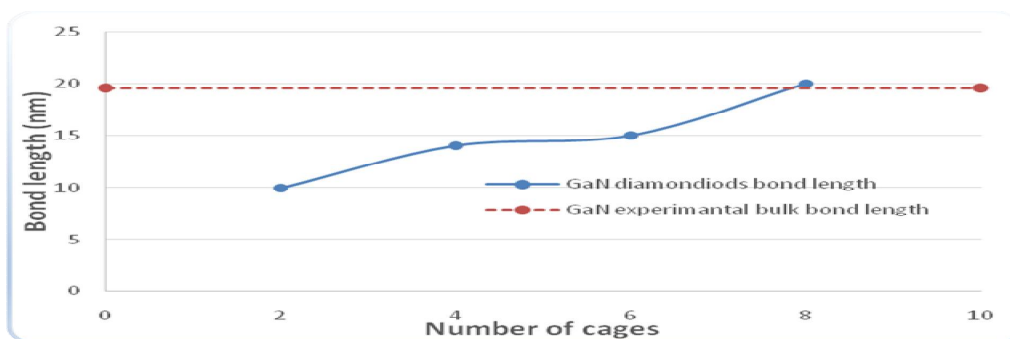


Figure 5: Bond lengths of GaN Diamondoids .PBE/3-21G theory is used for the calculations of this figure. The dashed line represents the experimental bulk value of Ga-N bond length.

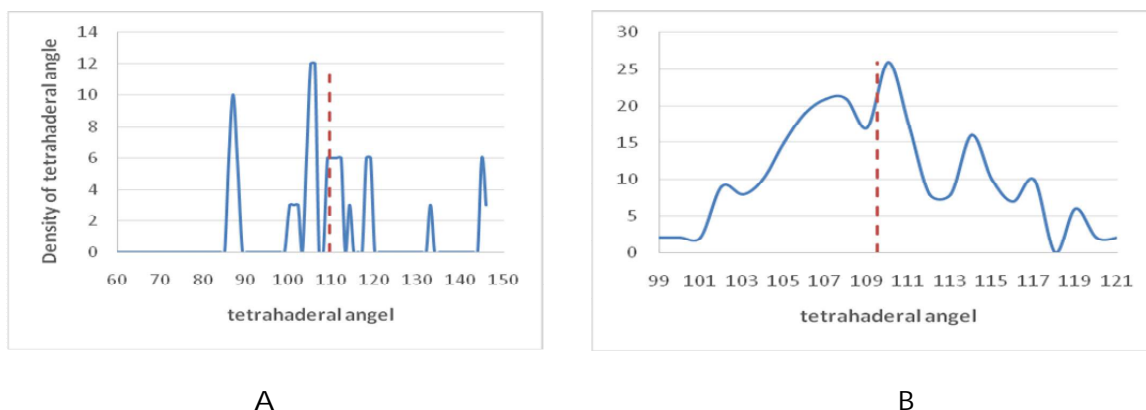


Figure 6: (A) Density of Tetrahedral Angles in GaN-diamantane and (B) Density of Tetrahedral Angles in GaN-octamantane. The dashed line represents the ideal value of Zincblende Structure Experimental at 109.47° [13].





Bilal Al-Rawi

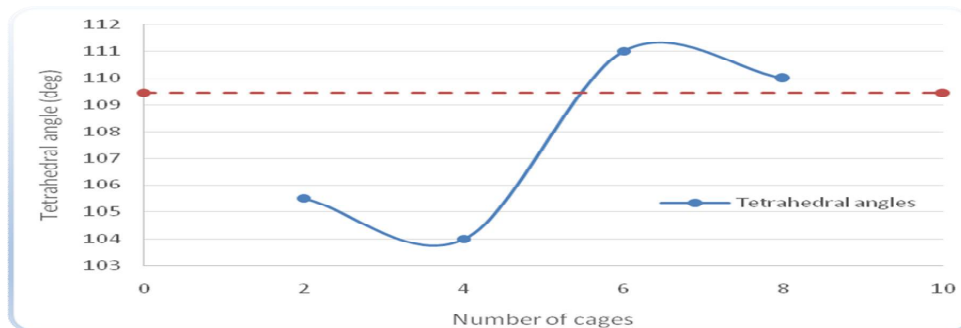


Figure 7: The variation of Tetrahedral Angle as a function of number of cages for GaN. This angle is compared with the Experimental Ideal Diamond and Zincblende Structure Tetrahedral Angle of 109.47°

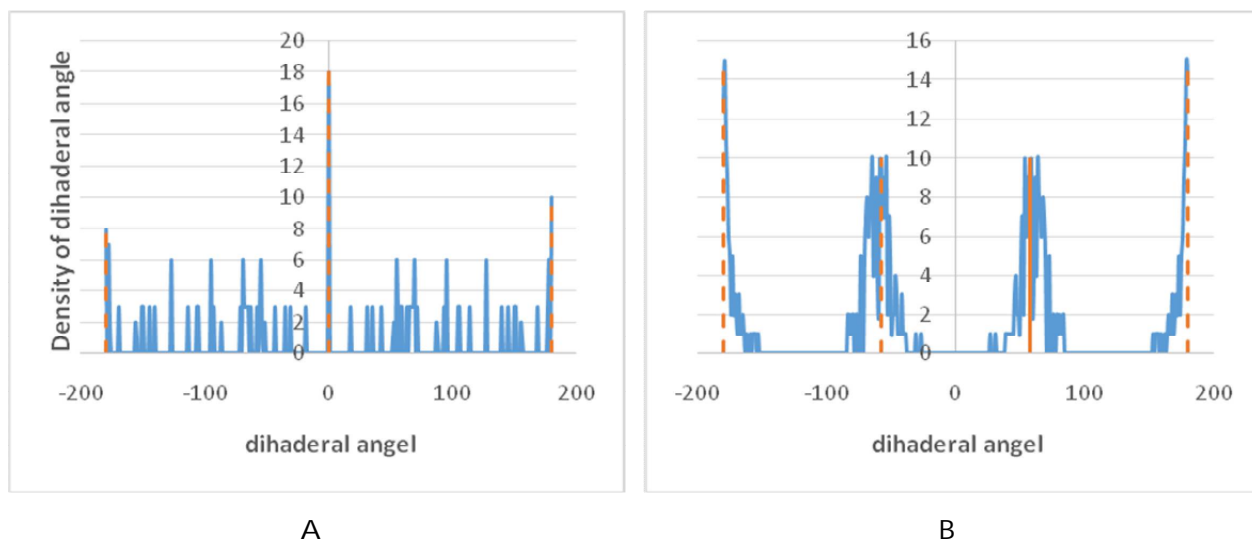
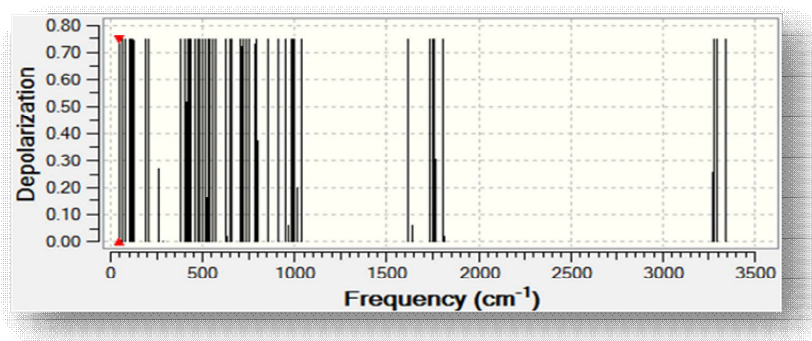


Figure 8: A) Density of Dihedral Angles in GaN-diamantane and B) Density of Dihedral Angles in GaN-Octamantane. Dashed lines show the experimental ideal value of this angle in bulk Zincblende Crystals i.e. $\pm 60^\circ$ or $\pm 180^\circ$ [16].





Bilal Al-Rawi

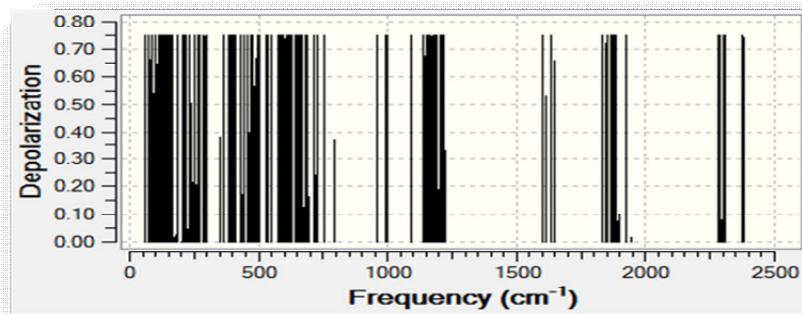


Figure 9: The Comparison between the pulsed Depolarization Spectrums in (a) GaN-Diamantane and (b) GaN-Octamantane.

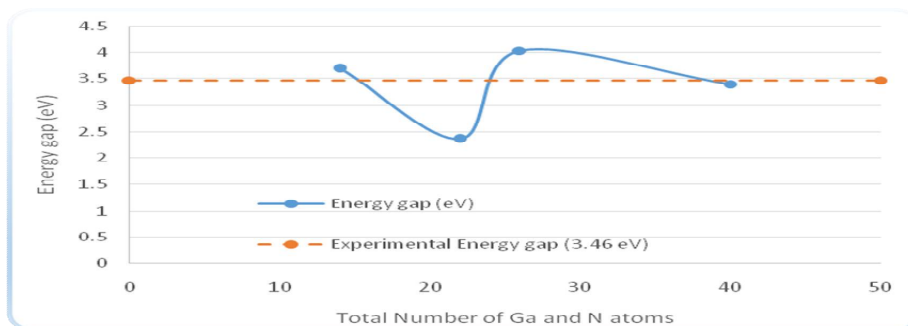


Figure 10: Energy Gap as a function of total number of Ga and N Atoms in GaN Diamondoids. The dashed line represents the experimental value of bulk GaN gap at 3.46 (eV).

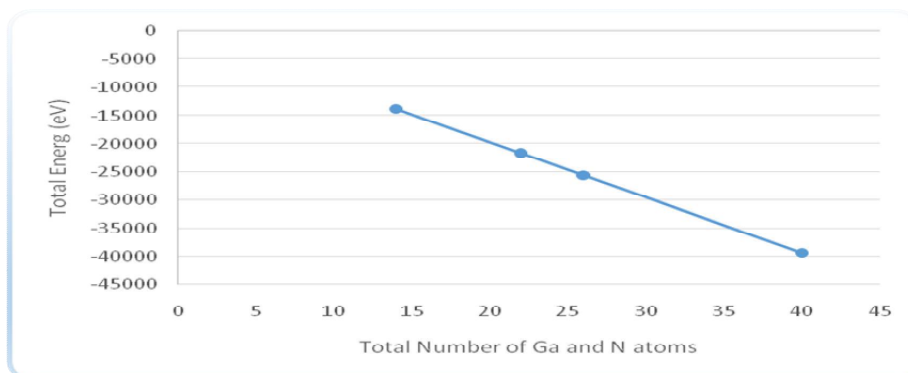


Figure 11: Total energy as a function of total number of Ga and N Atoms in GaN Diamondoids.





Empowerment and Employment Generation among Ksheerasagaram Beneficiaries of Wayanad District

Siddhartha Savale* and R.Senthil Kumar

Department of Veterinary and Animal Husbandry Extension, Kerala Veterinary and Animal Sciences University, Pookode, Wayanad – 673576, Kerala, India.

Received: 07 Aug 2017

Revised: 27 Aug 2017

Accepted: 15 Sep 2017

*Address for correspondence

Siddhartha Savale

Department of Veterinary and Animal Husbandry Extension,
Kerala Veterinary and Animal Sciences University,
Pookode, Wayanad – 673576, Kerala, India.
E.mail: sssiddharth757@gmail.com



This is an Open Access Journal / article distributed under the terms of the **Creative Commons Attribution License** (CC BY-NC-ND 3.0) which permits unrestricted use, distribution, and reproduction in any medium, provided the original work is properly cited. All rights reserved.

ABSTRACT

Kudumbashree has evolved over the past across Kerala into various operating activities and to a varying degree of success. Livestock farming is one among them which has thriven to a better extent. The present study was carried out to analyse the empowerment level of Ksheerasagaram beneficiaries of Wayanad district. Multi stage sampling technique was adopted and data was collected using the personal interview. The total number of beneficiaries selected was 75. Findings revealed that majority of the Ksheerasagaram beneficiaries studied were of middle age, belonging to Hindu religion and unreserved communities. It could also be observed that majority of them were living as nuclear families and size of the family was three to four members. Primary occupation was agriculture and secondary occupation being animal husbandry with above ten years of experience. Land owned by majority of beneficiaries was below one acre with small herd size. There is significant variation in annual income before and after joining SHG. With respect to empowerment majority of the beneficiaries were less empowered and economic empowerment was ranked first followed by informational and technological, psychological and social empowerment.

Keywords: Ksheerasagaram, Empowerment and Kudumbashree.

INTRODUCTION

Women across India and in many other countries have still not been able to gain freedom from injustice. To gain a rightful and dignified status in the society women have to be empowered which will expose their inner strength, capabilities and creativity. Education being a potent tool is empowering women at various circumstances. Women



**Siddhartha Savale and Senthil Kumar**

have also become the change agents by educating and empowering other women about standing for themselves and raising their voice.

Women self help groups are the ones which have evolved as a catalyst and have shattered all barriers of restrictions and have assisted women with all sorts of needs. In the year 1998 in Kerala, Kudumbashree was established to empower women on various dimensions, an institution for promoting self-help group as a tool for women empowerment. Kudumbashree is the poverty eradication and women empowerment programme implemented by the State Poverty Eradication Mission (SPEM) of government of Kerala. Different income generating activities are being carried out by Kudumbashree for women empowerment by training them. Ksheerasagaram i.e. dairy farming is one among such activities where the venture envisages providing loan assistance to members for establishment of dairy farms at subsidised rates. A group of 5-10 beneficiaries submit a loan proposal to the bank and based on the merit of the proposals submitted the bank grants the loan to the beneficiary. An amount at the rate of 33% of the granted loan would be deposited in the loan account of the beneficiary as subsidy by the apex body of the Kudumbashree at the district level. Procurement of animals is from local market and each beneficiary is allotted with two cows. Three months of concentrate feed is provided at start-up of enterprise. Revenue is generated from marketing of milk, calves, dung etc.

MATERIALS AND METHODS

The present study was aimed to analyse empowerment of Ksheerasagaram beneficiaries of Wayanad district. Multi stage sampling procedure was adopted for selection of beneficiaries. Wayanad district was purposively selected for the study which consisted of three taluks namely Vythiri, Mahanantavady and Sultan Bathery. Five groups were selected at random from each taluk. Each group consisted of five beneficiaries. The total sample size was 75 for the present study. For data collection interview schedule was prepared and was subjected to relevancy testing among seven subject matter specialists based on their suggestions the schedule was modified. The interview schedule was pretested by conducting a pilot study among 15 unsampled beneficiaries at Muttill based on results obtained further modifications were done and a well-structured interview schedule was prepared for data collection. The variables for assessing socio-economic profile in the study included age, religion, caste, family type, family size, primary occupation, secondary occupation, experience, land owned and herd size. Empowerment scale was developed to analyse level of empowerment by modifying scale developed by Kavitha, 2005. Data was analysed using simple statistical tools such as Frequency, Percentages, Mean score and Dalenius Hodges cumulative square root frequency.

RESULTS AND DISCUSSION

Graph 1 clearly indicates that there is increase in income after joining SHG when compared to before joining SHG, 61.33 per cent of Ksheerasagaram beneficiaries had an annual total income of below 25,000 rupees followed by 50,000 to one lakh rupees (20.00%), 25,000 to 50,000 rupees (17.33%) and above one lakh rupees (1.33%) before joining SHG. Income after joining SHG has increased to some extent, 36.00 per cent of Ksheerasagaram beneficiaries had an annual total income of below 25,000 rupees followed by 50,000 to one lakh rupees (29.33%), above one lakh rupees (26.67%) and 25,000 to 50,000 rupees (8.00%) after joining SHG. Based on the above findings it could be interpreted that there was a substantial reduction in the proportion of the beneficiaries in the category of annual income below Rs.25000 and they shifted to the annual income of above Rs.25000 categories due to the livestock income generating activities. The movement to higher categories of annual income was remarkable where only just above one-fifth of the respondents were belonging to annual income of Rs.50000 and above before joining the SHGs but later as a result of adoption of dairy farming as an income generating activity more than half of them moved to the annual income categories of after joining the SHG were shifted to the categories belonged to Rs.50000 and above. With regard to



**Siddhartha Savale and Senthil Kumar**

level of empowerment (Table 2) nearly half (45.33%) of had high level of empowerment followed by 26.67 per cent, 14.67 percent and 13.33 per cent with low, very high and very low level of empowerment respectively.

Analysis of dimensions of empowerment (Table 3) revealed that the dairy enterprise brought about a significant economic, information and technological and psychological empowerment. Though social empowerment was also high, as evidenced from high score of that dimension, the strength was relatively low since it was ranked last. The main objective of establishment of Kudumbashree organization was all-round empowerment of the women force through provision of income generating assets. Regular income to the beneficiaries, better marketing infrastructure, better control over productive resources, etc. were supposed to be some of the factors that could be attributed for higher economic empowerment. Further employment generation was analysed as the individual time spent in farming activities per day. The average of number of hours employed in farming activities was calculated for all beneficiaries. Results revealed that the employment generated in Ksheerasagaram was 5.45 hours per day. The time consumed in routine activities in dairy farming was more such as cleaning of sheds and animals, milking, feeding, harvesting and chaffing of green fodder, delivery of milk for marketing, nursing of calves which were done twice a day.

CONCLUSION

The results of the study revealed that majority of Ksheerasagaram beneficiaries had high level of empowerment. Evaluation of empowerment under different dimensions revealed that economic empowerment was higher. Direct involvement in marketing of milk, regular payment directly to the beneficiaries and better control over economic resources could be some of the reasons for higher economic empowerment of Ksheerasagaram beneficiaries. Employment generation was observed higher in Ksheerasagaram as the activities involved in the management of dairy animals for production of milk are more and time consuming. Moreover the degree of successful management would be reflected daily in the form of milk yield and any pitfall would cause immediate economic impact. These factors could have forced the Ksheerasagaram beneficiaries to allot more time for their enterprise.

REFERENCES

1. Bhushan, B., Sudan, R.S. and Sethi, S. 2015. Analysis of socio-economic characteristic of SHG (Self-Help Group) of women associated with dairy farming. *J. Ani. Res.* 5(4).
2. Chethan, G.N. 2014. Impact assessment of the Livestock Development for Livelihood Support Programme in Wayanad district. *M.V.Sc thesis*, Kerala Veterinary and Animal Sciences University, Pookode.
3. Khode, N.V., Sawarkar, S.W., Banthia, V.V., Nande, M.P. and Basunathe, V.K. 2016. Adoption of improved dairy cattle management practices under Vidarbha development programme package. *Ind. Res. J. Ext. Educ.* 9(2): 80-84.
4. Rahman, S. and Gupta, J. 2015. Knowledge and adoption level of improved dairy farming practices of SHG members and non-members in Kamrup district of Assam, India. *Indian J. Ani. Res.* 49(2): 234-240.
5. Rewani, S.K. and Tochwang, L. 2014. Social empowerment of women self help group members engaged in livestock rearing. *Ind. Res. J. Ext. Educ.* 14(2): 116-119.
6. Tajpara, M.M., Chandawat, M.S., Bhorniya, M.F., Bochalya, B.C. and Kalsariya, B.N. 2016. Knowledge level of beneficiaries dairy farmers about recommendations of saus on improved animal husbandry practices. *Int. J. Agri. Sci.* 8(21): 1396-1398.





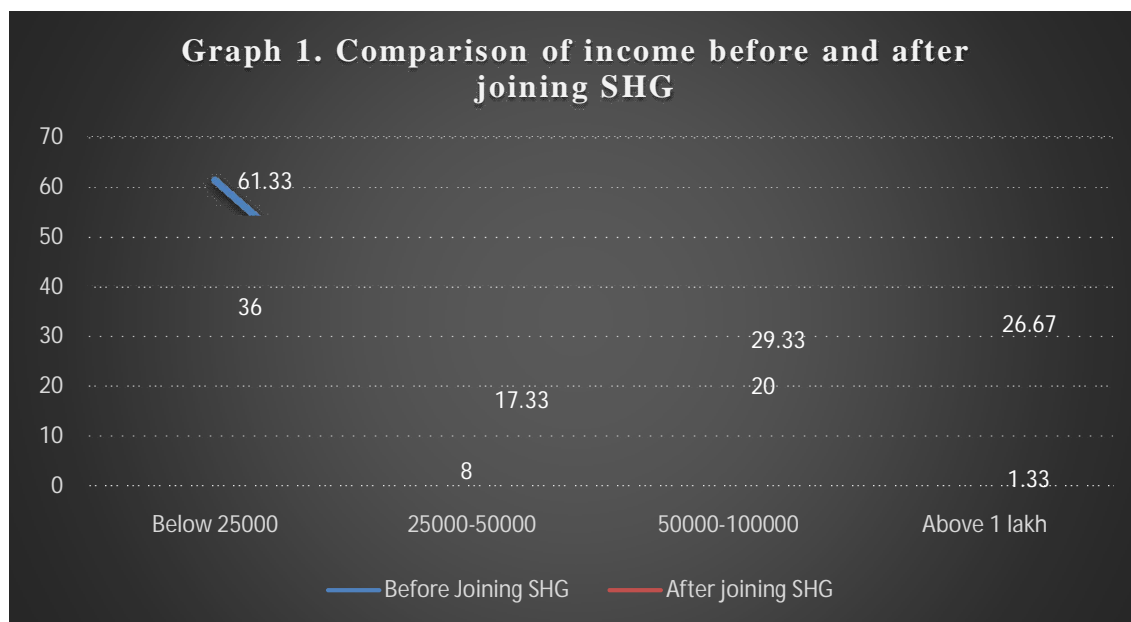
Siddhartha Savale and Senthil Kumar

Table 1. Distribution of Ksheerasagaram beneficiaries based on the level of Empowerment n=75

Empowerment	Frequency	Percentage
Very low (74-90)	10	13.33
Low (90.01-94)	20	26.67
High (94.01-102)	34	45.33
Very high (102.01-108)	11	14.67
Total	75	100

Table 2. Study of different dimensions of Empowerment of Ksheerasagaram beneficiaries.

Sl. No.	Dimensions	Mean score	Rank
1	Economic empowerment	1.87	I
2	Information and technological empowerment	1.85	II
3	Psychological empowerment	1.84	III
4	Social empowerment	1.64	IV





RESEARCH ARTICLE

Assessment PM₁₀, PM_{2.5} and TSP Concentrations Emitted from Cement Factory

Anmar Dherar Kusag

Department of Physics, College of Education for Pure Sciences, Anbar University, Anbar, Iraq.

Received: 29 Nov 2017

Revised: 18 Dec 2017

Accepted: 04 Jan 2018

*Address for correspondence

Anmar Dherar Kusag

Department of Physics,

College of Education for Pure Sciences,

Anbar University, Anbar, Iraq.

E.mail: dr.anmardhr@gmail.com



This is an Open Access Journal / article distributed under the terms of the **Creative Commons Attribution License** (CC BY-NC-ND 3.0) which permits unrestricted use, distribution, and reproduction in any medium, provided the original work is properly cited. All rights reserved.

ABSTRACT

Particulate matter concentrations were measured at different sizes (PM₁, PM_{2.5}, PM₇, PM₁₀ and Total Suspended Particles). Measurements were taken at a total of 39 sites within the case study factory, distributed in areas of suspected emission, including the offices, workers' dormitories, and neighboring residential areas. Pollutants were measured in the vicinity of emission sources so as to monitor their impact on individuals working in these places. In each site 30 samples were collected at various times, amounting to a total of 1170 samples, collected according to specific measuring process. According to the instructions of the National Emission Standards of Activities and Businesses Act no. (3) of 2012, analysis of samples showed that the ratios of excess emissions reached 0%, 56%, 80%, 97%, and 98% for particulate matters at (TSP, PM₁₀, PM₇, PM_{2.5}, PM₁) respectively.

Keywords: particulate matter; cement factories; PM₁₀; PM_{2.5}; TSP.

INTRODUCTION

Cement factories are classified as class "A" in the environmental classification of sources of pollution according to the Environmental Protection and Enhancement Act no (27) in 2009. In the article on environmental instructions for industrial, agricultural, and service projects, class "A" includes large industrial projects, which are expected to cause more environmental pollution [1]. It has been scientifically proven that emissions from this type of industry pose a great threat to human health [2], surrounding environment [3], and infrastructure [4]. Suspended particles that result from breaking, mixing, grinding, burning, and subsequent cooling and packaging of raw materials cause the greatest danger because they contain harmful toxic substances such as carbon compounds, acidic condensates, or metals, including lead, cadmium, sulfurs, and nitrates [5], in addition to the dangers of gaseous and dust emissions of sulfur



**Anmar Dherar Kusag**

oxides, nitrogen, carbon dioxide, cement dust, silicon dioxide, tricalcium silicate, aluminum oxide, ferrous oxide, kaolin and bentonite clays, and calcium sulfite, all expected to be emitted during various processes of production.

Accordingly, if environmental guidelines are ignored, cement production can have tremendous adverse effects on the environment. It was deemed necessary to devote this study to research the effects of emissions from Fallujah Cement Factory, identify their sources, and reveal their potential dangers, due to the large number of workers in the factory and due to its proximity to large residential areas.

AIMS OF STUDY

This study aims to identify emission rates at Fallujah Cement Factory from their various sources, compare them to standard values accepted locally, and identify the sites of excess pollution and their levels, in an effort to limit emissions, in order to protect the health of workers and the neighboring populations, and to preserve a clean and pollutant-free environment inside the factory.

METHOD OF STUDY**The case of Study**

The case of study is Fallujah Cement Factory which located at 33°22'15.97" N longitude and 34°51'06.19" E latitude.

The first production line was operated in 1976, and was increased to two production lines in 1982 after expanding the factory. The total number of workers is currently (555); (530) of whom are males and (25) females. A worker works at the factory 5 days a week, 4 of which on day shifts and 1 on a night shift, averaging 38 hours per week. The factory operates by a dry production line, at a rate that reaches 10,000 tons per month.

Measured Samples

The process of measurement relied on three principal determinants to achieve optimal results at every measurement location, including the type of operating units, their operating durations, which depend on the factory's operating circumstances, and the type of pollutants expected from each unit. Hence, concentrations of emissions were measured at all possible source locations in the factory, in addition to the administrative offices, resting locations for workers, and the surrounding residential areas. Also, the level of pollutants was measured at the vicinity of the sources of emission, in order to register the extent of their effects on the workers present at these specific sites; focusing on areas pertinent to the factory's state of active operation. Measurements were taken at a fixed distance from the sources of emission, 1m away from walls and 2m away from entrances, corners, and intersections, to avoid measuring pollutant levels in concentrated pockets which do not reflect actual conditions.

Accordingly, measurements were performed at 39 sites within Fallujah Cement Factory, as illustrated in figure (1), and 30 specimens were collected at each site, over various times, totaling 1170 samples, in compliance with the conditions and specifications of the aforementioned process of measurement, so as to obtain the best possible results by reducing factors of error.

At each location, the concentrations of different suspended particles of various sizes were measured, including (PM1, PM2.5, PM7, PM10), in addition to measuring the concentration of Total Suspended Particles (TSP) in mg/m³.

An American AEROCET 531 laser particle counter was used in measurement.



**Anmar Dherar Kusag****Analysis of Measured Samples**

Analysis depended mainly on the instructions of the National Emissions Standards of Activities and Businesses no (3) of 2012, since the Fallujah Cement Factory is an establishment of Ministry of Industry and Minerals in Iraq, and it abides by Iraqi laws and guidelines.

Subsequently, after measuring particles of different sizes (PM1, PM2.5, PM7, PM10), and measuring TSP, measured concentrations were compared to the National Emission Standards illustrated in table (1). Statistica 8 was used to graph and analyze results.

RESULTS AND DISCUSSION**Concentration of Suspended Particles of less than 1 μ m (PM1)**

These are the small particles of less than 1 μ m in diameter. They include very small particles of less than 0.1 μ m, which do not precipitate, but assemble with each other, or with larger particles resulting in bigger particles, the majority of which are in the range of PM1. These particles do not constitute great danger to human health, even though they reach the lungs readily, as the lungs are capable of expelling them through exhalation [9].

The Environmental Protection and Enhancement Act did not specify a standard acceptable level for PM1, and only defined levels for PM10 and PM2.5. Thus, we compared the measured PM1 concentrations with the standard acceptable level for PM2.5 which is 0.06mg/m³, given that the standard acceptable concentration for PM2.5 is most certainly greater than that for PM1. Fallujah Cement Factory did not exceed this limit at any of the measured sites, as illustrated in figure (2), and this could be attributed to relatively large granular size of white cement; a factor which reduces the probability of emitting this type of particles.

To demonstrate the extent of impact emission of these particles has on surrounding areas, a contour line was drawn for the emitted particles at all measurement sites. Results showed that despite falling within acceptable limits at all measured sites, the principal source of emission was identified as the rock grinder, the filler factory, and the fuel tanks, as their concentrations fell between 0.0054-0.016mg/m³, whereas emissions lessened at the rotating furnace, the storage houses of rock, clay, and raw materials, and at the offices, gradually declining in concentration until they diminish at the electrical power generator and the mechanic workshop, as clarified by figure (3) and table (2).

Concentration of Suspended Particles of 2.5 μ m (PM2.5)

These are particles suspended in the air with diameters of less than (2.5 μ m), primarily comprised of secondary compounds resulting from the chemical transformation of various gaseous forms, and these particles contain some toxic chemicals which can cause dangerous pulmonary diseases upon entering the human body [9, 10].

The standard concentration limit of particles less than 2.5 μ m according to the law of Environmental Protection and Enhancement is 0.06 mg/m³, and more than half the measurement locations at Fallujah Cement Factory surpassed these levels by ratios of up to 56%, wherein the highest concentration of emissions was 0.507 mg/m³ at the rotating furnace, packaging, cement grinder, cement silos, and mixture storage houses, whereas the lowest concentrations were found at the offices, the mechanic workshop, the electrical power generator, the canteen, reception, and provisioning, which recorded 0.026mg/m³, as illustrated in figure (4) and table (2). This is a very serious indicator that requires the prompt identification of possible industrial flaws within the sources of emission, as well as providing the proper precipitation systems for maintaining the wellbeing of factory workers.



**Anmar Dherar Kusag**

Due to the increasing sources of emission of these particles at all the studied locations, and their overt exceedance of acceptable limits, the impact of these emissions extended onto the surrounding areas, as is shown in figure (5), which demonstrates contour levels of PM_{2.5} concentrations measured at all studied locations.

Concentration of Suspended Particles of less than 7 μ m (PM7)

These are particles of less than (7 μ m) in size, form through mechanical processes, and their composition resembles that of the earth's crust, and they are also emitted upon use of heavy fuel at industrial establishments such as cement factories. These particles have an adverse effect on human health, affecting the pulmonary system and lungs [75, 76].

Since the standard limits for PM7 have not been defined by the Environmental Protection and Enhancement Act as mentioned previously, the standard level of PM₁₀ was adopted as a reference limit, maintaining that relying on local standard limits, albeit approximate, is more appropriate than relying on other standards, taking into account that such local regulations do in fact govern these factories, whereas no substitute binding law exists to legally impel other standards. 80% of all measurement sites in Fallujah Cement Factory exceeded the permissible limits of 0.15 mg/m³, and the highest concentration of PM7 at Fallujah Cement Factory was 9.625 mg/m³, recorded at the rotating furnace, packaging and fuel storage, whereas the lowest level was 0.086 mg/m³, recorded at the filler factory, provisioning, and mixture storage houses, as illustrated in figures (6) and (7), and table (2).

Concentrations of Suspended Particles of Diameters of less than 10 μ m (PM10)

These are particles of less than (10 μ m), and are regarded as the most dangerous to human health [11, 12]. The upper acceptable limit of these particles in the air according to the Iraqi Environmental Protection and Enhancement law is 0.15 mg/m³, however, recordings at Fallujah Cement Factory reached an unprecedented breach of those levels of up to 97%, which indicates that the concentration of these particles exceeded the permissible levels at all measurement sites, including the administrative office buildings, as illustrated in figure (8) and table (2). The plant emits particles that fall in this particular range and are leaked all along the production line as a result of collisions between various factory machines and inadequate number of precipitants to reduce the concentration of these pollutants in the air. With time, these particles precipitate on the ground, inside and outside the factory, as well as on the roads, despite the weekly factory cleaning, and due to their light weight, they return to the air with even the slightest air currents, which constitutes an additional source of emission that is increasingly exacerbated the more it is neglected, exacting its toll on factory workers who are exposed to the highest concentrations and for the longest period of time.

Although there are several sources of emission for these particles, there remain a primary and lesser secondary sources identified at Fallujah Cement Factory, and their contour levels were outlined as illustrated in figure (9). The highest concentration for these particles was found at the packaging and fuel storage areas, reaching (15.23mg/m³), while its lowest concentration was (0.2 mg/m³) at the rock and clay storage areas, as well as at the reception, oil tanks, electrical power generator, mechanic workshop, rock grinder, provisioning and the fire department.

Total Suspended Particles (TSP)

It is the mass concentration of aerosol particles suspended in the air. The maximum permissible level of these particles is 0.25 mg/m³ according to the Iraqi Environmental Protection and Enhancement Act, and they cannot reach the human respiratory system due to the nasal filtration process, nevertheless, the majority of particles are transferred into the mouth as a result of capillary effect, and are swallowed afterwards [78]. Since particles larger than PM₁₀ are far fewer than those which fall below this range, results reached by this study were fairly identical to the results of PM₁₀. Fallujah Cement Factory exceeded the permissible level by 98% as illustrated in figure (10) and table (2).





Anmar Dherar Kusag

After plotting the contour levels shown in figure (11), the highest concentration of these emissions were found at the packaging and fuel storage areas, reaching (19.78mg/m³), whereas their lowest concentration reached (0.2 mg/m³) and was found at the clay and rock storage areas, reception, provisioning area, fuel tanks, mixing storage areas, electrical power generator, mechanic workshop, rock grinder, fire department, and raw material storage houses.

CONCLUSION

After measuring and analyzing 1170 collected specimens from 39 test locations distributed throughout the sites of possible emission of particles at Fallujah Cement Factory, and according to the Instructions of the National Emission Standards of Activities and Businesses Act no. (3) of 2012, it was found that:

- The concentration of suspended particles smaller than 1µm did not exceed the standard limit at any of the measured sites.
- More than half of the measurement sites exceeded the standard concentration limits for suspended particles smaller than 2.5µm in diameter by a ratio of 56%.
- 80% of all measurement sites at Fallujah Cement Factory exceeded the permissible levels for suspended particles of less than 7µm in diameter.
- 97% of the sites measured for concentrations of suspended particles smaller than 10µm exceeded the permissible level.
- Fallujah Cement Factory surpassed the permissible standard limit for TSP by a ratio of 98%.

REFERENCES

1. Republic of Iraq: Environmental Protection and Enhancement Act, Article (A) and as per the law by Iraqi Council of Representatives.
2. Chun, Y. Y. et al. *Enviro. Res.*2003, 92, 64.
3. Marta, S. et al. *Enviro.Res.*2004, 95, 198.
4. Cristina,B. et al.*Enviro.Pollu.*2008, 151.292.
5. Saleh, I.K. *Engen. and tech.* 2007,2,34.
6. Eduardo, Y. et al. *Environ. Sci. Pollut. Res*, 2011, 18. 64.
7. Traversi, D. et al.*Mota. Res.* 2011. 54. 726 .
8. Republic of Iraq: National standard of emissions Act, 2012, No.3.
9. Ahmed M.O. MSc. Department of physics , college of science, almustansiria univ. IRAQ, 2004.
10. Hone,J.C. et al,*Atmo. Enviro.*2012, 54.728.
11. Waleed, M.A., Msc, Faculty of Meteorology, Environment and Arid Land Agriculture, KAU univ., 2009
12. Shahsavani A. et al. *Jour.of Arid Enviro.*2012, 72, 77.

Table (1) demonstrates the maximum permissible limits for air pollutants emitted from stationary sources.

Air Pollutant	Scientific symbol	Upper Accepted Limit µg/m ³
Total Suspended Particles	TSP	250
Total Suspended Particles less than 10µm	PM ₁₀	150
Total Suspended Particles less than 7µm	PM ₇	150
Total Suspended Particles less than 2.5µm	PM _{2.5}	60
Total Suspended Particles less than 1µm	PM ₁	60





Anmar Dherar Kusag

Table (2) Values of measured pollutants at all measurement locations in Fallujah Cement Factory.

Sample No.	PM1	PM2.5	PM7	PM10	TSP
1	0.005467	0.014233	0.0446	0.0928	0.1571
2	0.0043	0.011	1.9934	3.0444	5.0531
3	0.003533	0.6553	3.0348	9.995	13.68863
4	0.014667	0.085933	0.3142	0.9443	1.3591
5	0.006067	0.154767	9.6251	9.9966	19.78253
6	0.006167	0.1545	9.6254	9.996	19.78207
7	0.005167	0.004833	0.0251	0.375	0.4101
8	0.004867	0.0155	0.1846	0.2423	0.447267
9	0.003633	0.053433	0.5342	0.8549	1.446166
10	0.0043	0.036333	0.2848	0.4154	0.740833
11	0.0044	0.0354	0.243	0.3946	0.6774
12	0.0059	0.0361	0.2057	0.2948	0.5425
13	0.005	0.0264	0.1767	0.2546	0.4627
14	0.0057	0.026	0.166	0.2347	0.4324
15	0.0042	0.0236	0.1453	0.2054	0.3785
16	0.006	0.0244	0.1247	0.2361	0.3912
17	0.0055	0.035	0.1755	0.2856	0.5016
18	0.0053	0.0357	0.2249	0.3749	0.6408
19	0	0.0668	1.1562	9.9972	11.2202
20	0.0048	0.1469	4.1443	8.2569	12.5529
21	0.0052	0.031	0.3754	1.64	2.0516
22	0.0054	0.3279	1.6047	1.8666	3.8046
23	0.0163	0.2646	1.9941	2.6483	4.9233
24	0.0153	0.2357	1.7057	2.1645	4.1212
25	0.0046	0.1451	1.0862	1.3065	2.5424
26	0.0052	0.1249	0.8243	1.365	2.3194
27	0.0146	0.156	1.2632	1.7258	3.1596
28	0.0046	0.0652	0.4259	0.6641	1.1598
29	0.0062	0.065	0.4641	0.6054	1.1407
30	0.0046	0.0652	0.4259	0.6641	1.1598
31	0.0058	0.066	0.4654	0.6054	1.1426
32	0.004967	0.0756	0.3187	0.469	0.868267
33	0.004933	0.0756	0.3091	0.4452	0.834833
34	0.004767	0.065	0.4259	0.6635	1.159167
35	0.004967	0.0756	0.334	0.4712	0.885767
36	0.009267	0.035	0.1803	0.2458	0.470367
37	0.0144	0.0244	0.9536	1.4048	2.3972
38	0.0162	0.0652	1.9921	2.9847	5.0582
39	0.0045	0.027867	0.2185	0.2941	0.544967





Anmar Dherar Kusag



Figure (1) Illustrates the location and description of all measurement sites at Fallujah Cement Factory.

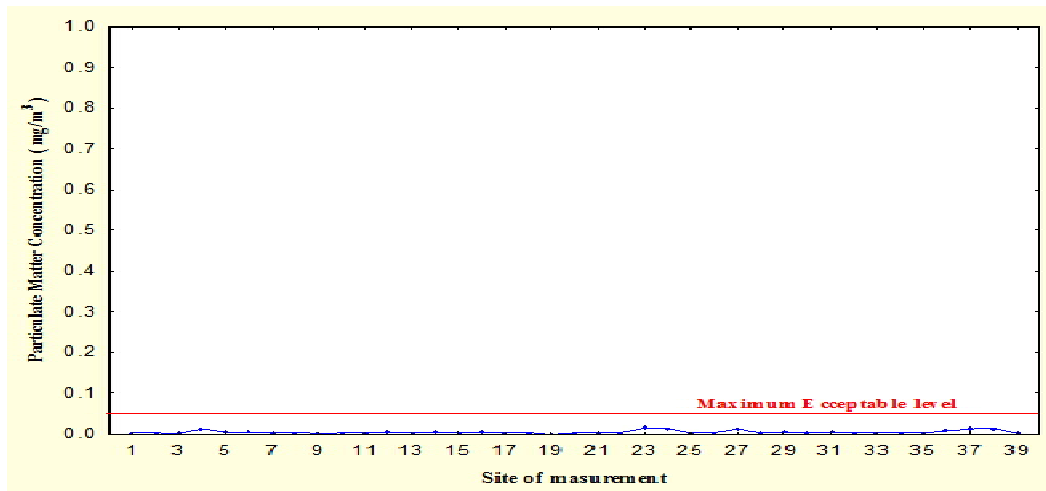


Figure (2) Illustrates the measured concentration levels of PM1 compared to standard limits.

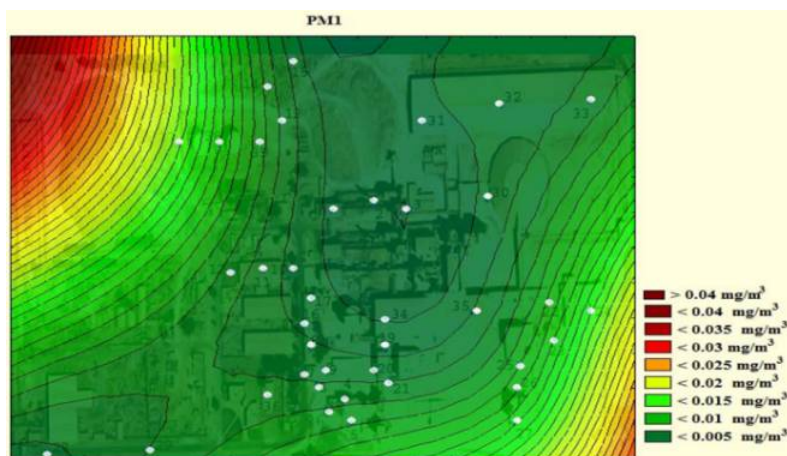


Figure (3) Demonstrates a contour line distribution of PM1 concentrations at Fallujah Cement Factory.





Anmar Dherar Kusag

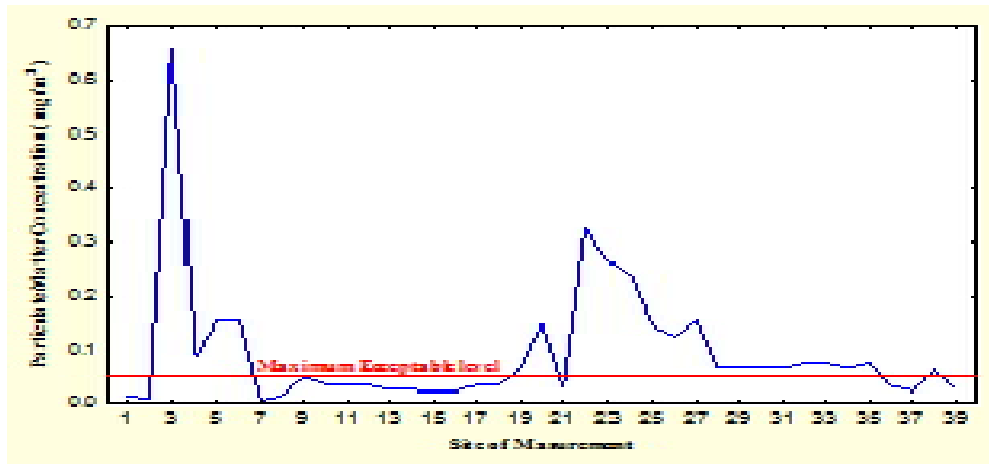


Figure (4) Illustrates the measured concentration level of PM2.5 compared to the standard limit.

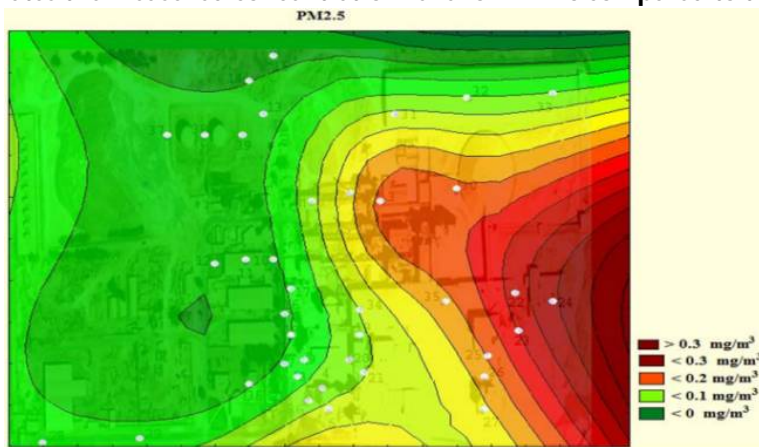


Figure (5) Shows contour distribution of PM2.5 concentration levels at Fallujah Cement Factory.

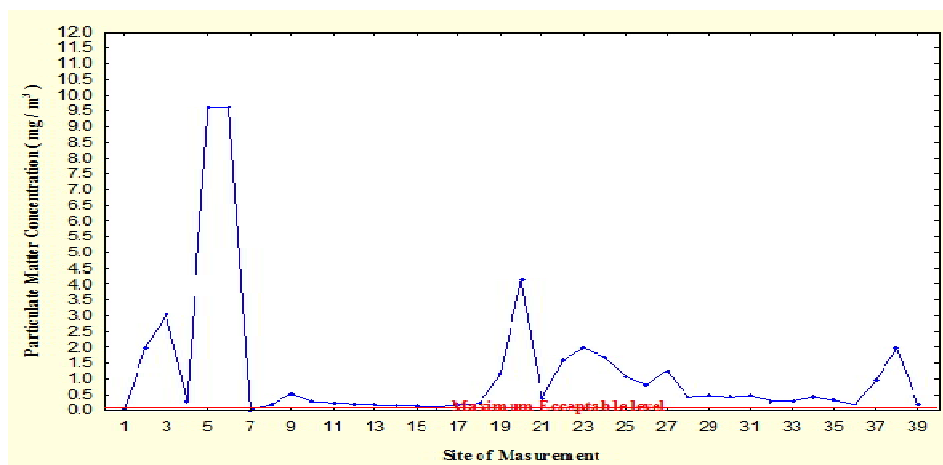


Figure (6) Shows the measured concentration level of PM7 compared to the standard level.





Anmar Dherar Kusag

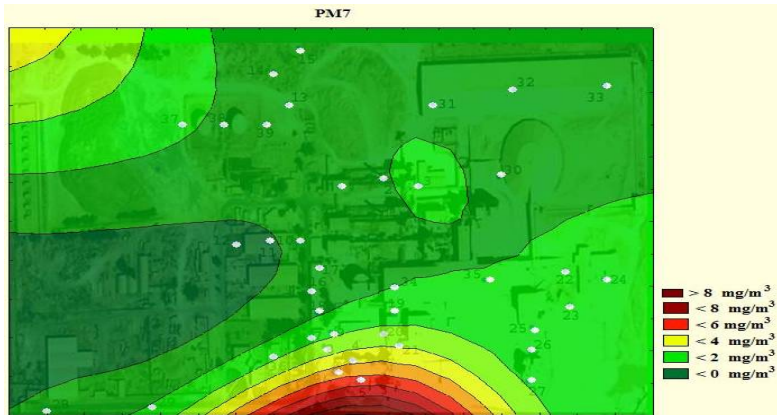


Figure (7) Shows contour distribution of PM7 concentration levels at Fallujah Cement Factory.

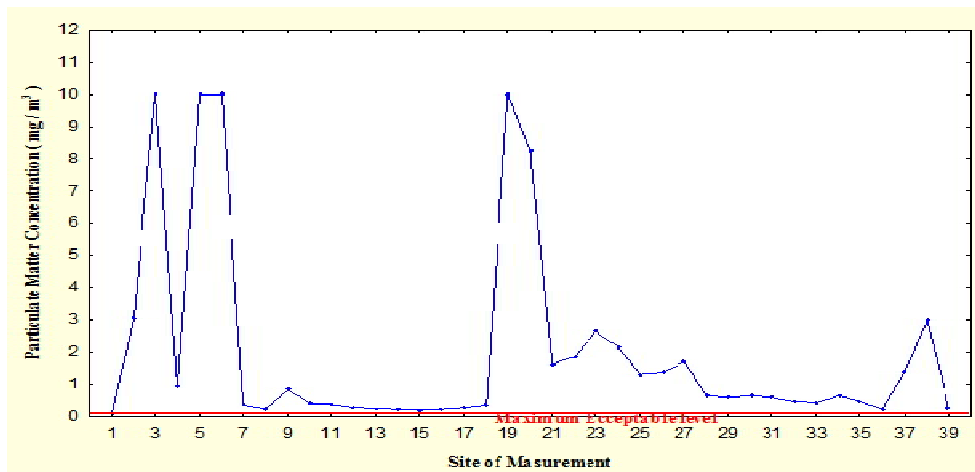


Figure (8) Shows the measured concentration levels of PM10 compared to the standard level.

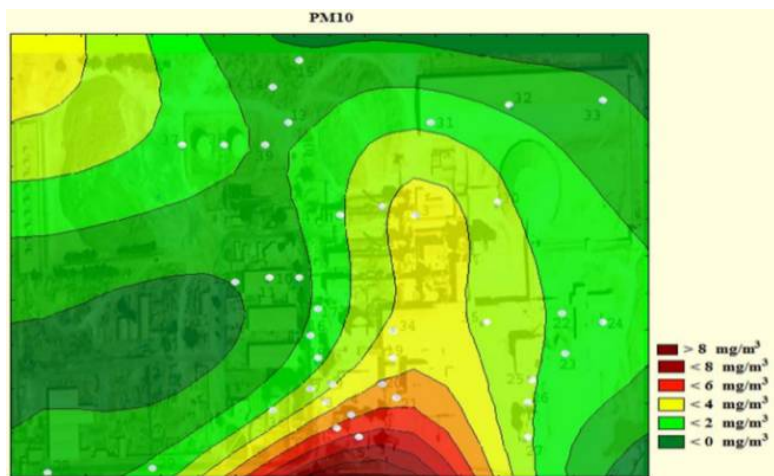


Figure (9) Demonstrates contour distribution for the concentration level of (PM10) at Fallujah Cement Factory.





Anmar Dherar Kusag

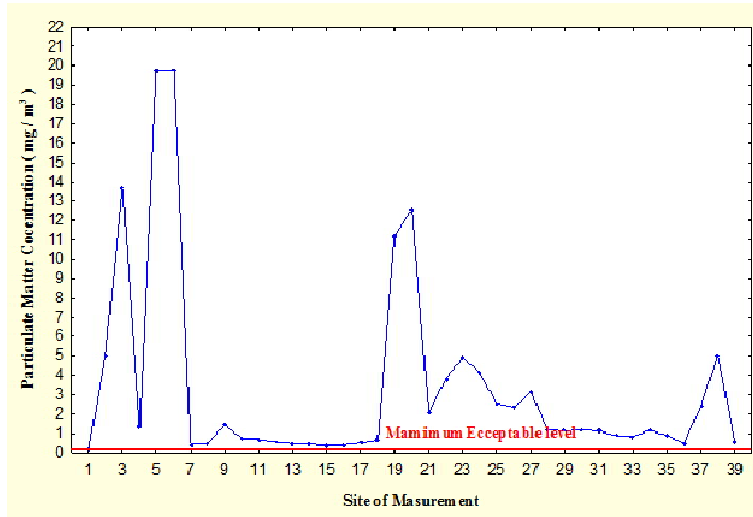


Figure (10) Demonstrates the measured TSP concentration level compared to the standard level.

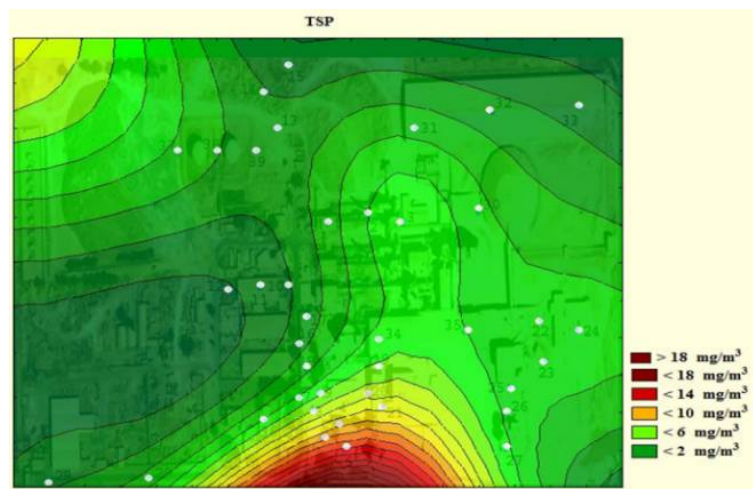


Figure (11) Demonstrates the contour distribution for TSP concentration levels at Fallujah Cement Factory.





Finger Length Ratio in Adults with Stature and Gender

Mar Mar Wai^{1*}, Tahamida Yesmin², Myint Myint Soe³, Fazlin Zaini⁴, Sandheep Sugathan⁵ and Myo Than⁶

¹Senior Lecturer, Department of Anatomy, Faculty of Medicine, University Kuala Lumpur, Royal College of Medicine Perak, Ipoh, Perak, Malaysia.

²Lecturer, Department of Anatomy, Faculty of Medicine, University Kuala Lumpur, Royal College of Medicine Perak, Ipoh, Perak, Malaysia.

³Associate Professor, Department of Public Health, Faculty of Medicine, University Kuala Lumpur, Royal College of Medicine Perak, Ipoh, Perak, Malaysia.

⁴Lecturer, Department of Anatomy, Faculty of Medicine, University Kuala Lumpur, Royal College of Medicine Perak, Malaysia.

⁵Senior Lecturer, Department of Public Health, Faculty of Medicine, University Kuala Lumpur, Royal College of Medicine Perak, Ipoh, Perak, Malaysia.

⁶Professor, Department of Anatomy, Faculty of Medicine, University Kuala Lumpur, Royal College of Medicine Perak, Ipoh, Perak, Malaysia.

Received: 03 Dec 2017

Revised: 21 Dec 2017

Accepted: 17 Jan 2018

*Address for correspondence

Mar Mar Wai

Senior Lecturer, Department of Anatomy,
Faculty of Medicine, University Kuala Lumpur,
Royal College of Medicine Perak,
Ipoh, Perak, Malaysia,
E.mail: dmmwai@gmail.com



This is an Open Access Journal / article distributed under the terms of the **Creative Commons Attribution License** (CC BY-NC-ND 3.0) which permits unrestricted use, distribution, and reproduction in any medium, provided the original work is properly cited. All rights reserved.

ABSTRACT

A personal identification is one of the significant aspects of forensic investigation. Every part of human body has more or less constant relationship with stature. The appendages of the body represent specific relationship to the stature. The length of the index (2D) and ring fingers (4D) are under control of prenatal estrogen and testosterone and their ratio is sexually dimorphic trait and remains fairly stable postnatally. This study is to estimate the correlation between the index finger to ring finger ratio with the stature and gender. This cross-sectional study support that there is positive result with negative correlation between index to ring finger ratio (2D:4D) and height and relationship between 2D:4D ratio with stature and gender. Thus, we can predict height and gender based on 2D:4D ratio.

Keywords: Finger length, Index and ring finger ratio, stature, sex determination.





INTRODUCTION

Age and sex along with stature constitute important criteria for establishing the identity of a human¹. Personal identification either in living individual, dead person or the remains is one of the significant aspects of forensic medicine. Every part of human body has more or less constant relationship with stature². Stature estimation from skeletal remains and body parts is based on the principle that the height of an individual has a definite and linear relationship with various parts of the body and long bones of an individual³. The estimation of stature is more accurate and reliable using long bones than any other parts of the body. The trunk and limbs have their own consistent ratio in relation to human height. The appendages of the body represent certain relationship to the total stature. The stature can be estimated from long bone and its prediction occupies relatively a central position in anthropological research and in identification necessities by medico-legal experts⁴. The ratios between body parts also depend on age, sex and race^{5, 6}, and have been known that men and women have different body proportions². In women the index and ring finger tend to be almost equal in length and in men the ring finger tends to be much longer. Index and ring finger ratios become a significant parameter for determining sex and are related to the amount of testosterone exposure during pregnancy. Higher prenatal testosterone level is associated with shorter index finger in comparison to the ring finger. The ratio of the lengths of the index finger (2D) and the ring finger (4D), 2D:4D is sexually differentiated, where men tend to have lower 2D:4D than women^{4,9}.

This ratio is a popular predictor for various personality and behavioral trait as the growth of the ring finger is promoted by pre-natal testosterone, and index finger is promoted by pre-natal oestrogen⁴ and this ratio is established in utero⁵. Exposure to prenatal androgens is also essential for sexual differentiation and has profound, permanently masculinizing effects on human neural circuitry and peripheral tissues, and health-related human sex differences seen in later postnatal life⁷. A number of studies suggested that 2D:4D ratio is lower in foetus exposed to high level of testosterone and the ratio is higher when the foetus was exposed to high level of oestrogen. A low ratio is considered masculinized, while a high ratio is feminized⁸. Sex differences have been documented from various ratio between different finger lengths and sexual dimorphism is most marked for second and fourth digit ratio⁷. Personal identification is an integral part of the investigation in cases of crimes or disasters where disintegrated and amputated body organs are found very frequently. Estimating stature from various parameters based on the above mentioned evidences become one of the most important and essential exercise for personal identification. The purpose of this study is to find the correlation between the index and ring finger ratio to the gender and stature of an individual that will provide relevant information for further investigation in forensic field

MATERIAL AND METHODS

It was the cross-sectional study conducted on 150 healthy students (75 male and 75 female) age between 19- 23 years in UniKL RCMP, Ipoh, Perak, Malaysia.

Length of the fingers was measured as the linear distance from the flexion crease at the base of the finger to the tip of the finger by using sliding caliper.

Length of the index finger (IFL): 2D in mm

The distance between the mid-point of the proximal most flexion crease at the base of the index finger and the tip of the finger in the midline on the palmar surface.



**Mar Mar Wai et al.****Length of the ring finger (RFL): 4D in mm**

The distance between the mid-point of the proximal most flexion crease at the base of the ring finger and tip of the finger in the midline on the palmar surface.

Height

It was measured as vertical distance from the vertex to the floor by stadiometer with the head of the subject held in the Frankfurt Horizontal plane. The subject was bare footed during the measurement. Height of the stature was taken in term of cm.

Ethical consideration

Ethical approval was obtained from the University ethical committee and informed consent of the students were taken for the measurements. Students who did not consent and those with poorly defined wrist creases, deformities of the vertebral column and limbs were excluded.

Data Entry and Data Analysis

The data were tabulated and entered into Microsoft Office Excel 2010 and then transferred into Statistical Package for Social Sciences software (SPSS, version 23) for statistical analysis.

DISCUSSION

The results of our study showed that index to ring finger ratio (2D:4D) was lower in male when compared to female. It was found to have (0.977) in female and (0.958) in male for right hand while for the left hand is (0.984) for female and (0.963) for male. The mean index to ring finger ratio (2D:4D) in males was significantly lower than females in both hands. The p value was <0.005 . Our findings were comparable to observations in other studies^{4,9} where on average males showed lower digit ratios (2D:4D) than female, based on the fact that increased prenatal testosterone exposure in male the ring finger tend to be much longer than the index finger. In female, the index and ring fingers tend to be almost equal in length, thus the index and ring finger ratio becomes a significant parameter for sex determination². Women usually show higher 2D:4D than men¹⁰. High prenatal testosterone level that was responsible for masculinization, whereas decreased levels are assumed to feminize a foetus¹¹. Thus the 2nd to 4th finger length ratio (2D:4D) showed strong correlation with sexual dimorphism. Furthermore, prenatal testosterone might play a crucial role in the differentiation of the brain and adult sexual orientation¹². In our research, the Pearson correlation coefficient (r) between height and index to ring finger ratio (2D:4D) of the right hand show negative correlation (-0.212) and is statistically significant (0.009) whereas for the left hand also show negative correlation (-0.114) but it is statistically not significant. This finding is consistent with Ibegbu^{13,14}, who reported that correlation between stature and 2D:4D ratio in a Nigerian ethnic tribe was not statistically significant. From the scattered plot graph of the right hand, the R^2 linear is 0.045 which means that 4.5% prediction of relationship between height and index to ring finger ratio can be made while for the left hand, the R^2 linear is 0.013 which means that 1.3% prediction can be made.

CONCLUSION

It can be suggested that the ratio of index finger and ring finger length (2D:4D) is a useful parameter in estimation for sex determination that can predict height and gender.



**Mar Mar Wai et al.**

ACKNOWLEDGMENTS

I would like to take this opportunity to express my heartfelt thanks to the authority of the UniKL for the support and cooperation by providing the grant of STRG and to students who participate in this research.

REFERENCES

1. Rastogi P, Kanchan T, Menezes RG, Yoganarasimha K. (2009) Middle finger length – a predictor of stature in the Indian population. *Med Sci Law*; 49: 123-6
2. Manning, J. T., Scutt, D., Wilson, J., & Lewis-Jones, D. I. (1998). The ratio of 2nd to 4th digit length: A predictor of sperm numbers and concentrations of testosterone, luteinizing hormone and oestrogen. *Human Reproduction*, 13, 3000–3004.
3. K. Krishan et al. (2012). Estimation of stature from index and ring finger length in a North Indian adolescent population. *Journal of Forensic and Legal Medicine* 19, 285-290
4. Varocek, M., Manning, J. T. & Dressler, S.G. (2007) Repeatability and interobserver error of digit ratio (2D:4D) measurements made by experts. *American Journal of Human Biology*; 19: 142-146
5. Kiran G T et al. (2013). Relationship of stature of an individual with second and fourth digit lengths among medical student belonging to Southern part of India. *Indian Journal of Forensic Medicine & Toxicology*, Vol. 7, No. 2, 61-63
6. L Meadows, R L Jantz. (1992) Estimation of stature form metacarpal lengths. *Journal of Forensic Sciences*; 37(1): 147-54
7. Cohen-Bendahan, C.C.C., van de Beek, C., Berenbaum, S.A. (2005) Prenatal sex hormone effects on child and adult sex-typed behaviour: methods and findings. *Neurosci. Biobehv. Rev.* 29, 353-384
8. Alyson B. and Minna L. "An investigation into the relationship between digit length ratio (2D: 4D) and psychopathy", *British Journal of Forensic Practice*, published online by © Pier Professional Ltd, Vol 12 Issue 2, May 2010
9. Peters M, Mackenzie K, Bryden P. (2002) Finger length and distal finger extent patterns in humans. *Am J Phys Anthropol*, 117(3): 209-17
10. Ellis L, Ames MA: Neurohormonal functioning and sexual orientation: a theory of homosexuality-heterosexuality. *Psychol Bull* 1987; 101: 233–258.
11. McIntyre, M.H. (2006). The use of digit ratios as markers for perinatal androgen action. *Reprod. Biol. Endocrinol.*, 4: 10.
12. Wilson G. D. (1983). Finger length as an index of assertiveness in women. *Preconality and Individual Differences*, 5, 195-201
13. A.O. Ibegbu et al. (2012). Anthropometric Study of the Index (2nd) and Ring (4th) Digits in Epira Ethnic Group of Nigeria. *Asian Journal of Medical Sciences* 4(2): 79-84
14. Tanuj Kanchan, G Pradeep Kumar, Ritesh G. Menezes. Index and ring finger ratio- A new sex determinant in South Indian population. *Forensic Science International* 181(2008)53-e1 53-e4.





Mar Mar Wai et al.

TABLE 1: The Relationship between Digit Ratios with Gender (Frequency / Percentage of Index to Ring Finger Ratio (2D:4D) among male and female in both hands)

GENDER	DIGIT RATIO	Less than 1 (<1)		1		More than 1 (>1)	
		n	%	n	%	n	%
Female (n=75)	Right	56	74.67	1	1.33	18	24
	Left	26	34.67	1	1.33	48	64
Male (n=75)	Right	71	94.67	0	0	4	5.33
	Left	67	89.33	1	1.33	7	9.33
Total (n=150)	Right	127	84.67	1	0.67	22	14.67
	Left	113	75.33	2	1.33	35	23.33

TABLE 2: Descriptive Statistics mean (± SD) of index to ring finger ratio in both gender

GENDER		RATIO (2D:4D)			
		RIGHT	P VALUE	LEFT	P VALUE
FEMALE (n=75)	Mean (± SD)	0.98 (±0.03)	0.000	0.98 (±0.03)	0.000
MALE (n=75)	Mean (± SD)	0.96 (±0.03)	0.000	0.96 (0.03)	0.000
Total (n=150)	Mean (± SD)	0.97 (±0.03)	0.000	0.97 (±0.04)	0.000

Table 3: T-Test (Relationship between Index to Ring Finger Ratio (2D:4D) and gender

	GENDER	Mean (± SD)	Sig. (2-tailed)
RATIO (RIGHT)	MALE	0.96 (±0.029)	.000
	FEMALE	0.98 (±0.031)	.000
RATIO (LEFT)	MALE	0.96 (±0.034.)	.000
	FEMALE	0.98 (±0.034)	.000

Table 4: Pearson Correlation between Index to Ring Finger Ratio (2D:4D) and Height (Cm) in Total Population

		HEIGHT (cm)	RATIO (RIGHT)	RATIO (LEFT)
HEIGHT (cm)	Pearson Correlation	1	-.212**	-.114
(n=150)	Sig. (2-tailed)		.009	0.166

** . Correlation is significant at the 0.01 level (2-tailed)





Mar Mar Wai et al.



Fig. 1. Tresna Sliding Caliper

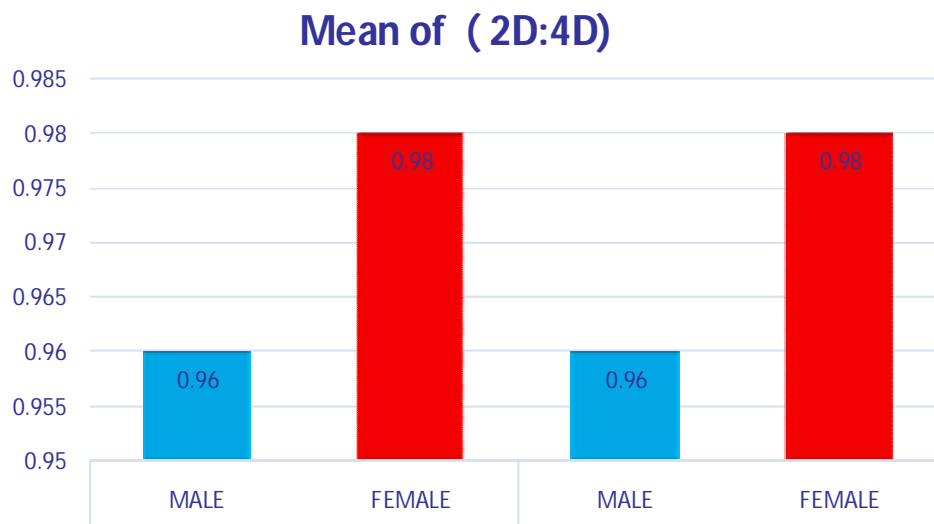
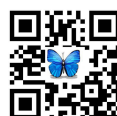


Fig. 2. Bar Diagram Showing the (2D:4D) in male and female in both hand.





Mar Mar Wai et al.

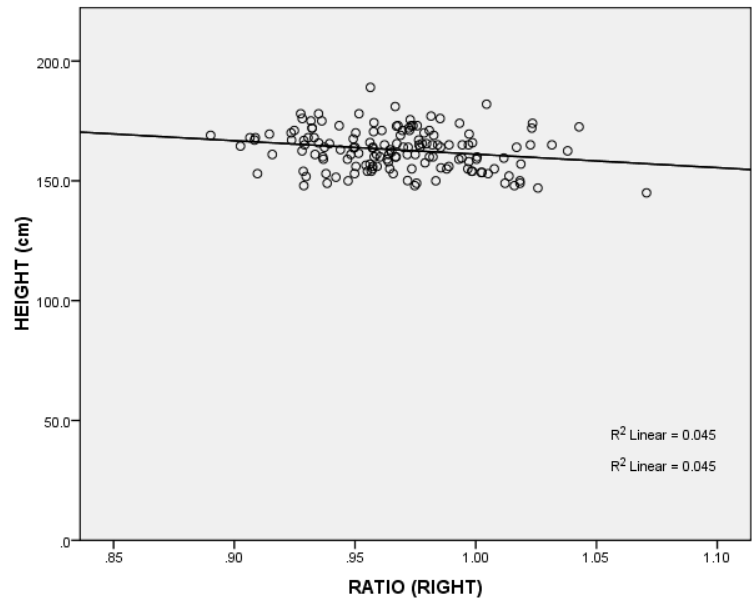


Figure 3: Relationship between index to Ring Finger Ratio Andheight (Cm) for Right Hand

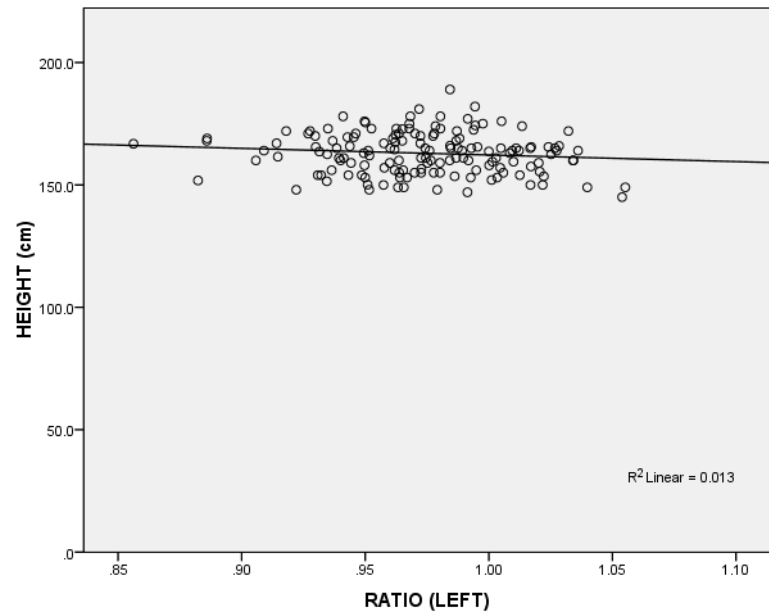


Figure 4: Relationship between index to Ring Finger Ratio and Height (Cm) for Left Hand





RESEARCH ARTICLE

Effect of *Eruca sativa* Leaves Extract on Osteoporosis induced by Phosphoric Acid in Adult Male Rabbits

Sawsan Kadhim Mashi* and Dina Saadoon Dheyab

Department of Physiology and Pharmacology, College Veterinary Medicine, University of Baghdad, Iraq.

Received: 23 Nov 2017

Revised: 17 Dec 2017

Accepted: 08 Jan 2018

*Address for correspondence

Sawsan Kadhim Mashi

Department of Physiology and Pharmacology,

College Veterinary Medicine-University of Baghdad,

Baghdad, Iraq.

E.mail: saosanmashi@gmail.com



This is an Open Access Journal / article distributed under the terms of the **Creative Commons Attribution License** (CC BY-NC-ND 3.0) which permits unrestricted use, distribution, and reproduction in any medium, provided the original work is properly cited. All rights reserved.

ABSTRACT

The current study intended to determine the effect of *Eruca sativa* leaves extract on osteoporosis induced by phosphoric acid and his to pathological changes of bone in adult male rabbits. Twenty healthy adult male rabbits were used, animals randomly divided into 4 groups treated for 30 days as the following: control group (C) : rabbits in this group were permitted to ad libitum provide of drinking water, (T₁) group : rabbits in this group were allowed to drinking water containing 1530 mg /kg b.w of phosphoric acid, (T₂) group : rabbits in this group received 250 mg/ kg b.w aqueous extract of *Eruca Sativa* orally and 1530 mg /kg b.w of phosphoric acid in drinking water , (T₃) group : rabbits in this group received 250 mg/ kg b.w aqueous extract of *Eruca sativa* orally. The results of this study revealed that oral intubation of phosphoric acid for 30 days caused osteoporosis manifested by a significant elevation(P<0.05) in the serum ALP and phosphorus while there is a significant decrease in vitamin D (P>0.05) . On the other hand animals received *Eruca Sativa* with phosphoric acid for 30 days showed a considerable decrease (P>0.05) in serum ALP and significant increase in vitamin D (P<0.05) . The histological section showed pathological changes in the bone in T₁ group while giving *Eruca Sativa* extract with and without phosphoric acid was effective in modified these changes into semi normal.

Keywords: Osteoporosis, Phosphoric acid, *Eruca Sativa*, vitamin D, ALP, Magnesium, Phosphorus and Calcium.

INTRODUCTION

Osteoporosis means that the bones become weak and breakable, resulting in a higher threat of fractures than in regular bone. Osteoporosis take place when bones lose minerals, like calcium, fastly than the body can replace them leading to a loss of bone thickness (density or bone mass). As a result, bone becomes less dense and thinner therefore



**Sawsan Kadhim Mashi and Dina Saadoon Dheyab**

even a minor hit or fall can cause severe fracture. Medical plants take a vital part in our life since they're broadly used for the prevention and treatment of different diseases including osteoporosis because it contains active pharmacological compounds in high amount. *Eruca sativa* L. which is also called Rocket, it is from the Brassica family (Cruciferae), it originated in Mediterranean area and currently is established around the world [1]. It is mostly used as vegetable and spice, in addition the plant has medicinal uses commonly it is used as digestive, astringent, emollient, tonic, diuretic, depurative, laxative, rubefacient and stimulant [2]. It is also used as aphrodisiac, eye infection and for digestive and kidney problems [3]. Furthermore the plant used for its anti genotoxic effect against human hepatoma (HePG2) cells because of the presence of erysolin and erucin compounds in the plant [4]. It is also used as hepatoprotective activity, antihyperlipidemic, and antiephrolethiatic [5]. Rocket contains a collection of anticancer components such as glucosinolates which have antioxidant activity, and are strong stimulant of natural detoxifying enzymes in the body, such compounds also have anti-ulcer, cytoprotective and anti-secretary effects in the ethanolic extracts of the plant in rats [6]. Furthermore the plant has antifungal activity due to the existence of antioxidant ingredient like flavonoids, glucosinolate, carotenoids as well the volatile fractions [7]. Besides *Eruca sativa* assists regulate blood pressure, adjust cholesterol levels, improve wound healing and helps in loss weight [8]. The rocket plant contains minerals for instance (N, P, K, Ca, Mg, Na, Fe, Cu, Mn and Zn) [9], in addition Rocket is abundant with the natural antioxidants like (vitamin C, vitamin K, and vitamin A) [10]. Phosphoric acid is a mineral inorganic acid having the chemical formula (H_3PO_4), a large amount of Phosphoric acid about (80%) is utilized in the manufacture of agricultural fertilizers, and the rest being used for detergent additives (about 10%), insecticide production, cleaners and cattle feed additives. In the steel manufacturing, it is used to clean and rust-proof, besides It is used as a flavoring agent in carbonated beverages, jellies, jams and cheeses. In foods, phosphoric acid provides a sharp, acidic taste. Moreover phosphoric acid is used in producing water softeners [11].

OBJECTIVE

The aim of recent study was to detect the possible effects of aqueous extract of *Eruca sativa* on osteoporosis induced by phosphoric acid.

MATERIALS AND METHODS

Twenty healthy adult male rabbits, weighted (1000-1500 g) were used. Rabbits were housed in iron cages and kept for ten days for acclimatization. Room temperature was maintained at (22-25°C). Animals were allowed freely access to water and pellets along the experimental time. Rabbits were housed in an animal's house /Department of physiology and pharmacology/College of veterinary medicine/ University of Baghdad. Animals were randomly separated into four equal groups (5rabbits/group) and treated for 30 days as follows: control group (C) : rabbits in this group were permitted to ad libitum provide of drinking water, (T₁) group : rabbits in this group were allowed to drinking water containing 1/10 of lethal dose (1530 mg /kg b.w) of phosphoric acid [12], (T₂) group : rabbits in this group received 250 mg/ kg b.w aqueous extract of *Eruca Sativa* orally [13] and 1/10 of lethal dose 1530 mg /kg b.w of phosphoric acid, (T₃) group : rabbits in this received 250 mg/ kg b.w aqueous extract of *Eruca Sativa* orally. Blood samples were collected after 30 days of the experiment, blood was collected directly from heart, centrifuged at 3000 rpm for 15 min. and then kept at -8 C until thawed for analyses, serum samples were used to measure the following parameters that related with bone metabolism: calcium (Ca), magnesium (Mg), phosphorus (P) and alkaline phosphatase (ALP) by using specialized kits from Biosystem company and the Measuring of vitamin D was by using HPLC, in brief, the method uses a reversed phase HPLC technique that exhibits a obvious solution of Vitamin D. The movable phase is an acetonitrile extract of serum by solid phase extraction C18/ODS 4.6 ×25, wave (265nm), HPLC was carried out by using a Shimadzu LC- 2010AHT system with Shima -dzu LC-2010 pump (Japan) [14].

For histological studies the animals bone samples have immersed in 10% formalin for seven days. After well fixation, each bone sample transformed into decalcified solution which composed of equal parts of Formic acid solution [250



**Sawsan Kadhim Mashi and Dina Saadoon Dheyab**

ml formic acid (98%) + 250 ml Distal water] and Sodium citrate solution [50 gr. Sodium citrate +250 ml Distal water]. The decalcified solution have been used for 10 days and the solution changed every five days to achieve well decalcification, [15], Then the sections processed upgrading with ethanol alcohol for paraffin technique and sectioned serially at (5-6) μm . The prepared tissue sections were stained with the Hematoxylin and Eosin stain [16].

Preparation of Plant Extracts

Plant leaves were obtained from local market, leaves were cleaned with water then dried at room temperature, after that the dried plants were kept in (-20°C) until used. Dried leaves (50 g) were extracted by adding 500 ml of distilled water and boiling for 30 min. The extract was then filtered and lyophilized, after that the extract was reserved at -20°C [17].

Statistical Analysis

Data are shown as the Mean \pm SE. Data were analyzed by using one way analysis of variance (ANOVA) within SPSS program. Means were tested by t test at probability level of ($p < 0.05$) [18].

RESULTS AND DISCUSSION

The effect of *Eruca sativa* and phosphoric acid on bone in male rabbits for 30 days represented in table-1. Results revealed that the differences in Ca were significant ($P < 0.05$) in T_2 and T_3 groups (11.30 \pm 0.37), (11.48 \pm 0.33) as compared with T_1 group (9.28 \pm 0.66). On the other hand there was a significant increase in serum P ($P < 0.05$) in T_1 group (7.45 \pm 0.71) in compared to T_2 and T_3 groups (5.05 \pm 0.75), (4.76 \pm 0.68). Also, there was a significant change ($P < 0.05$) in Mg in T_3 group (2.44 \pm 0.04) as compared with control, T_1 and T_2 groups (2.13 \pm 0.03), (1.94 \pm 0.11), (2.10 \pm 0.12). The highest estimate of ALP was detected in T_1 group (360.31 \pm 74.45) which differed significantly ($P < 0.05$) as compared with control, T_2 and T_3 groups (150.62 \pm 8.92), (148.25 \pm 14.87), (157.34 \pm 6.26). Data showed a significant increases ($P < 0.05$) in vitamin D level in T_2 group (3.59 \pm 0.71) comparing with control group, T_1 and T_3 groups (1.74 \pm 0.30), (1.48 \pm 0.51), (1.69 \pm 0.40).

The current experiment demonstrate that the phosphoric acid caused considerable elevation in serum P in T_1 group while there was a marked decrease in Ca and Mg at the same group in compared to other group, this is may be attributable to many reasons first, increase utilization of phosphoric acid may minimize the body's calcium/phosphorus ratio [19], this denotes that least calcium is obtainable for bone mineralization than phosphorus in view of the fact that both calcium and phosphorus are necessary to compose the basic units of the bone, lower calcium-phosphorus ratio does not ameliorate bone forming. Secondly, phosphoric acid binds calcium and magnesium in the digestive tract. Salts of calcium and phosphorus (calcium phosphate) are identified as apatites and they form the bulk of the bone. However, these salts are just good for bone healthiness as long as they are formed in the bone. yet, the salts of calcium and phosphoric acid created in the gut are not easily absorbed in the intestine, for that reason the consumption of phosphoric acid may possibly diminish the absorption of calcium and magnesium. as both minerals are essential for bone health, phosphoric acid can reduce the amount of calcium and magnesium existing for bone mineralization. Lastly, the acidifying effect of phosphoric acid is also a reason of bone loss. Some experienced have argued that phosphoric acid might acidify the blood enough for the body to equalize it by stripping calcium from the bone [20]. Furthermore the results of present study showed no significant increase in vitamin D in T_1 group on the contrary there was an elevation in vitamin D in T_2 group. Arugula promises to keep the bones in appropriate shape and teeth strong. The calcium content in plant is very high which is the major building block of our body, in addition Arugula also rich in vitamin K which works as a glue that deposits and connects calcium with each other, as well this process minimizes bone impairment and damage [21]. The active form of vitamin D-1 25(OH)2D plays a substantial role in calcium metabolism, e.g. by rising calcium absorption in the gut.



**Sawsan Kadhim Mashi and Dina Saadoon Dheyab**

[22, 23]. The S-1, 25(OH)₂D concentration raises in response to a lowering in calcium absorption [24]. Also the present study showed significant increase in ALP in T₁ group as compared to other groups. Alkaline phosphatase is an essential ingredient in hard tissue formation, its exact role is still unidentified, but it appears to works both to raise the local concentration of inorganic phosphate (a mineralization promoter) and to reduce the concentration of extracellular pyrophosphate (an inhibitor of mineral formation) [25]. Phosphoric acid, or other acidic solutions dissolve the calcium precipitates, it makes sense that osteoblasts by creating a local environment of alkalinity through alkaline phosphatase assists build bone. It also reveals that in order to slow bone loss, one cannot be in an acidic state. Being a product of osteoblasts raised serum levels of alkaline phosphatase point out condition of increased bone turnover [26].

In compare with sections of control group (fig.1), the section of T₁ group showed sever disorganization and disarranged of osteons. There were thinning of compact part of bone with poor remodeling at the Endostium and Periosteum surfaces which revealed undulating surfaces. The outer circumferential lamellae of bone showed basophilic staining feature which revealed sever demineralization of inorganic part of bone (fig.2). The magnified sections revealed dilatation of Haversian canals and lost the normal architecture of osteons with marked spaces of depletion of part of compaction associated with poor mineralization and multiple line of cracks (fig.3&4), these pathohistological changes perhaps related to the long time of exposure to phosphoric acid. The sections of T₂ group showed little spots of basophilia around some of osteons while other changes showed normal endosteal and periosteal surfaces (fig.5), while the sections of T₃ group showed mild changes and characterized by normal endosteal and periosteal surfaces with mild basophilia which seen near endostium. In some region of bone the concentric lamellae of osteon were arranged closely and displaying small size and lightly basophilic staining (fig.6&7). the effect of *Eruca Sativa* extract in T₂ and T₃ groups was effective in modified these changes into semi normal, this effect possibly due to its potent antioxidant effects on bones.

CONCLUSION

Aqueous extract of *Eruca sativa* leaves can improve osteoporosis induced by phosphoric acid along 30 days of treatment.

ACKNOWLEDGEMENTS

The authors would like to extend their deep thanks and appreciation to Dr. Dhyaa Ab. Abood for his assistance in the histopathological part of this research.

REFERENCES

1. Al-Qurainy F, Alameri A A and Khan S. RAPD profile for the assessment of Genotoxicity on a medicinal plant; *Eruca sativa* .J.Med.Plants Res 2010;4(7):579-586.
2. Alam M S, Kaur G, Jabbar Z, Javed K and Athar M. *Eruca sativa* seed possess antioxidant activity and exert a protective effect induced on mercuric chloride induced renal toxicity. Food and Chem Toxicol 2006;45:910-920.
3. Yaniv Z, Schafferman D and Amar Z. Tradition uses and biodiversity of Rocket(*Eruca sativa* Brassicaceae)in Israeel J.Econom Bot 1998; 52(4):394-400.
4. Lamy E, Shoder J, Paulus S, Brenk P, Stahi T and Sandermann V M. Antigeno- toxic proprieties of *Eruca sativa* (Rocket plant), erocin and erysolin in human hepatoma (HePG2) cells towards benzo(a)pyrene and their mode of action. Food and ChamToxicol 2008; 46(7):2415-24210.
5. Bukhashi E, Maliki S A and Ahmed S S. Estimation of nutritional value and trace elements content of *Carthamus oxycantha* ,*Eruca sativa* and *Plantago ovanta*. Pak J.Bot 2007; 30(4):1181-1187.





Sawsan Kadhim Mashi and Dina Saadoon Dheyab

6. Al-qasomi S, Al-sohaibani M, Al-Howriny T, Al-Yahya M and Rafatullah S. Rocket(*Eruca sativa*):a salad herb with potential gastric anti-ulcer activity. World J.Gastroenterol 2009 ;15(6):1958-1965.
7. Hanafi E M, Hegazy E M, Riad R M and Amer H A. Bio-protective effect of *Eruca sativa* seed oil against the hazardous effect of Aflatoxin B1 in male rabbits. J.Acad Research 2010; 2(2):670-674.
8. Anac D and Martin-Prevel P. Improved crop quality by nutrients management .Kluwer Academic Publisher 1999 ; pp:1-13.
9. Neriman Tuba Barlas*, Mehmet E_ref Irget and Mahmut Tepecik. Mineral content of the rocket plant (*Eruca sativa*) African Journal of Biotechnology 2011; 10(64): 14080-14082.
10. Marwat S.K, Rehman F and Khan A A. Phytochemistry and pharmacological values of rocket (*Eruca sativa* Miller) A review, International Journal of Horticulture2016; 6(21): 1-7 .
11. Prof. Shakhshiri. www.scifun.org. General Chemistry.2008
12. Biofax. Datasheet 19-4 /70.Northbrook, IL:Biofax industrial Bio-test Laboratories Inc 1970.
13. Mahdy SS.The antigenotoxicity of *Eruca Sativa* Mill extract on bone marrow cells of male albino mice treated with Vincristine. Ibin Al-Haitham Jou. For pure and Applied 2012; NO.2. Vol.25.
14. Amy, K , Thomas Bremner J E and Sayed M H .Quantification of Serum 25-Hydroxyvitamin D2 and D3 Using HPLC–Tandem Mass Spectrometry and Examination of Reference Intervals for Diagnosis of Vitamin D Deficiency. Am J. Clin Pathol 2006;125:914-920.
15. Luna G.. "Manual of Histological Staining Methods of The Armed Forced Institute of pathology". 3rd Ed. McGraw Hill book Co. New York 1968 ; Pp: 71, 98.
16. Bancroft J D and Marilyn G..Theory and practice of histological techniques.6th ed.London, Elsevier Limited 2008 ; Pp:168-173.
17. Aysen Yarat*, Ozlem Sacan, Serap Akyuz, Burcin Alev, Rabia Pisiriciler, Esin Ak and Refiye Yanardag. In vitro effect of aqueous plant extracts on antioxidant parameters in saliva samples. Journal of Medicinal Plants Research 2013 ; 7(3):118-125.
18. SAS. SAS/STAT Users Guide for Personal Computer. Release 9.1..SAS Institute, Inc., Cary, N.C., USA 2010.
19. Garcia-Contreras F, Paniagua R and Avila-Diaz M et al. Colabeverage consumption induces bone mineralization reduction in ovariectomized rats. Arch Med Res 2000; 31:360–5.
20. Tucker KL1, Morita K, Qiao N, Hannan MT , Cupples L A and Kiel D P . Colas, but not other carbonated beverages, are associated with low bone mineral density in older women: The Framingham Osteoporosis Study. Am J Clin Nutr 2006; 84(4):936-42.
21. Flore R¹, Ponziani F R , Di Rienzo T A , Zocco MA , Flex A, Gerardino L , Lupascu A , Santoro L , Santoliquido A, Di Stasio E, E. Chierici , Lanti A, Tondi P and Gasbarrini A. Something more to say about calcium homeostasis: the role of vitamin K2 in vascular calcification and osteoporosis. Eur Rev Med Pharmacol Sci 2013; 17(18):2433-40.
22. Li YC, Pirro AE, Amling M, Dellling G, Baron R, Bronson R, Demay MB. Targeted ablation of the vitamin D receptor: an animal model of vitamin D-dependent rickets type II with alopecia. Proc Natl Acad Sci U S A 1997;94:9831–9835.
23. Yoshizawa T, Handa Y, Uematsu Y, Takeda S, Sekine K, Yoshihara Y, Kawakami T, Arioka K, Sato H, Uchiyama Y, Masushige S, Fukamizu A, Matsumoto T, Kato S. Mice lacking the vitamin D receptor exhibit impaired bone formation, uterine hypoplasia and growth retardation after weaning. Nat Genet 1997;16:391–396.
24. Dawson-Hughes B, Harris S, Kramich C, Dallal G and Rasmussen H.M, Calcium retention and hormone levels in black and white women on high- and low-calcium diets. J Bone Miner Res 1993; 8:779–787.
25. Ellis E. Golub and Kathleen Boesze-Battaglia. The role of alkaline phosphatase in mineralization. Current Opinion in Orthopaedics 2007; 18:444 – 448.
26. Van Straalen JP, Sanders E, Prummel MF and Sanders GT. Bone alkaline phosphatase as indicator of bone formation. Clin Chim Acta 1991; 201:27-33.





Sawsan Kadhim Mashi and Dina Saadoon Dheyab

Table 1: illustrate the effect of *Eruca sativa* leaves extract and phosphoric acid on Calcium, Phosphorus, Magnesium, ALP and vitamin D.

Parameters	Calcium mg/dl	Phosphorus mg/dl	Magnesium mg/dl	ALP U/L	Vit. D ng/ml
control	10.37±0.45ab	6.13±0.19ab	2.13±0.03b	150.62±8.92 b	1.74±0.30 b
T ₁	9.28±0.66b	7.45±0.71a	1.94±0.11b	360.31±74.45a	1.48±0.51b
T ₂	11.30±0.37a	5.05±0.75b	2.10±0.12b	148.25±14.87b	3.59±0.71a
T ₃	11.48±0.33a	4.76±0.68b	2.44±0.04a	157.34±6.26 b	1.69±0.40 b
LSD	1.4775	2.0098	0.2846	114.98	2.11991

Small superscript denote significant (p<0.05) difference between groups (rows).

C : control group

- T₁: Animals received drinking water contain 1530 mg /kg b.w of phosphoric acid .

- T₂ : Animals received 250 mg/ kg b.w aqueous extract of *Eruca Sativa* orally and 1530 mg/kg b.w of phosphoric acid.

- T₃ : Animals received 250 mg/ kg b.w aqueous extract of *Eruca Sativa* orally.

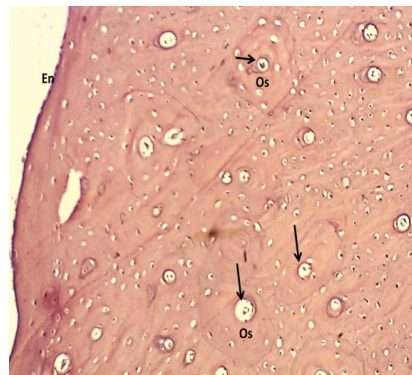


Figure 1: Section of bone (control) shows: Endostium (En), osteons (Os) and Haversian canal. H&E stain .100x

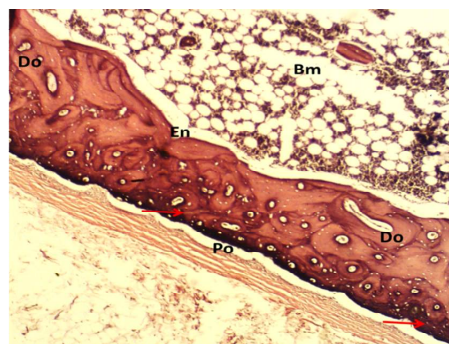
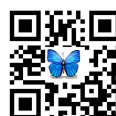


Figure 2: Section of bone in T₁ group shows: poor remodeling of Endostium (En) and periosteum surfaces (Po) , disarranged osteons (Do) with basophilic of outer circumferential lamellae . H&E stain.40x.





Sawsan Kadhim Mashi and Dina Saadoon Dheyab

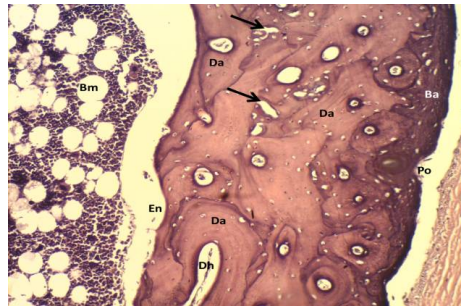


Figure 3: Magnified section of bone in T₁ group shows: poor remodeling of Endostium (En) and periosteum surfaces (Po), disarranged osteons (Da) with basophilic of outer circumferential lamellae (Ba), depletion of organic part of bone (arrows) and dilatation of Haversian canal (Dh). H&E stain.100x.



Figure 4: Magnified section of bone in T₁ group shows: marked spaces of depletion (De) with poor mineralization (dm), basophilic of outer circumferential lamellae (Ba), and multiple line of cracks (arrows). H&E stain.400x

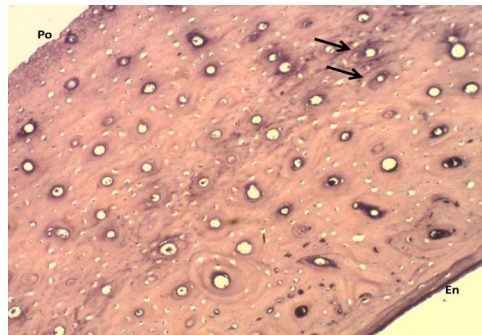


Figure 5: Section of bone in T₂ group shows: mild basophilic at sub endostium region (arrows), periosteum (Po) and endostium (En). H&E stain.40x.





Sawsan Kadhim Mashi and Dina Saadoun Dheyab

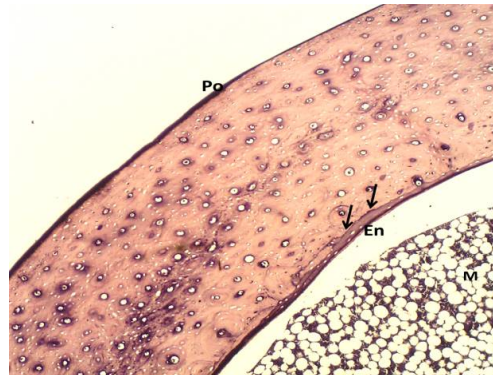


Figure 6: Section of bone in T₃ group shows: mild basophilic at sub endostium region (arrows), periosteum (Po) and endostium (En) . H&E stain.40x.

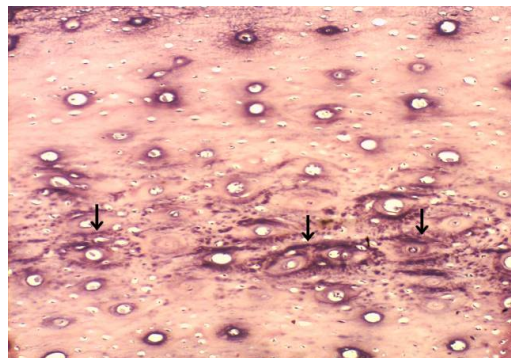


Figure 7: Section of bone in T₃ group shows: the concentric lamellae displaying small size and lightly basophilic staining (arrows). H&E stain.100x.

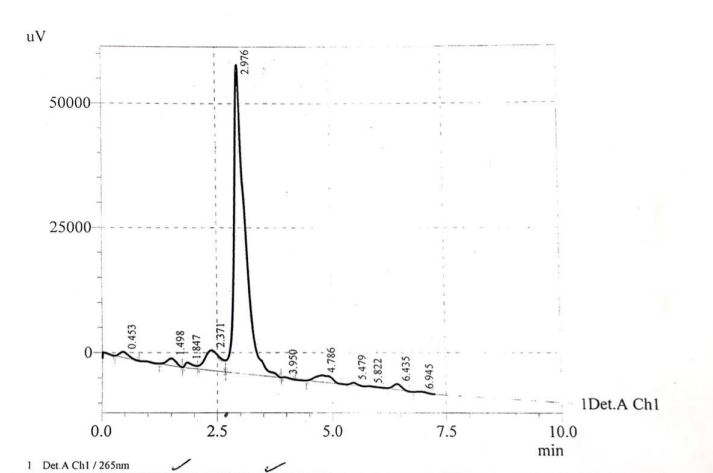


Fig 8 : Vitamin D Standard HPL-C Technique





Sawsan Kadhim Mashi and Dina Saadoon Dheyab

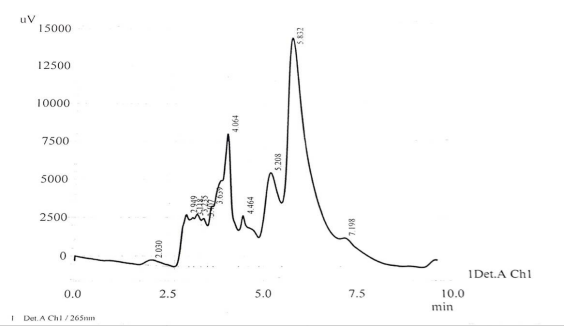


Fig. 9: Chromatogram of Vitamin D in control group.

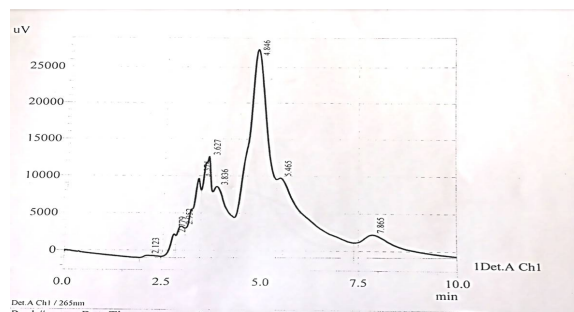


Fig. 10: Chromatogram of Vitamin D in T₁ group

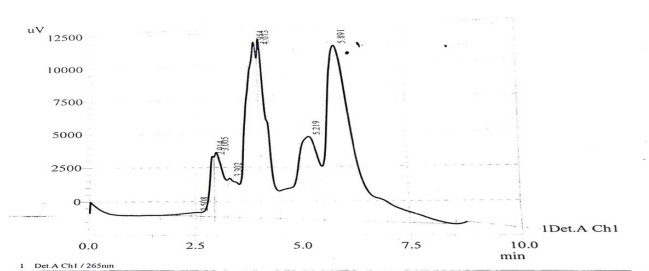


Fig. 11: Chromatogram of Vitamin D in T₂ group

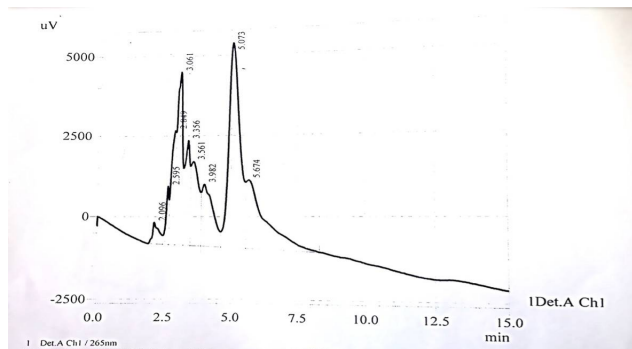


Fig. 12: Chromatogram of Vitamin D in T₃ group





Histological and Histochemical Features for Jacobson's Glands in Male *Gazella subgutturosa*

Dhyaa Ab. Abood* and Zahraa M Hussein

Department of Anatomy and Histology, College of Veterinary Medicine, University of Baghdad, Baghdad, Iraq.

Received: 03 Dec 2017

Revised: 29 Dec 2017

Accepted: 25 Jan 2018

*Address for correspondence

Dhyaa Ab. Abood

Department of Anatomy and Histology,
College of Veterinary Medicine,
University of Baghdad, Baghdad, Iraq.
E.mail: sabahali503@yahoo.com



This is an Open Access Journal / article distributed under the terms of the **Creative Commons Attribution License** (CC BY-NC-ND 3.0) which permits unrestricted use, distribution, and reproduction in any medium, provided the original work is properly cited. All rights reserved.

ABSTRACT

The present work was investigated the histological and histochemical features of Jacobson's glands in *Gazella subgutturosa*. Six adult Gazelle were used for this work. The tissue sections were stained with H&E, combine Alcian blue-PAS and Alcian blue- aldehyde foccine stains. The results showed that the Jacobson glands were dispersed throughout the connective tissue of the incisive duct and along the entire length of vomer nasal duct. They compound tubuloalveolar type consisted mainly of mucus alveoli which build up by low columnar cells and enclosed by myoepithelial cells. The ducts system of glands consisted of intercalated, striated and common ducts. The mucous secretion of gland was drained by two main ducts at the dorsal and ventral commissures of vomer nasal duct in addition for groups of ducts those opened throughout the respiratory epithelium of lateral wall of vomer nasal duct. Histochemically with combined Alcian blue (2.5pH) & PAS stains, most of the glandular alveoli were containing positive PAS secretory granules and little of these alveoli were containing positive granules for Alcian blue (2.5pH), few alveoli were positive for both AB& PAS stains. The glandular alveoli were negative for Alcian blue (1 pH), and mucin was carboxylated types with Alcian blue- Aldehyde fuchsine stain. Our Conclusion showed clear differences when compared to other literatures, the mucus secretion composed of both acid and neutral types, the glands appear unlikely to other which secreted mixed fluid in the vomer nasal organ by the same secretory units which has mucous nature and showed nil serous type would thus have to be derived.

Keywords: Jacobson gland, histochemical, histological, vomer nasal organ.





INTRODUCTION

In all vertebrates, except birds there is an olfactory system which responsible for pheromones detection called "vomeronasal organ" which represents the second one responsible for specific pheromone smelling [1][2]. Vomeronasal organ consists of paired tubular structure on both side and / or the base of nasal septum [3] [4]. In ruminant the vomeronasal tubes continuous with outer environment throughout the nasopalatine duct, incisive papilla at oral cavity and the opening of nasopalatine duct at the vestibule of nasal cavity while in equine and carnivores it open into vestibule of nasal cavity [5][6] [7]. As well as other body system, the vomeronasal organ has blood supply [8], it encircled by vomeronasal cartilage [4],[5]. The vomeronasal duct composed of soft tissue which contained the functional units of vomeronasal organ included both sensory epithelium in addition of respiratory epithelium and sub epithelial soft tissue which include wide veins, axons of accessory olfactory nerve and vomeronasal gland or Jacobson gland [4], [9] [10]. The main function of vomeronasal organ is dealing with specific sex pheromones [11], also this gland conceded as the lubricatory system in the vomeronasal organ [12] such function required a medium for dissolving these pheromones which done by seromucous secretions of this gland, scarce histochemical data is available on the Jacobson glands in *Gazella subgutturosa* so present article aimed to illustrate the histological and histochemical structure of Jacobson glands of vomeronasal organ in indigenous Gazelle (*Gazella subgutturosa*).

MATERIALS AND METHODS

Six healthy, adult male *Gazelle subgutturosa* were obtained from (AL-Madaen Animal Reservoir) in Baghdad provinces. The animals were euthanized by slaughter under low of department of public health ethics in college of veterinary medicine at university of Baghdad. The animals heads have been removed immediately from the body and the incisive papilla were infused with Bouin's solution, solution throughout the orifices of incisive papillae, then the nasal region included the hard palate and leaves for 48 then heads was immersed in 10% formalin for seven days [13]. The nasal region including hard palate has been cutting up into four transversal sections involved incisive duct, rostral, middle and caudal portions of vomeronasal organ. Each section has been trimmed to achieve the regions which include the basal part of nasal septum. For easy dealing with soft tissue the bony elements of each transversal sections were decalcified by a decalcification formula composed of equal parts of Formic acid solution [250ml formic acid (98%) + 250ml Distal water] and Sodium citrate solution [50 gr. Sodium citrate +250 ml Distal water]. The decalcified solution haven been used for 10 days and the solution changed every five days to achieve well decalcification [14], then the sections processed upgrading with ethanol alcohol for paraffin technique and sectioned serially at (5-6) μm . For general description of glands the prepared tissue sections were stained with Hematoxylin and Eosin. For histochemical description, the tissue sections were stained with combine Alcian blue (2.5pH) - Periodic Acid-Schiff (PAS) to differentiate the neutral and acidic mucosubstances and glycogen. Alcian blue (2.5pH) (blue) for acidic mucins and carboxylated or weakly sulphated acid mucosubstances. Aldehyde fuchsin-Alcian blue stains to differentiate the acidic carboxylated mucin (blue) from that acidic sulphated type (purple) [15].

RESULTS

The results showed that, the vomeronasal organ has composed of conducting part which involved (Incisive & papilla and incisive duct) and olfactory part which involved the vomeronasal duct. The Jacobson glands of *Gazella subgutturosa* were observed throughout the connective tissue components at the middle and caudal portions of the incisive duct (Fig.1&2) and extended along the entire length of vomeronasal duct of vomeronasal organ (Fig.3). The Jacobson's gland has been classified as compound tubuloalveolar type consisted mainly of mucus alveoli, the mucous alveoli were large size and lined by low columnar cells and enclosed by myoepithelial cells (Fig.4). The ducts system of Jacobson's glands has begun with intercalated duct which lined by low cuboidal cells and extended from the alveolar part of gland to drains the secretion into the next striated duct. Striated duct was lined by tall columnar cells, had wide lumen and surrounded by myoepithelial cells, it was connected between the intercalated duct and the





Dhyaa Abood and Zahraa Hussein

common duct. (Fig.5). Common duct was large, had a wide lumen and lined by tall columnar cells (Fig.5), their epithelial cells showed secretory activities. The Jacobson glands were drained their mucous secretion by two main ways: (i) the two main ducts at the dorsal and ventral commissures of vomer nasal duct, (ii) Groups of common ducts which opened through the lining epithelium of vomernasal duct (Fig.6). Histochemical results of Jacobson gland have shown that, with combined Alcian blue (2.5pH) & PAS stains, most of the alveoli were containing positive PAS secretory granules and little of these alveoli were containing positive granules for Alcian blue (2.5pH) (fig.7 & 8), on the other hand few alveoli showed positive for both AB&PAS stains (Fig.9). The alveoli of Jacobson's glands were negative for Alcian blue (1 pH) (Fig.10). With Alcian blue-aldehyde fuchsin the glandular alveoli were stained with blue color which indicated for carboxylated acid mucin type produced by these alveoli (Fig.11).

DISCUSSION

Histologically, the presences and distribution of lubricatory system (Jacobson glands) in *Gazella subgutturosa* were recorded of [5] [7] & [16], this results suggest that almost the glands were located near the common ducts of dorsal and ventral commissures especial at the incisive duct, rostral and middle portions where the luminal diameter of vomernasal duct was the widest [13] [17], on the other hand this result disagree with [9] & [18] who referred for opinion says that "the duct system of Jacobson glands empty their secretions into the lumen via short epithelial ducts at different locations through the luminal epithelium only", on other hand such lubricatory system was not present in other terrestrial vertebrates (tetrapods) such as (turtles) [19] and frog [20]. The turtles and frogs are aquatic or marine vertebrates live in aquatic environment they dispense with such system of lubrication so, sensory epithelium lacking glands, this suggests that these animals would be able to sense not only air-borne, but also water-borne odors during their adult terrestrial life. Even in squamates (Snakes or Lizard) [21] this suggests that these squamates live underground in dark environment and use such chemoreceptor organ for feeding rather than use their eyes or hear. The current results revealed the Jacobson glandular secretory units were mucous alveoli, such type was also recorded by [22] in Angora goats and [3] in Tammar wallaby, While the serous type was observed by [9] in Egyptian goat, [23] & [7] in Egyptian Buffaloes, [24] in camels, on the other hand three types involved (i) mixed seromucous, (ii) serous and (iii) mucous were stated by [18], also [25] stated the seromucous type in buffaloes, [26] in male red fox, [27] in sheep and [17] in mouse. Our results revealed the shape of alveolar secretory units was low columnar cells such result disagree with result of Moawad et al., [9] who referred for the pyramidal-shaped cells, the present result suggest that the shape of glandular epithelium is changes with their functional status that supported by results of Donjacour [28] who referred that the underneath extra cellular matrix play a role in affection the epithelial function by changing cell shape. The current results revealed that most mucous alveoli of *Gazella subgutturosa* Jacobson glands were PAS positive which referees for the presences of neutral or weakly acidic glycoproteins, on the other hand there were little alveoli showed sever reaction (positive) for Alcian blue (pH 2.5) which indicates the presence of acidic mucosubstances in the *Gazella subgutturosa*, this result was accords with [29], [30] in giraffes and disaccord with result of [9] in Egyptian goat, [3] in Tammarawilbe, [7] in buffaloes, the present result suggest that the presence of two types reactions revealed various function beyond each type, the PAS positive mucopolysaccharid and or glycoprotein secretion (neutral pH) act as pheromones fixing molecule's to surface microvilli of neuroepithelium as well as act as dissolving medium for odoriferous molecule's [13] [31], on the other hand the acidic mucopolysaccharid it play as role of local defense mechanism against mucous sniffed microorganisms which proofed by presence of carboxylated mucin which play the powerful antimicrobial agent [15].

ACKNOWLEDGEMENTS

The authors would like to acknowledge all technical staff and assistances in department Of Anatomy, Histology & Embryology-College of veterinary Medicine at University Of Baghdad.





Dhyaa Abood and Zahraa Hussein

REFERENCES

1. Igbokwe ECO. The role of main olfactory and vomeronasal system in animal behavior and reproduction. *Anim Res Int* 2009;6:1093–1101.
2. Brennan PA. The vomer nasal system. *Cell Mol life Sci*.2001; 58:546–555.
3. Schneider NY, Fletcher TP, Shaw G, Renfree MB. The vomeronasal organ of the tammar wallaby. 2008 *J Anat* 2008; 213: 93–105.
4. Abood DA, Hussein ZM. Histological features of Vomer nasal organ in Indigenous Gazelle (*Gazella subgutturosa*). *J Entomol Zool Studies* 2017; 5: 598-604.
5. Abood DA. Morphological and Histological features of Naso-palatine Duct of Indigenous Buffalo (*Bos indicus*). *Inter J Adv Biol Res* 2017; 253-256.
6. Hytell P, Sinowatz F, Vejlsøe M, Betteridge K. *Essentials of Domestic Animal Embryology*. Philadelphia: Saunders Elsevier, 2010; 372.
7. Kassab A, El-Shafey A. Light and Scanning Microscopic Study on the Vomeronasal Organ of the Buffalo (*Bos bubalis*). *Global Vet*.2012;8:491–497.
8. Besoluk K, Eken E, Bahar S. The branches of the descending palatine artery and their relation to the vomer nasal organ in Angora goat. *Vet Med* 2006; 51: 55-59.
9. Moawad UK, Awaad AS, Abedellaah BA. Morphological, histochemical and computed tomography on the vomeronasal organ (Jacobson's organ) of Egyptian native breeds of goats (*Capra hircus*). *J Basic Appl Sci* 2017;6:174–183.
10. Salazar I, Lombardero M, Cifuentes J M, Quinteiro PS, Aleman N. Morphogenesis and growth of the soft tissue and cartilage of the vomeronasal organ in pigs. *J Anat* 2003;202:503-514.
11. Keller M, Baum MJ, Brock O, Brennan PA, Bakker J. The main and the accessory olfactory systems interact in the control of mate recognition and sexual behavior. *Behav Brain Res* 2009, 268–276.
12. Rehoresk SJ, Firth BT, Hutchinson MN. The structure of the nasal chemosensory system in squamate reptiles. 2. Lubricatory capacity of the vomeronasal organ. *J Biosci* 2000;25:181–190.
13. Altai DA. Anatomical and Histological Study of Vomeronasal organ in Iraqi native cattle (*Bos indicus*). A thesis degree of master from university of Baghdad, college of veterinary medicine 2010.
14. Luna G. *Manual of Histological Staining Methods of the Armed Forces Institute of Pathology*. 3rd Ed. New York: McGraw Hill book Co; 1968;71, 98.
15. Bancroft JD, Marilyn G. *Theory and practice of histological techniques*. 6th Ed. London: Elsevier Limited; 2008;168-173.
16. Onwuaso IC, Chima NI. HISTOLOGICAL STUDIES OF THE VOMERONASAL ORGAN OF AFRICAN GIANT RAT (*Cricetomys gambianus*, WATERHOUSE). *Anim Res Inter* 2009;6: 1003-1008.
17. Roslinski DL, Bhatnagar KP, Burrows AM, Smith TD. Comparative morphology and histochemistry of glands associated with the vomeronasal organ in humans, mouse lemurs, and voles. *Anat Rec* 2000; 260:92-101.
18. Knetch M, Kuhnu D, Huttenbrink KB, Witt M, Hummel T. Frequency and localization of the putative vomeronasal organ in humans in relation to age and gender. *Laryngoscope* 2001;111: 448–452.
19. Gerlach J. The Complex Vomeronasal Structure Of *Dipsochelys* Giant Tortoises And Its Identification As A True Jacobson's Organ. *Herpetological J* 2005; 15:15-20.
20. Jungblut LD, Pozzi AG, Paz DA. Larval development and metamorphosis of the olfactory and vomeronasal organs in the toad *Rhinella* (*Bufo*) *arenarum* (Hensel, 1867). *Acta Zool (Stockholm)* 2011; 92: 305–315.
21. Gharzi A, Abbasi M, Yusefi P. Histological studies on the Vomeronasal organ of the worm like snake, *Typhlops vermicularis*. *J Biol Sci* 2013;13:372-378.
22. Besoluk O, Eken P, Boydak M. The vomeronasal organ in Angora goats (*Copra hircus*). *Vet Archiv* 2001;71:11–18.
23. Abbasi M. The vomeronasal organ in buffalo. *Italian J Anim Sci* 2007;6:991– 994
24. Karimi H, Mansoori-Ale Hashem R, Ardalani G, Sadrkhanloo R, Hayatgheibi H. Structure of Vomeronasal Organ (Jacobson organ) in Male *Camelus Domesticus* Var. *dromedaris persica*. *Anat. Histol. Embryol* 2001;43: 423–428.





Dhyaa Abood and Zahraa Hussein

25. Ardalani GH, Sadrhanloo AA, Abbasi M. Anatomy and histology of vomeronasal: organ of buffalo. J Fac Vet Med 2001 55, 5–11.
26. Karimi H, Hassanzadeh B, Razmaraii N. Structure of vomeronasal organ (Jacobson) in the male red fox (*vulpesvulpes*). Anatomical Sciences. 2016; 13:47-54.
27. Abbasi M, Khosravinia M. Vomeronasal organ of Lori sheep. J Fac Vet Med 2004;58:279–282.
28. Donjacour AA, Cunha GR. Stromal regulation of epithelial function. In: Lippman M.E., Dickson R.B. (eds) Regulatory Mechanisms in Breast Cancer. Cancer Treatment and Research, 53. Springer, Boston, MA, 1991: 335-364.
29. Lee KH, Park C, Kim J, Moon C, Ahn M, Shin T. Histological and lectin histochemical studies of the vomeronasal organ of horses. Tissue Cell 2016;48:361–369.
30. Kondoh D, Nakamura KG, Ono YS, Yuhara K, Bando G, Watanabe K, Horiuchi N, Kobayashi Y, Sasaki M, Kitamura N. Histological features of the vomeronasal organ in the giraffe, *Giraffacamelopardalis*. Microsc Res Tech 2017;00:1–5.
31. Takami S, Getchell ML, Getchell TV. Resolution of sensory and mucoid glycoconjugates with terminal α -galactose residues in the mucomicrovillar complex of the vomeronasal sensory epithelium by dual confocal laser scanning microscopy; Cell Tissue Res 1995; 280:211–216.

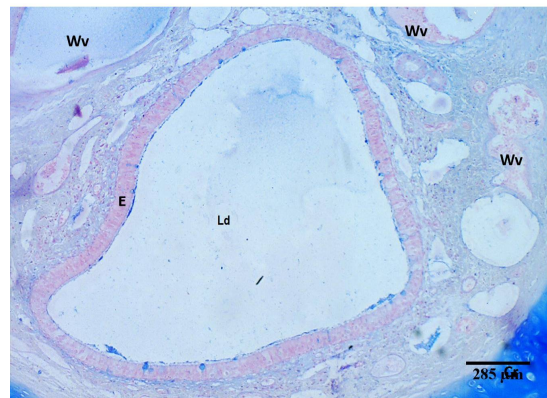


Figure1: Section at rostral portion of incisive duct shows: lumen of incisive duct (Ld), epithelium (E), wide veins (Wv), & cartilage (Cr), Alcian blue stain.

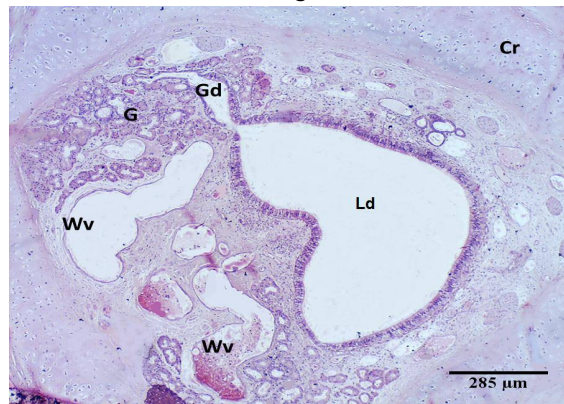


Figure2: Transverse section at the middle portion of the incisive duct shows: Lumen of incisive duct (LD), cartilage (Cr), wide vein (Wv), glandular tissue (G), common duct of Jacobson gland (Gd). PAS stain.





Dhyaa Abood and Zahraa Hussein

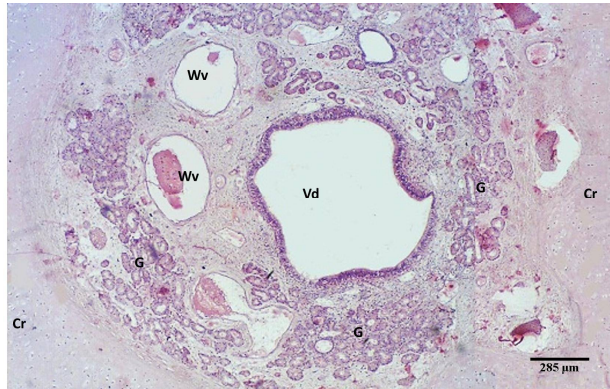


Figure 3: Transverse section at the vomer nasal duct shows: Lumen of vomer nasal duct (Vd), cartilage (Cr), wide vein (Wv), glandular tissue of Jacobson gland (G). PAS stain.

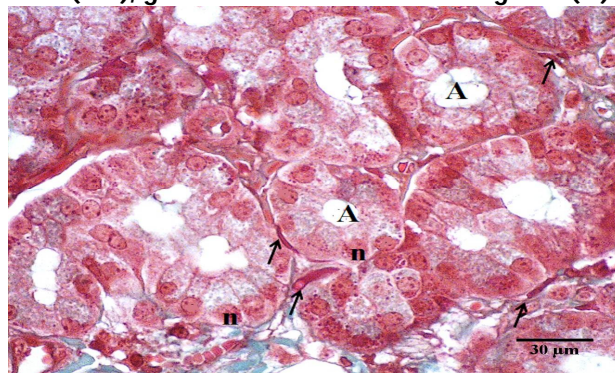


Figure 4: Section of Jacobson's gland shows: alveoli (A), nuclei (n) & nuclei of myoepithelial cells (arrows).Masson's trichrom stain.

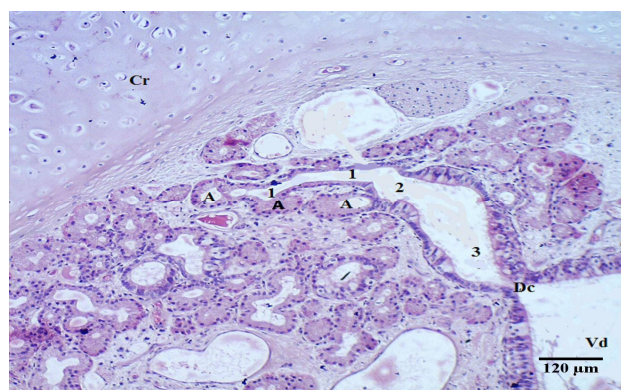


Figure 5: Section of the duct system of Jacobson's glands shows: cartilage (Cr), Alveoli (A), intercalated duct (1), striated duct (2), common duct (3), opening of dorsal commissure (Dc) & vomer nasal duct (Vd). H&E stain.





Dhyaa Abood and Zahraa Hussein

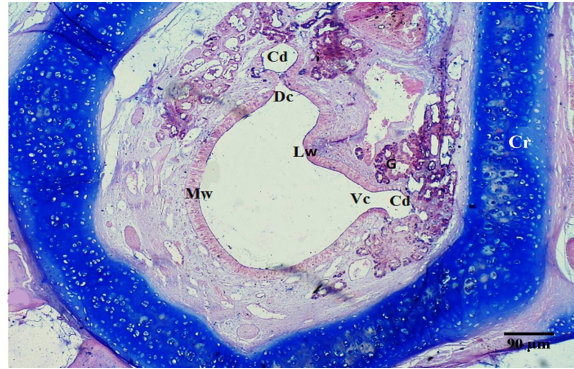


Figure 6: Section of vomer nasal duct shows: Jacobson's glands (G), common duct (Cd), medial wall (Mw) & lateral wall (Lw) of vomer nasal duct, dorsal commissure (Dc), ventral commissure (Vc) & cartilage (Cr). Combine AB& PAS stain.

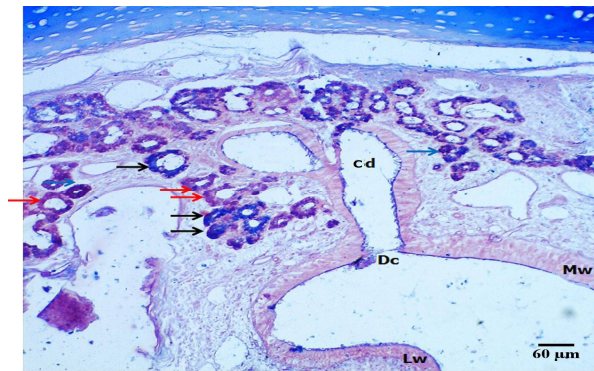


Figure 7: Section of Jacobson's glands shows: Alveoli which contained PAS positive secretion (Red arrows), Alcian blue positive secretion (Black arrows), common duct (Cd), lateral wall (Lw) & medial wall (Mw) of vomer nasal duct & dorsal commissure (Dc). Combine AB (2.5pH) & PAS stains.

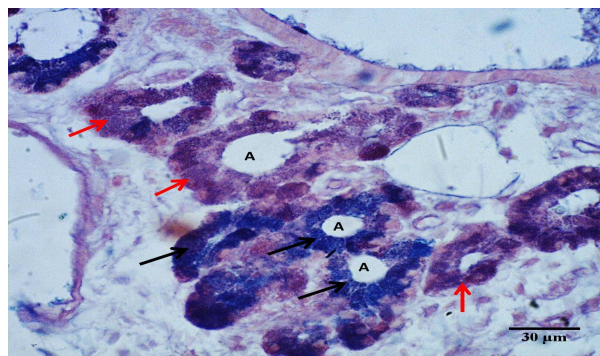


Figure 8: Magnified section for alveoli of Jacobson's glands shows: two types of alveoli (A), that the Alcian blue positive stain (Black arrows) & positive PAS stain (Red arrow). Combine AB (2.5pH) & PAS stains.





Dhyaa Abood and Zahraa Hussein

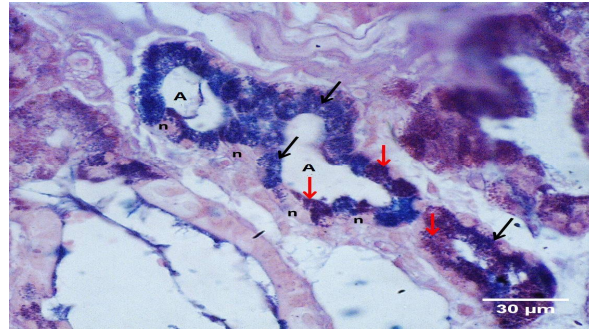


Figure 9: Magnified section for alveoli of Jacobson's glands shows: the alveoli (A), that have both Alcian blue positive stain (Black arrows) & positive PAS stain (Red arrow). Combine AB (2.5pH) & PAS stains.

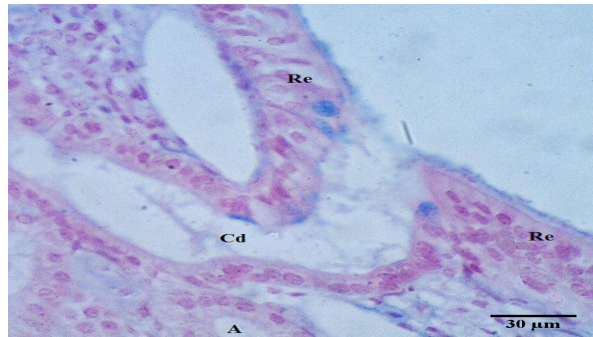


Figure10: Magnified section of Jacobson's gland shows: alveoli (A) which give the negative result for Alcian blue (1 pH) & nuclei of acinus cells (n).

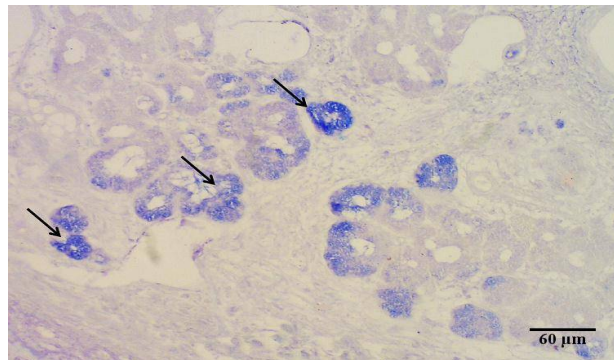


Figure 11: section of Jacobson's gland shows: alveoli which give the positive result (arrows) for carboxylated mucin. Alcian blue-aldehyde fuchsin stain.





Pressure effect on Superconducting Properties of $\text{Bi}_2\text{Pb}_2\text{Sr}_2\text{Ca}_2\text{Cu}_{3-x}\text{Co}_{0.2}\text{O}_{10+\delta}$ system

Amal K. Jassim* and Asmaa A.Hussien

Department of Physics, College of Science, Baghdad, University of Baghdad, Baghdad, Iraq.

Received: 01 Dec 2017

Revised: 23 Dec 2017

Accepted: 25 Jan 2018

*Address for correspondence

Amal K. Jassim

Department of Physics,
College of Science, Baghdad,
University of Baghdad, Baghdad, Iraq.
E.mail: amelalmalki1974@yahoo.com



This is an Open Access Journal / article distributed under the terms of the **Creative Commons Attribution License** (CC BY-NC-ND 3.0) which permits unrestricted use, distribution, and reproduction in any medium, provided the original work is properly cited. All rights reserved.

ABSTRACT

Bulk polycrystalline $\text{Bi}_2\text{Pb}_{0.3}\text{Sr}_2\text{Ca}_2\text{Cu}_{3-x}\text{Co}_x\text{O}_{10+\delta}$ sample with ($x=0, 0.2, \dots$) was prepared by a solid state reaction method. The effects of pressure (press) have been investigated to obtain the optimum conditions for the formation and stabilization of the superconducting phase. An increase of critical temperature was found when the pressure increases from 0.3 GPa to 0.7 GPa. On the other side an increases of the pressure to 0.9 GPa decrease of the T_c .

Keywords: BCCO System, Superconductor Properties, x-ray diffraction.

INTRODUCTION

To get a high – T_c superconductors, can changed many parameters such as sintering temperature, pressure and substitution or addition of other element in the Cu and Bi sites. Therefore, Pb is the most important substituting element that influences the microstructure, phase composition, and the related superconducting properties of the BSCCO system. The presence of Pb in the initial mixture favors the reaction kinetics of the Bi- (2223) phase [1,2,3]. Aydin et al. (2009) [4] investigated the influence of the addition of Gd to $\text{Bi}_{1.8}\text{Pb}_{0.35}\text{Sr}_{1.9}\text{Ca}_{2.1}\text{Cu}_3\text{Gd}_x\text{O}_y$ superconductor for $x=0.1-0.5$ prepared by solid state reaction methods. They found that the transition temperatures, Vickers hardness, young modulus, yield strength and fracture toughness values of the samples strongly dependent on the Gd addition and decreased with an increase the Gd addition. From XRD they found that the addition of Gd degraded the formation of high- T_c phase.

Jannah et al. (2011) [5] studied the effect of nano Co_3O_4 addition on the properties of BPCCO system prepared by solid state reaction method. Two kinds of precursor powder were studied; pure Bi(Pb)-Sr-Ca-Cu-O and mixture of Bi(Pb)-Sr-Ca-Cu-O with nano Co_3O_4 powder (0.01 wt% to 0.04 wt%). Co_3O_4 act as the magnetic impurities in the superconductor system. From the results, they showed that a low concentration and appropriate amount of magnetic





Amal Jassim and Asmaa Hussien

impurities enhanced the critical temperature of Bi (Pb)- Sr-Ca-Cu-O superconductor and the samples contained both the high T_c phase(2223) and the low T_c phase (2212). Ghazala *et al.*(2013) [6] investigated the influence of the Pressure on the Superconducting and Mechanical Properties of $\text{Bi}_{1.6}\text{Pb}_{0.4}\text{Sr}_{1.8}\text{Ba}_{0.2}\text{Ca}_2\text{Cu}_{2.2}\text{Ni}_{0.8}\text{O}_{10+\delta}$ System. An improvement of mechanical properties was found when the pressure increases from 0.3 GPa to 0.9 GPa. On the other side an increases of the pressure to 1.1 GPa decrease in the micro hardness, Young modulus and yield strength. Ebtisam (2015) [7] studied the effect of vanadium addition on the properties of $\text{Bi}_{1.7}\text{Pb}_{0.3}\text{V}_x\text{Sr}_2\text{Ca}_2\text{Cu}_{3-y}\text{Ti}_y\text{O}_{10+\delta}$ system prepared by solid state reaction method. The XRD analyses showed an orthorhombic structure with two phases high-2223 phase and low-2212 phase in addition to that an impure phase was found. The higher T_C value was 123K which found for the higher value of oxygen content for the bulk composition $\text{Bi}_{1.7}\text{Pb}_{0.3}\text{V}_{0.2}\text{Sr}_2\text{Ca}_2\text{Cu}_{2.8}\text{Ti}_{0.2}\text{O}_{10+\delta}$.

EXPERIMENTAL

The system of $\text{Bi}_2\text{Pb}_{0.3}\text{Sr}_2\text{Ca}_2\text{Cu}_{3-x}\text{Co}_x\text{O}_{10+\delta}$ with($x=0, 0.2$) was prepared by a solid state reaction method by mixing oxides, carbonates and nitrates $\text{Bi}_2(\text{CO}_3)_3$, Pb_3O_4 , $\text{Sr}(\text{NO}_3)_2$, CaCO_3 , CuO and CoO with molecular weights (Wm) equivalent to the proportion of high purity powders (99.9%), Then pressed the mixture into pellets under different pressures (0.3, 0.5, 0.7, and 0.9GPa) using hydraulic press type (Specac). Resistance-temperature data were obtained by using four point probe DC method at temperature range (77 - 300) K to determine the critical temperature (T_c). The crystal structure of the prepared samples were obtained by x-ray diffraction(XRD) method, using x-ray diffractometer type Philips Source: $\text{Cu } K\alpha$. The lattice parameters were calculated by using a computer program based on Cohen's least square method[8]. The oxygen content in the ceramic oxide superconductor samples was determined by using iodometric titration technique which is a simple chemical method [9].

RESULTS AND DISCUSSION

The critical temperature dependence of the resistivity (ρ) for the samples of the nominal composition $\text{Bi}_2\text{Pb}_{0.3}\text{Sr}_2\text{Ca}_2\text{Cu}_3\text{O}_{10+\delta}$ and $\text{Bi}_2\text{Pb}_{0.3}\text{Sr}_2\text{Ca}_2\text{Cu}_{2.8}\text{Co}_{0.2}\text{O}_{10+\delta}$ sintered at 830°C for 140 h under different pressures (0.3, 0.5, 0.7, and 0.9GPa) are shown in Figs. (1 and 2).

From these figures and Table(1) note that the values of the critical temperature (T_c) enhance with increasing pressure from 0.3GPa and 0.5GPa to 0.7GPa. It is believed that this behavior may due to the increases carrier concentration n_h in the CuO_2 planes, the change of n_h within the unit cell resulting in the improvement of the critical temperature[10].The best pressure is 0.7GPa where T_c equal to (114, 116)K at $x=0, 0.2$.

While the decreases of T_c with increasing pressure to 0.9GPa as shown in Fig.(3) may be due to that pressure induced change in carrier concentration assuming that the change distribution among the crystallographically in equivalent CuO_2 layers in nonhomogeneous Or can explain this behavior as "the deviation from stoichiometry and disordering of these compound lead to decrease the value of T_c with increasing pressure to 0.9GPa" This results agreement with Vonsovsky *et al.*[11].

The x-ray diffraction patterns with Miller indices for all the superconductor samples sintered at 830°C for 140h under different pressures for compositions $\text{Bi}_2\text{Pb}_{0.3}\text{Sr}_2\text{Ca}_2\text{Cu}_3\text{O}_{10+\delta}$ and $\text{Bi}_2\text{Pb}_{0.3}\text{Sr}_2\text{Ca}_2\text{Cu}_{2.8}\text{Co}_{0.2}\text{O}_{10+\delta}$ are shown in Figs. (4, 5). These figures indicate that all the samples have orthorhombic structure with lattice constants (a , b and c) listed in Table (2).

All the major peaks correspond to the Bi-2223 phase, the minor impurity phases detected include $\text{Sr}_2\text{Ca}_2\text{Cu}_7\text{O}_8$ and unknown phase. Also we have seen an improvement in the structure properties that appears with increasing pressure up to 0.7GPa. It observed from Figs.(4 and 5) that peaks intensity for the free sample such as $h(0012)$ and





Amal Jassim and Asmaa Hussien

H(0014)] increases with increasing the value of pressure. New peaks were appearance attributed to Bi-2212 phase belongs to L(0211), L(113) and L(008) with increasing the value of pressure to 0.9GPa.

Values of lattice parameters a, b, c, unit cell volume, c/a ratio, density of unit cell and volume fraction of high TC phase and low TC phase have been calculated for the compositions $\text{Bi}_2\text{Pb}_{0.3}\text{Sr}_2\text{Ca}_2\text{Cu}_3\text{O}_{10+\delta}$ and $\text{Bi}_2\text{Pb}_{0.3}\text{Sr}_2\text{Ca}_2\text{Cu}_{2.8}\text{Co}_{0.2}\text{O}_{10+\delta}$ for different pressure (0.3, 0.5, 0.7 and 0.9GPa) as shown in the Table (2). Little and random variation is found for these values as pressure is varied. The best value of pressure on the powder to form a pellet is about 0.7GPa for x=0 and 0.2, which produces samples with the highest values of c, c/a and V_{2223} .

According to the high pressure, two phenomenological models are adopted in order to indicate which parameters could play an important role in reaching a higher T_c based on the crystal structures. In the first model Wheatley *et al.* [12] assumed that the charge carriers or holes are distributed equally between all the CuO_2 layers within a unit cell regardless of their number. While the second model Haines *et al.* [13] suggested that the possibility of a nonhomogenous charge distributed among the bioequivalent CuO_2 layers in the compounds is explicitly taken into account. It should be pointed out that pressure larger 0.5 is not suitable and produce melted pellets for samples with x=0.4, 0.6, 0.8, 1, 2 and 3.

Excess of oxygen content (δ) has been measured by using the idiometric titration method for the samples Table (3) show the variation of the transition temperatures and oxygen content (δ) for the nominal compositions of $\text{Bi}_2\text{Pb}_{0.3}\text{Sr}_2\text{Ca}_2\text{Cu}_3\text{O}_{10+\delta}$ and $\text{Bi}_2\text{Pb}_{0.3}\text{Sr}_2\text{Ca}_2\text{Cu}_{2.8}\text{Co}_{0.2}\text{O}_{10+\delta}$ prepared under different pressures. This Table show a direct relationship between O content and transition temperature.

From this Table we can notice that the values of δ increased for the samples prepared under pressures 0.3Gpa, 0.5Gpa and 0.7Gpa, besides that T_c was increased this may be due to the pressure enhancement hole concentration in the Cu-O₂ layers. while increases pressure to 0.9GPa decreases the oxygen content (δ) and the critical temperature T_c .

CONCLUSIONS

The conclusion from the results can be summarized as follows:

- The highest critical temperature 116K was obtained for $\text{Bi}_2\text{Pb}_{0.3}\text{Sr}_2\text{Ca}_2\text{Cu}_{2.8}\text{Co}_{0.2}\text{O}_{10+\delta}$ sample which pressed under pressure 0.7Gpa with optimum value of excess oxygen ($\delta=0.292$).
- XRD pattern analyses have shown orthorhombic crystal structure for all samples with two phases high- T_c phase (2223) and low- T_c phase (2212). In addition to that impure phase was found.

REFERENCES

1. J.M.Tarascon, Y.Le Page, L.H.Greene, B.G.Bagley, P.Barboux, D.Hwang, G.W.Hull, W.R.Mckinnon and M.Giroud; *Phys.Rev.* B38- 2504(1988).
2. D. Azhar, "The effect of n variation on the high- T_c super. behavior of the $\text{Bi}_2\text{Sr}_2\text{Ca}_n\text{Cu}_n\text{O}_{2n+4}$ system", Ph.D. Thesis, Al-Nahrin University, College of Science, (2000).
3. M.Mizuno, H.Endo, J.Tsuchiya, N.Kijima, A.Sumiyama and Y.Oguri; Kitazawa, Ishiguro (Eds), *Advances in Superconductivity*, ISEC, Aug. 28-31, Nagoya, 3-15, Springer – Verlag, (1988).
4. H. Aydin, O. Cakiroglu, M. Nursoy, and C. Terzioglu, *1, 47, 2*, (2009).
5. A. N. Jannah, R. Abd- Shukor, H. Abdullah, A. Agail. *American Institute of Physics conference series V. 1415, P.83*, (2011).





Amal Jassim and Asmaa Hussien

6. Ghazala Y. Hermiz, Bushra A. Aljurani, Hassan A. Thabit, Advances in Materials Physics and Chemistry, V3, p 42, (2013).
7. Ebtisam Khalil Alwan Al-Bayati, "Effect of Vanadium addition on superconducting thin film of Bi_{1.7}Pb_{0.3}Sr₂Ca₂Cu_{3- γ} Ti _{γ} O_{10+ δ} system" A Thesis Submitted to the Council of the College of Science, University of Baghdad,(2015).
8. P.Komarck, Supercond.Sci Technol.V.13, P.456. (2000).
9. M. Manthiram , J.S.Swinnea, Z T.Sui,H.Steinink , and J.B.Good enough, J.Am.chm.soc. V.109. P.6667 (1987).
10. X. J. Chen, H. Q. Lin and C. D. Gong "Pressure Dependence of T(c) in Y-Ba-Cu-O superconductors" Physical .Review latter, No.10, V.85, P.2180, (2000).
11. S.V.Vonsovsky, Yu. A. Lzumov and E. Z. Kurmaev "Superconductivity of transition meatels" Ch.6, Spring – Verlag Berlin Heidelberg New Yourk (1982).
12. M. Wheatley, T. C. Hsu,and P.S.W. Aderson :Nature (Landon). V.333, P.121 (1983).
13. E. M. Haines and J. L. Tallon, Phys Rev B,V.45, P.3172 (1992).

Table (1): Critical temperature (TC) for different pressure for the composition Bi₂Pb_{0.3}Sr₂ Ca₂Cu_{3-x} Co_xO_{10+ δ} with x=0, 0.2.

x	Pressure GPa	T _c (K)
0.0	0.3	106
	0.5	112
	0.7	114
	0.9	101
0.2	0.3	107
	0.5	113
	0.7	116
	0.9	105

Table (2): Variation of values, lattice parameters , c/a, volume fraction and density ρ_m for different pressure of composition Bi₂Pb_{0.3}Sr₂ Ca₂Cu_{3-x} Co_xO_{10+ δ} (x=0,0.2).

X	PG Pa	a (Å)	b(Å)	c (Å)	c/a	V (Å ³)	ρ_m (gm/cm ³)	V ₂₂₂₃ %	V ₂₂₁₂ %
0	0.3	5.44	5.394	37.084	6.816	1088	1.437	76.643	22.467
	0.5	5.365	5.454	37.212	6.936	1088	1.436	79.554	19.556
	0.7	5.492	5.337	37.272	6.786	1092	1.431	71.943	27.167
	0.9	5.414	5.292	37.009	6.835	1060	1.474	65.732	32.378
0.2	0.3	5.381	5.401	37.081	6.891	1077	1.469	75.568	23.542
	0.5	5.447	5.361	37.149	6.783	1055	1.452	51.723	47.387
	0.7	5.413	5.512	37.196	6.871	1109	1.426	70.632	28.478
	0.9	5.423	5.338	37.08	6.837	1073	1.474	68.783	30.327





Amal Jassim and Asmaa Hussien

Table (3): The values of oxygen content(δ) and critical temperature (T_c) for the samples nominal composition of $\text{Bi}_2\text{Pb}_{0.3}\text{Sr}_2\text{Ca}_2\text{Cu}_3\text{O}_{10+\delta}$ and $\text{Bi}_2\text{Pb}_{0.3}\text{Sr}_2\text{Ca}_2\text{Cu}_{2.8}\text{Co}_{0.2}\text{O}_{10+\delta}$ for sintering temperature 830 °C under different pressure.

Pressure Gpa	X	Oxygen content(δ)	T_c (K)
0.3	0.0	0.1933	102
0.5		0.2347	112
0.7		0.2794	114
0.9		0.1902	99
0.3	0.2	0.1894	107
0.5		0.2434	113
0.7		0.2923	116
0.9		0.1784	104

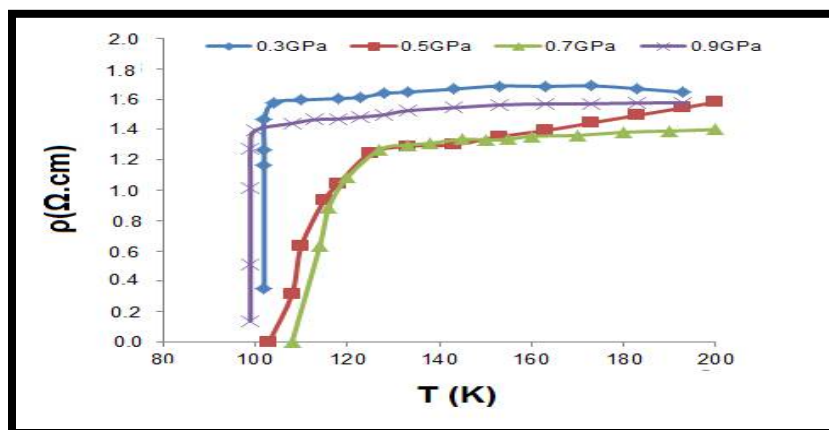


Fig.(1): Temperature dependence of resistivity for $\text{Bi}_2\text{Pb}_{0.3}\text{Sr}_2\text{Ca}_2\text{Cu}_3\text{O}_{10+\delta}$ sintered at 830°C for 140h with different pressure.

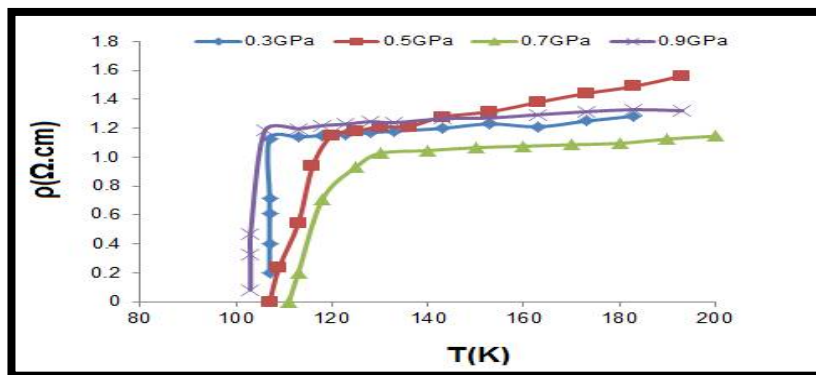


Fig.(2): Temperature dependence of resistivity for $\text{Bi}_2\text{Pb}_{0.3}\text{Sr}_2\text{Ca}_2\text{Cu}_{2.8}\text{Co}_{0.2}\text{O}_{10+\delta}$ sintered at 830°C for 140h with different pressure.





Amal Jassim and Asmaa Hussien

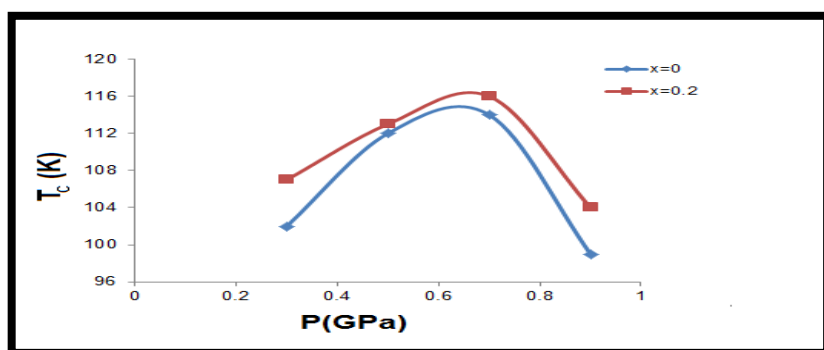


Fig.(3): The critical temperature for the compositions $\text{Bi}_2\text{Pb}_{0.3}\text{Sr}_2 \text{Ca}_2\text{Cu}_3 \text{O}_{10+x}$ and $\text{Bi}_2\text{Pb}_{0.3}\text{Sr}_2 \text{Ca}_2\text{Cu}_{2.8} \text{Co}_{0.2} \text{O}_{10+x}$ as a function of pressure.

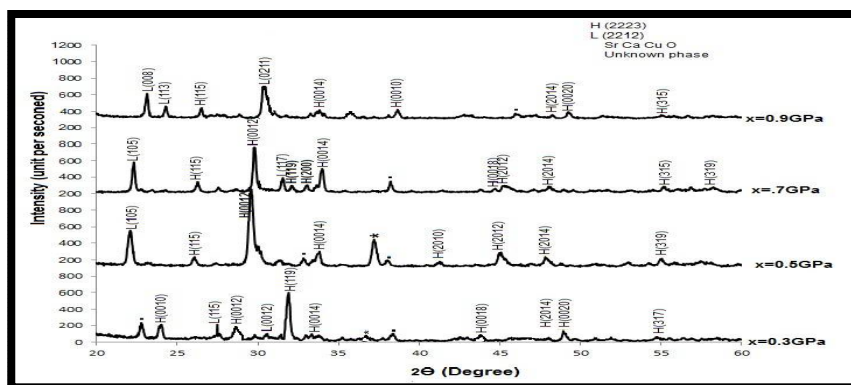


Fig.(4): XRD patterns for $\text{Bi}_2\text{Pb}_{0.3}\text{Sr}_2 \text{Ca}_2\text{Cu}_{3-x}\text{Co}_x\text{O}_{10+x}$ ($x=0$) sintered at 830°C for 140h under different pressure.

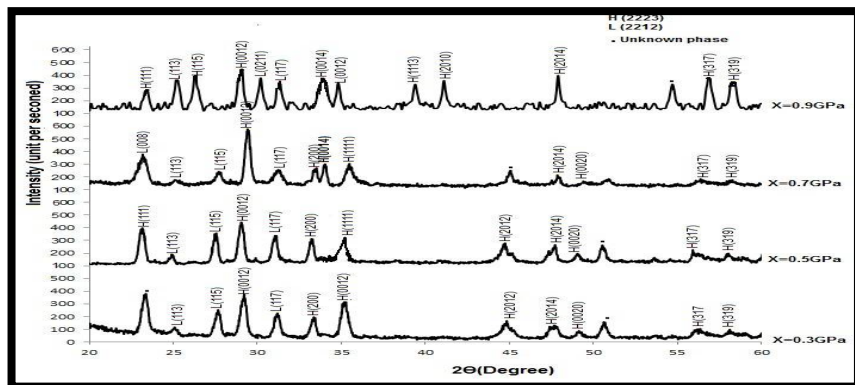


Fig.(5): XRD patterns for $\text{Bi}_2\text{Pb}_{0.3}\text{Sr}_2 \text{Ca}_2\text{Cu}_{3-x}\text{Co}_x\text{O}_{10+x}$ ($x=0.2$) sintered at 830°C for 140h under different pressure.





Attitude and Knowledge of Adugramam Beneficiaries in Goat Farming in Wayanad District

Siddhartha Savale* and R.Senthil Kumar

Department of Veterinary and Animal Husbandry Extension, Kerala Veterinary and Animal Sciences University, Pookode, Wayanad – 673576. Kerala, India.

Received: 01 Sep 2017

Revised: 13 Sep 2017

Accepted: 27 Oct 2017

*Address for correspondence

Siddhartha Savale

Department of Veterinary and Animal Husbandry Extension,
Kerala Veterinary and Animal Sciences University,
Pookode, Wayanad – 673576. Kerala, India.
E.mail: sssiddharth757@gmail.com



This is an Open Access Journal / article distributed under the terms of the **Creative Commons Attribution License** (CC BY-NC-ND 3.0) which permits unrestricted use, distribution, and reproduction in any medium, provided the original work is properly cited. All rights reserved.

ABSTRACT

Kudumbashree, being the pioneer of women empowerment in Kerala, is empowering women through various income generating activities and microenterprises. There are several livestock enterprises selected by the Kudumbashree units and one such livestock activity is Adugramam, a goat farming venture. A study was carried out to analyse the knowledge of Adugramam beneficiaries about goat farming in Wayanad district. By adopting multi stage sampling technique 25 beneficiaries were selected randomly from each taluk i.e. Vythiri, Mananthavady and Sulthan Bathery. The total sample size was 75 and data was collected using the personal interview. Attitude scale developed by Rajkamal and Kunzru (1998) and knowledge test developed by George (2010) was used to measure the beneficiaries' attitude and knowledge about goat farming. The study revealed that majority of the Adugramam beneficiaries studied were of middle age, with secondary level education, belonging to Hindu religion and unreserved communities. It could also be observed that majority of them were living as nuclear families and family size was three to four members. Primary occupation was agriculture and secondary occupation being animal husbandry with above ten years of experience. Land owned by majority of beneficiaries was below one acre with small herd size. The study revealed that a slight majority of the beneficiaries had unfavourable attitude and low knowledge about goat farming.

INTRODUCTION

Women being the pillars of the family unit present a picture of poverty and exploitation both inside and outside the home. Traditionally women's role is confined to four walls of the household where they are engaged in all household works which make them work longer than men every day. Women have lot of opportunity for development but there are barriers which are hindering them from achieving these values. All that is required is to break all those



**Siddhartha Savale and Senthil Kumar**

barriers and participate in all activities needed for development (Ukabhai, 2013). Income generating activities are most effective initiatives which are trending these days by empowering women in all sorts of dimensions. These activities make women economically independent, self-reliable and have cleared many hurdles which hinder women empowerment. Kudumbashree, a poverty eradication and women empowerment programme implemented by State Poverty Eradication Mission (SPEM) of government of Kerala. Kudumbashree is aiding self help groups through microfinance and pleasing them to carry out various income generating activities. Adugramam – Goat farming is one such income generating activity which is empowering women by providing employment and additional source of income to the family. In the present context, it is imperative to study their feeling aspects goat farming and also to analyse the adequacy of knowledge in scientific goat farming to make it a profitable venture. The outcomes of the study are likely to serve as valuable feedback to the policy makers of Kudumbashree organization and other stakeholders to formulate and improvise suitable strategies for enhancing the productivity and transform it as a sustainable venture for improving the livelihood of farm women.

MATERIALS AND METHODS

The research design adopted for the present study was Ex Post facto research design. The unit of study was Livestock based Women Self Help Group (LWSHG) members. Multi stage sampling technique was used to select the final respondents for the study. At first stage Wayanad district was purposively selected for the study followed by selection of three taluks namely Vythiri, Mananthavady and Sulthan Bathery of the district in the second stage. The third stage was selection of LWSHG at the block level. Five groups each consisting of five members were selected randomly from each of the three taluks of the district thus making 75 respondents for the study. Interview schedule was used as a tool to collect information from the respondents. The interview schedule included socio- economic variables such as age, religion, caste, family type, family size, education, primary occupation, secondary occupation, activity experience, land owned and livestock possession. To measure the attitude of beneficiaries towards goat farming attitude scale developed by Rajkamal and Kunzru (1998) was used. To analyse knowledge level of beneficiaries in goat farming knowledge test developed by George (2010) was used. Data was analysed using simple statistical tools such as Frequency, Percentages, Mean score and Dalenius Hodges cumulative square root frequency.

RESULTS AND DISCUSSION

The socio-economic profile of respondents of the study sample is tabulated in the Table 1. It can be observed that 60.00 per cent of the beneficiaries belonged to middle (36 to 55 years) age followed by 22.67 per cent and 17.33 per cent of the beneficiaries were in to old (≥ 56 years) age and young (≤ 35 years) age group respectively. The reason may be due to the fact that middle aged persons are more capable to carry out activities of the farm in addition to household work. Another reason may be that there was the age limit to join as a member of Adugramam is 60 years. The above finding was in agreement with Chetan (2014) and Soni (2016). Half of the beneficiaries 50.67 per cent were Hindus followed by Christians (38.67%) and Muslims (10.67%) and evaluation of caste pattern revealed that 60.00 per cent of the beneficiaries belonged to general caste followed by STs (20.00%), OBCs (18.67%) and SCs (1.33%). As per 2011 census report of religion wise population of Wayanad district Hindu population is highest in the district and hence this might be the reason why majority of beneficiaries were Hindus.

It is also curious to note that the second highest proportion of beneficiaries of Aadugramam was belonging to Scheduled Tribes. The habitat of the Tribes close to forest which would facilitate the access of goats to the forest for browsing, relatively higher skill required for dairy farming, constraints in marketing of milk, etc. might have forced them to join Aadugramam. Analysis of family type revealed that 64.00 percent of the beneficiaries belonged to nuclear family followed by joint family (36.00%). This reflects the trend of modern social system where the desire to live an independent life, insulation against probable familial conflicts, tendency of the parents to give their children a



**Siddhartha Savale and Senthil Kumar**

separate living space, etc. This finding was in line with Thangamani and Muthuselvi (2013). Size of family varied from three to four members for 62.67 per cent of the beneficiaries followed by five to six members (29.33%), one to two members (6.67%) and seven to above (1.33%). As most of the beneficiaries were belonged to middle age category with nuclear family type usually the family would be consisted of parents with one or two children. The above finding was in line with Rathod and Damodhar (2014).

With respect to educational status 33.33 per cent of beneficiaries had secondary education while the beneficiaries belonging to illiterate, primary, higher secondary and diploma education categories were 16.00 per cent, 24.00 per cent, 22.67 per cent and 4.00 per cent respectively. None of the beneficiaries had education of graduation and above. Compulsory and free education up to primary level, equal opportunities for females, realization of importance of education, etc. were the facilitating factors for the increased literacy rate of the respondents. The present finding was in agreement with Haque *et al.* (2014). Primary occupation for 78.67 per cent of the beneficiaries was agriculture followed by farm laborers (9.33%), self-employment (8.00%) and animal husbandry (4.00%). None of the beneficiaries were neither unemployed nor government employees. Secondary occupation for 96.00 per cent of the beneficiaries was animal husbandry followed by agriculture (2.67%) and self-employment (1.33%), and none of them were belonging to farm laborer category. This might be due to the fact that Wayanad is basically an agrarian district and majority of the beneficiaries of the three projects were mostly hailing from these families.

Experience of the members revealed that 85.33 per cent of the beneficiaries were having high experience in goat farming followed by moderate experience (12.00%) and less experience (2.67%). Agriculture and animal husbandry are being considered as family occupation the beneficiaries had relatively more experience in the selected livestock activities. The above finding was in line with Chethan (2014). Land owned by 54.67 per cent of the beneficiaries were of below one acre followed by up to 10 cents (21.33%), one to two acres (16.00%) and above two acres (8.00%) and none of the beneficiaries were landless. The smaller landholding might be due to increased population results in fragmentation and subdivisions of land by family members. The above finding is in line with that of Chethan (2014). Livestock possessed by 25.33 per cent of the beneficiaries were ranging from three to four goats followed by 22.67 per cent, 20.00 per cent, 13.33 per cent, 10.67 per cent and 8.00 per cent with five to six goats, one to two goats, seven to eight goats, nine to ten goats, above 11 goats respectively.

Data in table 2 revealed that 28.00 per cent of beneficiaries were having favourable attitude towards goat rearing whereas 26.67 per cent, 25.33 per cent and 20.00 per cent of beneficiaries were having very less favourable, less favourable and very high favourable attitude towards goat farming respectively. The more number of years of experience in respective livestock farming activities interwoven with their daily life processes would have created a psychological association with their enterprise which might have reflected in their favourable attitude. As pursuing livestock enterprise not considered as white collar occupation they lack status in the society which deserve to them and which would have been echoed in their unfavourable attitude. This also could be due to non-scientific goat farming, which is evidenced from a slight majority of members expressed unfavourable attitude towards goat farming, result in low remuneration accrued to them.

Table 3 indicated that 40.00 per cent, 25.33 per cent, 21.33 per cent and 13.33 of the beneficiaries were having low, high, very high and very low knowledge about goat farming respectively. Since majority of the beneficiaries had primary to secondary level education that could have posed some constraints on learning through digital media, understanding and adopting the modern farming techniques for improved production etc. The gender also could have created restriction on acquiring knowledge from cosmopolite sources. The results were identical to Kumari (2014) but were in contrast with findings of Chethan (2014) who noted that most of the respondents had medium knowledge.





CONCLUSION

The study revealed that a slight above half of the respondents had unfavourable attitude towards goat farming and were having low level of knowledge in scientific goat farming. Though majority of them highly experienced in goat farming it was not favourably transcended into the attitude and scientific goat farming. Hence there is an urgent need to impart training on improved goat farming practices to perform the activity efficiently and economically.

REFERENCES

1. Chethan, G.N. 2014. Impact assessment of the Livestock Development for Livelihood Support Programme in Wayanad district. *M.V.Sc thesis*, Kerala Veterinary and Animal Sciences University, Pookode.
2. George, A., Rajkamal, P.J. and Jiji, R.S. 2010. Analysis of socio-personal profile of livestock based self help group members of Thrissur district. *J. Ind. Vet.Ass.* 10(1): 38-42.
3. Kumari, N. 2014. Study on status and constraints of goat rearing in and around Ranchi district. *M.V.Sc thesis*, Birsa Agricultural University, Ranchi, Jharkhand.
4. Rajkamal, P.J. and Kunzru, O.N. 1998. A scale to measure attitude of farmers towards goat rearing. *J. Ext. Edu.* 9: 2177-2182.
5. Rathod, M.K. and Damodhar, P. 2014. Impact of MAVIM Activities on Empowerment of Rural Women. *Ind. Res. J. Ext. Educ.* 15(1): 8-11.
6. Soni Arti, N., Pandya C.D. and Patel G.R. 2016. Impact of self help groups on socio-economic status of tribal women in adopted villages of KVK, Tapi, Gujarat, India. *Int. J. Agri. Sci.* 8(20): 1357-1361.
7. Thangamani, S. and Muthuselvi, S. 2013. A study on women empowerment through self-help groups with special reference to Mettupalayam Taluk in Coimbatore District. *J. Bus. Mgmt.* 8(6): 17-24.
8. Ukabhaj, C. K. 2013. Participation of farm women in decision making process with respect to animal husbandry practices. *Ph.D. thesis*, Junagadh Agricultural University, Junagadh.

Table 1. Socio economic profile of respondents

Variables	Category	Frequency
Age (years)	Young (≤ 35)	13 (17.33)
	Middle Age (35 to 50)	45 (60)
	Old Age (≥ 50)	17 (22.67)
Religion	Hindu	38 (50.67)
	Muslim	8 (10.67)
	Christian	29 (38.67)
	Others	0
Caste	General	45 (60)
	SC	1 (1.33)
	ST	15 (20)
	OBC	14 (18.67)
Education	Illiterate	12 (16)
	Primary	18 (24)
	Secondary	25 (33.33)
	Higher secondary	17 (22.67)
	Diploma	3 (4)
	Under graduation	0




Siddhartha Savale and Senthil Kumar

	Post-graduation	0
	Doctoral	0
Family type	Joint	27 (36)
	Nuclear	48 (64)
Family size	1 to 2 Members	5 (6.67)
	3 to 4 Members	47 (62.67)
	5 to 6 Members	22 (29.33)
	7 to 8 Members	1 (1.33)
Primary occupation	Unemployed	0
	Agriculture	59 (78.67)
	Animal husbandry	3 (4)
	Govt. employee	0
	Self-employment	6 (8)
	Farm labour	7 (9.33)
	Any other	0
Secondary occupation	No secondary occupation	0
	Animal husbandry	72 (96)
	Farm labour	0
	Agriculture	2 (2.67)
	Self-employment	1 (1.33)
	Any other	0
Experience	Least (Less than 1 year)	0
	Less (1 to 5 years)	2 (2.67)
	Experienced (5 to 10 years)	9 (12)
	Highly experienced (Above 10 years)	64 (85.33)
Land owned	Landless	0
	Up to 10 cents	16 (21.33)
	Below 1 acre	41 (54.67)
	1-2 acres	12 (16)
	Above 2 acres	6 (8)
Livestock possession	1 to 2 Goats	15 (20)
	3 to 4 Goats	19 (25.33)
	5 to 6 Goats	17 (22.67)
	7 to 8 Goats	10 (13.33)
	9 to 10 Goats	8 (10.67)
	Above 11 Goats	6 (8)

Values in the brackets are percentages





Siddhartha Savale and Senthil Kumar

Table 2. Distribution of Adugramam beneficiaries based on attitude towards goat farming n=75

Attitude towards goat farming	Frequency	Percentage
Highly unfavorable(16-20)	20	26.67
Unfavorable(20.01-22)	19	25.33
Favorable(22.01-25)	21	28.0
Highly favorable(25.01-28)	15	20.0
Total	75	100

Table 3. Distribution of Adugramam beneficiaries based on knowledge about goat farming n=75

Knowledge about Goat farming	Frequency	Percentage
Very low(7-13)	10	13.33
Low (13.01-17)	30	40
High (17.01-19)	19	25.33
Very high (19.01-26)	16	21.33
Total	75	100





Detection of Single Nucleotide Polymorphisms (SNPs) in *INSR* (Insulin Receptor Gene) in Iraqi women with Polycystic Ovarian Syndrome (PCOS).

Noor H.Mohammad* and Abdul Kareem A. AL-Kazaz

Department of Biotechnology, College of Science, University of Baghdad, Baghdad, Iraq.

Received: 04 Dec 2017

Revised: 23 Dec 2017

Accepted: 17 Jan 2018

*Address for correspondence

Noor H. Mohammad

Department of Biotechnology,
College of Science, University of Baghdad,
Baghdad, Iraq.
E.mail: noorgardinia@yahoo.com



This is an Open Access Journal / article distributed under the terms of the **Creative Commons Attribution License** (CC BY-NC-ND 3.0) which permits unrestricted use, distribution, and reproduction in any medium, provided the original work is properly cited. All rights reserved.

ABSTRACT

In this case-control design study , 50 clinically diagnosed Polycystic Ovarian Syndrome (PCOS) in Iraqi female and 20 healthy Iraqi female were enrolled for analysis of the Exon 17 C/T Single Nucleotide Polymorphisms in *INSR* gene as predisposing molecular marker for PCOS and its relationship with diabetes.

Genomic DNA was extracted from whole blood of each subject using wizard genomic DNA purification kit. Specific primers for Single Nucleotide Polymorphism (SNPs) analysis of *INSR* Exon 17, Intron 8 and Intron 3 were used Single Nucleotide Polymorphism-Polymerase Chain Reaction (SNPs-PCR) amplification reaction. Post PCR Restriction Fragment Length Polymorphism (PCR-RFLP) was done for PCR-Products using the Restriction Enzyme PMLI.

In conclusion, the Exon 17 C/T Single Nucleotide Polymorphism in *INSR* gene can consider as predisposing molecular marker for PCOS that can transmit offspring, CRC and Breast Cancer in Iraqi patients and the Intron 8 Single Nucleotide Polymorphism can consider as predisposing molecular marker for PCOS and Diabetes that can be transmitted offspring in Iraqi patients.

Keywords: PCOS, Diabetes , *INSR*.





INTRODUCTION

Polycystic ovarian syndrome, which used to be called Stein-leventhal Syndrome, is a common condition affecting 5-10% of women of childbearing age. This disorder is probably the most common hormonal abnormality in women of reproductive age. In 95% of women with PCOS, an ultrasound of the ovaries will reveal cysts that can be seen on the surface of the ovary. These ovarian cysts are often lined-up to form the appearance of a "pearl necklace" (4). The susceptibility genes for PCOS are unknown; several candidate genes have been evaluated. Most of researchers found the evidence that *INSR* gene show consistent linkage and association with PCOS. The *INSR* receptor gene comprises 22 exons spanning 120kb on chromosome 19. Mutations in exon 17 and intron 13, 8 that encode the tyrosine kinase domain of the insulin receptor, have been shown severe insulin resistance and hyperinsulinemia. Two possible approaches are used to identify a genetic locus for PCOS genes: (i) association studies where a predisposing allele is expected to be found more frequently in the affected population than the normal individuals and (ii) linkage studies where the probands and their families are investigated to determine if particular genomic landmarks are distributed independently or in linkage with the phenotype. While the mode of inheritance is not required for the association studies, it requires a relatively large set of individual for a clear conclusion (5). Many genes presented expression suggesting thus that the genetic abnormality in PCOS affects signal transduction ruling insulin action and their secretion. Although the cause of PCOS is not well understood, insulin resistance may be a key factor. Insulin is vital for the transportation and storage of glucose at the cellular level; it's helps to regulate blood glucose level and has a role in carbohydrate and lipid metabolism. These conditions put those with PCOS at a higher risk of developing type 2 diabetes and cardiovascular disease (2, 1). The aims of this study is to examine whether the insulin receptor *INSR* gene contributes to genetic susceptibility to the PCOS and to analyze the exon 17 C/T single nucleotide polymorphism in *INSR* a predisposing molecular marker for PCOS.

MATERIALS AND METHODS

DNA extraction

Approximately (3-5ml) of blood was taken from each patient by sterile syringe and places EDTA tubes.

- Each blood sample was placed into 15 ml tube.
- Cell lysis solution was added to the sample about 6 ml.
- Blood and cell lysis were mixed together by inverting the tubes several times and incubate them for 10 minutes in room temperature.
- Samples were centrifuged at 10000 rpm for 20 minutes.
- The supernatant was discarding by using a pipette to avoid losing the pellet.
- Add 2 ml of nucleic lysis buffer to the samples.
- The mixtures were mixed by inversion.
- Then 2 ml of protein precipitation solution and vortex the samples for 20 seconds.
- Centrifuge the samples at 10000 rpm for 10 minutes.
- After the centrifugation, the supernatant were transfer to new tubes that contain Isopropanol about 2 ml.
- The mixtures were centrifuged at 10000 rpm for 20 minutes.
- Then discard the supernatants and add 2 ml of 70% ethanol.
- Centrifuge the sample again at 10000 rpm for 10 minutes.
- Aspirate the ethanol and dry the pellet for 10 – 15 minutes.
- The final step is (100µl) of DNA rehydration was added to the samples and storage them overnight at 4 °C.
- At the next day the samples were taken to estimate the DNA concentration by Nanodrop (www.promega.com).



**Noor Mohammad and Abdul Kareem AL-Kazaz****Estimation of the DNA concentration by the Nanodrop equipment**

The DNA concentration was determined by using the Nanodrop about 2µl of each sample which gives the measurement the optical density (O.D) at wave length of 260 nm and 280nm that lead to estimate DNA purity ratio according to this formula.

$$\text{DNA purity ratio} = \text{O.D at 260} / \text{O.D at 280}$$

This ratio was used to detect nucleic acid contamination with protein preparation. DNA quality also can assess by simple analyzing the DNA by Agarose gel electrophoresis (3).

Agarose Gel Electrophoresis

The separation of DNA fragments in Agarose gels in different concentration were used 0.8% for extracted DNA while 1% using for visual checking of specific PCR product. Gels were run horizontally in 0.5 X TBE buffer, DNA sampling were mixed with loading buffer and loaded into the wells of the gel for checking of total DNA, in this steps there will be checking for PCR product that haven't loading dye because of green master mix reaction buffer that contain a compound which increase the density of the sample with blue and yellow dyes. That works as a loading dye when reaction products were analyzed by gel electrophoresis.

Electrophoresis buffer was added to cover the gel and run for 1-2 hours at 5 V/cm. Agarose gel were stained with Ethidium bromide 0.5 g/ml for 20 – 30 minutes. The DNA bands were visualized by U.V transilluminator at 365 nm wavelength (Maniatis *et al.*, 1982). Then the gel documentation system was used for document the bands.

Amplification of DNA by PCR technique.**Specific PCR****PCR reaction performed using the following****Specific primers and their preparation.**

There are variant SNPs in the *INSR* gene were selected based on Xu Xinghua *et al.* (2011) that used in this study. Three pairs of specific primers were provided by (Alpha DNA – Canada) for this marker. The details of these primers which including sequence and their chromosomal locations are presented in table (1). Which provided in lyophilized form and dissolved in sterile distilled water to have the final concentration of 10 pmol/µl.

Go Taq@ Green Master Mix

The master mix reactions were used to achieve the homogeneity of reagents and reduced the risks of contamination. All amplifications were performed on ice in aseptic condition using a laminar air flow hood (6).

Protocol of specific PCR

This protocol consists of:

PCR primers

The specific PCR primers reported into table (2-3)



**Noor Mohammad and Abdul Kareem AL-Kazaz****PCR Mix**

Contain the reaction in tube of 1 ml on ice

Amplification reaction

To Amplify the INSR genes, which present in genomic DNA of PCOS patient, following the reactions that used:

Then add genomic DNA 2 μ l (100ng/ μ l) + mix 23 μ l = 25 μ l.

The quantity and amplification size of PCR product were confirmed by Agarose gel electrophoresis of 5 μ l of amplified DNA on 2% Agarose gel (1 hour and 0.5 X Tris Borate Buffer). The gel stained with Ethidium bromide which visualize the PCR product by U.V transilluminator and then were imaged by gel documentation system. The specific size of PCR products were estimated by comparing with the ladder bench top PCR markers (100bp) (6).

There were some problems appeared on the gel such as:

- Primer dimer
- Unspecific product.

The suitable solution for avoiding these problems by using optimization PCR reaction which consist:

Changing in aneling temperatures

That means using different temperatures one less than the original temperature (58°C less than 60°C) and three temperatures more than the original (62°C , 64°C , 66°C more than 60°C), to know at which temperature that the primer work well and can give a sharp band.

Using 0.7 μ l of primer volume instead of 1 μ l illustrated in PCR master mix (optimization).

Then adding genomic DNA 2 μ l (100ng/ μ l) + mix 23 μ l = 25 μ l.

Changing in time of annealing temperature by using 45 sec. instead of 30 sec

Then The quantity and amplification size of PCR product were confirmed by Agarose gel electrophoresis of 5 μ l of amplify DNA on 2% Agarose gel (1 hour and 0.5 X Tris Borate Buffer). The gel stained with Ethidium bromide which visualize the PCR product by U.V transilluminator and then were imaged by gel documentation system. The specific size of PCR products were estimated by comparing with the ladder bench top PCR markers (100bp) (6, 4).

RESULTS**Blood Sampling**

Sixty eight human blood samples were collected from AL- Yarmok Hospital in Baghdad province, from 17 December 2013 to 17 June 2014, consisting of 46 samples infected with PCOS that have different ages ranged between 11-67 years old and their weight ranged between 30-120 kg as indicated in table (6).





Noor Mohammad and Abdul Kareem AL-Kazaz

According to these data there will be 4 groups that classified due to their ages and weight, these are the properties of each groups:

Group No.1

- Unmarried women with PCOS.
- Aged ranged between 11-35 years.
- Weight ranged between 30-85 Kg

Group No.2

- Married Women with PCOS.
- Aged ranged between 20-35 years.
- Weight ranged between 65-100 Kg .

Group No.3

- Married women with PCOS.
- Aged ranged between (36-51) years.
- Weight ranged between (60-90) Kg.

Group No.4

- Married women with PCOS.
- Aged ranged between (52-67) years.
- Weight ranged between (70-120)Kg.

Twenty blood samples were taken from pregnant women in AL-Yarmok Hospital as a control group which indicated in table (7).

DNA Extraction

DNA samples were extracted by three methods:

Extrip™ Method

In this method there was low DNA concentration with no purity as indicated in (Table 8).

Standard Method

In this method there was suitable DNA concentration with suitable purity amount as indicated in (Table 9).

Genomic® Wizard Purification Kit

There was high DNA concentration and purity as indicated in (Table 10).

This method was preferred among other two methods because of highly DNA concentration and purity, while the first one didn't used because it's gives low DNA concentration and purity, however the second method doesn't longley used because it's need long time for DNA extraction with high cost of material that used.



**Noor Mohammad and Abdul Kareem AL-Kazaz****Detection of INSR gene by Specific PCR Amplification**

The detection of INSR gene in DNA samples amplified by using specific PCR which is couple of specific primers. In the first PCR experiment, a standard concentration of 10 Pmol of each primer, 100 ng of template DNA was added and 35 cycles were performed. The PCR yield were bands of the desired product so; all reaction components were kept at the same concentration as indicated in figure (1).

As a complex multigenic disease various susceptibility genes of PCOS interest with each other and the environmental factors also influence the accuracy and development of the syndrome which is play an important role in the expression of hyperandrogenic phenotype.

Concerning molecular genetic studies, PCOS is one of the most extensively studied endocrinopathys in women and attention has been given to insulin resistance with special focus on the **INSR** gene. Therefore in this study we used family- based analysis in order to investigate the relationship between the INSR gene SNPs and the genetic component of PCOS (6, 5).

The achieving balance between reaction components is usually required to reduced none specific amplification and / or to enhance the yield of desired DNA product and reducing primer dimer that leads to doing an optimized the PCR conditions as indicated in figure (2).

Some samples were taken to amplified with PCR technique by using 3 primers, they are { rs 8108622 & rs10500204 (p1) , rs2059807 (p2) and rs1799819 (p3) }, to detect INSR gene in the DNA samples. The procedure of this technique consists of using 0.7µl from each primers and 2µl of DNA samples. Then the samples were migrated in 0.5X TBE buffer with 2% Agarose for 1 hour at 90V, the result was unclearly bands with unspecific product and primer dimer as indicated in figure (3).

To avoid these problems, using 0.5µl of the primer and migrated the samples with 0.5X TBE buffer and 0.5% Agarose for 45 second at 70V , the same procedure was used for 2 other primers (rs2059807 (p2) and rs1799819 (p3), as indicated in figures (4).

CONCLUSION

Based on the findings of the present study, it is possible highlight the following conclusions:

- The best method that used in this study to have high DNA concentration with high purity is Genomic® Wizard Purification Kit.
- Using fresh blood to have high quantity of DNA better than the frozen blood.
- LH values appears in high level in Women with PCOS either they were married or unmarried.
- FSH values appear in low level in married Women with PCOS.
- Most patients in this study were overweight or obese those mean their BMI value more than 30 kg/m² which cause in type 2 diabetes (T2D).
- The PCOS can happen in age ranged between (10-80 years)
- Find that rs1799817 was not significantly over transmitted to PCOS off spring from their parents and its association with increasing in CRC and breast cancer. While the rs8108622 & rs10500204 and rs2059807 were significantly over transmitted to PCOS off spring from their parents.
- The exon 17 C/T single nucleotide polymorphisms in INSR can't consider as predisposing molecular marker for PCOS in Iraqi women , while the SNPs in intron 3 and intron 8 can be consider as predisposing molecular marker for PCOS in Iraqi women.





Noor Mohammad and Abdul Kareem AL-Kazaz

- Type 2 diabetes can appear in the patients that have menopausal phase more than those who in the reproductive phase.

REFERENCES

1. Ewens, K.; Stewart, D.R. ; Ankenar, W.; Urbaneck, M.; Mcalliste, J.M.; Chen, C.; Baing, K.M.; Parker, S.C.J.; Franks, S. and Berga, S.L. (2012). Does PCOS have development Origins? *Fertil. Steril.* , 97:2-6.
2. Hoeger, K.M. and Oberfield, S.H.E. (2012). Do Women with PCOS have a Unique Predisposition to Obesity? *Fertil. Steril.* , 97:13-17.
3. Maniatis, T.; Fritsch, E.F. and Sambrook, J. (1982). *Molecular Cloning: A Laboratory Manual*, Cold Spring Harbor laboratory, N.Y.
4. Maysaa, A.R. (2013). Molecular Screening for Single Nucleotide Polymorphism in Insulin Receptor Gene in Iraqi Women with Polycystic Ovarian Syndrome. *Int. J. Mod. Biol. Med.*, 3(1): 17-26.
5. Moran, L.J.; Ko, H.; Misso, M.; Nonkes, M.; Talbot, M.; Freson, M.; Thendon, M.; Stepto, N. and Tedee, H.J. (2013). "Diery Composition in the Treatment of Polycystic Ovary Syndrome: A Systematic Review to Inform Evidence Based Guidelines ". *Hum. Reprod.* , 19(5):432.
6. Xu, X.; Zhao, H.; Shi, Y.; You, L.; Bian, Y.; Zhao, Y. and Chen, Z.J. (2011). Family Association Study between INSR gene Polymorphisms and PCOS in Han Chinese. *Reprod. Biol. Endocrinol.* , 9: 76.

Table: 1. The sequences and chromosomal locations of specific primers (Xu et al., 2011).

Primers	Sequence	Locations
*Rs8108622 / rs10500204 (reverse) Rs8108622 / rs10500204 (forward)	5`GAGAATTAGCCAAGCGAGAGTGT3` 5`GTCCCAGATACCAAGGATGTGC3`	INTRON 3
**Rs2059807(reverse) RS2059807 ((forward)	5`TGCTGAGCCCAGGAGTTTG3` 5`GACCCAGTATGCCATCTTTGTG3`	INTRON 8
***Rs1799817 (reverse) RS1799817 (forward)	5`TCCAGAAAGTGATGAGAACGTGAT3` 5`GGTCAACGAGTCAGCCAGTCT3`	EXON 17

*primer 1, **primer 2, ***primer 3

Table: 2. PCR master mix (final reaction volume = 25 µl)

Material conc.	Final conc.	Volume for 1 tube/ µl
D.W	-	8.5
Master mix	1X	12.5
Primer (forward) 10pmol/µl	1µl	1
Primer (reverse) 10pmol /µl	1µl	1
Total reaction volume		23

Table: 3. PCR programme

Steps	Temperatures	Time
Initial denaturation	95 °C	5 min (35 cycle)
Denaturation	94 °C	30 sec.
Annealing	60 °C	30 sec. (primer 1, 2, 3)
Extension	72 °C	1 min
Final extension	72 °C	7 min





Noor Mohammad and Abdul Kareem AL-Kazaz

Table: 4. Optimization PCR Programme:

Steps	Temperatures	Time
Initial denaturation	95 °C	5 min (35 cycle)
Denaturation	94 °C	30 sec.
Annealing	58 °C 60°C 62°C 64°C 66°C	45 sec. (primer 1, 2, 3)
Extension	72 °C	1 min
Final extension	72 °C	7 min

Table: 5. PCR master mix (optimization).

Material conc.	Final conc.	Volume for 1 tube / μ l
D.W	-	9 μ l
Master mix	1X	12.6 μ l
Primer (forward) 10pmol/ μ l	0.7 μ l	0.7 μ l
Primer (reverse) 10pmol / μ l	0.7 μ l	0.7 μ l
Total reaction volume		23 μ l

Table (6): Female blood samples with different ages and weight.

Samples ID	Ages (years)	Weight (Kg)
N1	40	85
N2	32	95
N3	28	82
N4	37	60
N5	36	74
N6	32	95
N7	48	75
N8	29	99
N9	30	75
N10	64	85
N11	21	75
N12	19	60
N13	31	75
N14	24	79
N15	18	60
N16	13	75
N17	47	68
N18	11	28





Noor Mohammad and Abdul Kareem AL-Kazaz

N19	27	60
N20	45	65
N21	35	65
N22	40	62
N23	22	55
N26	28	80
N27	45	75
N28	28	80
N29	39	68
N30	15	53
N31	67	114
N32	15	80
N33	30	88
N34	40	90
N35	28	60
N36	50	80
N37	47	74
N38	24	85
N39	12	80
N40	24	88
N41	30	67
N42	30	50
N43	41	75
N44	63	75
N45	21	65
N46	58	83

Table (7): Control samples from healthy pregnant women (women without PCOS).

Sample ID	Age (year)	Weight (Kg)	DNA Concentration ng/ml
C1	30	80	80.3
C2	26	82	110.5
C3	32	80	140
C4	43	85	223
C5	43	88	130
C6	20	83	259
C7	33	87	50
C8	22	75	109.5
C9	27	85	320
C10	30	88	100





Noor Mohammad and Abdul Kareem AL-Kazaz

C11	32	75	270
C12	20	75	90.1
C13	36	85	153.2
C14	25	110	160
C15	23	70	250
C16	19	85	300
C17	26	90	220
C18	22	70	195
C19	20	75	200
C20	33	95	158

Table (8): DNA samples were extracted by Exiprep® Method

Sample ID	DNA Concentration ng/ml	Purity
N1	6.4	1.1
N2	5.3	1.2
N3	13.7	1.3
N4	11.3	1.4
N5	23.6	0.55
N6	9.7	2
N7	11.9	1.6
N8	16.1	1.1
N9	10.8	1.2
N10	14	1.3
N11	17.3	1.3
N12	7.5	1.2
N13	9.9	1.1
N14	4.9	1.1
N15	9	1.1
N16	8.4	1.5
N17	6.8	1.7
N18	10	1.4
N19	5.6	1.2
N20	0.55	1
N21	3.4	1.2
N22	6.8	1.4
N23	1.6	1.3
N24	20.3	0.44





Noor Mohammad and Abdul Kareem AL-Kazaz

N25	11.2	0.55
N26	13.1	0.71
N27	4.6	0.53
N28	5.3	0.94
N29	5.5	0.45
N30	6.5	0.21
N31	9.5	0.77
N32	17.5	0.4

Table (9): DNA samples were extracted by standard Method.

Sample ID	DNA Concentration $\mu\text{g/ml}$	Purity
N1	150	1.5
N2	133	1.8
N3	156	1.6
N4	188	1.9
N5	200	1.8
N6	100	2
N7	179	1.7
N8	166	1.8
N9	145	1.8
N10	190	1.8

Table (10): DNA samples were extracted by Genomic® Wizard Purification Kit

Samples ID	DNA Concentration ng/ml	Purity
N1	2101.7	1.8
N2	200.7	1.6
N3	1306	1.9
N4	218.9	1.8
N5	74.5	1.7
N6	174.5	1.6
N7	100	1.5
N8	100	1.5
N9	178.1	1.6
N10	955	1.8
N11	182.5	2
N12	2023.5	2
N13	286	2



**Noor Mohammad and Abdul Kareem AL-Kazaz**

N14	66.5	1.8
N15	207.5	1.8
N16	10	1.8
N17	20.4	1.6
N18	240	1.9
N19	276	1.7
N20	20.5	1.8
N21	515	1.9
N22	37.5	1.6
N23	391	1.7
N26	15.5	1.6
N27	61	1.8
N28	47.5	1.8
N29	159.5	1.9
N30	78.6	1.8
N31	68.7	1.9
N32	10	2
N33	259	1.8
N34	116	2
N35	65.5	1.9
N36	16.6	1.8
N37	15	1.7
N38	20	1.8
N39	124	1.8
N40	340	1.8
N41	154	1.9
N42	20.5	1.9
N43	20.4	1.7
N44	52.7	1.8
N45	159	1.9
N46	573.6	1.7



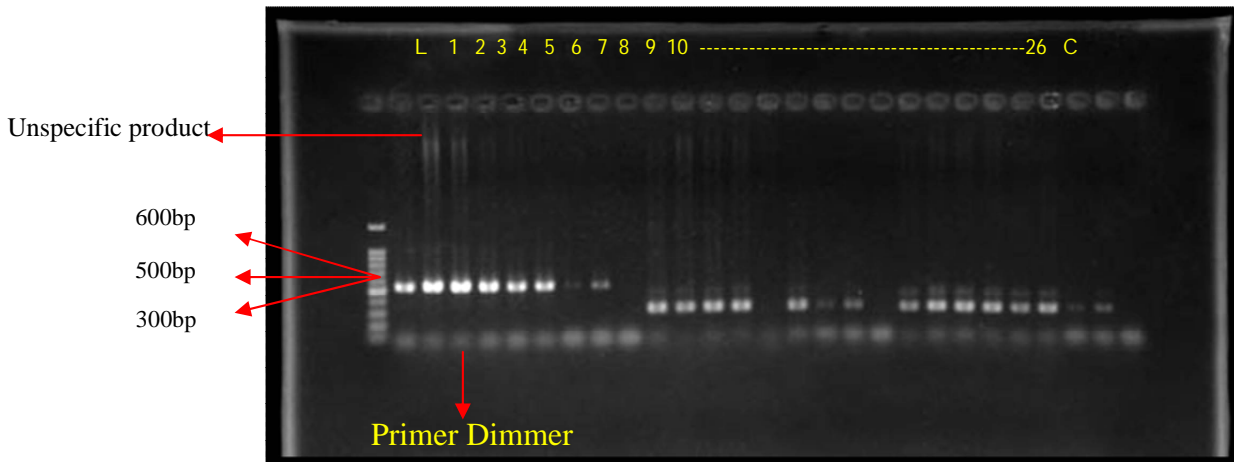


Figure (1): Agarose gel electrophoresis of the INSR gene in DNA samples by specific PCR. Fragments were fractionated by electrophoresis on 2% Agarose gel (1 hr/90V), 0.5X Tris –borate buffer and visualized by Ethidium Bromide staining. The first lane from (1-8) refers to primer 3 (rs1799817) while line (10-26) refers to primer 1 &2 (rs8108622 & rs10500304) and (rs2059807), L = ladder 100bp.

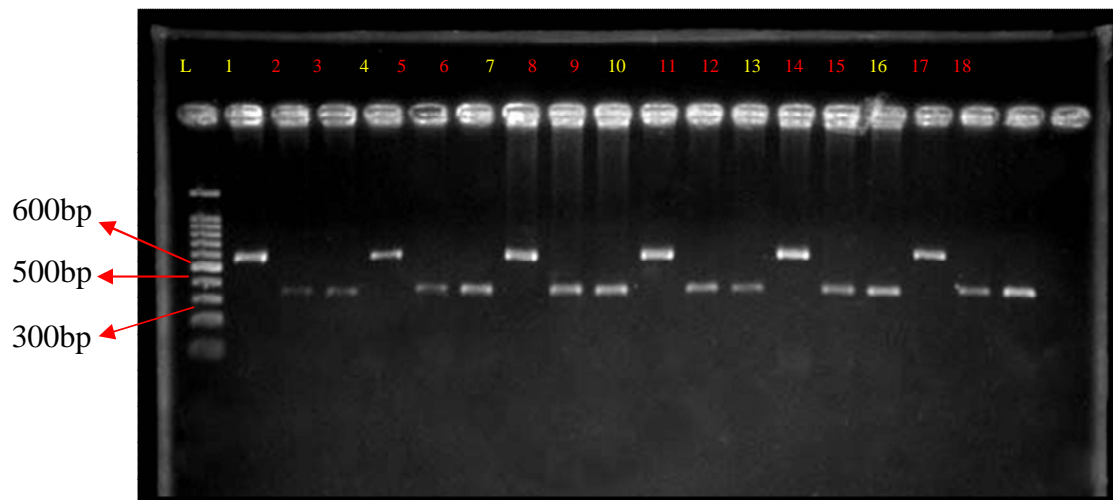


Figure (2): Agarose gel electrophoresis of the INSR gene in DNA samples after optimization reaction of general PCR. Fragments were fractionated by electrophoresis on 2% Agarose gel (1 hr/90V) 62°C, 0.5X Tris –borate buffer and visualized by Ethidium Bromide staining. , the lane (1,4,7,10,13 and 16) refers to primer 3 (rs1799817) and (2,3,5,6,8,9,11,12,14 and 15) refers to primer 1 & 2 (rs8108622 & rs10500204) and (rs2059807), L= Ladder 100bp.





Noor Mohammad and Abdul Kareem AL-Kazaz

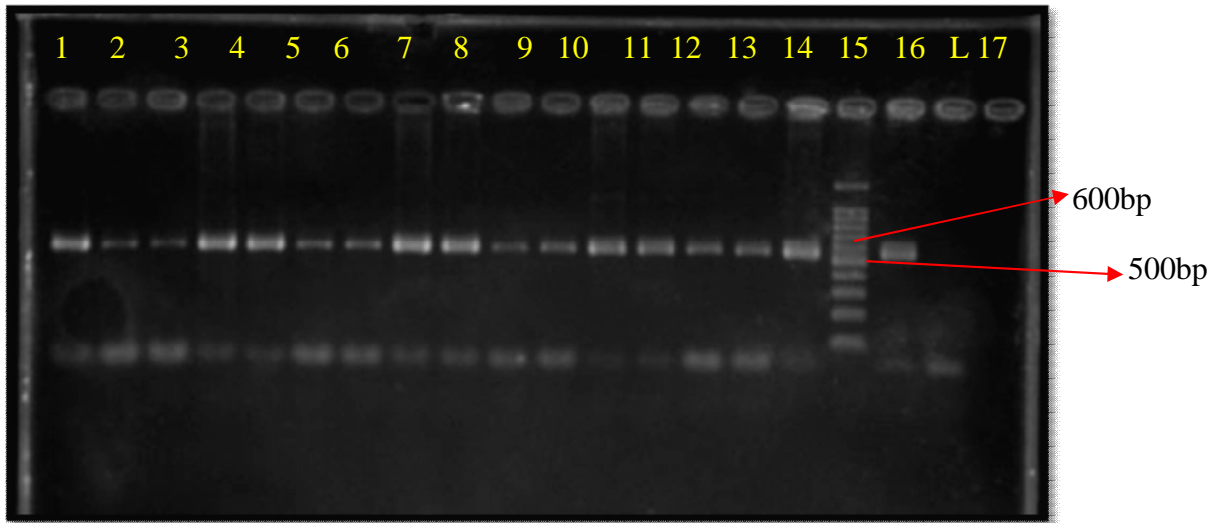


Figure (3): Agarose gel electrophoresis of the INSR gene in DNA samples before optimization reaction of general PCR. Fragments were fractionated by electrophoresis on 2% Agarose gel (1 hr/90V) 62°C, 0.5X Tris –borate buffer and visualized by Ethidium Bromide staining primer 3 (rs1799817), L= ladder 100bp.

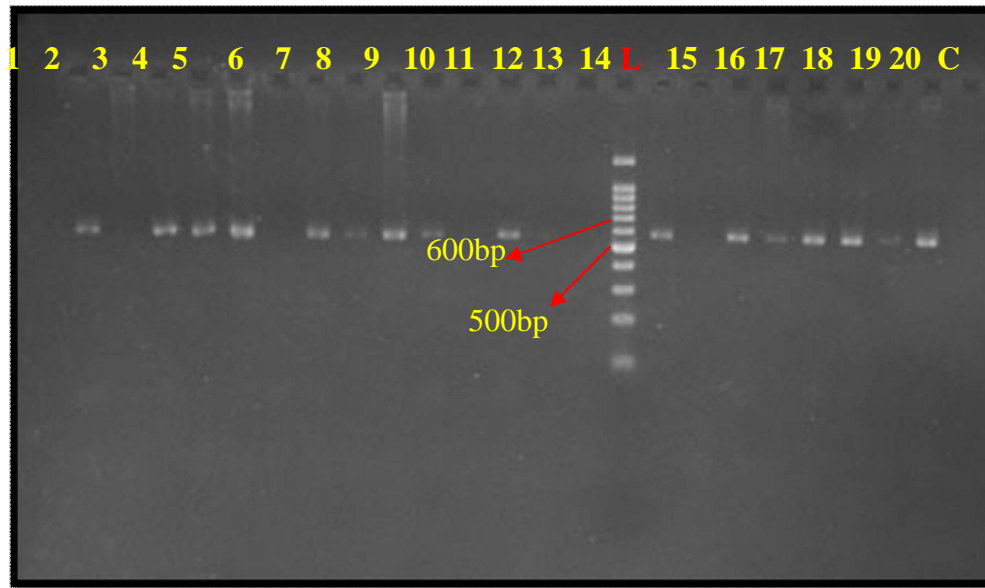


Figure (4): Agarose gel electrophoresis of the INSR gene in DNA samples of primer 3 after optimization reaction of general PCR. Fragments were fractionated by electrophoresis on 2% Agarose gel (1 hr/90V) 62°C, 0.5X Tris –borate buffer and visualized by Ethidium Bromide staining , L= ladder 100bp.





Dielectric and Magnetic Properties of Copper Substituted Manganese Ferrite

Saad F.Oboudi*

Department of Physics, College of Science, University of Baghdad, Baghdad, Iraq.

Received: 27 Nov 2017

Revised: 17 Dec 2017

Accepted: 12 Jan 2018

*Address for correspondence

Saad F.Oboudi

Department of Physics,
College of Science, University of Baghdad,
Baghdad, Iraq.
E.mail: saadoboudi@gmail.com



This is an Open Access Journal / article distributed under the terms of the **Creative Commons Attribution License** (CC BY-NC-ND 3.0) which permits unrestricted use, distribution, and reproduction in any medium, provided the original work is properly cited. All rights reserved.

ABSTRACT

A series of copper substituted manganese nano ferrites samples with the compositional formula $Mn_{1-x}Cu_xFe_2O_4$ ($x=0, 0.2, 0.4, 0.6, 0.8, \text{ and } 1.0$) were prepared by the conventional solid state reaction method, the samples sintered at 900°C for 5 hr. The X-ray diffraction patterns clearly exhibited the existence of single phase cubic spinel structure. With the increment of Cu content the X-ray density, porosity, and the grain size were found to increase, whereas the bulk density was found to decrease. The DC electrical properties were carried out by the two-probe method from room temperature up to 573 K. Electrical resistivity of all samples decreases with the increase of temperature ensuring the semiconducting nature of the ferrites. The DC electrical conductivity determined to increase with the increase of Cu content and reaches a maximum at $x=1.0$. The saturated magnetization of the samples decreased with x increase up to 1. All ferrite samples showed hysteresis characteristic of soft magnetic materials.

Keywords: Mn–Cu ferrite, DC electrical properties, Dielectric constant, Magnetic measurements.

INTRODUCTION

Ferromagnetic materials have attracted a considerable attention of the researchers through decades due to many reasons such as their interesting soft magnetic properties and micro wave frequency applications, they do not obey the reciprocity principle, and can control relatively high powers [1, 2]. They are mixed metal oxides with Fe^{3+} oxides the main component, it is a magnetic material exhibit in ferromagnetic ordering and magnetism due to the superexchange interaction [3]. Ferrites are polycrystalline ceramic materials that are typically formed using a high temperature sintering process [4,5]. They have been studied extensively due to easy to synthesis and abundant uses in many applications in the industry [6,7]. The featured properties and characteristics of ferrites are mostly depended on its chemical composition, preparation methods, sintering time, sintering temperature, nature and





Saad Oboudi

characteristics of the additives and their distribution in the compound. Substituted ferrites are more complex than regular ferrites. Sometimes ferric ions are replaced by trivalent ions of another metal, due to this replacement its physical properties depend on the site preferred by the substituent [8]. $Mn_{1-x}Cu_xFe_2O_4$ manganese copper ferrite belongs to the class of mixed spinel ferrite where “x” varies from 0.0 to 1.0. Manganese ferrite has the spinel structure where oxygen has fcc close packing and Mn^{2+} and Fe^{3+} can occupy either tetrahedral or octahedral interstitial sites [9]. Cu^{2+} is the divalent ion which occupies essentially tetrahedral sites depending on the sample preparation when substituted in ferrites [10]. In order to incorporate the spinel ferrites for a wide range of applications, it is essential to control the electrical resistivity and this can be achieved by controlling the sintering temperature and by proper elemental substitution.

Mixed spinel ferrites show unexpected properties at the nano regime due to the redistribution of cations, cation ionic radii, presence of ion to specific site, crystal field effect, ionic charge [11]. Due to their typical electrical and magnetic properties for technological applications, Cu-containing ferrites form an important and interesting group of ferrites [12]. On the other hand, manganese copper ferrites are low cost materials. The electrical conductivity and dielectric properties of spinel ferrites are most important in ferrites which depend on preparation conditions as it gives important information about the conduction mechanism [13]. Moreover, the nano-sized material is a physical object that is different in properties from the corresponding bulk materials [14]. In order to improve spinel ferrite properties, it is of prime importance to control the preparation conditions such as sintering time, sintering temperature, type, and quality of substitutions. The presence of Cu ions in ferrites activates the sintering process leading to an increase in density and decrease in losses. While Mn content presence plays an important influence on the magnetic properties of ferrites. Because of the normal spinel structure of $MnFe_2O_4$ and the inverse spinel structure of $CuFe_2O_4$. Samples of $Mn_{1-x}Cu_xFe_2O_4$ ($x=0, 0.2, 0.4, 0.6, 0.8$ and 1.0) nanoparticles have been systematically investigated as a research topic. The electrical and magnetic characterization of mixed manganese/copper ferrite samples have been mentioned in the context of temperature-structured resistivity, and frequency-established dielectric constant (ϵ'), tangent of dielectric loss angle ($\tan\delta$), and dielectric loss factor (ϵ'').

EXPERIMENTAL DETAILS

Samples of $Mn_{1-x}Cu_xFe_2O_4$ ($x=0, 0.2, 0.4, 0.6, 0.8$, and 1.0) ferrites have been prepared by the conventional solid state reaction method. The raw materials were high purity powders of low cost MnO (99.9%), CuO (99.9%), and Fe_2O_3 (99.9%). Respective stoichiometric amount of required powders were mixed thoroughly to prepare the ferrite samples, 3% PVA solution was added as a binder for improving compaction to the mixed powder. Grinding of every sample with specific composition was carried out in an agate mortar and pestle for 2 h, and then calcined at $150^\circ C$ for 2 h in air. The sintered powders were mixed with 2% of PVA as a binder, each sample was ground again for 2 h, and then pelletized at a pressure of about 5 tons for 3 minutes using Apex hydraulic press. The samples were sintered in a muffle furnace at $900^\circ C$ for 5 h in order to remove the organic binder and get the required phase. The temperature ramps were $5^\circ C/min$ for both heating and cooling. The crystal structure investigation was carried out using XRD measurements were performed [PHILIPS-PW-3040] with $CuK\alpha$ radiation ($\lambda=1.5418\text{\AA}$). Surface morphology and microstructural features such as grain size and porosity were examined using Hitachi S-3400, scanning electron microscopy (SEM). The two-probe method was employed to determine the electrical resistivity of the samples by using Keithley 2400 source/measure unit and the temperature was varied at a rate of 5 K/min from room temperature up to 573 K. The frequency characteristics of the samples such as dielectric constant and dielectric loss were investigated using a QuadTech-1920 LCR Meter at room temperature in the frequency range (1 KHz to 1 MHz). The magnetic properties were carried out at room temperature by means of a vibrating sample magnetometer (VSM) Lakeshore model 7404. The magnetic parameters: coercive field H_c , and saturation magnetization M_s , were determined by the hysteresis curves with an applied field of 15 kG.





RESULTS AND DISCUSSION

The X-ray diffraction patterns of the synthesized ferrite $Mn_{1-x}Cu_xFe_2O_4$ have been shown in Figure 1, it can be seen that the composite consists of manganese ferrite, copper substituted manganese ferrite and copper ferrite. The patterns analysis confirm the formation of the single phase of cubic spinel structure for the compositions $0.0 < x < 1.0$. Peak intensity is indicative of a high degree of crystallinity of the prepared ferrites. The existence of the (222), (200), (222), (422), (440), (531) and (533) major lattice planes confirms the formation of spinel cubic structure. The intensity of (311) peak decreases with the increasing of (Cu) content. It can be seen from Table I that the value of the particle size varies from 35.15 nm to 51.75 nm. Though all the samples were prepared using the same conditions, the crystallite size was not the same for the Cu substituted samples. This was probably due to the preparation condition followed here which gave rise to different rate of ferrite formation for different concentrations of Cu, favoring the variation of crystallite size.

Table I shows that the X-ray density D_x increases from 5.211 gm/cm³ to 5.701 gm/cm³ and bulk density D decreases from 4.935 gm/cm³ to 4.772 gm/cm³ with the increase of Cu ion content, these results can be attributed to the atomic weight and density of Copper (63.546, 8.96 gm/cm³) which are higher than those of manganese (54.93, 7.21 gm/cm³). The oxygen ions which diffuse through the material during sintering also accelerate the densification of the material. The X-ray density is higher than the apparent value due to the existence of pores which depends on the sintering condition. These results were in good agreement with those reported by Deraz et al. [15].

Figure 2 indicates that the porosity increases by Cu content increase which reflects the similar behavior of X-ray density, it is due to the larger ionic radius of Cu (0.73 Å) compared to Mn (0.46 Å).

Figure 3 shows the representative micrographs of the prepared ferrite samples that reveal the surface morphology by using scanning electron microscope. The images show that Cu²⁺ influences the microstructure. The grain size increases with the increase of Cu²⁺ content in the series refers to the more porous samples. It facilitates the grain growth and the grain growth reflects the competition between the driving force for grain boundary movement and the retarding force exerted by porous [16] as is evident from the increased value of porosity which discussed earlier.

The DC electrical properties were carried out as a function of composition and temperature for the prepared Mn-Cu nano ferrite samples by the two probe method. It can be notably observed from Figure 4 that the resistivity of all samples rises as a function of inverse temperature and it follows Arrhenius plot. This behavior proved the semiconductor nature of the ferrite samples. Basically, the activation energy in ferrites is often associated with the variation of mobility of charge carriers rather than their concentration. In Mn-Cu nanoferrite system, the values of activation energy play an essential role in overcoming the electrical energy barrier experienced by the electrons during hopping process, which in turn, contributes towards conductivity. Decreasing of activation energy may be attributed to the creation of a small number of oxygen vacancies [17]. It may also be justified due to the increase in conductivity of the nano ferrite material with the increase in Cu concentration as reported by Islam et al. [18] and DeOliveira et al. [19]. This behavior can be understood considering the conduction mechanism at a lower temperature which takes place mainly through the hopping probability which depends upon the separation of ions involved (Fe²⁺ and Fe³⁺) and the activation energy, whereas the conduction at a higher temperature is due to the hopping of polarons [20,21]. The hopping of electrons between Fe²⁺ and Fe³⁺ at B-sites on tetrahedral sites increases the conduction with the increasing of Cu content, which is produced during sintering process as explained by Verwey et al. [22]. This decrease in resistivity is due to the fact that Cu has a smaller value of resistivity (1.7×10^{-6} Ω-cm) as compared to that of Mn (144×10^{-6} Ω-cm). The Cu²⁺ → Cu¹⁺ transition with the variation of Cu concentration in Mn-Cu ferrite gives further reason for the decrease of DC electrical resistivity [23].





Saad Oboudi

The variation in dielectric constant is directly related to space charge polarization. The presence of higher conductivity phases in the grain boundaries of a dielectric produces the localized accumulation of charge under the influence of an electric field, results in space charge polarization [24]. Figure 5 shows the variation of dielectric constant (ϵ') with the rise of frequency up to 1 MHz. The value of ϵ' is higher at lower frequencies and is found to decrease continuously with increasing of frequency. A continuous increase in field reversal frequency results in a point where space charge carriers cannot remain preserved with the field and the alternation of their direction lags behind the field, resulting in a reduction of the dielectric constant of the material. In ferrites, polarization can also be regarded as a similar process to that of conduction. The hopping of electron between Fe^{2+} and Fe^{3+} ions results in local displacement of electrons determining the polarization of the ferrites. When the frequency is increased, polarization decreases until attaining a constant value. Beyond this critical value of frequency, the electron exchange between the two cations, cannot follow the alternating field. In addition, space charge polarization also results from the inhomogeneous dielectric structure of the material which can be explained on the basis of Koop's theory [25], which assumes that the ferrites are made up of well-conducting grains separated by a thin layer of poorly conducting grain boundaries [26].

It can be notably observed from Figure 6 that the tangent of dielectric loss angle ($\tan \delta$) is decreased with the increase of frequency. It is important to mention here that the value of $\tan \delta$ depends on different factors such as stoichiometry, Fe^{2+} content, material and structural homogeneity. Those factors, in turn, depend upon the composition of the ferrite samples and their preparation conditions inclusive of sintering temperature and sintering time [19]. The decrease of $\tan \delta$ with the increase of frequency might be also explained on the basis of Koop's phenomenological model.

A critical part of the entire core loss in ferrites is called dielectric loss factor (ϵ). Figure 7 shows the plot of frequency established dielectric loss factor. As the number of hopping electrons increase, the extent of local displacement within the direction of the electric field will increase, causing an increase in the electric polarization, which in turn enhances dielectric loss. The dielectric losses in ferrites are exhibited at some point of conductivity measurements, as highly conducting materials display high losses [20]. Consequently, the present ferrite series with relatively low losses might be useful in technological applications at higher frequencies.

The magnetic properties of a material are usually characterized by the magnetic hysteresis loop which gives the behavior trend of a material when excited by an external magnetic field. A typical magnetization versus magnetic field (M-H) loop of $\text{Mn}_{1-x}\text{Cu}_x\text{Fe}_2\text{O}_4$ nanoferrite collected on a VSM at room temperature under an applied field of 15 kOe is shown in Figure 8 which exhibits an increase in the magnetization as the magnetic field increases. In the spinel ferrite, the variation of saturation magnetization can be correlated to the interaction of Fe^{3+} (Tetrahedral) and Fe^{3+} (Octahedral) ions will be dominant. The collected curves are characteristic of soft magnetic materials. In $\text{Mn}_{1-x}\text{Cu}_x\text{Fe}_2\text{O}_4$ samples, the occupation of most Cu^{2+} at the octahedral sites and the transfer of Fe^{3+} from octahedral sites to tetrahedral sites strengthen the interactions between Fe^{3+} (Tetrahedral) and Fe^{3+} (Octahedral). Also, the magnetic anisotropy is strengthened due to the Jahn-Teller effect of the octahedral copper ions. The saturation magnetization of $\text{Mn}_{1-x}\text{Cu}_x\text{Fe}_2\text{O}_4$ nano ferrite is 17.82 emu/g for $x=0.0$ and it decreases to 16.05 emu/g with copper content increasing to $x=1.0$ at B equal to 7.1 kOe. The molecular magnetization (M) is given by the difference between the magnetization of MB and MA octahedral and tetrahedral sites, respectively, in which subnet B has a higher magnetization. Although Cu^{2+} ions have a magnetic moment less than Mn^{2+} ions and have a tendency to occupy octahedral sites, some of them may enter into tetrahedral sites in the spinel ferrite, the replacement of Cu^{2+} ions by Mn^{2+} ions in octahedral sites should result in increased M_s . The Cu^{2+} are substituted for some Fe^{3+} in the tetrahedral sites and more Fe^{3+} occupy the octahedral sites when the copper content is low. With the increase in the copper content, most Cu^{2+} entered into the octahedral sites and the ferromagnetic interactions between Fe^{3+} at the octahedral sites are disturbed. The transfer of Fe^{3+} from octahedral sites to tetrahedral sites leads to the decrease in saturation magnetization [27]. The maximum coercivity appears for CuFe_2O_4 nanoparticles where its value is higher than those of other samples. The higher coercivity of CuFe_2O_4 nanoparticles confirms its relatively strong magnetocrystalline anisotropy. The strengthening of





Saad Oboudi

the magnetic anisotropy results from the distortion of the spinel lattice due to the Jahn-Teller effect of the octahedral copper ions, similar results were reported by Tailhades et al.[28]. With all these characterization techniques we infer that the ceramics exhibited characteristics of a soft magnetic material with high electric conductivity.

CONCLUSIONS

Copper substituted Mn-Ferrite materials prepared by the conventional solid state reaction technique and investigated as potential materials for devices electronic, results exhibited single phase cubic spinel structure having nano-sized crystallite size. The decrease in dc electric resistivity of all the samples with increasing temperature depicts the semiconductor-like behavior of the samples. The reason for the decrease in saturation magnetization with increasing Cu^{2+} contents in the Mn-Cu nanoferrite series could be understood considering the non-magnetic nature of copper. The dielectric constant, tangent of dielectric loss and dielectric loss factor, all showed decreasing trend with increasing frequency ensuring high-frequency applications of the Cu substituted Mn-ferrite samples.

ACKNOWLEDGMENTS

This work was performed in the Superconductivity Lab, Physics Department, College of Science, University of Baghdad, Baghdad, Iraq, the Microstructure laboratories / Technique Physic (TEP), University of Wurzburg, Wurzburg, Germany, and the McLennan Physical Laboratories, University of Toronto, Toronto, Canada.

REFERENCES

1. Muhammad Ajmal, Asghari Maqsood, Structural, electrical and magnetic properties of $\text{Cu}_{1-x}\text{Zn}_x\text{Fe}_2\text{O}_4$ ferrites ($0 \leq x \leq 1$), Journal of Alloys and Compounds 460, 1–254-59 (2008)
2. M. F. Huq, D. K. Saha, R. Ahmed, and Z. H. Mahmood: Journal of Scientific Research 5(2), 215-233 (2013)
3. Mahmood Asif, Ramay Shahid Mahmood, Al-Zaghayer Yousef S., Alhazaa A. N., Al Masary Waheed A., Atiq Shahid, Au doping effect on the electrical and magnetic properties of Fe_3O_4 nanoparticles, Modern Physics Letters B (2015) DOI: 10.1142/S0217984915502139
4. M. Molaahmadi, S. Baghshahi, A. Ghasemi, Effect of Cu^{2+} substitution on structural and magnetic properties of Ni-Zn ferrite nanopowders, Journal of Materials Science: Materials in Electronics 27, 11 (2016)
5. J.F. Huheey and E.A. Keiter: College Publishers, Harper Collins, (1993)
6. H. M. El-Sayed: Journal of Alloys and Compounds 474 (1-2), 561-564 (2009)
7. A Lakshman, P S V Subba Rao, B Parvatheeswara Rao, and K H Rao, Electrical properties of In^{3+} and Cr^{3+} substituted magnesium-manganese ferrites, Journal of Physics D: Applied Physics 38, No.5 (2005)
8. Ph. Tailhades, C. Villette, A. Rousset, G.U. Kulkarni, K.R. Kannan, C.N.R. Rao, M. Lenglet, Cation Migration and Coercivity in Mixed Copper-Cobalt Spinel Ferrite Powders, Journal of Solid State Chemistry, 141, 56-63 (1998)
9. S. M. Ramay, Saadat A. Siddiqi, S. Atiq, M. S. Awan, S. Riaz: Structural, Magnetic, and Electrical Properties of Al^{3+} Substituted CuZn-ferrites: Chinese Journal of Chemical Physics Vol. 23, No. 5 (2010)
10. Krupicka S. and Novak P.: Oxide spinels in Ferroelectric Materials, edited by Wohlforth E. P., North-Holland, Amsterdam, 3 (1982)
11. Shahida Akhter, D. P. Paul, M. A. Hakim, S. Akhter, D. K. Saha, B. Anjuman, F. Islam, Microstructure and Complex Permeability Spectra of Polycrystalline Cu-Zn Ferrites, Journal of Scientific Research 4, No 3 (2012)
12. Sridhar Rapolu, D. Ravinder, and K. Vijaya Kumar., Synthesis and Magnetic Properties of Ni-Cu Nano-Magnetic Ceramics, Processing and Properties of Advanced Ceramics and Composites VI, 71-81 (2014) DOI: 10.1002/9781118995433.ch8
13. A. Tawfik, O. M. Hemeda, D. M. Hemeda, M. Mostafa, Structural and magnetocaloric properties of nano Zn ferrite doped with Ni under hydrothermal conditions, The European Physical Journal Plus, 129:278 (2014)





Saad Oboudi

14. Gul, I. H.; Maqsood, A., Influence of Zn Zr ions on physical and magnetic properties of co-precipitated cobalt ferrite nanoparticles, *Journal of Magnetism and Magnetic Materials*, 316, Issue 1, 13-18(2007)
15. Deraz M. N., Alarifi A.: *Int. J. Electrochem. Sci.* 7, 5534-5543 (2012)
16. Farhad Alam, Mohammad H. R. Khan, Hari N. Das, Akther A. K. M. Hossain: *Materials Sciences and Applications* 4, 831-838 (2013) <http://dx.doi.org/10.4236/msa.2013.412106>
17. Valesca Donizeti de Oliveira, Rero Marques Rubinger, Manoel Ribeiro da Silva, Adhimar Flávio Oliveira, Geovani Rodrigues, Vander Alkmin dos Santos Ribeiro, *Magnetic and Electrical Properties of Mn_xCu_{1-x}Fe₂O₄ Ferrite: Materials Research*, 19 No.4 (2016) <http://dx.doi.org/10.1590/1980-5373-MR-2015-0511>
18. Islam M. U., Chaudhry M. A., Abbas T., and Umar M.: *Mater. Chem. Phys.* 48, 227-229 (1997)
19. Valesca Donizeti de Oliveira, Rero Marques Rubinger, Manoel Ribeiro da Silva, Adhimar Flávio Oliveira, Geovani Rodrigues, Vander Alkmin dos Santos Ribeiro: *Materials Research* 19(4) 786-790 (2016) DOI: <http://dx.doi.org/10.1590/1980-5373-MR-2015-0511>
20. Klinger M. I.: *Journal of Physics C: Solid State Physics* 8 (21) 3595 (1975) <http://dx.doi.org/10.1088/0022-3719/8/21/029>
21. Klinger M. I.: *Physica Status Solidi (B)* 79 (1), 9-48 (1979)
22. Verwey E. J. W., De Boer J. H.: *Rec. Trans. Chim. de Pays-Bas* 55, 531 (1936)
23. Nam J. H., Jung H. H., Shin J. Y., and Oh J. H.: *IEEE Trans. Magn.* 31, 3985-3987 (1995)
24. Chanda M.: *Science of Engineering Materials* 3, The Machmillan Company of India Ltd., New Delhi (1980)
25. Koops C. G.: *Phys. Rev.* 83, 121 (1951)
26. Ravi Kumar G., Vijaya Kumar K., Venudhar Y. C.: *IJMER* 2 (2), 177-185 (2012)
27. Massart R., Zins D., Gendron F., Rivoire M., Mehta R. V., Upadhyay R. V., Goyal P. S., Aswal V. K.: *J. Magn. Magn. Mater.* 201, 73-76 (1999).
28. Tailhades P., Villette C., Rousset A., Kulkarni G. U., Kannan K. R., Rao C. N. R., Lenglet M.: *J. Solid State Chem.* 141, 56-63 (1998).

Table I: Particle Size, X-ray Density, Bulk Density, and Porosity with composition of mixed Mn-Cu nano ferrites

Composition (x)	Particle Size (nm)	X-ray Density (gm/cm ³)	Bulk Density (gm/cm ³)	Porosity (%)
0.0	51.75	5.211	4.935	7.125
0.2	43.87	5.272	4.904	8.854
0.4	47.23	5.345	4.877	10.208
0.6	43.24	5.485	4.822	12.566
0.8	50.05	5.574	4.801	14.459
1.0	35.15	5.701	4.772	16.912



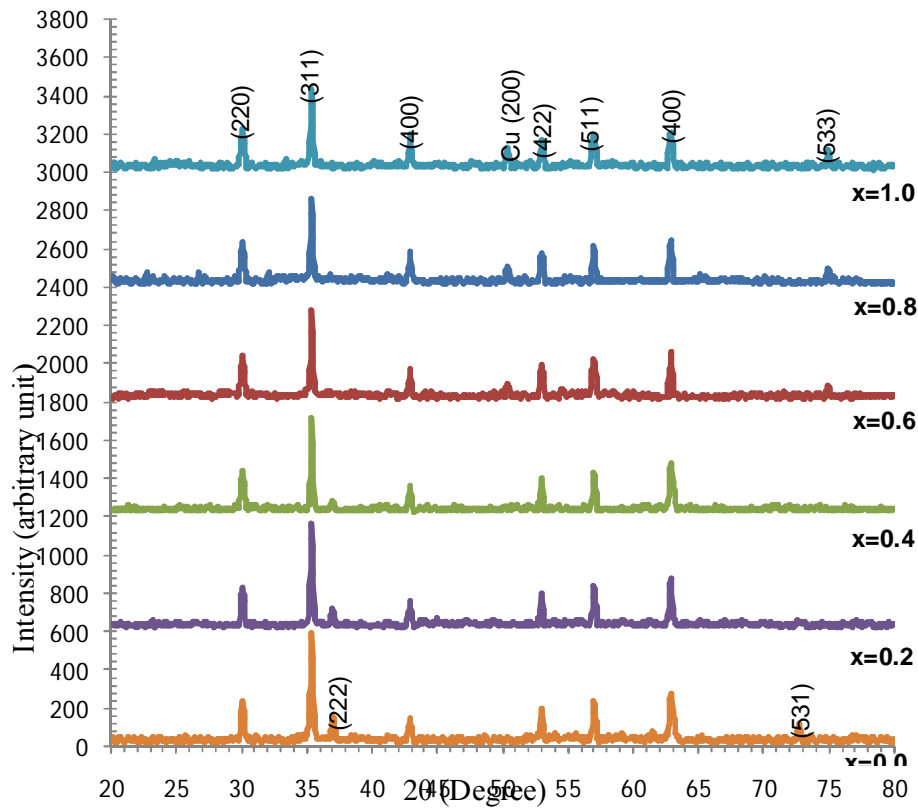


Figure1.X-Ray Diffraction Pattern of $Mn_{1-x}Cu_xFe_2O_4$ Ferrites.

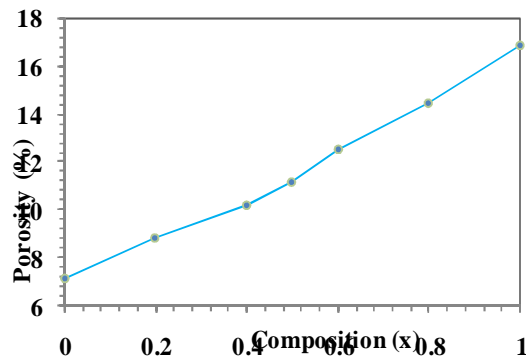
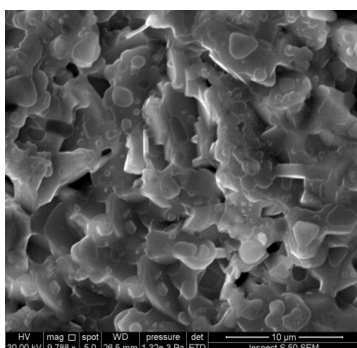


Figure 2. Variation of Porosity with Cu content.

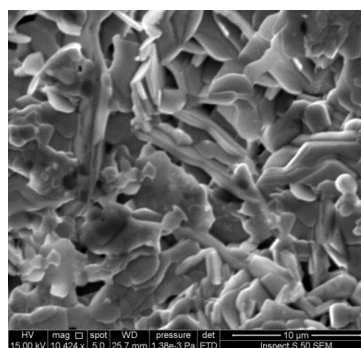




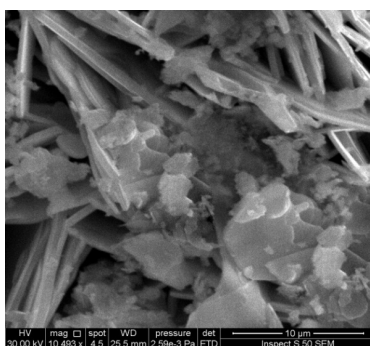
Saad Oboudi



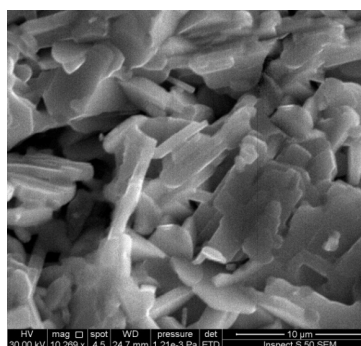
x=0



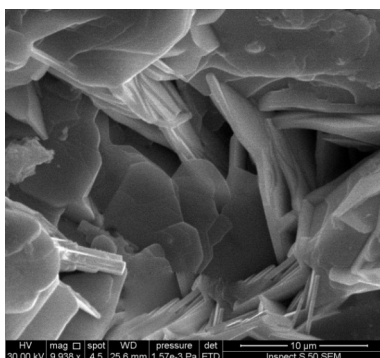
x=0.2



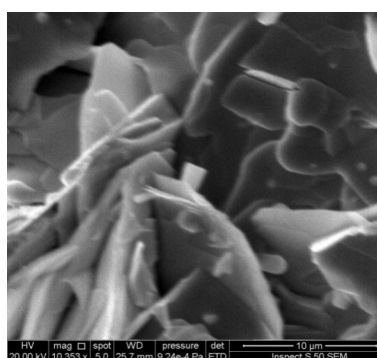
x=0.4



x=0.6



x=0.8



x=1.0

Figure 3. Scanning Electron Micrographs of $Mn_{1-x}Cu_xFe_2O_4$.



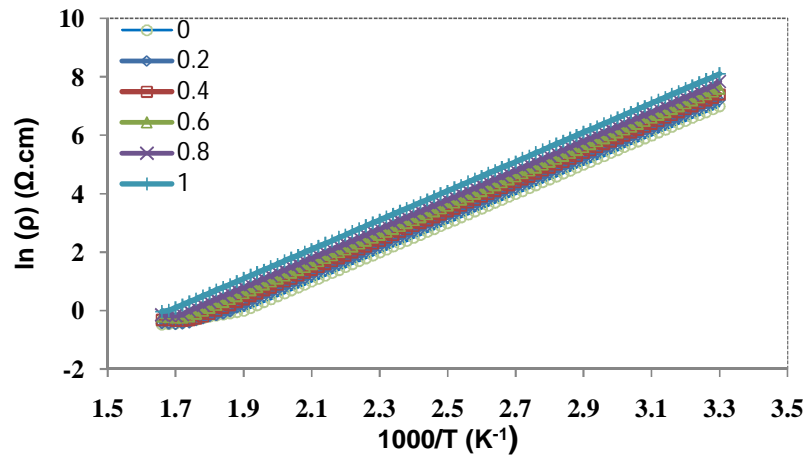


Figure 4. Variation of DC Electrical Resistivity with Inverse Temperature.

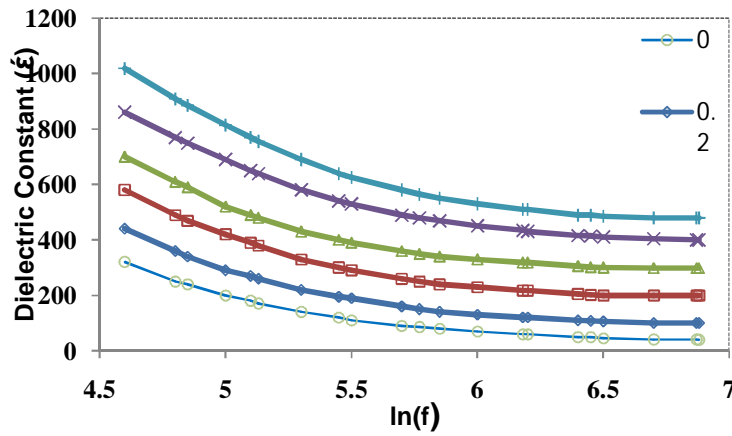


Figure 5. Dielectric Constant Plotted against Frequency.

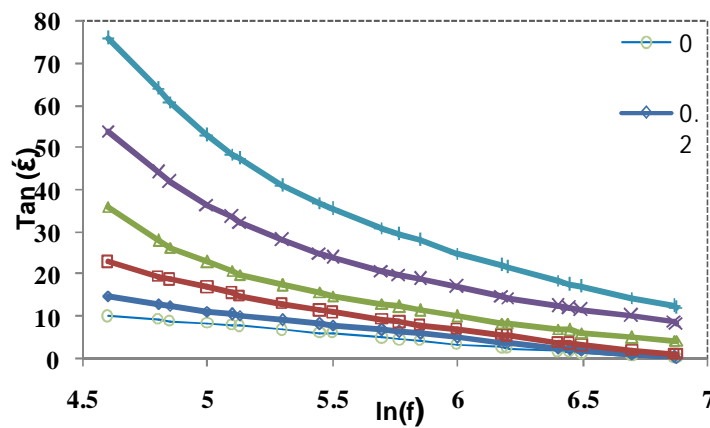


Figure 6. Tangent of Dielectric Loss Angle Plotted against Frequency.





Saad Oboudi

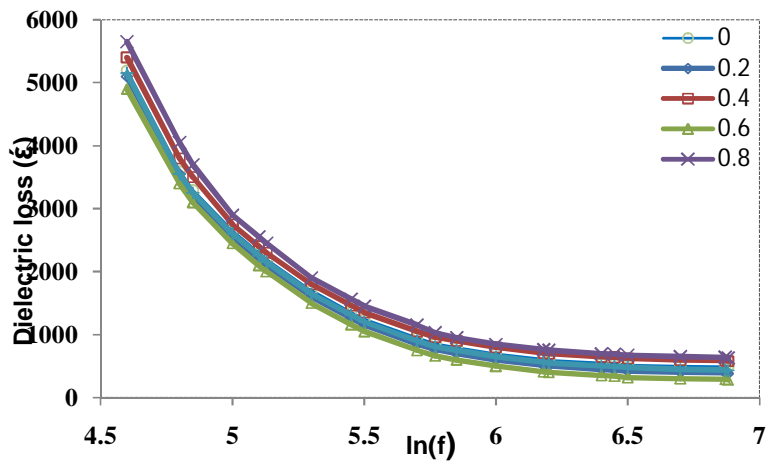


Figure 7. Dielectric loss Factor Plotted against Frequency.

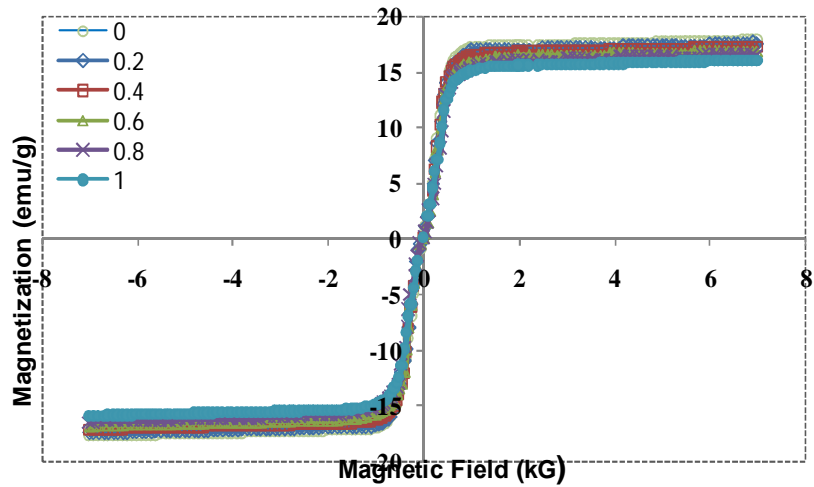


Figure 8. Hysteresis loops at room temperature of $Mn_{1-x}Cu_xFe_2O_4$ ferrite samples.





Broodstock Development and Induced Spawning of Mangrove Red Snapper *Lutjanus argentimaculatus*, Forsskal in Captivity.

T.Senthil Murugan*, K. Srinivasa Rao, N.Selvakumar and K.K.Philipose

Karwar Research Centre of ICAR-Central Marine Fisheries Research Institute, Karwar-581301, Karnataka, India.

Received: 17 Sep 2017

Revised: 25 Sep 2017

Accepted: 27 Oct 2017

*Address for correspondence

T.Senthil Murugan

Karwar Research Centre of ICAR-Central Marine Fisheries Research Institute,
Karwar-581301,
Karnataka, India.

E.mail: drtsenthilmurugan@gmail.com



This is an Open Access Journal / article distributed under the terms of the **Creative Commons Attribution License** (CC BY-NC-ND 3.0) which permits unrestricted use, distribution, and reproduction in any medium, provided the original work is properly cited. All rights reserved.

ABSTRACT

In order to augment the growing mariculture industry in India, brood stock development of another important candidate species mangrove red snapper, *Lutjanus argentimaculatus* was successfully carried out. The first trial on the spawning under captivity was tried successful and spawning was obtained. The fecundity of the spawn was about 1.2 million. However, the embryonic development was arrested in late neurula stage itself. It may be due to various factors including especially the brood stock diet. Further studies will be focussed on developing a specific brood stock diet in order to succeed in successful spawning and further higher rate of larval survival of this important species.

Keywords: Mangrove red snapper; *Lutjanus argentimaculatus*; Spawning under captivity.

INTRODUCTION

In the last fifty years, 80% of the wild fish stocks were fully or over-exploited due to the increased fishing efforts which resulted in stunning collapses, particularly in small pelagic fish stocks (Kleisner et al., 2013). Global capture by fisheries have remained constant at about 90 million tons in the last three decades even with the change in fishing effort towards alternative species to compensate for the loss of harvest in overfished stocks. At the same time, the growth in fish culture technologies permitted for the expansion of food fish production through farming at an average rate of 8.8% per year, outpacing population growth leading to an increase in per capita fish production (FAO, 2012). Regardless of the decreased contribution of marine fishes to global aquaculture production, major interest is being exhibited in developing the marine species since they support large markets. Controlled spawning is fundamental to the development of new aquaculture species. The main hurdle in developing technologies for aquaculture production of those species lies mainly in difficulties to achieve some essential life history phases in culture conditions. The main success for developing any fish fry production technology demands on developing and



**Senthil Murugan et al.**

maintaining healthy, hygienic and potential brooders. It is well understood that development of captive broodstock in proper environment and appropriate diet is the initial step required for seed production of any finfish. With the significant and growing start ups in the field of mariculture in India, technologies on producing fries in hatchery available almost for five species. This paper deals on developing technology for seed production of another important candidate species for mariculture the Mangrove red snapper *Lutjanus argentimaculatus*.

The snapper family Lutjanidae, a gonochorist (Grimes,1987), contains many commercially important species of tropical and subtropical coastal fisheries. The mangrove red snapper *Lutjanus argentimaculatus* (Forsskal) is widely distributed in the Indo-west Pacific from Samoa and the Line islands to East Africa, and from Australia northward to the Ryukyu Islands (Allen, 1985). Being a marine species also found in brackish mangrove estuaries and the lower reaches of freshwater streams. Usually migrates offshore to deeper reef areas, even penetrating depths exceeding 100 m (Allen, 1985,1987). Because of its high economic value and ability to adapt to various salinities and temperatures, it is considered as a good candidate species for mariculture (Chen et al., 1990; Estudillo et al., 2000). It is a high-priced food fish and the demand exceeds the supply. Especially in India, it can also be an alternate species for brackish water pond farming. Various spawning seasons were reported from different localities of the World. Singhagraiwan and Dol, 1993 reported the spawning occurs between January and November in Thailand. In Taiwan, spawning occurs between May and September (M.Y.Leu et. al., 2003) and in the Philippines in august (Emata et al., 1994). A lot of attentions have been given in the past ten years in mariculture of *L. argentimaculatus* concentrated efforts on problems related to spawning and larvae rearing. The foremost achievement in the spawning and larval rearing was obtained by Wudthisin (1984) in Thailand. This paper describes the successful development of a brood bank of *L. argentimaculatus* and spawning under captivity first time in India.

MATERIALS AND METHODS

Broodstock raising

The adult Mangrove red snapper *Lutjanus argentimaculatus* fishes were procured from a private brackish water cage farm near Uppunda, Karnataka in November 2015. The fishes were in the size range between 28.0cm and 34.0 cm and weight range between 2.0 and 2.40 kg. After bringing to marine cage farm facility of Karwar Research Centre of ICAR – Central Marine Fisheries Research Institute, each fish was tagged with Passive Integrated Transponder (PIT) tags individually. The tagged fishes were stocked in GI circular cage of 6 meter dia and 5 m depth. Fishes were fed on Oilsardine (*Sardinella longiceps*) @ 3% of the body weight. Fishes were sampled monthly for studying the growth. Once the fishes grown to a size of 1.0 kg monthly cannulation was executed in order to find out the first maturity size. After the fishes attained sexual maturity, cannulation was done fortnightly to find out the oocytes development.

Broodstock maintenance

3 numbers of matured females and 6 numbers of matured males were shifted to the hatchery facilities in September 2016 in order to be maintained in controlled conditions. 3 pairs consist of each 2 males and 1 female was stocked in 4 tons capacity circular 3 FRP tanks. Photoperiod of 14L:10D was maintained in all the brooders tanks during the entire study period. They were fed with prawns, squids and crabs enriched with multi vitamins, minerals, and astaxanthine at a minimum of 3% of the body weight daily. One hour after feeding the unfed wastes was removed and 100% water exchange was given for all tanks. After water exchange the tanks were given continuous flow through with a exchange rate of 45% daily. Throughout the rearing period salinity was in the range between 26 ppt and 31 ppt. Temperature in all the rearing tanks was maintained at 31.5 degrees by heaters with thermo stat controlling facility. Ovarian biopsies were collected periodically from the females and the ova diameter measured Fig.1.



**Senthil Murugan et al.**

Spawning and Egg production

For the first spawning trial in April 2017, a pair consisted of 1 female (3.8 kg) and 2 males (4.3 kg & 3.7 kg) were taken. Once the oocyte diameter of the female brooder reached 420-430 μ first injection of hCG (hCG care, Gufie Pvt. Ltd., Gujarat, India) at a concentration of 750 IU Kg⁻¹ was given. Males also given the same dose of hCG of first dose. The first dose injection was given around 11.45 am. 24 hours after the first dose, both female and males were given a second booster dose of hCG at the rate of 350 IU Kg⁻¹. After administration of the second booster dose, water was not exchanged in the tanks to avoid disturbance. The pre-spawning behaviour of brooders was observed on many occasions between 20 and 36 h after first injection. When spawning was confirmed time was noted. The fertilized eggs were collected after 5 hrs and incubated in the 500 litre capacity incubation tanks with slight flow through and gentle aeration without disturbing the eggs. A little egg were collected immediately after spawning and stocked in one glass aquarium tank of 200 litre capacity for studying the embryonic developments. The number of eggs was estimated volumetrically. Fertilization rate was estimated with 100 eggs from each spawn in a 1000- ml beaker of sea water.

RESULTS

From our regular monthly sampling of brood-stock in the cage, it was recorded that the males matured when they were 48 cm and 2.7 kg and females matured when they were 51 cm and 2.9 kg weight. As of now, more than 50 numbers of brooders are being maintained in the cage.

The following pre-spawning behaviour were observed; a.) male very often follow the female and moving close underneath. B.) erection of dorsal fin frequently by male. c.) male inclined head down towards female. After a period of 36 h post first injection, eggs were released and fertilization took place at 1200 hrs. Mangrove red snapper eggs are spherical, transparent, pelagic, positively buoyant measured from 780 μ to 810 μ diameter and with a single oil globule (0.14-0.16 μ diameter). The total fecundity of the first spawning was about 1.2 million. The unfertilized eggs settled in the bottom were removed by slowly siphoning without disturbing the fertilized eggs.

Embryonic development

The first cell division starts between 25 and 30 minutes. The eggs entered morula stage in a period of 1 hour 45 minutes. Blastula stage eggs were seen 2 hours 45 minutes post fertilization. The eggs entered gastrula in 4 h 50 minutes and neurula stage in 8h 10 minutes respectively. The embryonic development was arrested at this neurula stage further no development was observed Fig.2.

DISCUSSION

Hormone treatments are reliable methods of inducing spawning in *L.argentimaculatus* (Wudthisin, 1984; Lim and Chao,1993; Singhagraiwan and Doi, 1993;Emata et.al., 1994,1999). The fecundity obtained in this study again proved that mangrove red snapper are to be highly fecund and concurring with the earlier reports (Doi and Singhagraiwan 1993; Emata et. al., 1994 and Grimes 1987). Normally in mangrove red snapper the fecundity depend on the number eggs in the ovary over a critical minimum state of development, corresponding with a diameter of approximately 400 -450 μ m not on the female size.

The latent period observed in this present study more or less resembles the latent period reported for mangrove red snapper in Thailand (Doi and Singhagraiwan, 1993), Whereas a shorter period of 27 h reported by Emata et. al.,1994 for this species and similar latent period was reported for John's snapper *L.johnii* by Lim et. al., 1985 in Singapore; by





Senthil Murugan et al.

T.Senthil Murugan et.al., 2016 in India. Several studies on various fish species have shown inverse relationship to exist between latent period and water temperature (Stacey et al., 1979; Fortuny et al., 1988).

The duration taken for the earlier embryonic development obtained in this present study resembles the earlier report made by K.L.Cowden 1995 in Australia and with duration of 18 h 10 minutes for hatching. However Doi and Singhgraiwan (1993) and Emata et. al., 1994 reported 15 h and 16 h respectively for the hatching to commence.

The embryonic development of the fishes is controlled by many factors among them main two factors are temperature and brood stock nutrients. In this study the egg incubation also carried out in the same temperature similar to the spawning tank temperature. It may be concluded that the brood- stock nutrient might have played a major role in the arresting of embryonic development. Emata et. al., 2003 was able to obtain higher mean cumulative hatching and survival to normal larvae with the practical diet rather than raw fish in *L.argentimaculatus*. The present study may point out either the shifting from raw fish to a specific practical diet or combination of both for the mangrove red snapper brooders in the further spawning studies.

ACKNOWLEDGEMENTS

The authors are grateful to the Director, ICAR-Central Marine Fisheries Research Institute, Kochi for all the support rendered towards this work.

REFERENCES

1. Kleisner, K., Zeller, D., Froese R and Pauly, D., 2013. Using global catch data for inferences on the world's marine fisheries. *Fish and Fisheries*, 14, pp.293-311.
2. FAO, The state of the world fisheries and aquaculture (SOFIA). Rome: Food and Agriculture Organization of the United Nations, 2012, pp.1-230.
3. Grimes C.B., 1987. Reproductive biology of the Lutjanidae: a review. pp 239-294. In J.J. Polovina and S. Raiston (eds.). *Tropical snappers and Groupers. Biology and Fisheries management*. Westview Press, Boulder, Colorado. 659 pp.
4. Allen G.R., 1985. FAO Species Catalogue. Snappers of the World. An Annotated and Illustrated Catalogue of Lutjanid Fishes known to Date. FAO Fish. Synopsis No. 125, Vol.6. FAO, Rome. 208 pp.
5. Allen G.R. 1987. Synopsis of the circumtropical fish genus *Lutjanus* (Lutjanidae) pp. 33-87. In: J.J. Polovina and Raiston (eds.). *Tropical snappers and groupers: biology and Fisheries Management*. Westview Press, Boulder, Colorado. 650 pp.
6. Chen S.L., Ahyu C.Z, and M.Y. Lue, 1990. Tolerance of red snapper, *Lutjanus argentimaculatus*, fingerlings to temperature, salinity and dissolved oxygen. *Bull. Taiwan Fish., Res. Inst.*, 49: 37-42
7. Estudillo C.B., Duray M.N. marasigan E.T. and A.C. Emata, 2000. Salinity tolerance of larvae of the mangrove red snapper (*Lutjanus argentimaculatus*) during ontogeny. *Aquaculture*, 190: 155-167.
8. Singhgraiwan T. And M. Doi., 1993. Induced spawning and larval rearing of the red snapper, *Lutjanus argentimaculatus*, at the eastern Marine Fisheries Development Centre. *Thai. Mar. Fish. Res. Bull.* 4: 45-57.
9. Emata A.C., Eullaran B. And T.U. Bagarinao, 1994. Induced spawning and early life description of the mangrove red snapper, *Lutjanus argentimaculatus*. *Aquaculture*, 121: 381-387.
10. M.Y. Leu, I.H. Chen. and L.S. Fang, 2003. Natural spawning and rearing of mangrove red snapper, *Lutjanus argentimaculatus* larvae in captivity. *The Israel., Journal of aquacult.*, 55(1): 22-30.
11. Wudthisin., 1984. Propagation on the red snapper, *Lutjanus argentimaculatus*. Tech. Paper, Rayong Marine Fish. Stn., Marine Fish. Div., dept. Fish., Thailand. 58pp.
12. Lim H.S. and T.M. Chao, 1993. The spontaneous spawning of mangrove red snapper, *Lutjanus argentimaculatus* in net cages. *Singapore J. Pri. Ind.*, 21(2): 86-91.





Senthil Murugan et al.

13. Emata A.C., Damaso J.P. and B.E.Eullaran,1999. Growth, maturity and induced spawning of mangrove red snapper, *Lutjanus argentimaculatus*, broodstock reared in concrete tanks. Israeli J. Aquaculture. Bamidgeh, 51(2):58-64.
14. Doi M. and Singhagraiwan,1993. Biology and culture of the Red snapper, *Lutjanus argentimaculatus*. Res. Proj. Fish Resource Dev. Kingdom of Thailand, Eastern Marine Fish. Dev. Centre and Jpn.Int. Cooperation Agency, 51pp.
15. Lim L.C., Cheong L., Lee H.B. and H.H. Heng, 1985. Induced breeding studies of the John's snapper *Lutjanus johnii* in Singapore. Singapore J.Pri. Ind., 13: 70-83.
16. T, Senthil Murugan, D.Divu., K.Srinivasa Rao and K.K.Philipose.,2016. Broodstock development and induced spawning of the John's snapper *Lutjanus johnii* (Bloch, 1792) under controlled conditions. *Indian J. Fish.*, 63(1):117-119.
17. Stacey, N.E., Cook, A.F. and Peter, R.E., 1979. Ovulatory surge of gonadotropin in the gold fish, *Carassius auratus*. Gen. Comp. Endocrinol., 37: 246-249.
18. Fortuny, A., Espinach Ros, A. And Amutio,V.G., 1988. Hormonal induction of final maturation and ovulation in the Sabalo, *Prochilodus platensis*: treatments, latency and incubation times and viability of ovules retained in the ovary after ovulation. *Aquaculture*, 73: 373-381.
19. K.L.Cowden., 1995. Induced spawning and culture of Yellowfin Bream, *Acanthopagrus australis* and Mangrove jack *Lutjanus argentimaculatus*. Thesis for the degree of Doctor of Philosophy in the department of Zoology, James Cook University of north Queensland, Australia.
20. A.C.Emata. and I.G.Borlongan., 2003. A practical broodstock diet for the mangrove red snapper, *Lutjanus argentimaculatus*. *Aquaculture* 225:83-88.

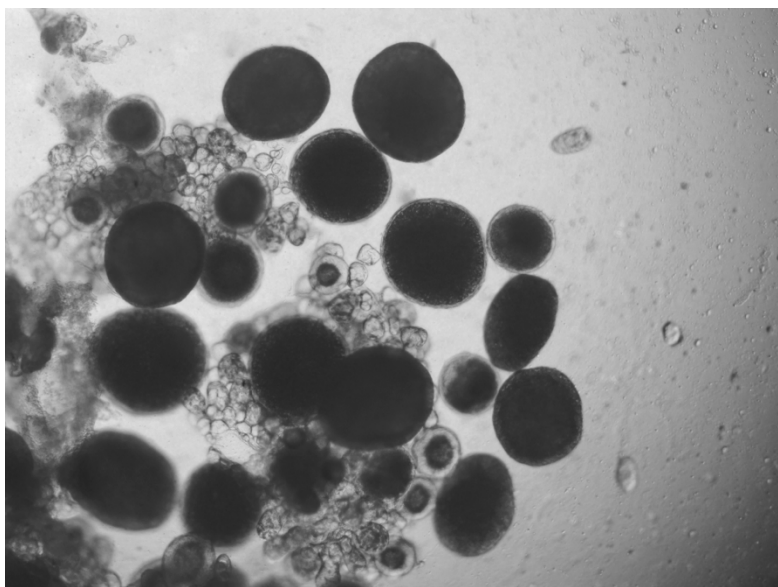
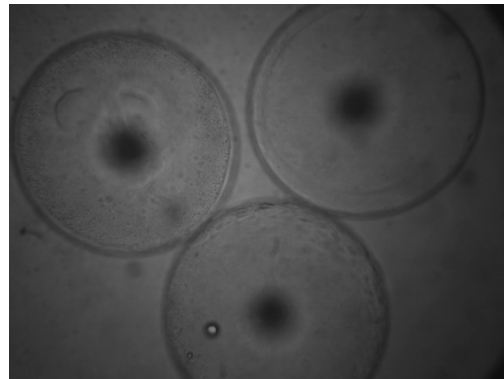


Fig. 1. Photomicrograph showing ovarian biopsy from mature *L. argentimaculatus*.

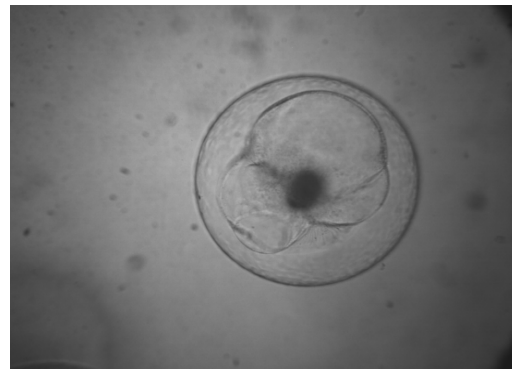
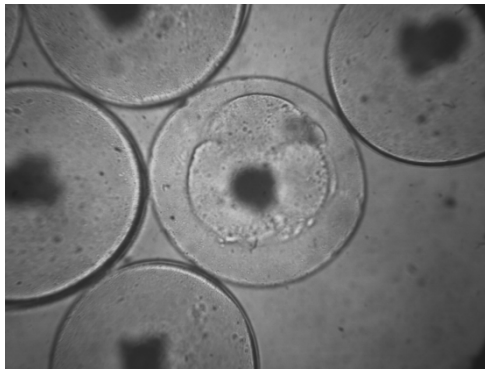




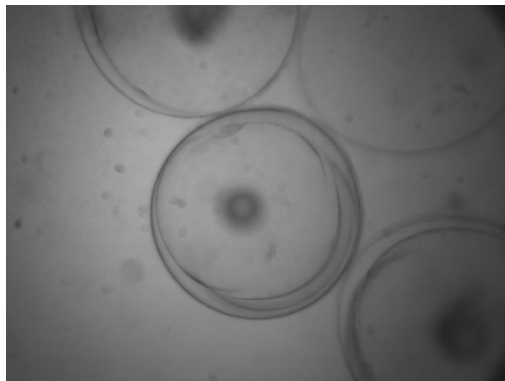
Senthil Murugan et al.



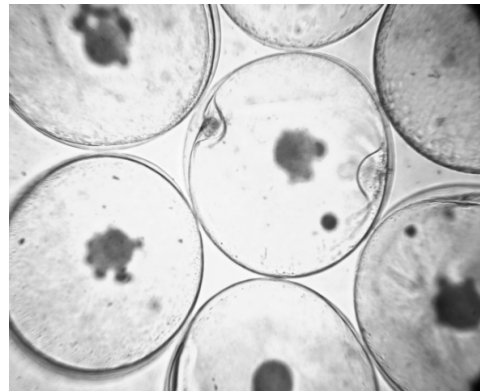
A



B

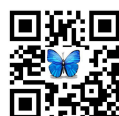


C



D

Fig. 2. Early embryonic development in *L. argentimaculatus* A. Fertilized egg B. Cell division stage C. Late Gastrula stage D. Neurula stage.





Influences the Number of Laser Pulsed on Optical and Structural Properties of $(\text{CuO})_x: (\text{Pb})_{1-x}$ Thin Films Prepared by Laser Induced Plasma Technique

Kadhim A.Aadim* and Ghaith H. Jihad

Department of Physics, College of Science, University of Baghdad, Iraq.

Received: 12 Dec 2017

Revised: 27 Dec 2017

Accepted: 28 Jan 2018

*Address for correspondence

Kadhim A.Aadim

Department of Physics,

College of Science,

University of Baghdad, Iraq.

E.mail: kadhim_adem@scbaghdad.edu.iq



This is an Open Access Journal / article distributed under the terms of the **Creative Commons Attribution License** (CC BY-NC-ND 3.0) which permits unrestricted use, distribution, and reproduction in any medium, provided the original work is properly cited. All rights reserved.

ABSTRACT

CuO:Pb nano films have been produced on glass substrates by Laser induced plasma (LIPS) technique in Vacuum ($p = 2.5 \times 10^{-2}$ mbar) using Nd:YAG laser with ($\lambda=532$ nm & 1064 nm) , $X=0.6,0.7$ and 0.8 and distance 10cm between laser and the substrate with thickness of films 108 nm. It is observed from optical properties that the films possess Absorption 75% in visible and near infrared region of spectrum and direct band gap values in the rang 2-2.8 eV at $\lambda=523$ nm while at $\lambda=1064$ nm the band gap in rang 2-2.6, also when increases no. of pulse the films are more homogenate.

Keywords: Laser Induced Plasma Spectroscopic (LIPS), Atomic Force Microscopic (AFM), X-Ray diffracting (XRD), Lead (Pb), Cupper mono Oxide (CuO).

INTRODUCTION

Copper oxide has varying optical behaviors and a range of direct optical band gaps due to stoichiometric deviations arising from the parameters and method of production[1], Copper oxides are considered important semiconductor of metal oxides, it nanomaterial because have the benefit of a low surface potential barrier which effects on electron field emission properties. There are two types of copper oxide formed from copper include : (CuO) and (Cu₂O) with narrow band gap energy 1.21 to1.51 eV and 2.1 to 2.6 eV respectively Potential field emitter has been copper oxide which a good gas sensing material as well as an efficient catalytic agent.[2] Copper oxide (CuO) is a semiconductor material which many application for fabrication of photovoltaic solar cells. The features of copper oxide semiconductors are high optical absorption and nontoxic and low cost fabrication. CuO are p-type semiconductors with band gaps 1.5 – 1.8 eV for indirect transition and 1.9 eV for direct transition which are close to the ideal energy gap for solar cells and allows for good solar spectral absorption due to this direct band gap. The lattice parameters of

13157





Kadhim A.Aadim and Ghaith H. Jihad

CuO are $a = 4.684 \text{ \AA}$, $b = 3.425 \text{ \AA}$, $c = 5.129 \text{ \AA}$ and $\beta = 99.28^\circ$ [3] CuO thin films have been prepared using various thin film deposition techniques such as chemical vapour deposition, vacuum evaporation, electro-deposition, thermal oxidation, sputtering process, electron-beam evaporation, chemical solution deposition, Laser induce Plasma System (LIPS) using Nd:YAG laser[4][5]. LIPS method is of particular interest because of its good control of stoichiometry ease of fabrication and low temperature synthesis. Since it is relatively new, hence a greater understanding is required before the film quality can be optimized. It was reported that LIPS derived thin films are thermodynamically stable. [5].

EXPERIMENTAL METHOD

Preparation of CuO film doped with Pb under Vacuum ($P=2.5 \times 10^{-2}$ mbar) at different weight using chemical mixed, Optical and Structural properties have been studied. The objectives of this study are observe the crystal structure, investigate the absorbance of CuO films with layer variation, and determine band gap energy with Pb doped variation at first and second harmonic of Nd:YAG laser.

CuO thin film has been synthesized by LIPS method under Vacuum. On to the microscope glass substrates ($1 \times 25 \times 75 \text{ mm}^3$) at energy value $E=900$ mj with different number of pulses at first & second harmonic of Nd:YAG laser, then prepare CuO:Pb films with different weight according to the following equation

$$W_{\text{CuO+Pb}} = X * (W_{\text{Cu}} + W_{\text{O}}) + (1-X) * W_{\text{Pb}} \quad (1)$$

The results for Mixing between CuO & Pb ($W_{\text{CuO+Pb}} = 3\text{gm}$)

X	CuO (gm)	Pb (gm)
0.6	0.831	2.169
0.7	1.417	1.582
0.8	1.816	1.183

The schematic arrangement of LIPS set-up is shown in Fig. (1). In which thin films are prepared under Vacuum with pressure tell to 2.5×10^{-2} mbar

RESULTS AND DISCUSSION

X-ray diffraction (XRD)

Figure (2 a and b) shows the results of XRD of the CuO powder and Pb Powder respectively. The XRD results of the film samples can be seen in Fig. 3. The location of the spikes in intensity on the XRD plot at the various 2θ angles of incidence can be related to the material composition and crystalline orientation. The 2θ angle values for each copper composition were taken from JADE5 PDF tables and can be seen in Tables (1,2). Consequently, it can be seen that under the Vacuum, the composition and orientation of the crystalline structure of the thin layers varies. These results agree with Yahya Alajlani [1], Xue Wang [6]. The maximum peak of CuO is at $2\theta = 38.537^\circ$ this results agreement with Ref.[1][2][7].

While Pb powder has different as shown in table (2).





Kadhim A.Aadim and Ghaith H. Jihad

After that we prepare CuO: Pb thin films with different weight by using LIPS with Nd:YAG Laser $\lambda=(532\text{nm} , 1064\text{nm})$, so the XRD pattern are shown in figure(3).The results from the fig. 3 that after doped CuO with Pb the compounded is more crystalline when X is increasing.

Atomic Force Microscopy (AFM)

Atomic force microscopy AFM used to study the Morphology of the surface and crystal structure of the surface thin films precipitated, and which was calculated average grains size, Figure (4) describe three-dimensional pictures and distribution of the grains respectively for surfaces of prepared thin film. Average diameters for particles are increased with increase the doping of Pb due to transmission.

Optical Measurements

The variation of absorbance of the CuO film as shown in Fig. 5. This spectrum reveals that as deposited CuO film has high absorbance in the visible region, which is the characteristic of CuO. Wavelength 500 nm to 1100 nm has low absorbance this agree with M. Dahrul.[3],

While The variation of absorbance of the Pb film is shown in Fig. 6.This spectrum reveals that as deposited Pb film has high absorbance in the visible region, which is the characteristic of Pb. Wavelength 500 nm to 1100 nm has low absorbance this agree with M. Dahrul.[3].From Fig.5 & Fig. 6 we conclude that the Absorbance of CuO & Pb thin films when prepared LIPS using 1st harmonic of Nd: YAG laser (i.e. $\lambda=1064$ nm) have more Absorbance than that using 2nd harmonic of Nd: YAG laser (i.e. $\lambda=532$ nm).

After mixed between CuO:Pb thin films with different X , the Absorbance can be shows in fig 7.From Fig.7 we conclude that the Absorbance of CuO & Pb thin films when prepared LIPS using 1st harmonic of Nd: YAG laser (i.e. $\lambda=1064$ nm) have more Absorbance than that using 2nd harmonic of Nd: YAG laser (i.e. $\lambda=532$ nm).

Direct energy gap for samples can be calculated using Tauc relation[8]:-

$$\alpha h \nu = B(h \nu - E_g)^{1/2} \quad (2)$$

Where B is a constant depends on the nature of the material, h is Planck's constant and ν is the photon frequency.The relationship between $(\alpha h \nu)^2$ and photon energy (h ν) and extended straight portion of the curve to cut the photon energy axis at the point $(\alpha h \nu)^2 = 0$ we get the value of the energy gap, with thickness measured by using Fizeu Fringes is equal to 100 nm . Figures (8) show the optical energy gap for direct transmission of the copper oxide films with different number of pulses at Energy (E=900 mj) under Vacuum with $P=2.5 \cdot 10^{-2}$ mbar.The following tables shows the variation of energy with number of pulses in LIPS techniques using 1st & 2nd harmonic of Nd:YAG laser as table 3 and 4.

From the tables 3 and 4 the value of energy gap are in nearly standard E_g [5][9], at $\lambda=532\text{nm}$ the experimental value of E_g range from (1.75-1.3) eV as number of pulsed increases while at $\lambda=1064\text{nm}$ the E_g range from (1.42-1) eV this fact is right because the relation between wavelength and energy is inverse proportional . As the number of shots increase the thickness of films increases this led the absorbance of the films increase so the energy gap decreases.

Figures shows that the variation of Energy gap with number of pulses when prepared films by using LIPS with 1st & 2nd harmonic of Nd:YAG laser .The variation of Energy gap with number of pulsed are shown in following table for $(\text{CuO})_x:(\text{Pb})_{(1-x)}$. From the tables the energy gap has a good value when the number of shot is high.



**Kadhim A.Aadim and Ghaith H. Jihad**

CONCLUSION

Copper oxide (CuO) thin films and $(\text{CuO})_x(\text{Pb})_{(1-x)}$ films were successfully prepared by Laser Induced Plasma method with number of layers variation using 1st and 2nd harmonic of Nd:YAG laser at $X = (0.6, 0.7, 0.8)$ under Vacuum. From the results we have obtained the following: The copper oxide (CuO) prepared has polycrystalline structure. The Structure of CuO films are more crystalline with doped by Pb at different concentrations. Particle size of the prepared thin films increases with concentration of Pb, as well as increases surface roughness and the average square root for both 1st and 2nd harmonic of Nd:YAG laser under Vacuum. The thin films prepared has direct energy gap and the value of the optical energy gap decreased with increasing the number of Pulses for both 1st and 2nd harmonic of Nd:YAG laser under Vacuum.

REFERENCES

- [1] Y. Alajlani, F. Placido, H. O. Chu, R. De Bold, L. Fleming, and D. Gibson, "Characterisation of Cu₂O/CuO thin films produced by plasma-assisted DC sputtering for solar cell application," *Thin Solid Films*, vol. 642, no. September, pp. 45–50, 2017.
- [2] A. A. Shehab, "Effect Of Annealing Temperature For CuO Thin Films Properties Prepared By Simple Chemical Methods," *J. Multidiscip. Eng. Sci. Stud.*, vol. 3, no. 3, pp. 1472–1480, 2017.
- [3] M. Dahrul, H. Alatas, and Irzaman, "Preparation and Optical Properties Study of CuO thin Film as Applied Solar Cell on LAPAN-IPB Satellite," *Procedia Environ. Sci.*, vol. 33, pp. 661–667, 2016.
- [4] Z. Zhang and P. Wang, "Highly stable copper oxide composite as an effective photocathode for water splitting via a facile electrochemical synthesis strategy," *J. Mater. Chem.*, vol. 22, no. 6, pp. 2456–2464, 2012.
- [5] Y.-F. Lim, C. S. Chua, C. J. J. Lee, and D. Chi, "Sol-gel deposited Cu₂O and CuO thin films for photocatalytic water splitting," *Phys. Chem. Chem. Phys.*, vol. 16, no. 47, pp. 25928–25934, 2014.
- [6] X. Wang, C. Hu, H. Liu, G. Du, X. He, and Y. Xi, "Synthesis of CuO nanostructures and their application for nonenzymatic glucose sensing," *Sensors Actuators, B Chem.*, vol. 144, no. 1, pp. 220–225, 2010.
- [7] N. A. Dahham, "Annealing temperature effect on the Structure, Morphology and Optical properties of Copper Oxide CuO thin Films," vol. 22, no. 6, 2017.
- [8] M. S. Dresselhaus, *Solid State Physics Part II - Optical Properties of Solids*. 2001.
- [9] S. Visalakshi, R. Kannan, S. Valanarasu, A. Kathalingam, and S. Rajashabala, "Studies on optical and electrical properties of SILAR-deposited CuO thin films," *Mater. Res. Innov.*, vol. 21, no. 3, pp. 146–151, 2017.





Kadhim A.Aadim and Ghaith H. Jihad

Table (1).The results of X-ray examination of CuO powder

material	2θ (Deg.)	FWHM (Deg.)	d _{hkl} Exp.(Å)	d _{hkl} Std.(Å)	hkl
CuO powder	32.5026	0.1400	2.7525	2.7510	(110)
	35.5375	0.2720	2.5241	2.5230	(111)
	38.7342	0.2600	2.3228	2.3230	(111)
	48.7494	0.3140	1.8665	1.8660	(202)
	53.4636	0.3590	1.7125	1.7140	(020)
	58.2992	0.3680	1.5814	1.5810	(202)
	61.5769	0.3840	1.5049	1.5050	(113)
	65.7651	0.7940	1.4188	1.1480	(022)
	66.2506	0.5080	1.4096	1.4100	(310)
	72.4216	0.4320	1.3039	1.3040	(311)
	75.1732	0.6140	1.2629	1.2620	(222)

Table (2).The results of X-ray examination of Pb powder

material	2θ (Deg.)	FWHM (Deg.)	d _{hkl} Exp.(Å)	d _{hkl} Std.(Å)	hkl
Pb powder	28.6382	0.647	3.1146	3.1090	(110)
	31.2482	0.126	2.8601	2.8550	(111)
	36.2254	0.144	2.4777	2.4750	(200)
	48.5471	0.233	1.8738	1.8714	(222)
	52.1890	0.153	1.7513	1.7412	(311)
	62.1030	0.090	1.4934	1.4930	(222)
	65.1986	0.084	1.4298	1.4291	(022)

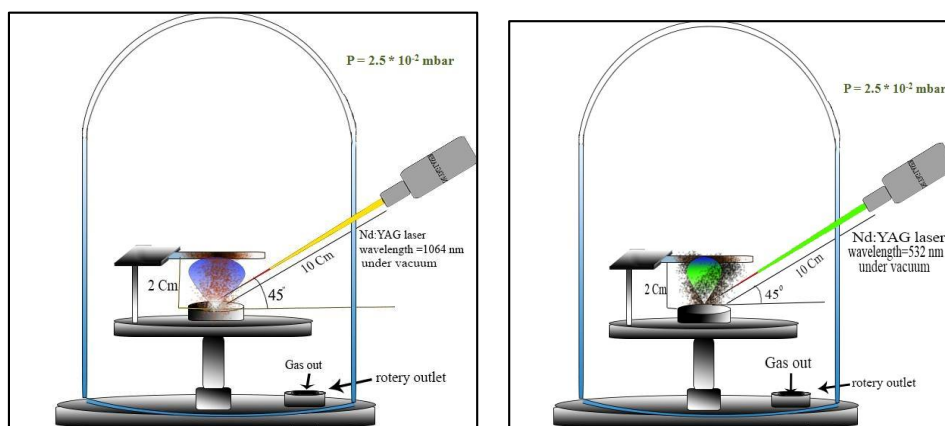


Fig (1).CuO:Pb films fabrications by using Laser Induced Plasma System under Vacuum with λ=(532nm,1064nm)





Kadhim A.Aadim and Ghaith H. Jihad

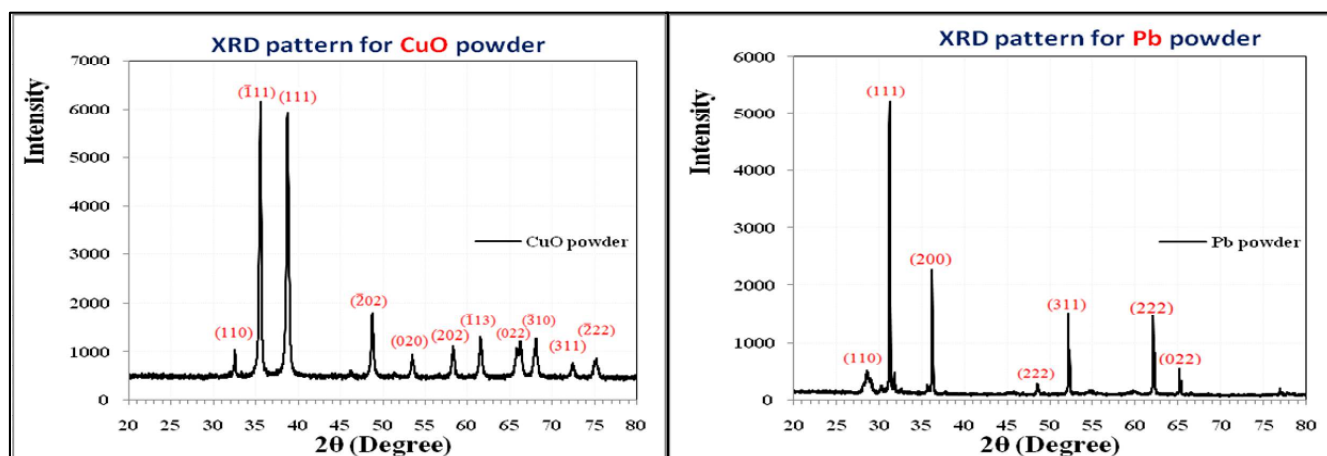
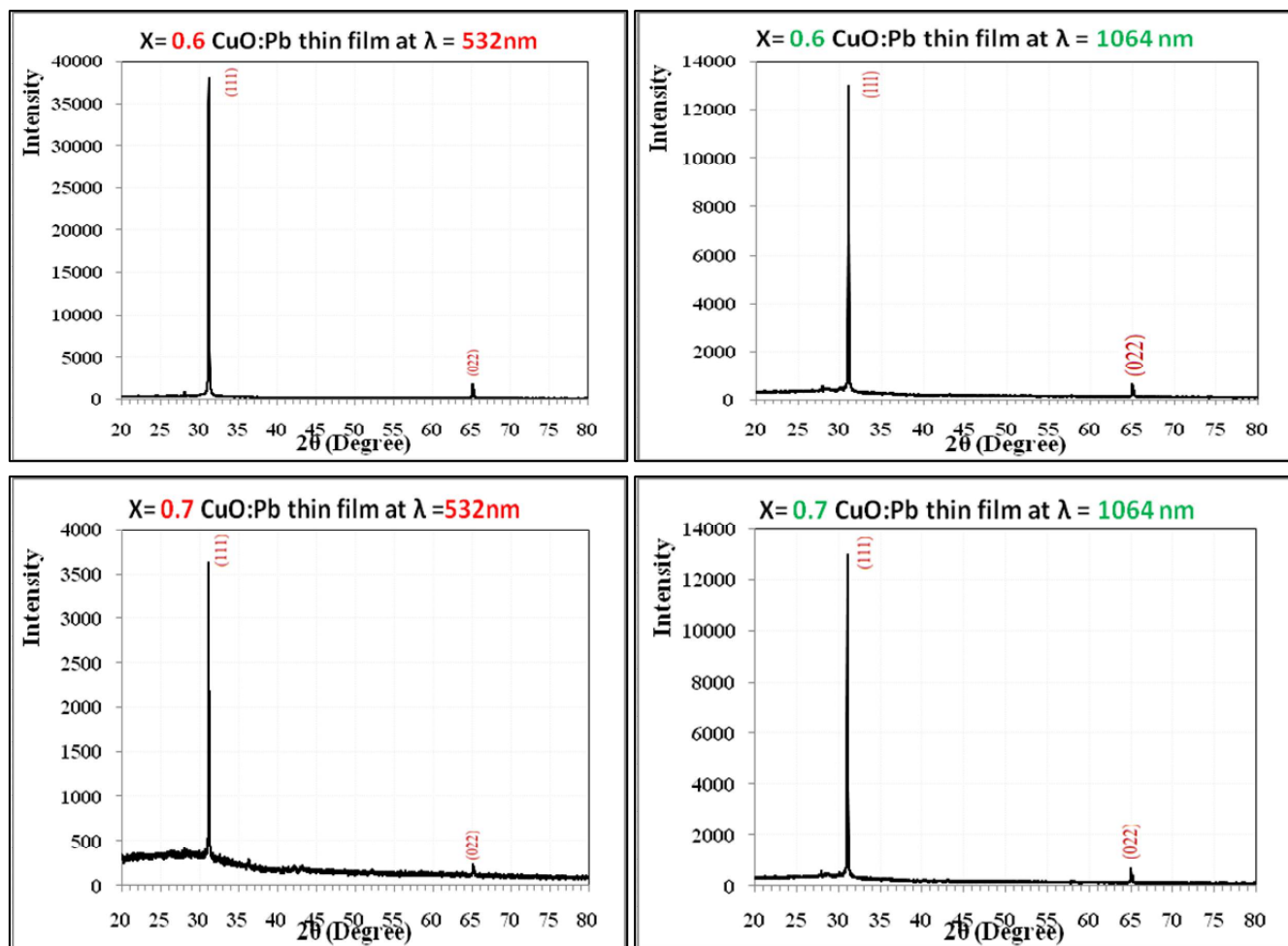


Fig (2.a): XRD patterns of CuO Powder

Fig (2.b): XRD patterns of Pb Powder



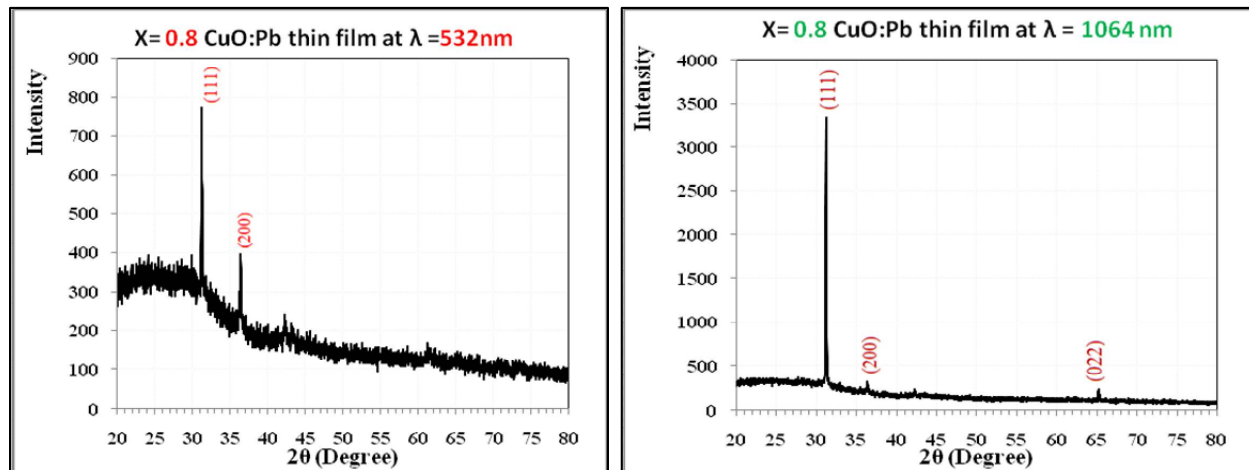


Fig (3): XRD patterns of the $(\text{CuO})_x(\text{Pb})_{1-x}$ thin films at energy $E=900$ mj using LIPS technique with $\text{NOP}=600$ Shots

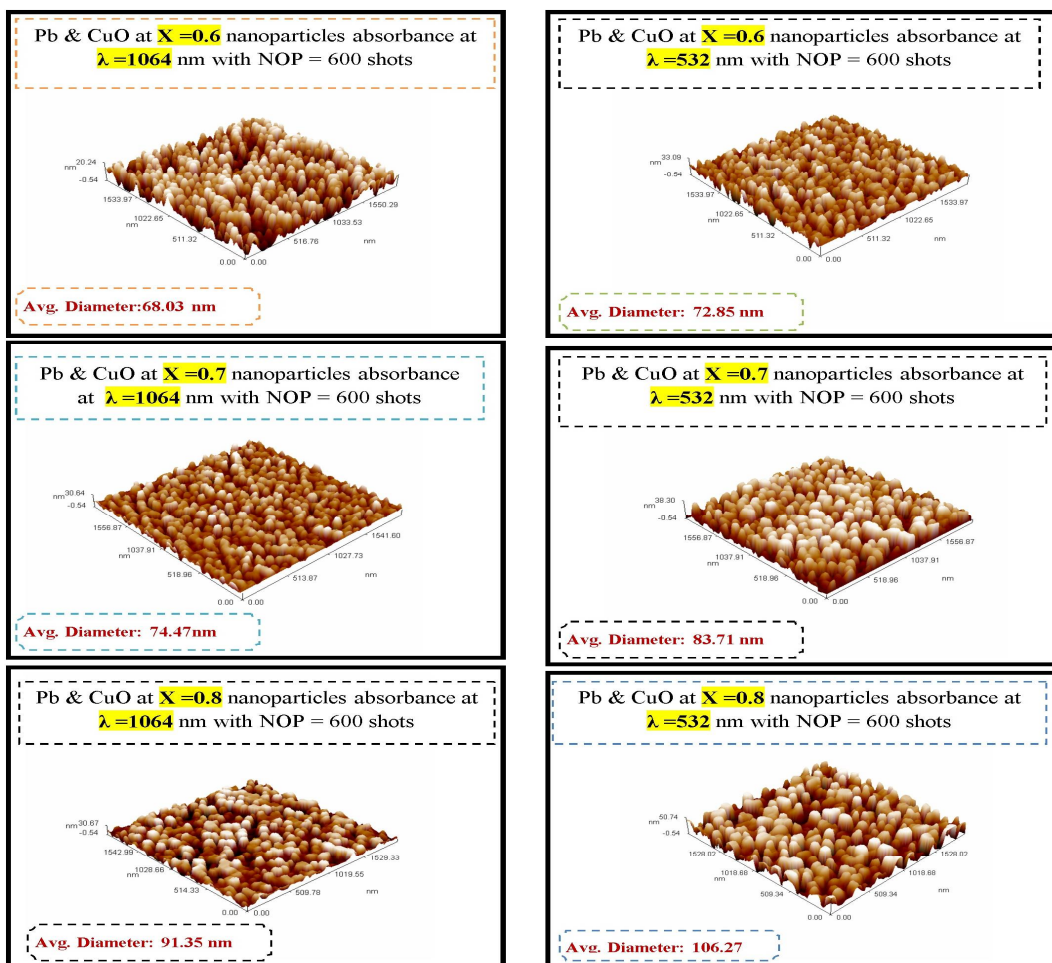


Figure (4): AFM of the prepared thin films of copper oxide (CuO) with Lead (Pb) at $\lambda = (532 \text{ nm} , 1064 \text{ nm})$, in 3D





Kadhim A.Aadim and Ghaith H. Jihad

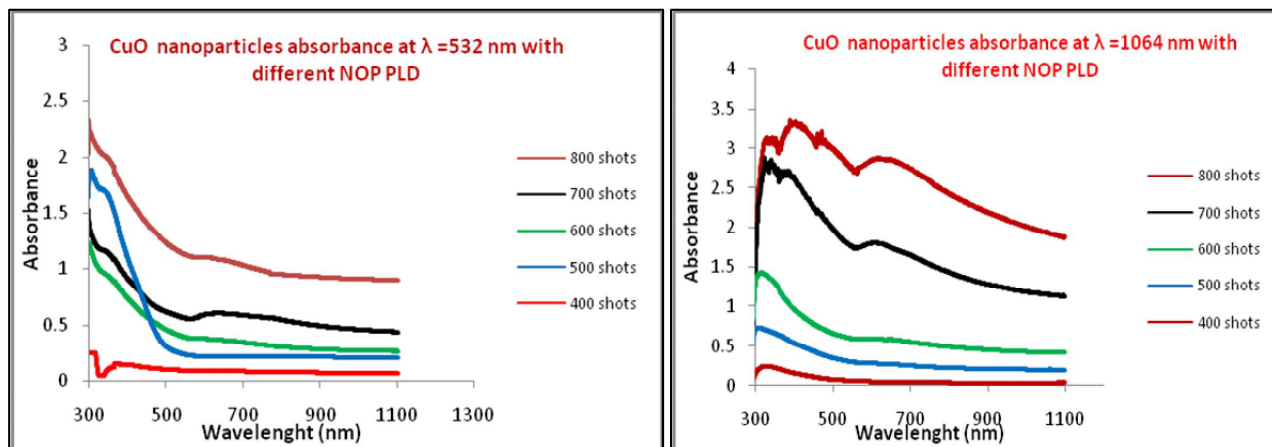


Fig. (5). Absorbance of CuO thin films prepared by LIPS using 1st & 2nd harmonic of Nd:YAG laser under vacuum

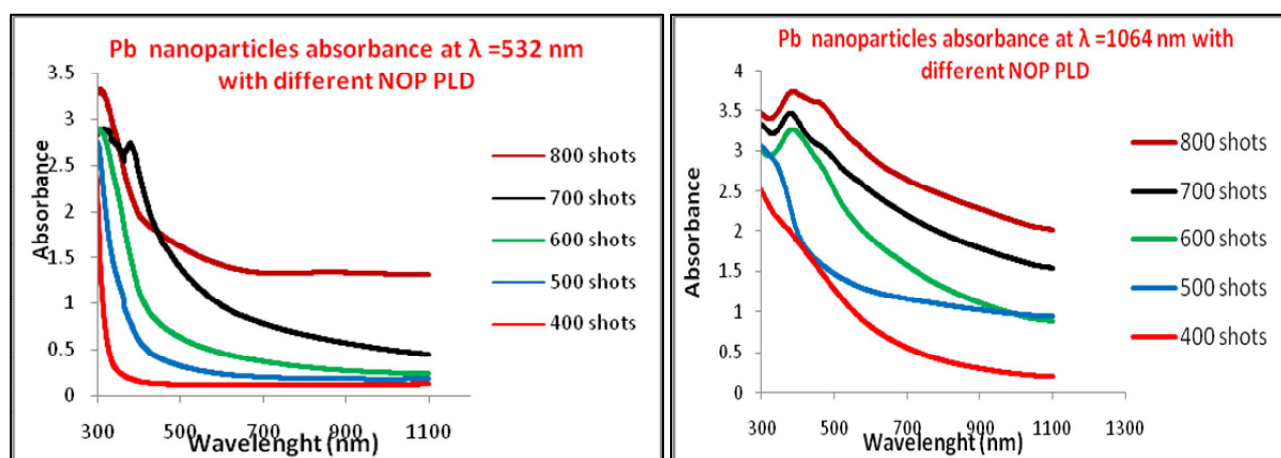
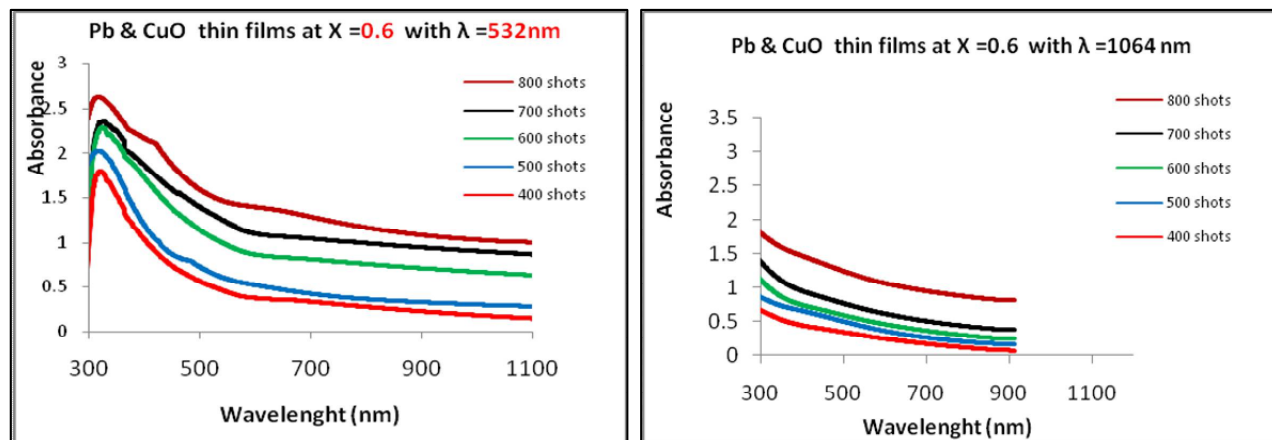


Fig. (6). Absorbance of Pb thin films prepared by LIPS using 1st & 2nd harmonic of Nd:YAG laser under vacuum





Kadhim A.Aadim and Ghaith H. Jihad

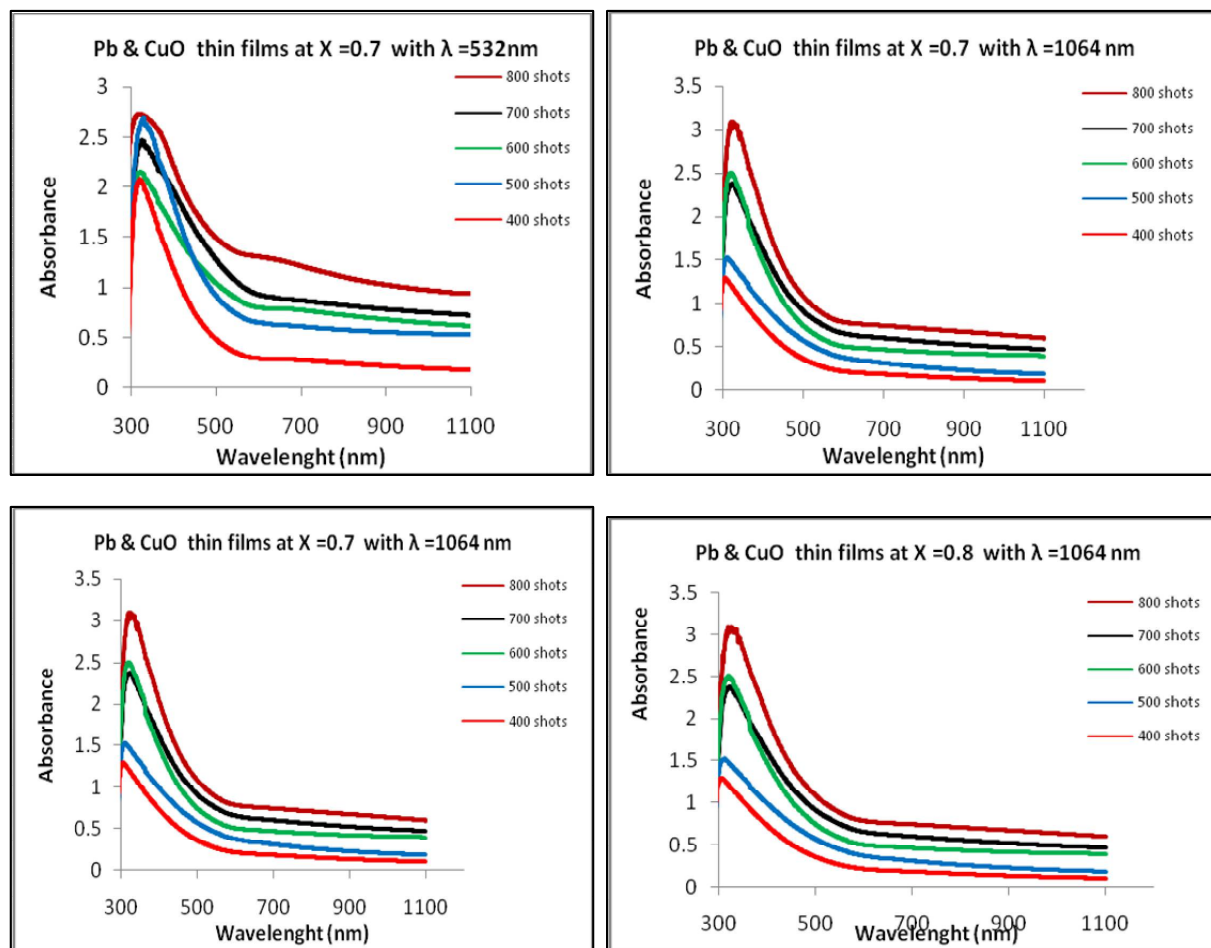


Fig. (7). Absorbance of $(CuO)_x : (Pb)_{1-x}$ thin films prepared by LIPS using 1st & 2nd harmonic of Nd:YAG laser under vacuum

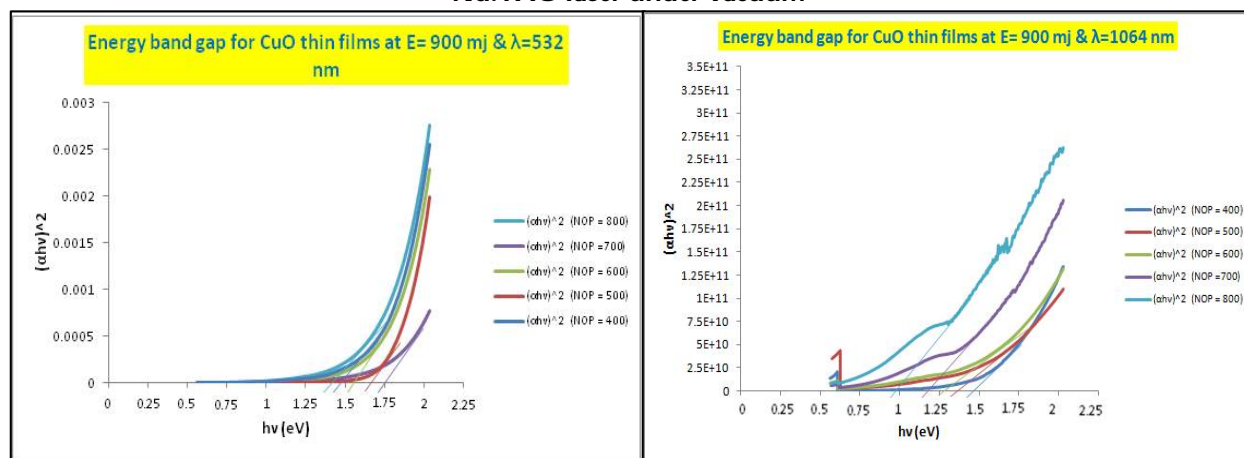


Fig. (8) Show the optical energy gap for direct transmission of the copper oxide films with different number of pulses at Energy (E=900 mj) under Vacuum.





Kadhim A.Aadim and Ghaith H. Jihad

Table (3) : The values of energy gap with NOP at $\lambda=532$ nm

Element = CuO thin film		E=900 mj			$\lambda=532$ nm		E _g (Standard)
NOP	400	500	600	700	800		
Energy gap(eV)	1.75	1.6	1.55	1.4	1.3	1.21-1.51 [5][9]	

Table (4) : The values of energy gap with NOP at $\lambda=1064$ nm

Element = Pb thin film		E=900 mj			$\lambda=1064$ nm		E _g (Standard)
NOP	400	500	600	700	800		
Energy gap(eV)	1.42	1.3	1.25	1.2	1	1.21-1.51 [5][9]	

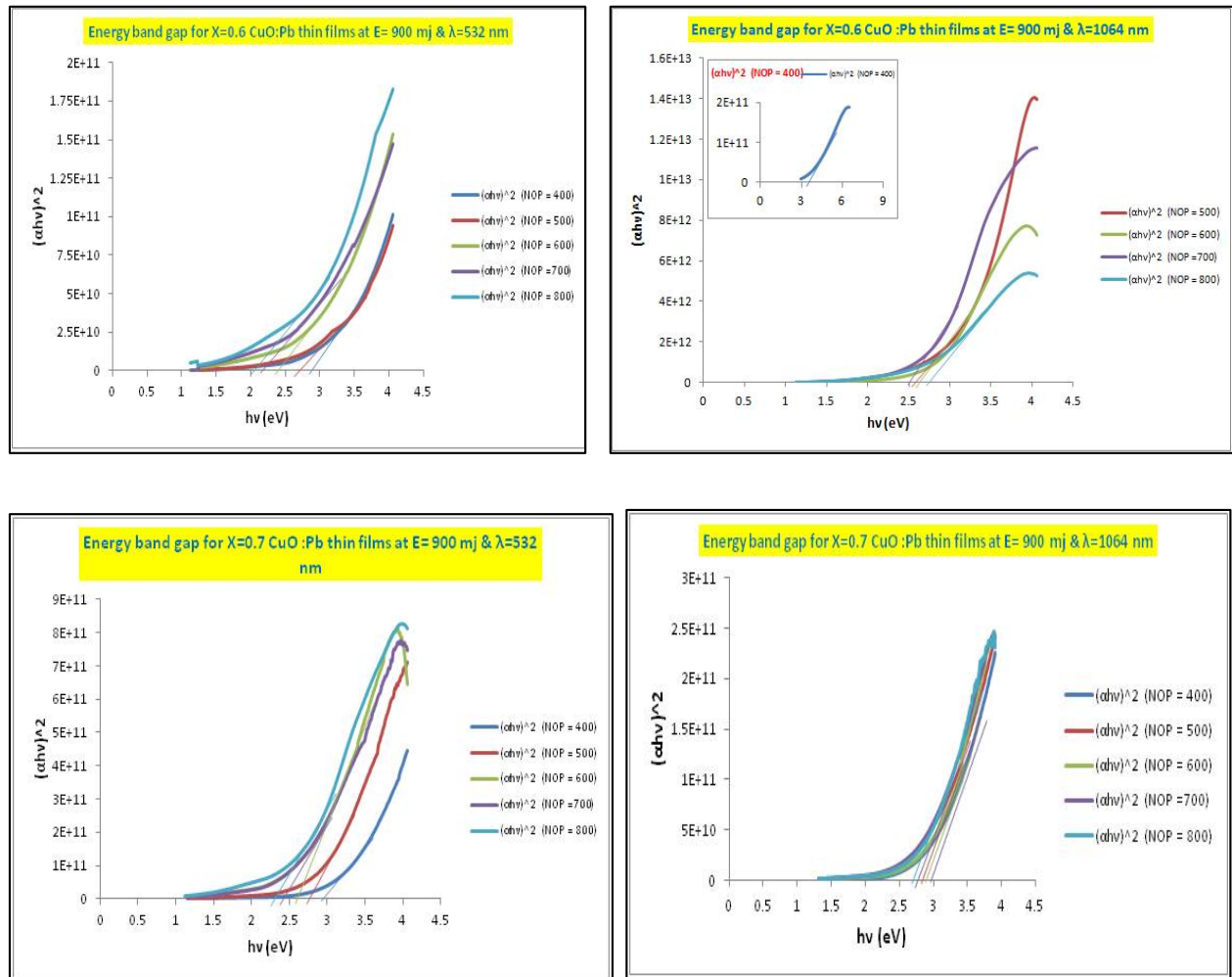


Fig.(9). Dependence of $(\alpha hv)^2$ on the photon energy. (The NOP dependence of the optical band gap)





Kadhim A.Aadim and Ghaith H. Jihad

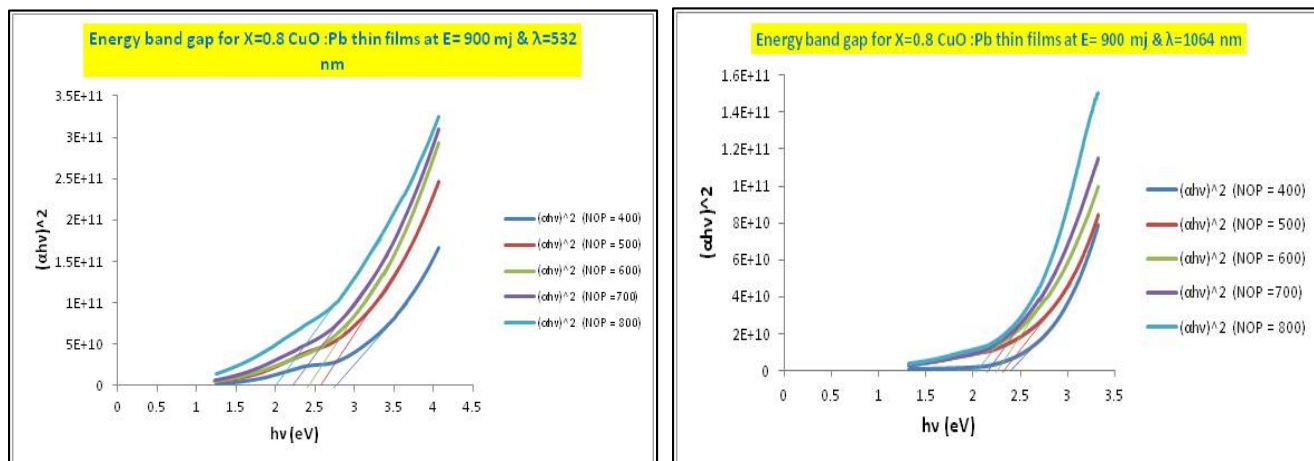


Fig. (10). Dependence of $(ahv)^2$ on the photon energy for mixing $(CuO)_x:Pb_{(1-x)}$ thin films prepared by using LIPS technique under Vacuum.

Table (5) : The values of energy gap with No. of pulse

Element = X=0.6 CuO:Pb thin film		E=900 mj			λ=523nm	
NOP	400	500	600	700	800	
Energy gap(eV)	2.8	2.6	2.4	2.2	2	
Element = X=0.6 CuO:Pb thin film		E=900 mj			λ=1064nm	
NOP	400	500	600	700	800	
Energy gap(eV)	2.8	2.7	2.62	2.59	2.49	
Element = X=0.7 CuO:Pb thin film		E=900 mj			λ=523nm	
NOP	400	500	600	700	800	
Energy gap(eV)	2.9	2.66	2.66	2.4	2.35	
Element = X=0.7 CuO:Pb thin film		E=900 mj			λ=1064nm	
NOP	400	500	600	700	800	
Energy gap(eV)	2.9	2.8	2.72	2.62	2.6	
Element = X=0.8 CuO:Pb thin film		E=900 mj			λ=523nm	
NOP	400	500	600	700	800	
Energy gap(eV)	2.7	2.55	2.45	2.25	2	
Element = X=0.8 CuO:Pb thin film		E=900 mj			λ=1064nm	
NOP	400	500	600	700	800	
Energy gap(eV)	2.4	2.3	2.25	2.2	2.1	





Technological Advancements in Manufacture of Heat cum Acid Coagulated Dairy Products---A Review

Siva Kumar S^{1*} and Rajinder Kumar²

¹College of Dairy Science and Technology, GADVASU, Ludhiana (Punjab) -141 004, India.

²Research Scholar, Division of Dairy Technology, NDRI Karnal, Haryana-132001, India.

Received: 15 Nov 2017

Revised: 17 Dec 2017

Accepted: 23 Dec 2017

*Address for correspondence

Dr.Siva Kumar S

Assistant Scientist,

College of Dairy Science and Technology,

GADVASU, Ludhiana (Punjab) -141 004, India

E.mail: drshiva2003@yahoo.com



This is an Open Access Journal / article distributed under the terms of the **Creative Commons Attribution License** (CC BY-NC-ND 3.0) which permits unrestricted use, distribution, and reproduction in any medium, provided the original work is properly cited. All rights reserved.

ABSTRACT

Paneer is the famous dairy product across Indian sub-continent obtained by heat treating the milk followed by acid coagulation using suitable acid. From the point of sensory evaluation, paneer is mild acidic flavour with slightly sweet taste, and a soft, cohesive and compact texture. Paneer is rich in nutrients and having enough moisture content in the product to permit growth of variety of microorganisms. The ambient storage conditions are generally favourable for their survival and rapid growth. The shelf life of the paneer is one day at room temperature and for about a week under refrigeration (7 °C). The spoilage of *paneer* is mainly due to bacterial action. Successful attempts have been made to enhance the shelf life of *paneer*. The Chhana is used extensively as the base and filler for the preparation of a variety of Indian sweets namely rasogolla, sandesh, cham-cham, rasamalai, rajbhog, chhana-murki. This review article deals with the technological advancements in manufacture of heat cum acid coagulated dairy products with respect to factors affecting physico-chemical, microbiological changes and nutritional profile, packaging and shelf life of the heat cum acid coagulated dairy products.

Keywords: Heat cum acid coagulated dairy products, paneer, chhana, packaging, storage changes, Shelf life.

INTRODUCTION

The development in paneer manufacturing is not well documented, but from the history, it was originated from nomads of southwest Asia who were the first to develop various kinds of cheeses. "Paneerkhiki" a distinctive cheese variety was developed first by the Iranian "Bakhtiari" tribe, in south-west Asian region. Paneer means container, "Khiki" means skin (Rennet form of goat / sheep was may be used to make it, hence the name). In the beginning,



**Siva Kumar and Rajinder Kumar**

paneer was prepared by curdling milk by using sour milk, pieces of creepers called “putika” or bark of “palaska” tree (Singh *et al* 1984). Paneer is a universally accepted product across Indian sub-continent. Cottage cheese manufactured by acid coagulation in western countries is similar product, Queso del pais, Queso Blanco, Quesocriollo and Quesodela Tierra are some of the similar products prepared in South and Central America. Chhana is more commonly known as paneer in certain parts of India. The main difference between paneer and chhana is pressing, the pressed chhana is called as paneer. Paneer market in India is the largest dairy product sold in terms of volume after liquid milk, 80% of which is sold as loose paneer by local milk vendors. Paneer plays a significant role in the Indian vegetarian diet owing to its high food and nutritive value. It contains high level of proteins, fat, minerals like calcium and phosphorus and vitamin A and D. Because of the above mentioned nutritional benefits, paneer is an ideal food for infants, adolescents, adults, growing children, sport persons and pregnant womens. The ability of paneer to be deep fried is one feature that has led to its wider acceptance and ideal for making snacks, pakoras or fried paneer chunks. Paneer is a rich source of animal protein, available at a comparatively lower cost and forms an important source of animal protein for vegetarians. The preparation and use of chhana for preparation of chhana based sweets are confined mainly to the eastern region of the country, notably West Bengal, which produce the maximum quantity (De 1983).

Definition of paneer

According to FSSR (2011), Paneer obtained from cow / buffalo milk or a combination thereof by precipitation with sour milk, lactic acid or citric acid. It shall not contain more than 70% moisture and the milk fat content shall not be less than 50% of the dry matter. Milk solids may also be used in preparation of the product. Paneer when sold as low fat paneer, it should confirm the following requirements i.e. Moisture not more than 70.0 percent and milk fat not more than 15.0 percent of dry matter.

Method of manufacture

Buffalo milk with 6% fat 9% SNF was heated to 90°C/ 5 minutes and cooled to 70°C. Standardization of Fat: SNF 1:1.65 was carried out using buffalo skim milk. Then citric acid solution (2-2.5 g/kg of milk) is added slowly with continuous stirring until a clear curd and whey is separated, then the mixture was allowed to settle down for 10 minutes and whey was drained out through a muslin cloth during this time. The curd was then collected and filled in a hoop lined with a clean and strong muslin cloth. The hoop had a rectangular frame with the top as well as bottom open. The hoop was then kept under pressure for 15-20 minutes. The pressed block of curd is removed from the hoop and cut into pieces and immersed in pasteurized chilled water (4–6 °C) for 2–3 h. The chilled pieces of paneer are then removed and placed on a wooden plank for 10–15 min to drain occluded water. Afterwards, these pieces were packed in LDPE materials and stored at refrigeration temperature (4±1 °C) (Bhattacharya *et al* 1971).

An industrial process for the manufacture of paneer has been developed by the NDDB. The milk is heated to 85°C through a plate heat exchanger, pumped to a paneer vat and cooled to 75°C. Hot milk is coagulated by adding citric acid solution with proper mixing. The curd is left to settle for 10 to 15 minutes without agitation. The whey is then drained and the curd heaps are filled in paneer hoops with a muslin cloth and pressed for 10 to 15 minutes at a pressure of 3 kg per sq. cm to remove the whey. The final blocks are dipped in pasteurized cold water at 4°C for 3 hours for cooling and firming the paneer (Aneja 2007).

Value addition –Different Types of paneer

Paneer is manufactured by using some modifications in different methods for different types of milk.

Difference between Cow milk paneer / buffalo milk paneer/mixed milk paneer

For getting good quality paneer from cow milk, certain additive to be added along with certain modifications in the manufacturing process is required. Paneer conforming the FSSAI standards was made from crossbreed cow milk with 3.7% fat and 8.25%-8.42% SNF (Pruthi and Koul 1989). Paneer made from cow milk is of inferior quality in



**Siva Kumar and Rajinder Kumar**

sensory characteristics as compared to buffalo milk is due to the different makeup of casein micelles and lower calcium and protein content. Buffalo milk with 5-6% fat was recommended for the manufacturing of paneer (Bhattacharya *et al* 1971) Fat globules and casein micelles of bigger size and higher concentration of fat, casein, calcium, phosphorus and lower voluminosity and solvation properties of casein micelles in buffalo milk makes it for paneer making with spongy character (Sindhu 1996). Paneer manufactured from 6% fat buffalo milk was best in quality. Better quality paneer was prepared with 20 parts of buffalo skim milk and 80 parts of cow whole milk. Buffalo and cow milk (65:35) having 5.18% fat was used for manufacture of paneer .Pal and Yadav (1991) recommended the use of mixed milk(50% cow milk and 50% buffalo milk) with fat level of 3.5% was used for the production of low-fat paneer.

Sheep/Goat milk paneer

Sheep milk could be used to manufacture paneer, which resembled buffalo milk paneer. Processing variables like heat treatment (90°C), coagulation temperature (90°C) and coagulant strength (2%) were standardized for the manufacturing of paneer from ewe's milk with 6.94 % fat (Pal *et al* 2008).

Conventional paneer and Low fat paneer

Milk with a fat to SNF ratio of 1:1.65 is preferred for the preparation of paneer (Khan and Pal 2011). Low fat paneer is a good alternative to high fat paneer .The high fat paneer, generally avoided by health conscious people due to its high fat content. In western countries skim milk paneer and low fat paneer are available with 13% fat and 24% fat, respectively on dry matter basis, from these two variants skim milk paneer had a chewy, hard body and rubbery texture. Paneer with acceptable quality can be obtained from milk with 3.5 % fat without incorporation of any additive. In addition to reduction in cost, sensory quality and rheological properties of low fat milk paneer was improved with addition of soya solids (Kanawjia and Singh 2000). Low fat paneer incorporated with soy fiber and inulin increased the sensory, rheological and nutritional parameters. Dietary fiber not only improves the sensory and textural properties of low fat paneer but also reduces the chances for colorectal cancer (Kanawjia and khurana 2006). Goel (2000) reported that the total solids, fat, protein, lactose and ash content of laboratory made paneer varied from 57.8 to 56.52, 25.0 to 26.0, 23.08 to 27.02, 2.29 to 2.52 and 1.195 to 1.305 per cent, respectively.

Recombined and Reconstituted milk paneer

The milk production during the summer season declines, this leads to lower availability of milk, not only for the production of milk but also for conversion into products. Good quality paneer was manufactured by using skim milk powder, whole milk powder and butter oil by using the required modifications in the processing parameters (Kanawjia and Khurana 2006).

Paneer Tikka

Paneer tikka, an exotic kebab a value added product, when vacuum packed using LLDPE/BA/Nylon-6/BA/LDPE and stored at 3±1 °C had shelf life of 40 days. Out of 3 packages studied, LLDPE/BA/Nylon-6/BA/LDPE was most effective in controlling the chemical changes during storage (Kunal and Goyal 2013).

Herb or vegetable impregnated paneer

Functional properties of paneer can be improved by incorporation of vegetables to paneer. Along with value addition, cost of the product is also decreased with a small decrease in sensory scores of the product. The incorporation of coriander and mint leaves in the range of 5-30% in buffalo milk (5% fat) increased the yield, crude fiber, ascorbic acid, iron, ash, and calcium content of the paneer (Bajwa *et al* 2005).



**Siva Kumar and Rajinder Kumar****Protein enriched paneer**

Non conventional low cost proteins are mainly used to improve its nutritional value, reduce the cost and sensory characteristics of low fat paneer. This is suitable for the consumers suffering from protein malnutrition and coronary complications (Khan and Pal 2011). Paneer with high nutritional value was manufactured by incorporating calcium salt and groundnut protein isolates in the skim milk and vegetable fat mixture (Kanawjia and Singh 2000). Soy protein isolate (SPI) was mainly added as a fat replacer for the preparation of low fat paneer. The addition of SPI increased the yield % and Protein % (Sivakumar *et al* 2011).

Filled paneer and Soymilk paneer

Preparation of filled paneer is a best alternative to utilize the skim milk during the flush season where the possibility of casein manufacture is not possible or the paneer demand is high. The skim milk (9 Part) is utilised by blending coconut milk (1 Part) or vegetable oil for preparation of filled paneer with acceptable sensory attributes (Venkateshwarlu *et al* 2003). Soy milk, vegetable protein incorporated in the milk products not only help reducing the cost but also increases the nutritive value of the final product. Coagulation of soya milk results into a soft, white and gelatinous mass. The soy milk @40% was added to buffalo milk to get the soya milk paneer, but the physical scores of all parameters decreased at this level (40%). The soy milk up to 20% level added to buffalo milk had no adverse effect on sensory characters. The addition of sodium caseinate further enhances the acceptability of soy paneer (Biradar *et al* 2012).

UF/MF Paneer

Membrane technology application in dairy sector provides great opportunities in terms of quality control, concentration and fractionation along with energy conservation. The shelf life of the paneer was 3 months at 35°C, this was manufactured by autoclaving the ultra filtered double toned milk was concentrated to 30% total solids and glucono- δ -lactone was added @0.9% before filling in retortable metalized polyester pouches. Retentate of microfiltration along with addition of calcium chloride @0.15% was used for manufacturing of paneer with improved textural and organoleptic properties (Kanawjia and Rizvi 2000).

Measures to improve shelf life of paneer

The shelf life of paneer was about 7 days at 7°C storage, however, its freshness was lost in just 3 days. Therefore, short shelf life of paneer is one of the major drawbacks, several methods have been tried so far by a few workers to enhance the shelf life of paneer. Kanawjia and Singh (2000) reported that packaging of chemical preservatives treated paneer with and without vacuum extended its shelf life up to 35 and 50 days, respectively at 8 °C. Rani *et al* (2014) reported that fresh skim milk (fat 0.5% and solid not fat (SNF) 8.7%), vegetable oil (soyabean oil), coriander leaves (1%), mint leaves (1%) and green chilies (0.3%), roasted and grounded cumin seeds (0.3%) and black pepper (0.3%) were used for preparation of brine dipped and dry salted masala paneer. Further, various measures were tried to improve shelf life of paneer which may be broadly categorized as use of antimicrobial agents, application of various treatments and use of hurdle technology.

Chhana and Chhana based Sweets

According to FSSR (2011), chhana means the product obtained from the cow or buffalo milk or a combination thereof by precipitation with sour milk, lactic acid or citric acid. It shall not contain more than 70.0 % moisture and the milk fat content shall not be less than 50.0% of the dry matter.

Method of Manufacturing of Chhana**Traditional Method and Continuous method**

In traditional method a small quantity of boiled milk is taken in a coagulating vessel. The required amount of coagulant is added to the milk and mixed till the coagulation is complete. The muslin cloth containing the curd mass





Siva Kumar and Rajinder Kumar

is hung to remove the whey further and to cool the chhana for further processing (Aneja *et al* 2002). In continuous method, a prototype machine with 40 kg chhana /per hour capacity consists of balance tank, injection chamber, holding coil, cooling chamber and strainer. Standardized cow milk (250 litres /hr) is pumped from a balance tank to an injection chamber where the steam is directly injected into the milk and the steam gets completely condensed in milk and temperature is increased to 90-95°C. Then the milk is brought in contact with the coagulant, which is regulated manually in proportion to the rate of milk flow. The mixture is circulated through a holding coil for complete coagulation of milk. The coagulated product, along with the whey is then pumped to a double-jacketed cooling tank, where it is cooled down to room temperature then the product is directed to a mechanical strainer, a double jacketed inclined sieve, where it is drained thoroughly. Chhana with 55-65% moisture is discharged through the outlet and collected in the basket and whey is transferred to a separate tank for subsequent use for conversion in to whey based products.

CONCLUSION

Indian milk sweets have played an important role in the socio-economic and religious aspect of the human being. Paneer, Paneer based products, Chhana and Chhana-based products have been prepared and marketed in India for quite long time, the main drawback is that they are in the hands of mostly unorganized sector and limited with organized sector. The market potential is huge and it surpasses the many western dairy products. The Indian milk sweets having high profit margins and export potential and this sector is need to modernize to produce high quality products with long shelf life.

REFERENCES

1. Aneja R P, Mathur B N, Chandan R C and Banerjee A K (2002). Technology of Indianmilk products. In Dairy India Publication Delhi, India.
2. Aneja R P (2007) East-West fusion of dairy products. In: Gupta S (ed) Dairy India 2007, 6th edn. Dairy India Yearbook, A Dairy India Publication, New Dehli, pp. 51–53.
3. Bajwa U, Kaur J and Sandhu K S (2005) Effect of processing parameters and vegetables on the quality characteristics of vegetable fortified paneer. *Journal of food Science and Technology* 42: 145–50.
4. Bhattacharya D C, Mathur O N, Srinivasan M R and Samlik O (1971). Studies on the method of production and shelf life of paneer (cooking type of acid coagulated cottage cheese). *Journal of Food Science and Technology* 8: 117-120.
5. Biradar G S, Gujar S K, Dande K G and Gaikwad S M (2012). Studies on Physico Chemical Quality of Paneer (Indian Cheese) Papered From Blends of Soymilk and Buffalo Milk. *Journal of Animal Production* 2: 142-45.
6. De S. (1983) Indian Dairy Products. In: "Outlines of Dairy Technology". First Ed. Oxford university press, Delhi, pp: 382-466.
7. FSSR (2011) Food Safety and Standard Regulations. Food Safety and Standard Authority of India, Ministry of Health and Family Welfare, Govt. of India, New Delhi .pdf (Accessed on 12.10.2017).
8. Goel B K (2000) Reduction in the level of air borne contamination by the use of air washing and UV rays and its effect on shelf life of paneer. Ph.D. Thesis Submitted to Gujarat Agricultural University, Anand Campus, Anand, Gujarat.
9. Jayaprakash K T (2003) Technological studies on the manufacture of Rasogolla using artificial sweeteners. M. Sc. Thesis, NDRI Deemed University Karnal
10. Kanawjia S K and Singh S (2000) Technological advances in paneer making, *Indian Dairyman* 52: 45–50.
11. Kanawjia S K and Rizvi S S (2000) Development of paneer from microfiltered milk. *Indian Journal of Dairy Bioscience* 11: 67–70.
12. Kanawjia S K and Khurana H K (2006) Development of paneer variants using milk and non-milk solids. *Process Food Industry* 9: 38–42.





Siva Kumar and Rajinder Kumar

13. Khan S U and Pal M A (2011) Paneer production: A review. *Journal of Food Science and Technology*. 48:645–60.
14. Kunal K A and G K Goyal. (2013) Combined effect of vacuum packaging and refrigerated storage on the chemical quality of paneer tikka *Journal of Food Science and Technology* 50: 620–23.
15. Mathur, G K and Singh V B (2001) Protein enriched rasogolla. *Indian Journal of Dairy Sciences* 54(6): 305-310.
16. Pal M A and Yadav P L (1991) Effect of blending buffalo and cow milk on the physico-chemical and sensory quality of paneer. *Indian Journal of Dairy Science* 44: 327–32
17. Pal D, Rajorhia G S, Garg F C and Verma B B (1993) Development of technology for dried rasogolla mix. National Dairy Research Institute, Karnal, Annual Report, 1992-93, pp.90.
18. Pal M A, Malik A H, Wani S A, Salahuddin M and Bhat A S. (2008) Quality and yield of ewe milk paneer under the influence of various processing variables. *Beverage Food World* 35: 44–48.
19. Pruthi T D and Koul J L (1989) Paneer from crossbred cows' milk. *Indian Journal of Dairy Science* 42: 403–04.
20. Rani M, Dabur R S, Garg S R and Jadhav V (2014) Preparation, storage and microbiological quality of ready-to-serve low cholesterol masala paneer. *Veterinary World* 7(6): 443-447.
21. Sharma D K and Reuter H (1991) A new method of chhana making by ultrafiltration technique. *Indian Journal of Dairy Sciences* 44: 89-95.
22. Sindhu J S (1996). Suitability of buffalo milk for products manufacturing. *Indian Dairyman* 48: 41–47.
23. Singh S, Kanawjia S K and Sachdeva S. (1984) Current status and scope for future development in the industrial production of paneer. *Indian Dairyman* 36: 581-585.
24. Singh S P (1991) Technological Studies on production of Rasogolla from Reconstituted milk. M.Sc. Thesis NDRI Deemed University, Karnal.
25. Singh S K, Dwivedi H B, Kumar R and Yadav M P S (2005) Use of chemical andherbal coagulants in Chhana production from cow milk. *Journal of Farm Sciences* 14(2): 71-72.
26. Siva Kumar S, Balsubramanian S, Biswas A K, Chatli M K, Devatkal S K and Sahoo J (2011) Efficacy of soy protein isolate as a fat replacer on physico-chemical and sensory characteristics of low-fat paneer. *Journal of Food Science and Technology* 48(4): 498–501.
27. Tewari, B D and De S (1976) Standardization of the Industrial Method of Production of Dried Chhana. *Indian Journal of Dairy Sciences* 29: 212.
28. Venkateswarlu U, Reddy Y K and Kumar S (2003) Preparation of filled milk paneer by incorporating coconut milk. *Indian Journal of Dairy Science* 56: 352–58.

Table 1. Microbiological parameters of paneer

Parameters	Requirements
Standard plate count per g (max.)	35 x 10 ⁴
Coliform per g (max.)	100
Yeast and Mold per g (max.)	150

Table 2. Cooked channa-juicy products

Cooked channa-juicy products	
Rassogalla- boiled in sugar syrup.	
Rasomalai- boiled in sugar syrup and then transferred to sweetened condensed milk	
Rajbhog- boiled same as rasogolla, The size is the difference between them. It is stuffed with khoa, spices and cardamom	
Chamcham- boiled similar as rasogolla but shaped cylindrical and decorated with grated khoa	
Cooked channa -dry products:	Sandesh- medium moisture content Koda pak sandesh- very low moisture content.
Fried channa pieces coated with sugar -----Chanar murki	





Siva Kumar and Rajinder Kumar

Table 3. Innovations in the manufacture of chhana based sweets

Chhana Powder	Chhana powder was produced using tray, roller and spray drying processes. The product was reconstituted into chhana for preparation of Sandesh and Rasogolla, but during boiling, the balls are broken in the sugar syrup. The shelf life of the product was 2 months (air tight) and 4 months (gas packing) conditions. (Tewari and De 1976).
Chhana by Ultra filtration	The application of ultra filtration increases the product yield because of recovery of additional whey proteins (Sharma and Reuter 1991).
Use of Herbal Coagulants	The two herbal coagulants (papaya extract and ginger extract) were used for preparation of chhana. The sensory and chemical quality of the chhana produced using herbal coagulants was not comparable with the conventional chhana. (Singh <i>et al</i> 2005)
Sugar-free rasogolla	The manufacturing of sugar free rasogolla using different artificial sweeteners. viz 41.77 % sorbitol and 0.08 percent aspartame. (Jayaprakash 2003)
Sandesh	80 % of chhana was produced into sandesh in West Bengal. Chhana obtained with citric acid was usually preferred for the manufacture of sandesh. (Aneja <i>et al</i> 2002).
Protein-enriched rasogolla	The protein-enriched rasogolla prepared by using Soya- protein isolate deoiled soya-flour and skim milk powder added to cow milk, buffalo milk, goat milk and mixed milk. The protein content was increased by 47%, as compared with the control, when 1.5% soya protein isolate was added to mixed milk. The sensory attributes were comparable with the control. (Mathur and Singh 2001).
Chhana from Concentrated and Dried Whole Milk	Good quality of chhana from concentrated and dried whole milk was prepared after it was reconstituted to 15% TS (Singh 1991).
Dried rasogolla mix	Skim milk was concentrated to the required total solids level by using ultra and diafiltration process, calculated fat was added to the retentate before spray drying it. Certain additives and binders were dry blended in the retentate powder to get dried rasogolla mix and this is having balanced flavor and spongy texture. (Pal <i>et al</i> 1993).





Ethics of the Environment from the Perspective of Islam

Mohammad Noor Sepahi^{1*} and Abdul WahhabJasim Mahdi²

¹Department of Environmental Science, SavitribaiPhule Pune University, India.

²Department of Environmental Science, Acharya NagarjunaUniversity, Guntur, AndhraPradesh,India

Received: 13 Dec 2017

Revised: 18 Dec 2017

Accepted: 27 Jan 2018

* Address for correspondence

Mohammad Noor Sepahi

Department of Environmental Science,
SavitribaiPhule Pune University, India
Ganeshkhind, Pune, Maharashtra 411007.
E.mail: mohammadnoor.sepahi@yahoo.com



This is an Open Access Journal / article distributed under the terms of the **Creative Commons Attribution License** (CC BY-NC-ND 3.0) which permits unrestricted use, distribution, and reproduction in any medium, provided the original work is properly cited. All rights reserved.

ABSTRACT

Losses of untapped use of nature and the appearance of various pollutants in the environment progress and development without comprehensive planning, which is associated with the degradation and pollution of the environment, a global look at the environmental components in the world shows the precarious situation. The necessity of elaboration of the principles of environmental ethics regarding the moral aspirations of God, and at the same time it includes the development and improvement of material life, more serious than ever. Such a set of principles and foundations cannot be formulated by a person or group as a community, because it requires the foundations of ontology and anthropology derived from the source of the transcendental nature of the teachings of the revelation. The environment is all that exists and affects us around us, and they affect us and include the natural environment, artificial environment and social environment. From the point of view of Islam, principles can be mentioned, most important of which are: environmental justice, the development of artificial environments, the invitation to protect the environment, the environmental impact of development plans, the prevention of environmental degradation and environmental pollution, optimum use, environmental health, water health, air health, sound health, land health, waste sanitation, creation of a recycling system, development of green space and implementation of national and international agreements.

Keywords: Principles, Ethics, Environment, Health, Islam.

INTRODUCTION

In the present world, human beings have noticed the harmful consequences of uncontrolled exploitation of nature and the appearance of various types of pollutants in their environment. Progress with and without comprehensive





Mohammad Noor Sepahi and Abdul WahhabJasim Mahdi

planning is accompanied by the destruction and pollution of the environment, the apparent progression of the existing practice has led to the use of some individuals or institutions and limited countries of these advances has multiplied their capital, facilities and prosperity, but on the contrary, Nature has been destroyed and pollution of land, climate and the environment has spread to the world. One of the most important problems in today's world is the environmental crisis. It seems that this problem started when modern man stopped understanding himself as the vicegerent and trustee of the All-Merciful God who must channel divine mercy to everything at his disposal or within his reach, and stopped understanding nature as a sacred sign and valuable trust from God.

Other harmful gases from the atmosphere of industrialized countries and only two percent of the share of Third World countries. In this regard, in the last two centuries, with the consumption of fossil fuels and the destruction of forests, the total amount of carbon dioxide in the atmosphere has risen by 25%. The global look at other environmental factors in the world also presents a risky situation. Pollution and destruction of the environment is like a fire that combines firewood, dry, sinner, and non-fossil, so all the inhabitants of the planet need sustainable development and participate in preventing the degradation of the environment and pollution. Another issue in the environmental crisis is the massive increase in the population. In Islamic sources, we have a narrative account of the increase in the Muslim population. But the big question is whether this is a rule and should be implemented at all times and that the population continues to increase, or that it is not a rule and merely a cross-sectional plan. In certain times and in a special location, population growth can increase community development and improve life. The same growth and development tool and power, if left beyond its borders, can become a destructive lever of economic forces and cultural and scientific backing. From the point of view of Islam, there is a desirable demographic increase in quality. That is, if it is impossible to educate them and to provide conditions for marriage, occupation and housing, the increase in population will cause the Islamic society to decline. And the Prophet's Hadith about boasting the Prophet to the Muslim community, it means that Muslims need not be poor and backward and addicted, and so on.

When the population increases, the community's production structures must be expanded in proportion to it, so that the community can meet its own needs, but if such a balance does not exist, the population will be in need and dependence. Today, the necessity of elaborating the ethics of the environment that addresses the divine ethical aspirations and at the same time embracing the development and improvement of material life is more serious than ever before. The environment is all that exists around us and affect them, and they also affect us. The environment has a variety of:

Natural environment

All natural factors that exist around us are not created by humans, but are in use. The natural environment includes the following: air, soil, plants, animals, and a summary of the whole surface of the earth and its surrounding atmosphere.

Artificial environment

All things created by humans, such as residential areas, industrial areas, roads, and so on.

Human social environment

An environment in which a nation or nation lives together with its own culture and creates social environments with mutual interactions.

Attention to the environment should be reviewed based on its definition, which includes all types of environment, and the most important principles are:

The principle of environmental justice

Justice is a general law that incorporates the entire system of creation, and the concept of justice is that the right of every being, as it deserves, is this definition of justice is a comprehensive definition and includes humans, animals,





Mohammad Noor Sepahi and Abdul WahhabJasim Mahdi

plants, and even seemingly invisible objects like water, rock and soil. The most important environmental causes related to justice can be found in the following areas:

1. The collapse of the human ecosystem by humans, which means the collapse of the rights of environmental elements and, in fact, the depletion of human natural resources from energy, underground reserves and food, and, in general, unrealized resources.
2. Contamination of the main elements of human nutrition, ie water and soil, air, and the accumulation of wastes and pollutants, which deprive them of the right to life of living beings, including humans.
3. The use of raw material and reserves of the earth for the purpose of producing deadly weapons or other unusable and harmful goods for human beings, which, in fact, has created an inadequate use of the abovementioned substances in the context of the environmental crisis.

The principle of security in the environment

The principle of security in the environment has a very important role in the natural environment, the artificial environment and the social environment. So that man does not lose it he does not appreciate it. The Holy Prophet (peace be upon him) has said that:

«نعمتان مذكورتان (مجهولتان) الامن والعافية»

(Security and health are two things that are unknown to everyone and, until they lose, they do not care for their existential significance)

Imam Ali (AS) considers the welfare and the material and spiritual progress of life in the shadow of security.

The principle of environmental degradation

One of the basic principles of jurisprudence that can be used to solve many environmental problems. This principle is, in fact, the dominant authority of all Islamic laws. Accordingly, in Islam, harming others is by no means legitimate, whether at the stage of the law or at the stage of its implementation. Therefore, if a law is passed that causes harm to a person or society or causes harm in the course of implementation, then it is not legitimate for Islam. Many environmental issues can be discussed in the framework of degradation rule:

1. Pouring garbage in places that are harmful to humans and the environment. Such as the impact of oil waste on groundwater aquifers.
2. Unauthorized exploitation of natural resources, such as oil and gas wells, which will be detrimental to future generations.
3. Use of smoke cars and non-standard plants, especially near cities.
4. Causing sound pollution in such a way as to disturb citizens, such as the sound of nearby factories in the city.

Principal development and creation of artificial environment

The human being is the Almighty God who gave him responsibility for the land of the earth.

« هو انشاكم من الارض واستعمركم فيها »

(He created you from the earth and left it to you)

(Holy Quran, Hood, 61)

In another verse, God forbids man from destroying and disrupting the coherent system of nature and destroying it:

« ولا تفسدوا افيا الارض بعد اصلاحها »

(And do not corrupt the earth after its correction)

(The Holy Qur'an, Arafeh, 56)

The above verses refer to the positive and negative aspects of human activity in the earth. Since the development and avoidance of every kind of devastation is in order to meet the needs and desires of mankind, So, in fact, this is a sustainable development project that is now being considered by environmental thinkers.





Mohammad Noor Sepahi and Abdul WahhabJasim Mahdi

The principle of the call for the protection of the environment

In the educational system of Islam, we are observing and caring for each other in society and protecting the meaning of "to promote virtue and prevent vice" and taking care of the human environment.

« ولتكننكم ممتدعون بالخير ويامر ونبال المعروف وينهى عن المنكر وأولئك هم المفلحون »

(You must have a collective invitation to goodness, and to promote virtue and prevent vice, and they are those who are prosperous)
(Tousi1415,gh,p20)

When the environment is affected by the effects of various types of pollution, or when the earth's surface is affected by various environmental crises, these issues do not only offend humans and offenders, but all human beings must pay for it. So nobody can say that because he has done his job.

The principle of preventing environmental degradation

Destruction in the environment is a clear example of corruption, because it is the opposite of reformation and peace, that is, compatibility in the system of nature. From the point of view of Islam, corruption is considered as a general crime, and coping with corruption is the secret of the survival of religion and autonomy and the system of nature. God Almighty says:

وَلَا تَكُلُوا مِمَّا آتَتْكُمْ الْأَرْضُ ضَلِيلًا يُعْبِدُونَهَا وَيُهْلِكُ الْحَرْثَ وَالنَّسْلَ وَاللَّهُ يُجِيبُ الْفَسَادَ

And when it comes to power and sovereignty, he tries to corrupt the land and destroy and destroy the generation, and God does not love corruption.
(The Holy Qur'an, Baqara, 99)

The following points are understood by the accuracy of the verse:

1. Destruction of plants and the generation of animals, birds and humans is corruption on earth. Which the commentators have specified (Tabatabai, p. 98)
2. The "generation" of the term in this verse is universal and includes the human race of animals and birds, and the destruction of plants is the cause of the disappearance of the generation of animals, birds and humans.
3. According to the commentators, the meaning of "الحَرْث" in the verse of the plant is generally understood to include farms, trees, plants and pastures.

Corruption also has a far-reaching concept that covers any disturbance, devastation, deviation and oppression. In other words, corruption is damaged and destructive, and it is said to break the current, well-balanced system, and the opposite is the correction that all constructive plans are in the sense of it.

Infecting water, soil, and air, as well as disturbing the living environment of different earthly habitats and disturbing the environmentally friendly and well-established system, is considered as a cornerstone of corruption and environmental degradation behaviors.

The important point to be mentioned in this discussion is the behavior that leads to environmental degeneration.

Principle of health and cleanliness of the environment

Health is one of the important issues that Islam has paid serious attention to. In order to protect the environment, Islam has presented numerous commands and programs in all aspects of human life, including spiritual, material, personal and social. So, considering the impact of these arenas on each other, they should not be discussed individually. The social environment of human life has inevitable effects on his psyche and his behavior. Man receives many of his attributes from the environment. Clean environments often nurse clean people and infected environments are often infected people.





Mohammad Noor Sepahi and Abdul WahhabJasim Mahdi

(والبلد الطيب يخر جنبا تهبانذر بهو الذبخي ثلايخر جالانكدا اكلنصر فالابا تاقو ميشكرون)

The land of cleanliness (and sweetness) of flowering comes under the command of the Lord, but the evil lands (and the dill) are not worthless but desirable. These are the verses (self) for those who are grateful.

(Holy Qur'an, Arafah, 58)

In this verse, the effects of the environment on psyche and human behavior are presented subtly. In this example, humans are likened to plants, and their environment lives on sweet and savory grounds. In a contaminated environment, although it is efficient to teach, it is difficult to cultivate clean humans, just as the rain does not go up on the earth. For this reason, in order to rehabilitate the people and strengthen the righteous ethics, we need to improve the environment. In recent years, the World Health Organization has redefined the issue of environmental health (Environmental health is the control of the factors of the living environment that have or will have a bearing on the health, physical, psychological and social health of humans) (Halm Sardash and Delpishe, 1382, p. 3).

In all divine religions, purity and non-pollution are religious duties. In Islam, according to the Hadith of «النظافة من الايمان» cleanliness is next to godliness or purity is maintained in all fields, including human, earth, water, air, etc. Therefore, the prevention of environmental pollution is not a matter of the day, but it has been important during the history of Islam. The Prophet says in the Hadith (to anoint the earth because he is good and kind to you) (Nahj Al-Fasahah).

Islam has been instrumental in the health, beauty and enjoyment of clean things in the living environment and even in worship. As Allah Almighty is decorated with the ornament of the stars:

(انارينا السماء الدنيا بزينة الكواكب)

(We decorate the sky of this world on the stars of the stars)

(Holy Quran, Sufat, 6)

CONCLUSION

Human is an integral part of the set of the system of being, its position against nature must be determined on the basis of the truth of creation. In Islamic ideology, such a connection is determined by someone who is the creator of the universe. God does not appoint duties and duties to his servants unless it is expedient that the world and the Hereafter reform them. Allah has not ordered except good and good things, and has not forbidden anything except the ugly things that cause the degeneration of the world and the life of the servants.

And man does not do any work according to this command, except that reason also likes it, and does not leave anything, except that reason also considers it worthwhile to leave.

The role of Islam in environmental ethics is important from a variety of dimensions:

- Adjusting the instincts and demands of the human being in the field of the environment.
- Education for environmental ethics.
- Environmental Law Enforcement.

"Behavior" is the same result and function of "ethics" that occurs after education and awareness, and in more precise terms, human work has a moral root. And for this reason, we seek the knowledge and knowledge of people's traits and traits in their behavior. So much so that the effect of believing in God in eradicating environmental degradation factors and in guiding people to good and good cannot be expected from any kind of organization and material power. Inviting people to preserve the environment without resorting to a religious root is ineffective or effective. For this reason, efforts should be made to eliminate environmental degradation factors in the light of faith and virtue.





Mohammad Noor Sepahi and Abdul WahhabJasim Mahdi

REFERENCES

- 1.Holy Qur'an
- 2.Halm Sardash and Delpishe, 1382, p. 3
- 3.Nahj Al-Fasahah
- 4.Tousi1415,gh,p20
- 5.Nahj al-Balagha
- 6.<https://www.al-islam.org/nahjul-balagha-part-1-sermons>
- 7.<http://quran.ksu.edu.sa/tafseer/katheer/sura2-aya205.html>
- 8.http://www.thinkingfaith.org/articles/20081111_1.html





Propolis Mediated Synthesis of Magnetite Iron Oxide Nanoparticles

Majida A.J.Al-Qayim^{1*} and Ryaidh, Sh, Al_Hussain²

¹Prof.Dr.Physiological Chemistry, Department of Physiology and Pharmacology, College of Veterinary Medicine, University of Baghdad,Iraq.

²Ministry of Science and Technology, Director of Material Research, Baghdad, Iraq.

Received: 15 Dec 2017

Revised: 26 Dec 2017

Accepted: 28 Jan 2018

*Address for correspondence

Majida A.J. Al-Qayim

Prof. Dr. Physiological Chemistry

Department of Physiology and Pharmacology

College of Veterinary Medicine, University of Baghdad, Iraq.

E.mail: dr.majida.alqayim@gmail.com



This is an Open Access Journal / article distributed under the terms of the **Creative Commons Attribution License** (CC BY-NC-ND 3.0) which permits unrestricted use, distribution, and reproduction in any medium, provided the original work is properly cited. All rights reserved.

ABSTRACT

Iron oxide nanoparticles have high potential in medical use for their benefit as a drug carrier, in MRI, in tissue repair, and in treatment of tumor and anemia. Effects of different pH and temperature on the characterizations of the IONPs propolis mediated biosynthesis were the aim of this research. IONPs were formed from a mixture of ferric and ferrous chloride salts reduced by water propolis extract in a 1:2 and 2: 1 v:v ratio under different Ph and temperature. The formed IONPs were separated and characterized by UV- VIS absorption spectroscopy, FTIR , XRD AND SEM techniques. The XRD results depending on the latency of the particles -at 2θ revealed the average particle size of magnetic NP formed under the temperature of 80 C and acidic pH (2.9) are found to be in the range 31,714 – 46,20nm, and with SEM of these nanoparticles showed an agglomeration. Inconclusion, the crystalizing shape and size of the prepared iron oxide nanoparticles in this study illustrates the reducing efficacy of propolis in the synthesis of biogenic metallic nanoparticles.

Keywords: Iron oxide nanoparticles, Propolis, Biosynthesis, Magnetite.

INTRODUCTION

In nature iron oxide found in many forms namely maghemite, γ -Fe₂O₃, magnetite, Fe₃O₄, and haematite, α -Fe₂O₃, among which magnetite, Fe₃O₄, is very promising, because of its proven biocompatibility (1). The most common methods for iron oxide nanoparticles synthesis including co-precipitation, thermal decomposition, hydrothermal synthesis, microemulsion, and so nochemical synthetic route can all be directed to the synthesis of high quality of iron oxide NPs (2,3,4). Biogenic synthesis of IONPs using papaya extracts get attention because is cost effective, eco-friendly, non toxic and promising for applications in medicine (5).Iron nanoparticles have been mostly synthesized



**Majida A.J.AI-Qayim and Ryaidh, Sh, AI_Hussain**

using different plant extracts, since plant extracts act as low-cost reducing and stabilizing agents. The commonly used for iron nanoparticle synthesis tea extract at room temperature.(6) in addition to Sorghum bran extract (7) and eucalyptus leaf extracts(8). Microorganism or bacterial synthesis especially the magnetotactic bacteria and iron reducing bacteria (9,10,11). Magnetic nanoparticle synthesis is affected by temperature and pH, carried out at room temperature or by the hydrothermal route by mixing plant extract with metal salt solution (12).

Propolis (bee glue) is a sticky dark coloured material that honeybees collect from living plants, mix with wax and use in construction and adaptation of their nests. It is a commercial resinous product and contains phenols and many other preventive agents. Propolis is used as a building material in order to strengthen the borders of combs and as a chemical weapon against the pathogen microorganisms (13). Its antinociceptive (14), antibacterial against many of pathogenic bacteria (15), antiviral activity against herpes virus (16), antitumor and antioxidant potential against prostate cancer (17). From different botanical and geographical origins of world, more than 300 compounds including volatile organic compounds, flavonoid aglycones, phenolic acids and their esters, phenolic aldehydes, alcohols and ketones, sesquiterpenes, quinones, coumarins, steroids, amino acids were reported to have been isolated from propolis (18, 19,15). The synthesis of nanoparticles by biological methods may lead to development of clean, environmentally acceptable and nontoxic nanoparticles. The biosynthesis of safe and easily distributed iron oxide nanoparticles using propolis extract from single and mixed iron salts was the aim of the present study.

MATERIALS AND METHODS

Biosynthesis of Iron Oxide Nanoparticles (IONPs)

Preparation of Propolis Extract

Crude propolis obtained from local market as an Iraqi propolis, after cutting the resins blocks of propolis, the extract was prepared by maceration method. Briefly, 50 gm of propolis mixed with 500ml distilled water by continuously stirred in 35 °C for 3 days. The formed suspension was filtered using filter paper. The filtered supernatant was cooled to room temperature and stored at 4 °C until use.

Preparation of Iron Oxide Nanoparticles

The preparation of iron oxide nanoparticles was made by mixing of ferric and ferrous chloride mixture solution (0.1M) with propolis extract in volume ratio 1:2 and 2:1 respectively. To investigate the influence of the pH on the biosynthesis of the IONPs by propolis extract, the mixture pH was changed using NaOH (0.1 N) as follows:

- 1- PrIONPs-1 : prepared by mixing of 0.1 M of FeCl_3 – FeCl_2 with propolis extract in volume ratio 1:2 in 80 °C and pH=4.3
- 2- PrIONPs- 2 : prepared by mixing of 0.1 M of FeCl_3 – FeCl_2 with propolis extract in volume ratio 1:2 stirring at 80 °C and pH=8.0
- 3- PrIONPs- 3 : prepared by mixing of 0.1 M of FeCl_3 – FeCl_2 with propolis extract in volume ratio 1:2 with stirring at 80 °C and pH 12.0
- 4- PrIONPs-4 : prepared by mixing of 0.1 M of FeCl_3 – FeCl_2 with propolis extract in volume ratio 2:1 stirring at 80°C and pH =4.3
- 5- PrIONPs-4 : prepared by mixing of 0.1 M of FeCl_3 – FeCl_2 with propolis extract in volume ratio 2:1 stirring at 80°C and pH =8.0

The formation of the nanoparticles was observed as changed in directing reduction of FeCl_2 - FeCl_3 to Fe_3O_4 . In all the previous circumstances the nanoparticles formed were isolated by centrifuge at 6000 rpm in 25 min, then the precipitate washed by absolute ethanol in volume ratio 1:2 and dried at 60°C and kept for further characterization





Majida A.J.AI-Qayim and Ryaidh, Sh, AI_Hussain

Characterization of iron oxide nanoparticles

UV-Visible Spectra Analysis: The various nanoparticles from different method were analyzed by UV – visible spectroscopy Shimadzu UV – 1600, Japan, with wave rang 190.00 – 800.00 nm, scan speed of sampling interval was 0.5min.

Fourier Transform Infrared [FTIR] Spectroscopy

The prepared iron oxide nanoparticles (IONP) analyzed by FTIR spectroscopy (ABB/spectro-lab/MB3000/UK) , Laser phase and the F , D amplitude 35 and the rejected scan counter about 24, FTIR characterization was carried out under classic KBr pellet technique that measures infrared intensity vs wavelength [wave number] of light from 400 – 4000 cm, it is used to determine the nature of associated functional groups and structural features of biological extracts with nanoparticles.

The X-ray diffraction (XRD) Analysis

The prepared particles were examined using XRD (6000/Shimadzu Japan) ,XRD patterns were calculated using X'per Rota flex diffraction meter using Cu K radiation and $\lambda = 1.5406 \text{ \AA}$, 40.0 kv voltage , 30.0 ma x ray current , the measurement of XRD obtain in 2θ , continues scan , rang (20.000 – 60.000 deg)speed about 50000 deg / min in 0.60 sec . Crystallite size is calculated using Scherrer equation (CS) as described by(20).

$$\text{Equation 1 } CS = K\lambda / \beta \cos \theta \quad (1)$$

Where CS is the crystallite size Constant [K] = 0.94 β is the Full Width at Half Maximum [FWHM].

Scanning Electron Microscopy (SEM) analysis

The iron oxide nanoparticles were examined by SEM (Tescan Vega III /Czech) to study the morphology and shape of the particles, to get the best view under SEM, samples were slightly pressed into pellets at 0.5 ton-load. SEM MAG 30.0 Kx, SEM HV 10.0 kV and the image were examined at 2 -10 μ m scale.

RESULTS

Ultraviolet – Visible spectroscopy analysis

This analysis shown in Table1 and Fig-1 illustrated that the prepared compounds from propolis and iron chloride salts strongly absorbed radiation at wide range of wave length of ultraviolet – visible spectra ranged from 190-800. This absorbance indicating formation of conjugated compounds. This appeared at indicator to formed iron oxide. The strongest absorbance of radiation at UV was by the PrIONPs and at the visible- spectroscopy all the prepared nanoparticles were with the same absorbance.

Fourier Transform Infrared [FTIR] Spectroscopy

The analysis of the chromatographic images of the FTIR of the present prepared compounds shown in Fig-2 and Table 2. Vibrations due to different IR absorption according to the wave length (cm) were divided in to four regions , 1st for vibrations appear in 4000-2500, 2nd for 2500-200, 3rd 200-1500, and the 4th for 1500-400. Each region of wave length indicate the presence of bound molecules. Results revealed that all the prepared iron oxide nanoparticles using propolis extract containing compounds rich with O-H , C-H , N-H and COOH at IR absorption 3400- 1500cm-





Majida A.J.AI-Qayim and Ryaidh, Sh, Al_Hussain

, in addition they showed an absorption in the fingerprint region below 750-480 which specifically for iron oxide bounds.

X – Ray Diffraction (XRD) analysis

The analysis of the XRD included the 2θ values of the differentiated peaks in Figure 3, and the crystallite particle sizes using Scherrer's formula for the different types of iron oxide nanoparticles prepared using propolis extract are shown in Table 3. Every crystalline material has its specific diffraction pattern in the 2θ by the XRD. In the present study the pattern of IONPs synthesized from propolis extract showed sharp diffraction peaks at 2θ angles according to the type of iron oxide that were formed, the phase identification and crystalline structure of nanoparticles and determination of the strong diffraction peak with 2θ values of 26.618° , 33.8515° , 35.05° , 39.07° , 46.375° , and 55.7° corresponding to the hkl values from (205), (109), (119), (222) and (422) crystal planes respectively PCPDFWIN – PDF #251402 Wavelength and PCPDFWIN – PDF # 160653 Wavelength equal 1.54056.

Scanning Electron Microscopy (SEM) analysis

The present results of the analysis of the SEM micrographs represented in Figure 4 show the size and morphology of magnetic nanoparticles which were synthesized by propolis extract. These images clearly show the agglomeration of iron oxide nanoparticles produced, with an average particle size of IONPs that was different because of the effect of the pH during the steps of preparation of the magnetic nanoparticles, the smaller particle size showing in acidic pH =4.3 with slight aggregation of IONPs.

DISCUSSION

The biogenic synthesis of iron oxide nanoparticles using propolis extract as a reducing agent was successful. The particles prepared from the addition of propolis extract to a mixture of iron chloride salts were colloidal and had a black color indicating the formation of iron oxide molecules. This color change was a result of the excitation of surface plasmon resonance (SPR) due to the formation of IONP (21), this may be highly excited in SPR due to the propolis extract rich in reducing agents such as polyphenol. The maximum UV absorption of Pr IONP1 in comparison with other prepared types of particles indicated the stability and photosensitivity of the synthesized magnetite iron oxide nanoparticles in an aqueous colloidal solution at pH =4.3. The optical absorption spectrum of iron salts depended on particle size, shape, state of aggregation and surrounding dielectric medium (22). This could be attributed to the acidity of the solution which enhanced the phytochemical in the propolis extract, mainly caffeic acid, to reduce the substrate for IONPs. Furthermore, the increasing ratio 2:1 for propolis extract applied a high concentration of the reducing molecules, which enhanced the formation of Fe_3O_4 . In this study FTIR analysis was confirmed in order to evaluate the functional groups on propolis extract and predict their role in the formation of IONPs. These molecules were OH, CH, COO, NH, C=O and Fe-O. This technique used to establish the metallic nature of particles gives information, namely where the atoms are located from peak intensities (23). The peaks found at 600cm^{-1} are mainly caused by the formation of Fe-O in addition to the other molecules formed. Synthesis of iron oxide nanoparticles using propolis extract in a 2:1 ratio to ferric chloride precursors at an acidic solution were the best by XRD analysis. The XRD indicated the effective characterization and confirmed the crystal structure of the synthesized magnetite nanoparticles. Scanning electron microscopy was employed to analyze the structure of nanoparticles that formed in the present study, that is, the particles were agglomerated, the size distribution and morphology is irregular, the magnetite nanoparticles shape showed cubic shape particles and different particle sizes due to the bioreduction of iron salts by propolis extract. This outcome can be explained by the fact that the polyphenol concentration in propolis extract plays a role in the formation of the final structure and particle size of these biosynthesized magnetite nanoparticles (24).





Majida A.J.AI-Qayim and Ryaidh, Sh, AI_Hussain

REFERENCES

1. Gupta AK, Gupta M. (2005). Synthesis and surface engineering of iron oxide nanoparticles for biomedical applications. *Biomaterials*. 2005 Jun; 26(18):3995-4021.
2. Hyeon,T." Chemical synthesis of magnetic nanoparticles" *CHEM. COMMUN.*, 2003, 927–934
3. Wu, W., He, Q. & Jiang, C. *Nanoscale Res Lett* (2008) 3: 397. <https://doi.org/10.1007/s11671-008-9174-9>
4. Chengyin Fu. And Ravindra N. M. "Magnetic iron oxide nanoparticles: synthesis and applications" *Bio-inspired, Biomimetic and Nano-biomaterials*, (2012),1: 229–244 .
5. Latha N. and Gowri M. "Biosynthesis and characterization of Fe₃O₄ Nanoparticles using caricaya papaya leaves extract " *international J. Sci. and Resea. (IJSR)*, (2012):1551 – 1556.
6. Hoag,G. E. Collins J. B.,a Jennifer L. H., Jessica R. H., Mallikarjuna N. N. and Rajender S. V. " Degradation of bromothymol blue by 'greener' nano-scale zero-valent iron synthesized using tea polyphenols" *J. Mater. Chem.*, (2009) 19, 8671–8677.
7. Njagi EC, Huang H, Stafford L, Genuino H, Galindo HM, Collins JB, Hoag GE, Suib SL." Biosynthesis of iron and silver nanoparticles at room temperature using aqueous sorghum bran extracts." *Langmuir*. 2011 4;27(1):264-71.
8. Wang T., Jin X., Chen Z., Megharaj M. and Naidu R. "Green synthesis of Fe nanoparticles using eucalyptus leaf extracts for Treatment of eutrophic wastewater" *Science of the Total Environment* , (2014) ,466–467 :210–213.
9. Xiangqian, Li., Huizhong, Xu. Zhe-Sheng C.and Guofang C. "Biosynthesis of Nanoparticles by Microorganisms and Their Applications" *Journal of Nanomaterials* 2011:1 – 16 .
10. Rita Kleemann, Rainer U. Meckenstock; Anaerobic naphthalene degradation by Gram-positive, iron-reducing bacteria, *FEMS Microbiology Ecology*, Volume 78, Issue 3, 1 December 2011, Pages 488–496,
11. Miguel E. Cueva and Louise E. Horsfall" The contribution of microbially produced nanoparticles to sustainable development goals" *Microbial Biotechnology* (2017) 10(5), 1212–1215.
12. Mihir, H., Siddhivinayak B. and Rakesh K." Plant-Mediated Green Synthesis of Iron Nanoparticles" *Journal of Nanoparticles* (2014):1 – 9.
13. Wollenweber,e. and Stephen L. B." Feral Honey Bees in the Sonoran Desert: Propolis Sources other than Poplars (*Populus* spp.)" *Z. Naturforsch.* (1997); 52c, 530-535.
14. Talla , E..Dabole ,b..Taiwe , G.S NgoBum , E..Mbafor , J.T.Atchade ,T..Malik , B.Zulfiqar ,A..Sidiki ,N.. Nguimbou M. and Choudhary I." Antinociceptive Pentacyclic Triterpenoids from the Cameroonian Brown Propolis" *Pharmacologia* , 2013. 4 (3):218 – 227 .
15. Alencar S.M.,Oldoni T. L. C. , Castro I.S.R., Cabral M.L. , Costa C.M.,Cury J. A. ,Rosalen P. L., and Ikegaki M. "Chemical Composition and biological activity of a new type of Brazilian propolis : red propolis" *J. Ethenopharmacology*, (2007),113:278 – 283 .
16. Nolkemper, S.; Urogenreichling, J.; Sensch, K.; Schnitzler, P." Mechanism of herpes simplex virus type 2 suppression by propolis extracts". *Phytomedicine*, (2010)17: 132-138.
17. Salim I., Afaf D ., Khalid M ., Dina SM ." Antitumoral and Antioxidant Potential of Egyptian Propolis Against the PC3 Prostate Cancer Cell Line" *Asian Pacific Journal of Cancer Prevention*, 2015,16:7641 – 7651.
18. Bankova, V., Castro, S.L., Marcucci, M.C., "Propolis: recent advances in chemistry and plant origin" *Apidologie*,(2000) 31, 3–15.
19. Marcucci, M.C., Bankova, V.S., 1999. Chemical composition, plant origin and biological activity of Brazilian propolis. *Current Topics in Phytochemistry* 2, 115–123.
20. Venkateswarlu S., SubbaRao Y., Balaji T., Prathima B.and Jyothi N.V.V." BiogenicsynthesisofFe₃O₄ magnetic nanoparticles using plant in peel extract", *Materials Letters*, (2013),100:241–244.
21. Shankars., Akhil,E.,Balapra ,S., Amit S.,Absar ,A. and Murali, S." Biological synthesis of triangular gold nanoprisms" *nature materials* (2004) ,3 ,482 – 488.
22. Ali A, Zafar H, Zia M, et al. Synthesis, characterization, applications, and challenges of iron oxide nanoparticles. *Nanotechnology, Science and Applications*. 2016;9:49-67. doi:10.2147/NSA.S99986.





Majida A.J.AI-Qayim and Ryaidh, Sh, AI_Hussain

23. Kuang y., Q. Wang, Z. Chen, M. Megharaj, and R. Naidu, "Heterogeneous Fenton-like oxidation of monochlorobenzene using green synthesis of iron nanoparticles," *J. Colloid Interface Sci.*, (2013.) 410, 67-73.
24. Shojae S. and Shahri M.M. "Green Synthesis and Characterization Of Iron Oxide Magnetic Nanoparticles Using Shanghi White Tea (Cameli Sinesis) Aqueous Extract" *J. Chemical and Pharmaceutical research* (2016), 8 (5):138 – 143.

Table 1: The ultraviolet- visible spectroscopy analysis of the different biosynthesis of iron oxide nanoparticles prepared using propolis

Symbol of the IOPs	Ratio of FeCl ₂ :FeCl ₃ :propolis	pH	Absorbance at UV(240-250)	Absorbance at Visible(400- 460)
Pr IONPs 1	1:2	4.3	3.7	3.6
Pr IONPs 2	1:2	8.0	2.9	4.0
Pr IONPs 3	1:2	12.0	3.0	4.0
Pr IONPs 4	2:1	4.3	3.1	4.0
Pr IONPs 5	2:1	8.8	3.0	4.0

Table 2 : The FTIR analysis of Fe₃O₄ nanoparticles by propolis extract

Symbol of the IOPs	Ratio of FeCl ₂ :FeCl ₃ :propolis	pH	Wave length (cm ⁻¹) Active molecule of propolis			
			4000-2500 O-H, COOH N-H	2500-2000 C-N C-C	2000-1500 C=C C=O	1500-400 Fe-O
Pr IONPs 1	1:2	4.3	2920	2360	1736-1625	480 - 1426
Pr IONPs 2	1:2	8.0	3408 - 2872	2360	1616	544 - 1456
Pr IONPs 3	1:2	12.0	3384 - 2880	2360	1616	1624 - 480
Pr IONPs 4	2:1	4.3	3392 - 2880	2360	1728,1624	1455 - 520
Pr IONPs 5	2:1	8.0	3408 - 2880	2360	1624	1472 - 528

Table 3: The XRD analysis of Fe₃O₄ nanoparticles by propolis extract. According to PCPDFWIN – PDF #251402 and PCPDFWIN – PDF #160653.

	Values of peaks on 2 theta	I/II	FWHM	Particle Size (nm) by Scherrer's	Type Of IONP
IONP1	26.6182 35.0557	100 97	0.58000 0.47140	31.714 46.20	Fe ₃ O ₄ , Fe ₂ O ₃ and FeOOH
IONP2	35.6123 26.997	100 86	0.85000 0.80000	26.819 23.23	Fe ₃ O ₄ , Fe ₂ O ₃ and FeOOH
IONP3	26.4984 26.6981	100 77	0.20000 0.30000	70.4314 46.9736	FeOOH ,Fe ₂ O ₃ and Fe ₃ O ₄
IONP4	27.5090 25.9838	100 25	0.12450 0.11280	151,15 160.55	Fe ₂ O ₃ ,Fe ₃ O ₄ Fe ₃ O ₄ and FeOOH
IONP5	27.6830 43.6204	100 58	0.14230 0.14210	133.11 236.83	FeOOH and FeO





Majida A.J.AI-Qayim and Ryaidh, Sh, Al_Hussain

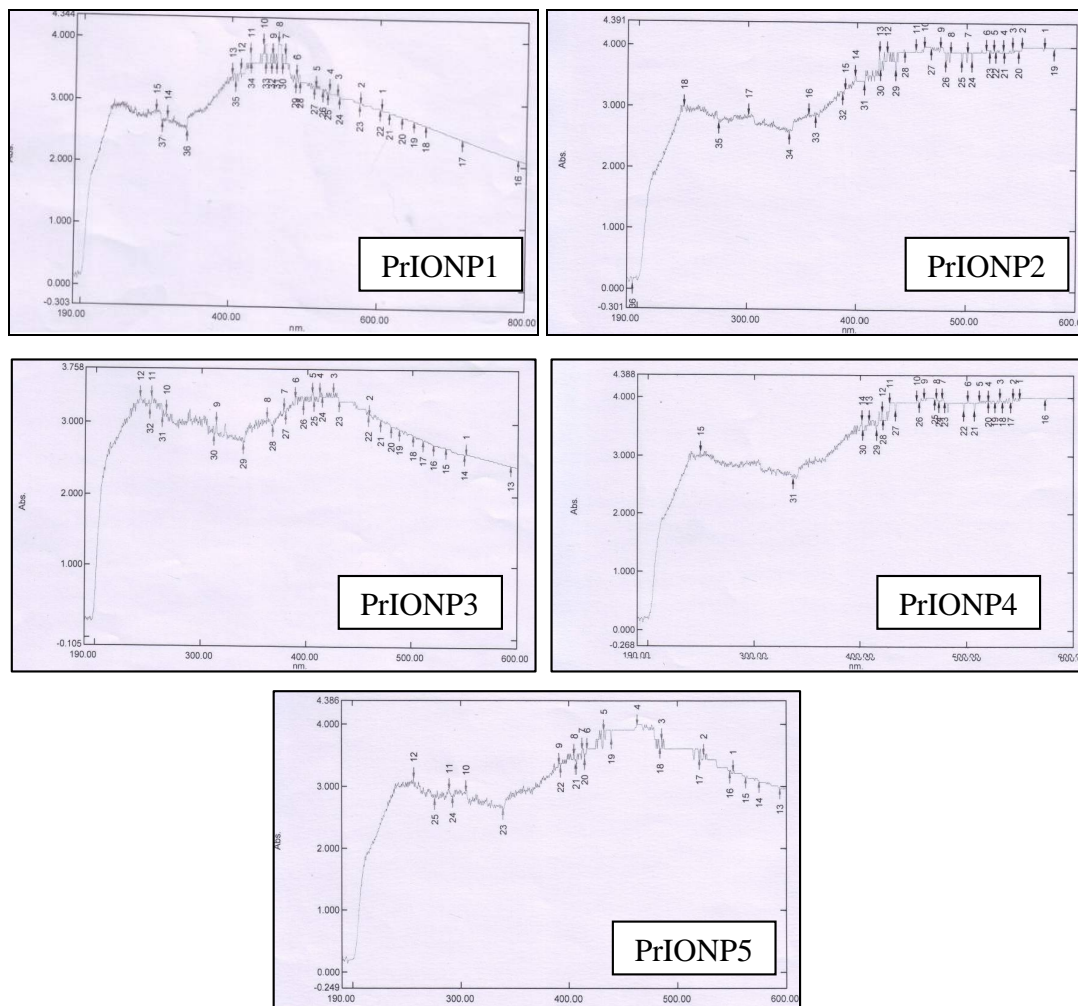
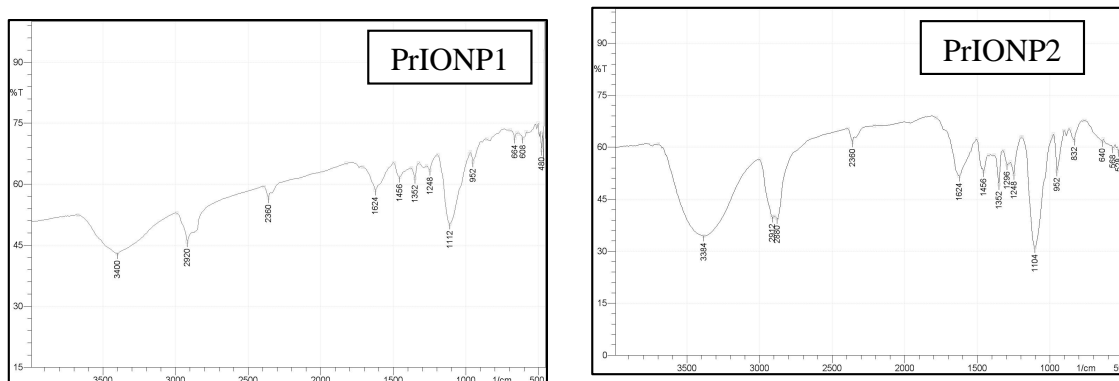


Figure 1: UV – Visible of iron oxide nanoparticles synthesis by propolis extract





Majida A.J.AI-Qayim and Ryaidh, Sh, AI_Hussain

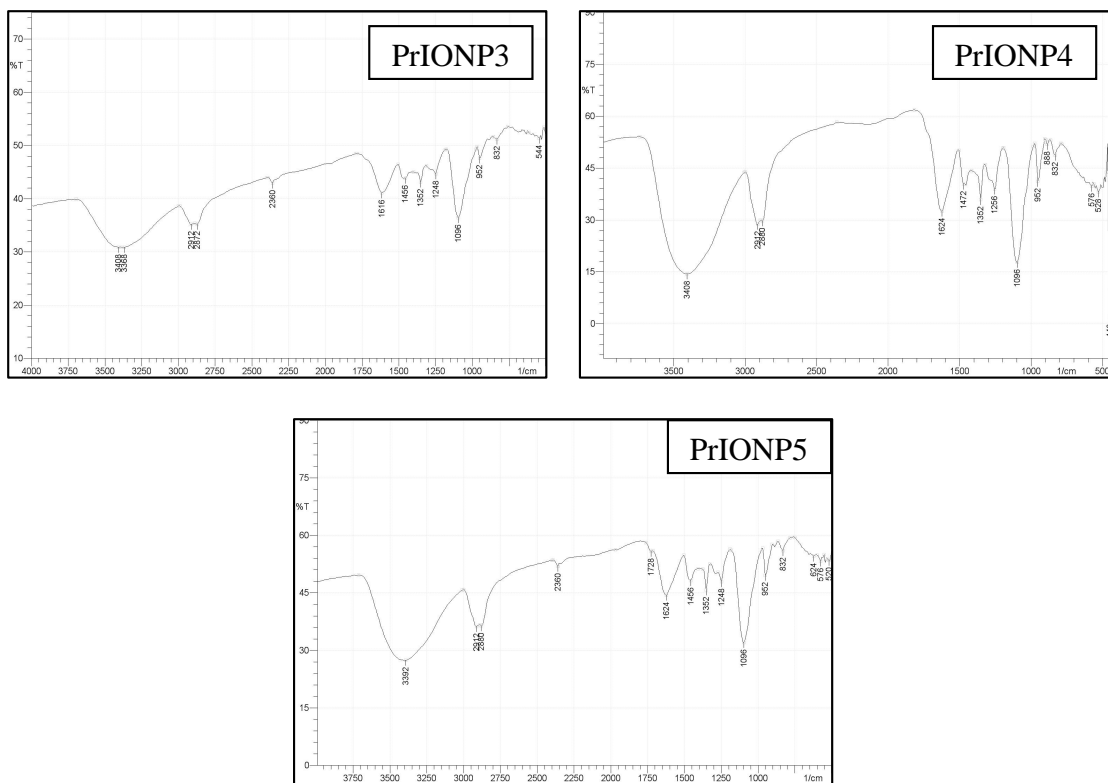
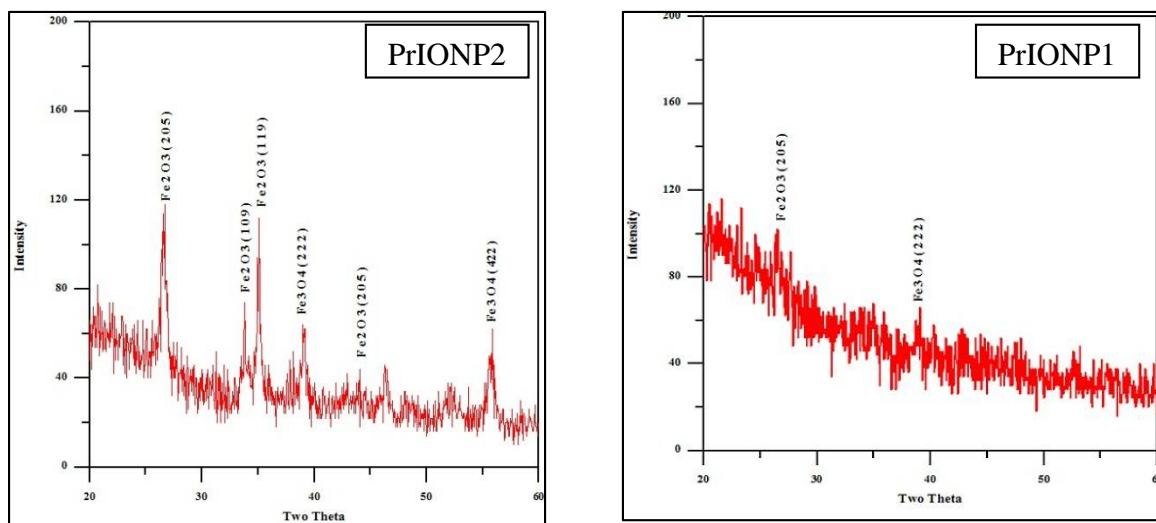


Figure 2. FTIR spectrum of iron oxide nanoparticles using mixture of FeCl₂, FeCl₃ and propolis extract.





Majida A.J.AI-Qayim and Ryaidh, Sh, AI_Hussain

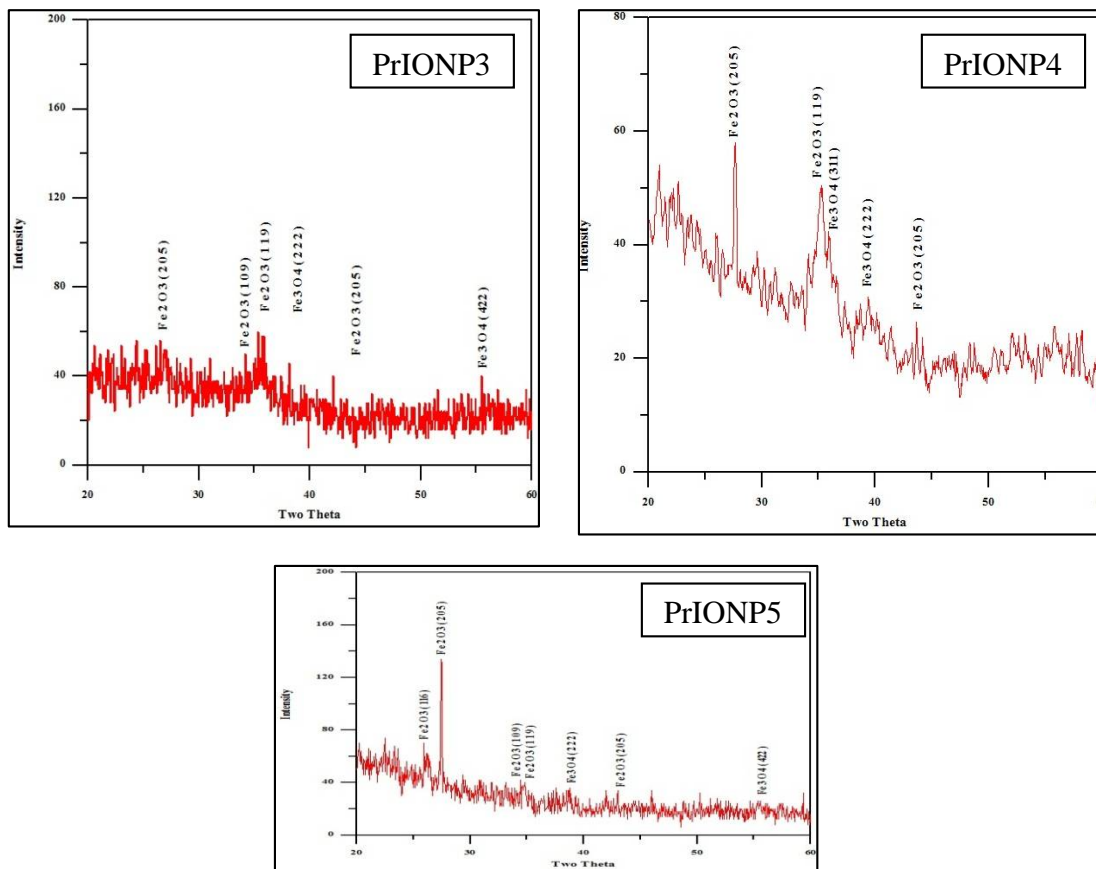
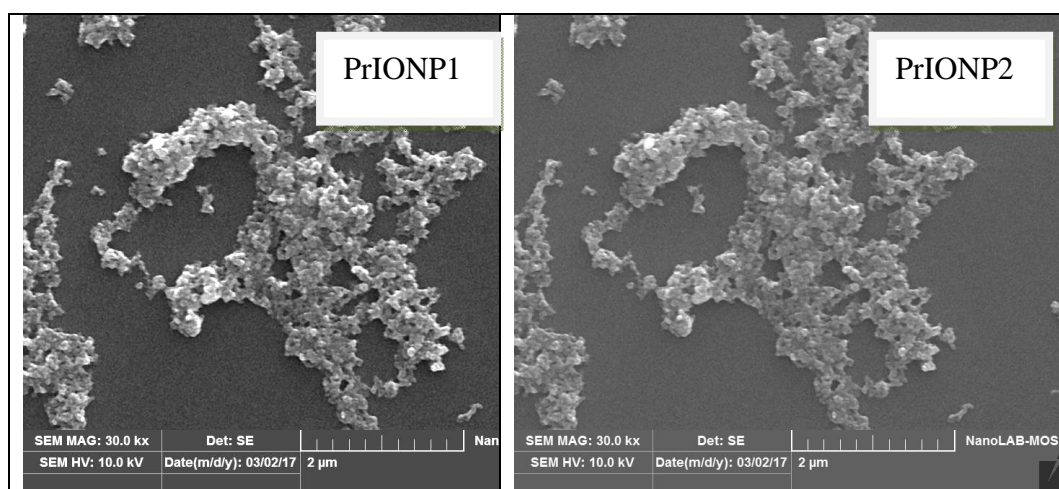


Figure 3. XRD spectrum of nanoparticles using mixture of $FeCl_2$, $FeCl_3$ and propolis extract





Majida A.J.AI-Qayim and Ryaidh, Sh, Al_Hussain

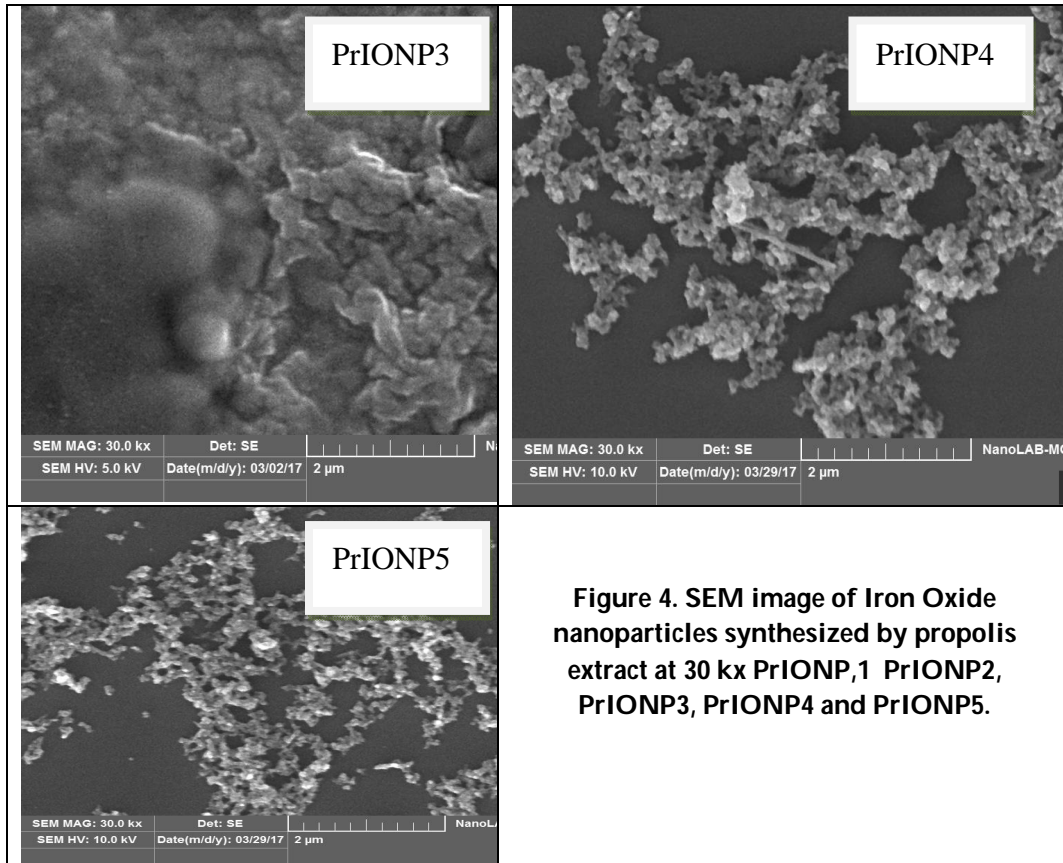


Figure 4. SEM image of Iron Oxide nanoparticles synthesized by propolis extract at 30 kx PrIONP,1 PrIONP2, PrIONP3, PrIONP4 and PrIONP5.





RESEARCH ARTICLE

Comparison between Software Empirical Equations and Ground Weather Station Solar Radiation in Iraq

Mohammed .T.Hussein* and Emad .J.Mahdi

Physics department, College of Sciences, University of Baghdad, Baghdad, Iraq.

Received: 12 Dec 2017

Revised: 23 Dec 2017

Accepted: 27 Jan 2018

*Address for correspondence

Mohammed .T.Hussein

Physics department, College of Sciences,

University of Baghdad,

Baghdad ,Iraq.

E.mail: mohammedtake@gmail.com , emad.jaleel@yahoo.com



This is an Open Access Journal / article distributed under the terms of the **Creative Commons Attribution License** (CC BY-NC-ND 3.0) which permits unrestricted use, distribution, and reproduction in any medium, provided the original work is properly cited. All rights reserved.

ABSTRACT

This article presents a comparison of solar radiation data measured at different sites in Iraq by ground weather station using Pyranometers are broadband instruments that used to measure global solar irradiance incoming from a 2π solid angle on a planar surface with software program has been used empirical equations with visual basic net language to locate the spatial and temporal distribution hourly solar radiation incident on a horizontal surfaces at four different latitude and longitude as follow ($32^{\circ}.19'N$ - $47^{\circ}.28'E$) ,($31^{\circ}.58'N$ - $46^{\circ}.33'E$),($32^{\circ}.41'N$ - $43^{\circ}.54'E$) and ($31^{\circ}.57'N$ - $44^{\circ}.46'E$) respectively. The results show a good agreement between measured and calculated data and this can be lead to used software program as solar radiation calculation.

Keywords: Software empirical equations, Pyranometers , solar radiation

INTRODUCTION

The knowledge of global solar radiation is essential for the optimal design and the forecast of the system performance in solar energy conversion systems. The solar radiation data are the fundamental inputs for solar project design, optimization and performance evaluation of solar technologies and applications such as solar thermal and photovoltaic systems for any project location [1,2]. There are various methods to estimate solar radiation. Favorable result for hourly solar radiation estimation was obtained by using atmospheric transmittance model at weather stations, the global solar radiation is generally measured on horizontal surfaces [2,3,4] .Hourly global solar radiation on tilt surfaces can be estimated from global solar radiation on horizontal surfaces using several mathematical models. The mathematical models can be used to estimate components of hourly global solar radiation on horizontal surfaces like direct and diffuse radiation and in inclined surfaces (for direct, diffuse, and ground-reflected radiation) [2,4,5] .





Mohammed .T.Hussein and Emad .J.Mahdi

Some of optical detectors have the ability to fully cover the spectrum of solar radiation, radiometers equipped with thermal detectors are widely used to measure broadband solar radiation, Pyranometers are broadband instruments that used to measure global solar irradiance incoming from a 2π solid angle on a planar surface [3,6,7].The mean solar constant H_0 is the rate of solar irradiation on the surface normal to the sun’s rays beyond the earth’s atmosphere and the mean earth-sun distance.Solar constant $H_0 = 1367 \text{ W/m}^2$, the solar irradiation from the sun varies by ± 3.5 percent.The extraterrestrial solar radiation H , varies by the inverse square law, as shown in the following equation [5,7,8,9]:

$$H = H_0 \left(\frac{D_0}{D} \right)^2 \tag{1}$$

Where D is the distance between the sun and the earth. The $\left(\frac{D_0}{D} \right)^2$ factor is approximated by [4,6,9]:

$$\left(\frac{D_0}{D} \right)^2 = 1.0001 + 0.034 \cos(X) + 0.0012 \sin(X) + 0.0007 \cos(2X) + 0.00007 \sin(2X)$$

Where $X = (360 \left(\frac{d_n - 1}{365} \right))$ (degree) (2)

Equation (1) can also be approximated by:

$$H = H_0 \left(1 + 0.034 \cos \left[\left(\frac{360 d_n}{362.25} \right) \right] \right) \tag{3}$$

Where d_n is the day’s number from year, $H_0 = (1367 \text{ W/m}^2)$

Terrestrial solar radiation, the sum of the beam radiation, $H_{b,h}$, and the sky diffuse radiation, $H_{d,h}$ [5,9,10,11,12,13]

$$H_{b,h} = H(C_0 + C_1 \exp(-k A_m)) \tag{4}$$

$$H_{d,h} = H \cos(Z_s) [0.2710 - 0.2939(C_0 + C_1 \exp(-K A_m))] \tag{5}$$

Where: $C_0 = 0.4237 - 0.00821(6 - AL)^2$, $C_1 = 0.5055 + 0.00595(6.5 - AL)^2$, $K = 0.2711 + 0.01858(2.5 - AL)^2$, AL : altitude above sea level and Z_s : is the sun’s zenith angle.

EXPERIMENTAL SITE AND DATA

The source of data used in present paper includes the solar radiation data in (W/m^2) provided by a fixed weather station installed in the multi sits in Iraqi cities. At latitude and longitude ($32^\circ.19'N$ - $47^\circ.28'E$), ($31^\circ.58'N$ - $46^\circ.33'E$), ($32^\circ.41'N$ - $43^\circ.54'E$) and ($31^\circ.57'N$ - $44^\circ.46'E$) respectively.

Estimate the amount of solar radiation falling on a horizontal surface at a given time and location, the radiation was estimated by design the Software program in visual basic net language using empirical equations to calculate the average daily global radiation on a horizontal surface. To compare with solar radiation data which measured by using ground weather stations instrument taken in to account land used and cover.

We choose a seasonal solstice days in long year (21 / 3, 21 / 6, 21 / 9, 21 / 12) for comparison between results which this days, there is a change in the rates of solar radiation and daylight hours. Inputs parameters for Software program are the latitude and longitude of the site and its elevation above sea level, the standard meridian for local time zone, solar constant, tilt angle, the date of day and number of month in year.





Mohammed .T.Hussein and Emad .J.Mahdi

RESULTS AND DISCUSSION

By inputs parameters supplied are latitude, longitude for weather stations sites like (32°19'N -47°28'E),(31°58'N-46°33'E),(32°41'N- 43°54'E) and (31°57'N- 44°46' E) , to calculate the hourly global for comparison between them , day and month number, solar constant 1367 W/m², and solar radiation data on horizontal surface. The program results give a clear idea about the behavior of hourly solar radiation , we are compares between the global solar radiation which incident on horizontal surface from the weather station and results of program , following figures present the (1-16) ,we notice on the other hand the hours near the sunrise and sunsets, the global solar radiation values on horizontal surface are close of to each other between the measured and calculate data , if there are The differences between the of solar radiation on a horizontal surface for any location between the measured and calculate data for all locations relying on solar constant value and the weather conditions surrounded station sites . This program provides a good calculation data for all on the horizontal surface and can be said the program performs well. The estimation provided by the program can be used for the estimation of potential energy for many technological applications.

CONCLUSION

The ability of the program to predict and describe the hourly solar radiation during different times, conditions and multi locations that is comparable with measure data. That is to leads us to the possibility of assessment mathematically of solar energy rates for any location in Iraq then use measured and calculated data to validation for any solar radiation rates.

REFERENCES

1. Yisehak Abate .Comparison of Different Empirical Models in The Estimation of Mean Global Solar Radiation Using Sunshine Durations Measured at Dire Dawa .Ethiopia .Haramaya university. may 2014 .
2. J. Radosavljevic, A. Dordevic .Defining of The Intensity of Solar Radiation on Horizontal and Oblique Surface on Earth . Facta universitates . Series: Working and Living Environmental Protection Vol. 2, No 1, 2001, pp. 77 – 86 .
3. F.Antonanzas-Torres,A.Sanz-Garciaa,F.J.Martínez-de-Pison,O.Perpignan-Lamigueiro.Evaluationand Improvement of Empirical Models of Global Solar. Irradiation: Case study northern Spain. Renewable Energy .60 (2013) 604-614.
4. S. Podder, R. Sayeed Khan, S. Ashraful Alam Mohon. The Technical and Economic Study of Solar-Wind Hybrid Energy System in Coastal Area of Chittagong, Bangladesh. Journal of Renewable Energy. Volume 2015, Article ID 482543, 10 pages. podder.shuvankar@gmail.com .
5. William B. Stine , Michael G. Power From The Sun . 2001 . [http:// www. powerfromthesun. net/ book.html](http://www.powerfromthesun.net/book.html).
6. C.Christopher Newton. A Concentrated Solar Thermal Energy System . (A Thesis submitted to the Department of Mechanical Engineering).The Florida state university famu - fsu college of engineering . 2007.
7. D. Vecan. Measurement and Comparison of Solar Radiation Estimation Models For Izmir/Turkey , Izmir institute of technology case . Izmir Institute of Technology . September 2011.
8. K. E. Holbert . Solar calculations. doc . 2007.
9. Shyam S. Chandel, Rajeev K. Aggarwal. Estimation of Hourly Solar Radiation on Horizontal and Inclined Surfaces in Western Himalayas. Smart Grid and Renewable Energy, 2011, 2, 45-55.
10. Abdullateef A. Jadallah, Dr. Dhari Y. Mahmood, Zaid A. Abdulqader. Estimation and Simulation of Solar Radiation in Certain Iraqi Governorates. International Journal of Science and Research (IJSR) . V. 3 Issue 8, August 2014.
11. Griffin Salima, Geoffrey M. S. Chavula. Determining Angstrom Constants for Estimating Solar Radiation in Malawi. International Journal of Geosciences, 2012, 3, 391-397.





Mohammed .T.Hussein and Emad .J.Mahdi

- 12. M. T. Y. Tadros, M. A. M. Mustafa, M. Abdel-Wahab. Estimation of the Global Horizontal Solar Radiation in Iraq. International Journal of Emerging Technology and Advanced Engineering . Volume 4, Issue 8, August 2014.
- 13. M. Ravi Kumar, B. Bala Sai Babu, M. Seshu. Estimation of Average Solar Radiation on Horizontal and Tilted. IOSR Journal of Electrical and Electronics Engineering (IOSR-JEEE) . e-ISSN: 2278-1676,p-ISSN: 2320-3331, Volume 11, Issue 3 Ver. IV (May. – Jun. 2016), PP 43-53.

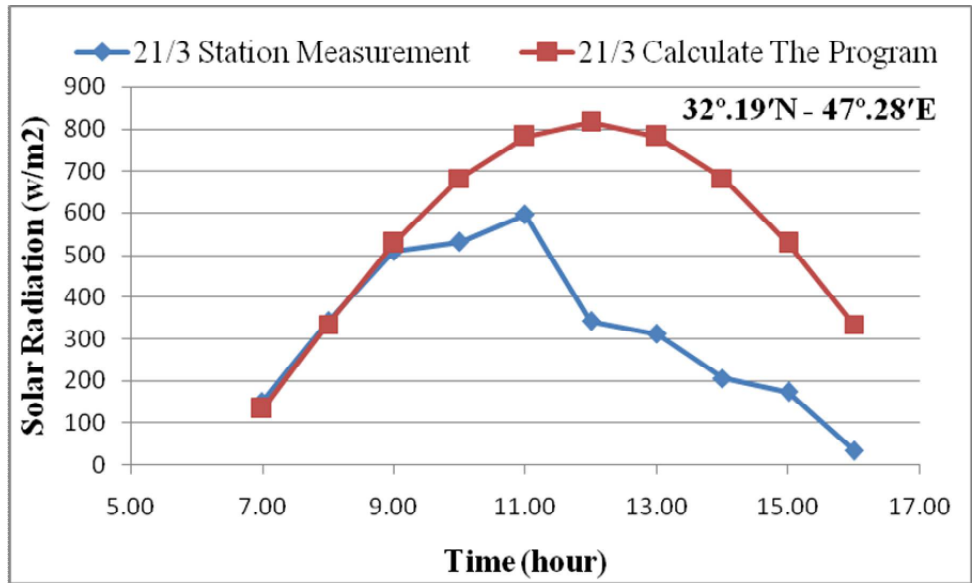


Fig (1) shows the comparison between the measured and calculate data of solar radiation with time for (32°.19'N- 47°.28'E) site

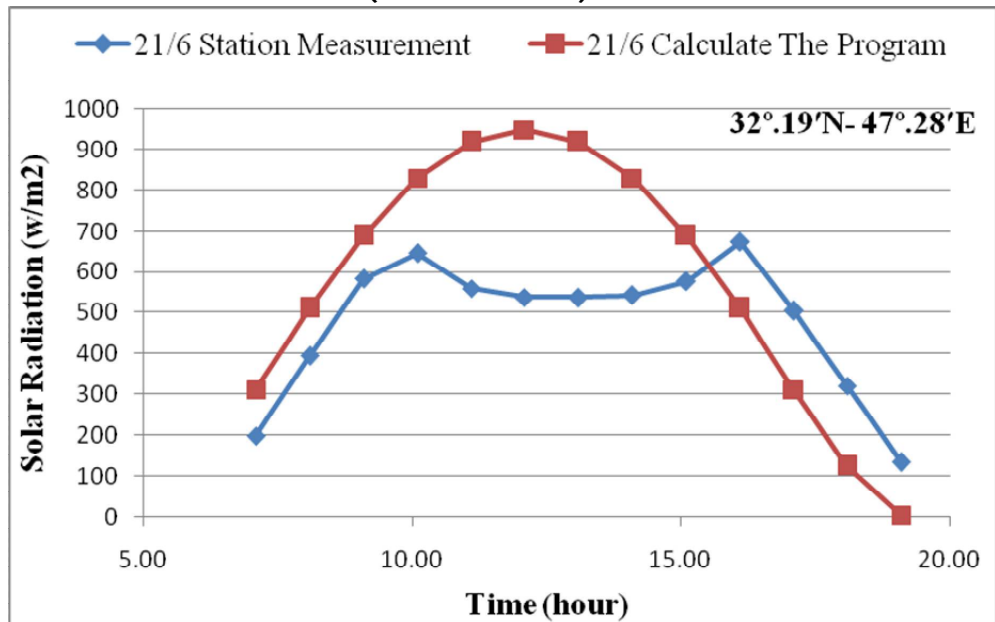


Fig (2) shows the comparison between the measured and calculate data of solar radiation with time for (32°.19'N - 47°.28'E) site





Mohammed .T.Hussein and Emad .J.Mahdi

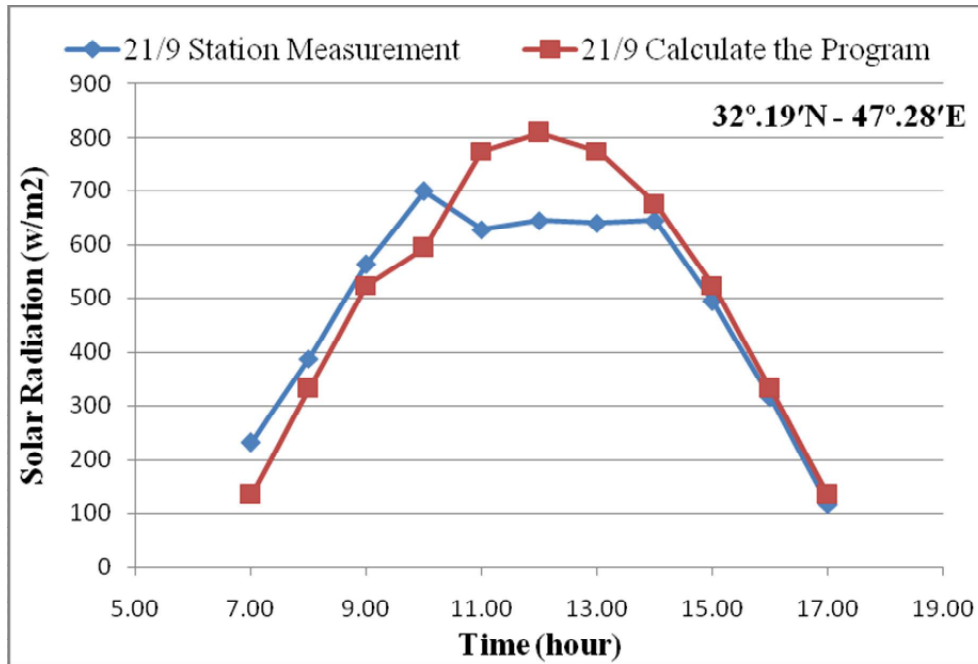


Fig (3) shows the comparison between the measured and calculate data of solar radiation with time in 21/9 for (32°.19'N - 47°.28'E) site

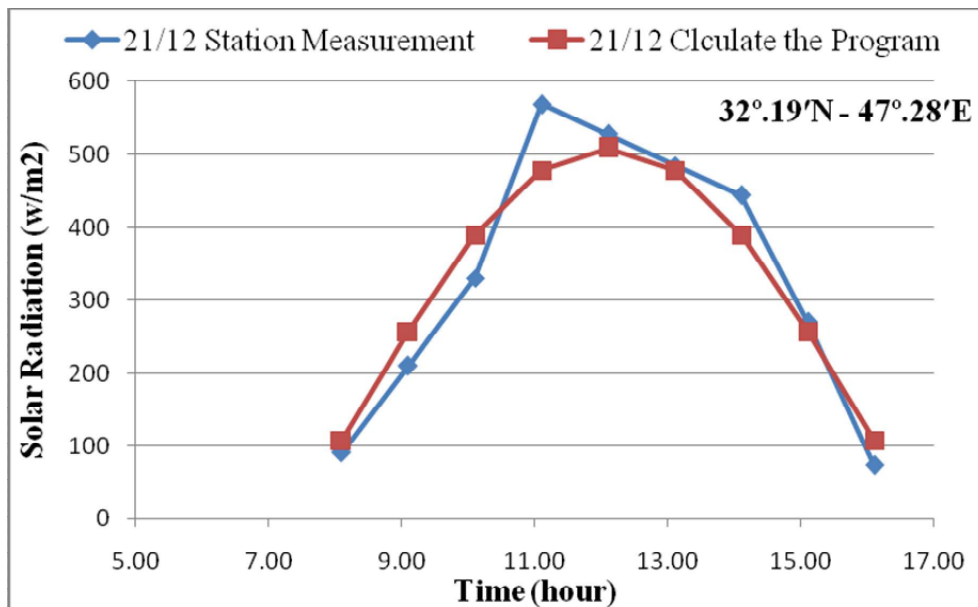


Fig (4) shows the comparison between the measured and calculate data of solar radiation with time in 21/12 for (32°.19'N - 47°.28'E) site





Mohammed .T.Hussein and Emad .J.Mahdi

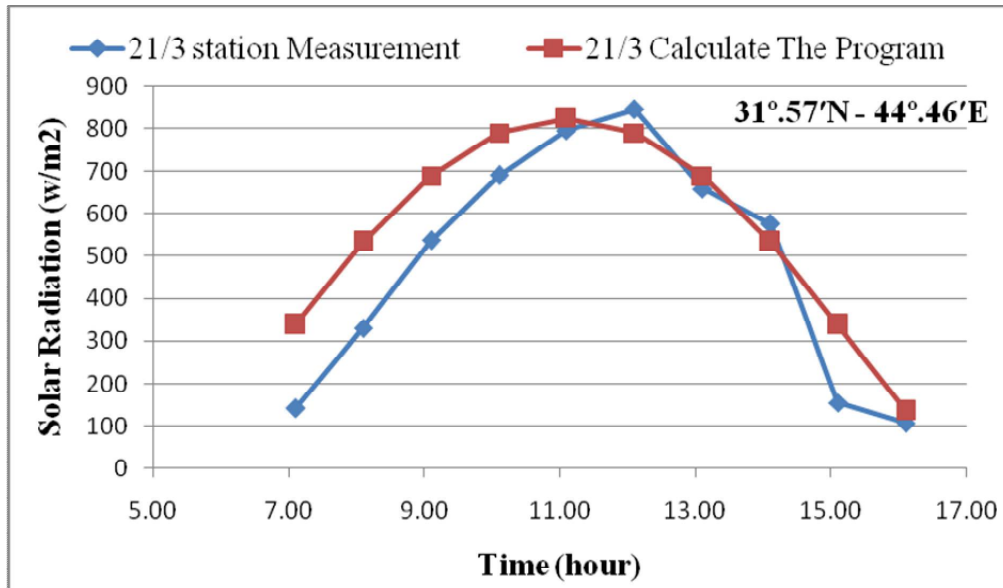


Fig (5) shows the comparison between the measured and calculate data of solar radiation with time in 21 /3 for (31°.57'N - 44°.46'E) site

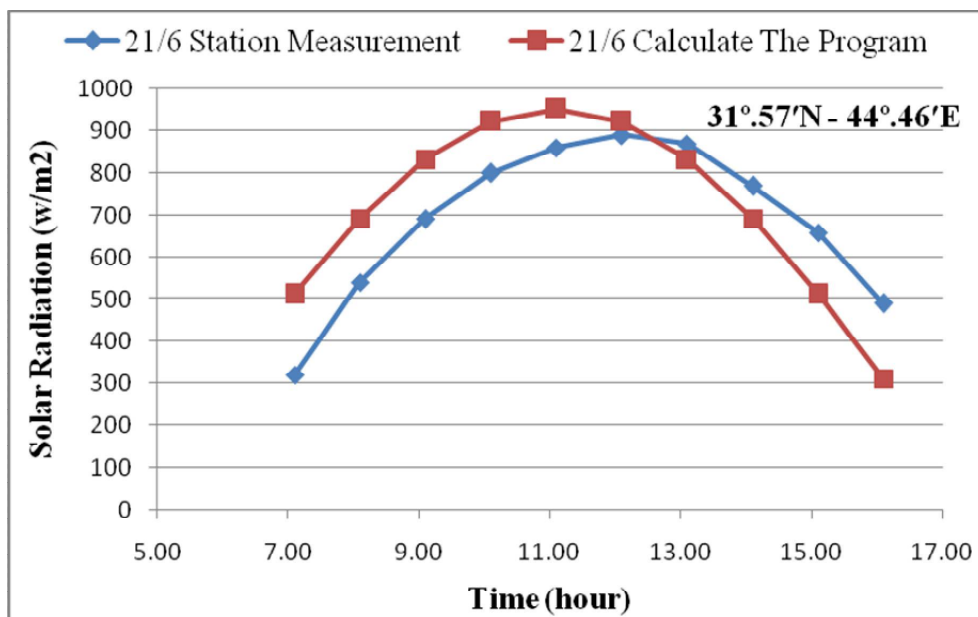


Fig (6) shows the comparison between the measured and calculate data of solar radiation with time in 21/6 for (31°.57'N - 44°.46'E) site





Mohammed .T.Hussein and Emad .J.Mahdi

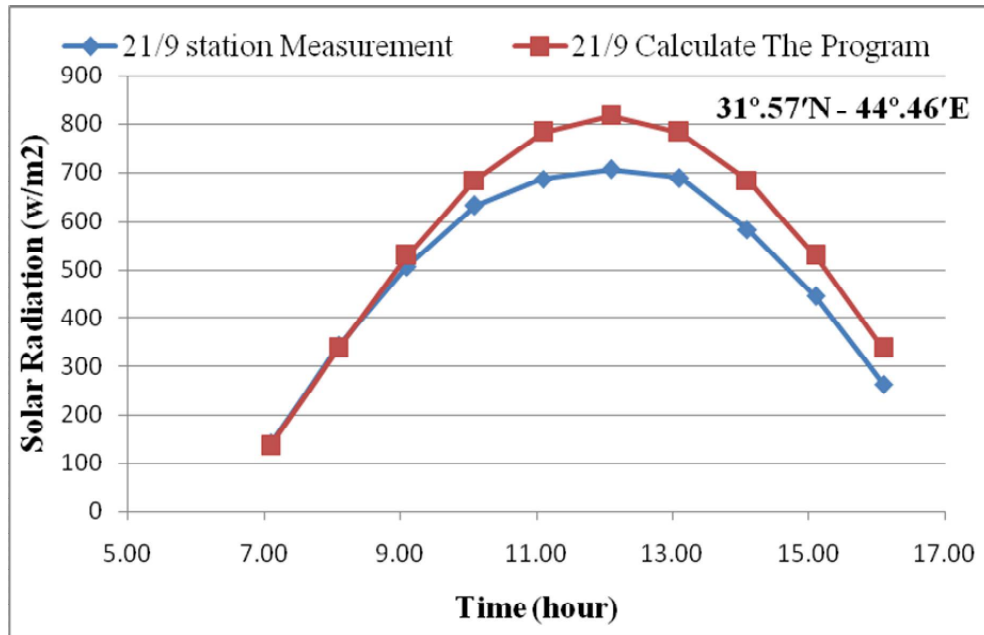


Fig (7) shows the comparison between the measured and calculate data of solar radiation with time in 21/9 for (31°57'N - 44°46'E) site

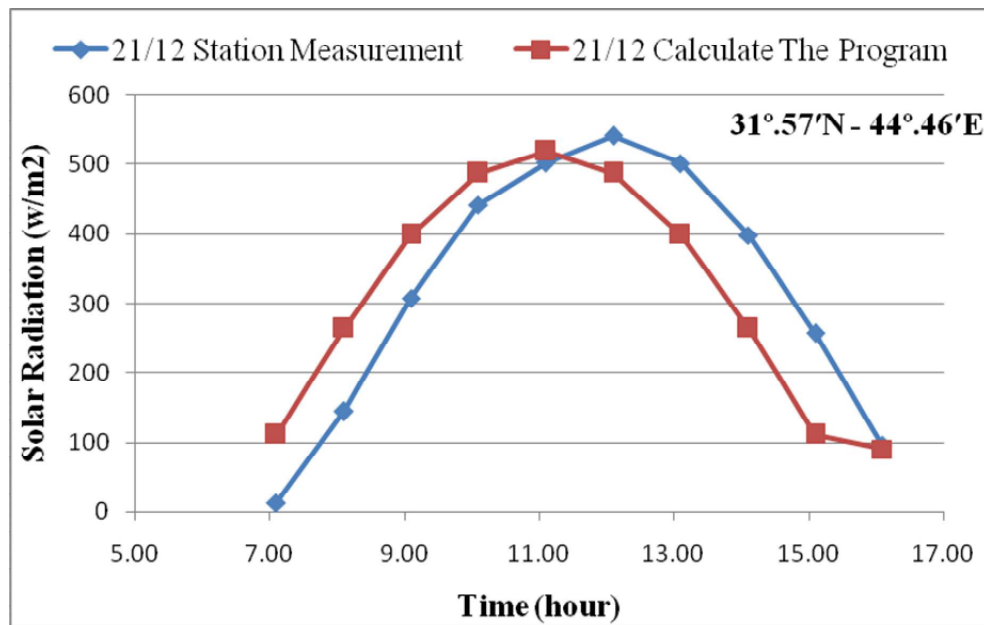


Fig (8) shows the comparison between the measured and calculate data of solar radiation with time 21/12 for (31°57'N - 44°46'E) site





Mohammed .T.Hussein and Emad .J.Mahdi

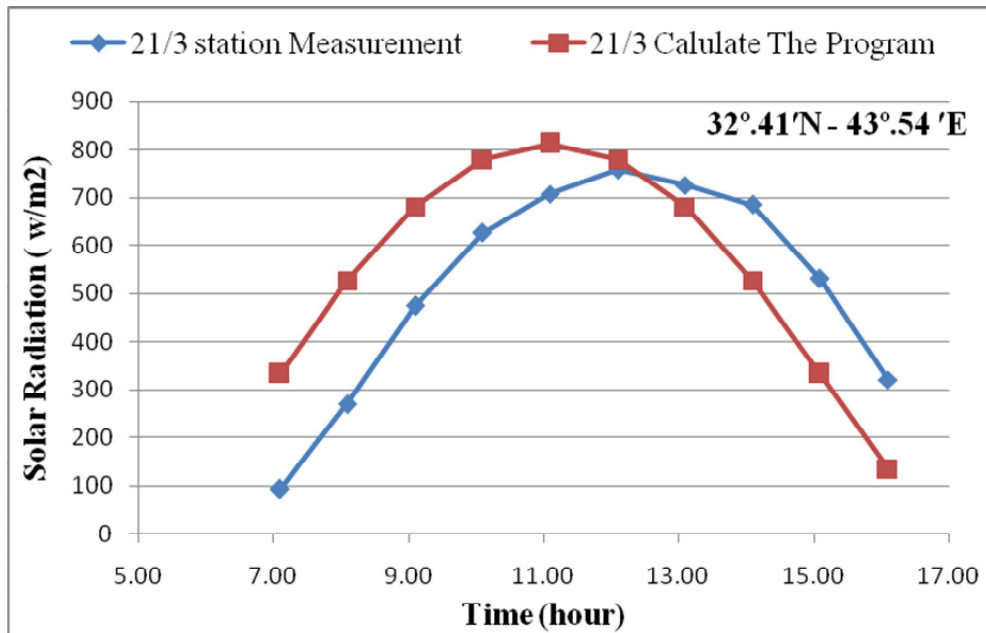


Fig (9) shows the comparison between the measured and calculate data of solar radiation with time in 21/3 for (32°.41'N - 43°.54'E) site

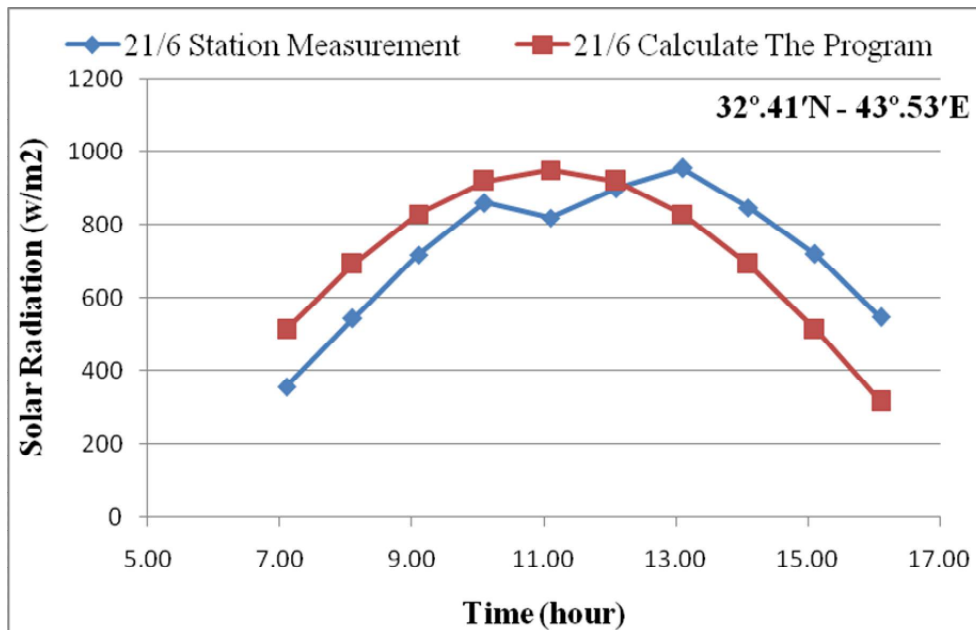


Fig (10) shows the comparison between the measured and calculate data of solar radiation with time in 21/6 for (32°.41'N - 43°.54'E) site





Mohammed .T.Hussein and Emad .J.Mahdi

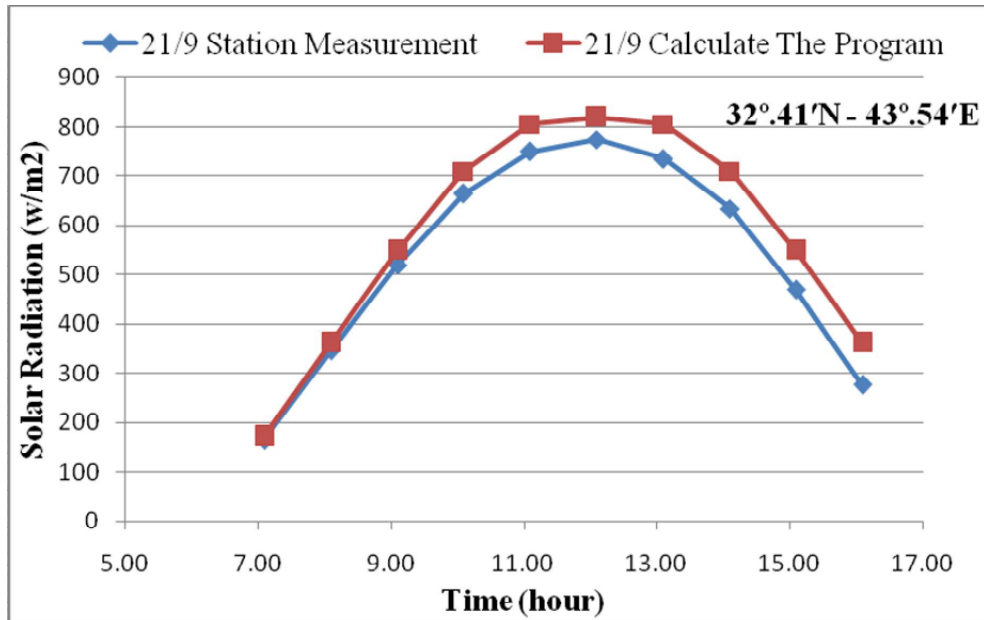


Fig (11) shows the comparison between the measured and calculate data of solar radiation with time in 21/9 for (32°.41'N - 43°.54'E) site

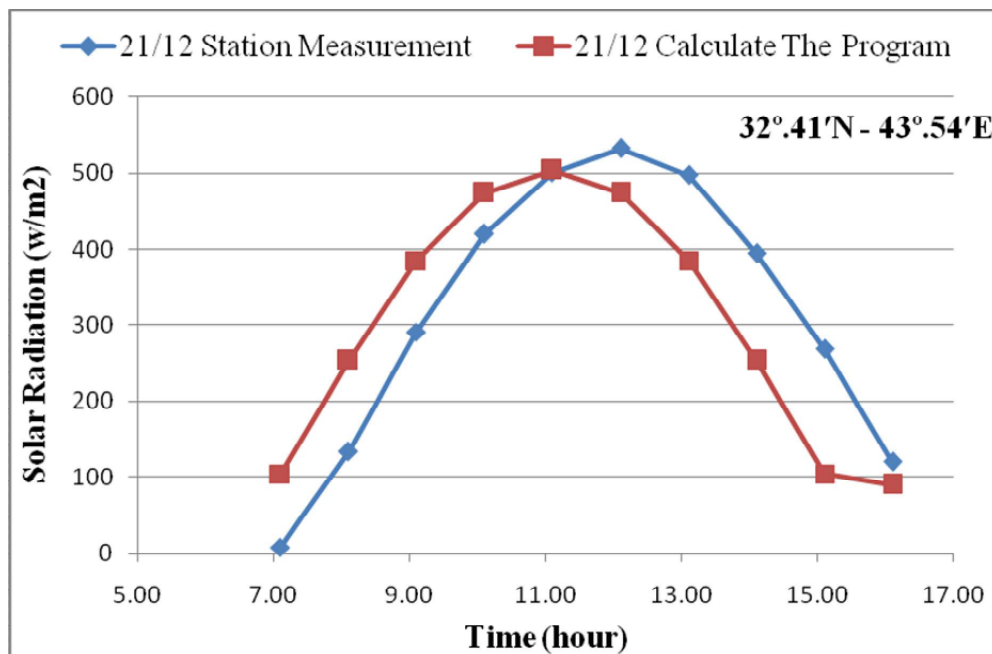


Fig (12) shows the comparison between the measured and calculate data of solar radiation with time for (32°.41'N - 43°.54'E) site





Mohammed .T.Hussein and Emad .J.Mahdi

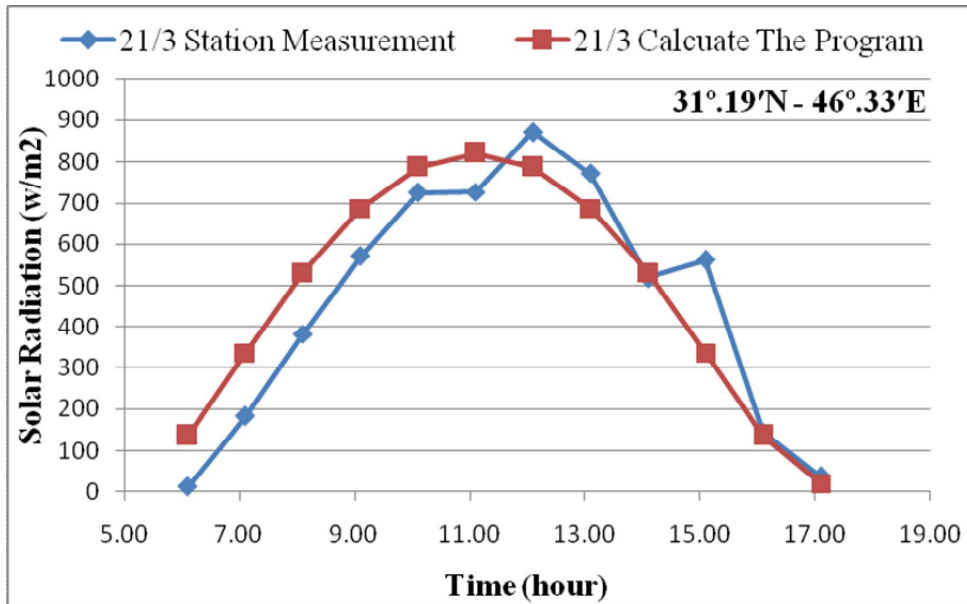


Fig (13) shows the comparison between the measured and calculate data of solar radiation with time in 21/3 for (31°.19'N - 46°.33'E) site

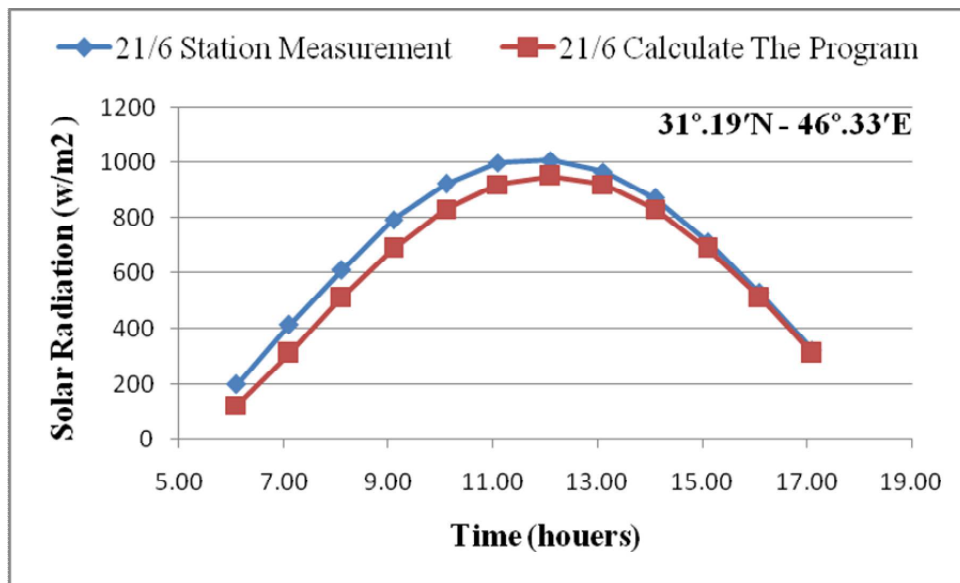


Fig (14) shows the comparison between the measured and calculate data of solar radiation with time in 21/6 for (31°.19'N - 46°.33'E) site





Mohammed .T.Hussein and Emad .J.Mahdi

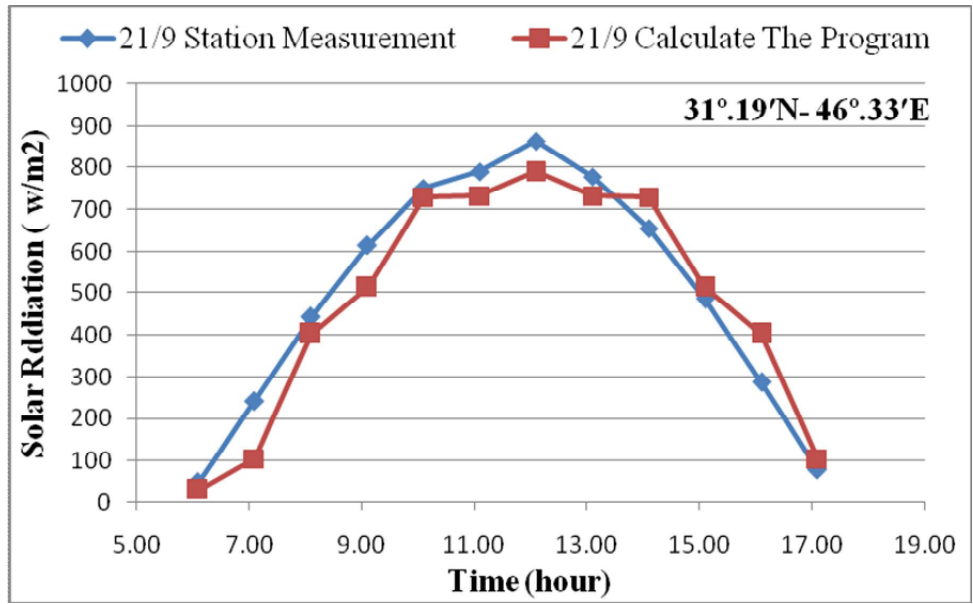


Fig (15) shows the comparison between the measured and calculate data of solar radiation with time in 21/9 for (31°.19'N - 46°.33'E) site

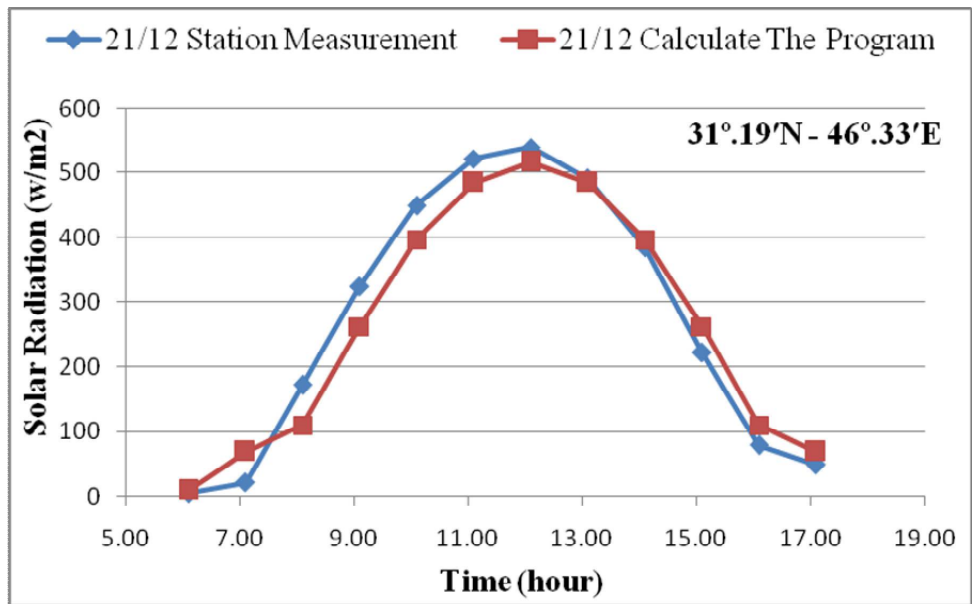


Fig (16) shows the comparison between the measured and calculate data of solar radiation with time in 21/12 for (31°.19'N - 46°.33'E) site





Isolation and Biochemical Characterization of Mycoplasma Species Associated with Respiratory Tract Infection of Sheep

M.Shivakumar^{1*}, P.T.Ramesh² and M.Narayana Bhat³

¹Principal, Animal Husbandry Polytechnic, Baragi, Gundlupete Taluk, Karnataka, India.

²Professor, Dept.of Veterinary Medicine, Veterinary College, Bangalore, Karnataka,India.

³Professor, Dept.of TVCC, Veterinary College, Bangalore, Karnataka, India.

Received: 11 Dec 2017

Revised: 22 Dec 2017

Accepted: 28 Jan 2018

*Address for correspondence

Dr.M.Shivakumar

Principal,Animal Husbandry Polytechnic,
Baragi, Gundlupete Taluk,
Chamarajanagar District – 571 111, Karnataka,India.
E mail: shiva5kid@gmail.com



This is an Open Access Journal / article distributed under the terms of the **Creative Commons Attribution License** (CC BY-NC-ND 3.0) which permits unrestricted use, distribution, and reproduction in any medium, provided the original work is properly cited. All rights reserved.

ABSTRACT

Irrespective of aetiology, infectious respiratory diseases of sheep and goats contribute to 5.6 percent of the total diseases of small ruminants. It often involves a combination of infectious causes as well as predisposing management factors, potentially leading to significant losses. The present investigation was carried out to comprehend the multifarious etiological mycoplasma species causing respiratory tract infection in sheep. A total of 180 swabs from the nasal cavity were processed by conventional methods for isolation and biochemical characterization of Mycoplasma species from sheep. The different species of mycoplasma isolated based on biochemical tests were *M.ovipneumoniae* (32), *M. arginini* (06), *M. agalactiae* (03) and *M.capricolum* spp *capricolum* (02). Biochemical tests revealed that all 43 isolates were inhibited by digitonin, 34 fermented glucose, six hydrolysed arginine and five isolates gave positive reaction to phenolphthalein test.

Keywords: Digitonin sensitivity, arginine hydrolysis glucose breakdown, *M.ovipneumoniae*, and biochemical tests.

INTRODUCTION

Small ruminants especially sheep and goats bestow significantly for the farmers economy in African, South Asian and Mediterranean countries. They are the valuable assets because of their prominent contribution towards milk, meat and wool production and their potential to grow and replicate rapidly. In developing country like India, sheep and goat has pivotal role in economy of poor, deprived, backward classes and landless labours. To make these small



**Shivakumar et al.**

ruminants based economy as sustainable, there is an urgent need for development of novel techniques for early and accurate diagnosis of complicated disease conditions (Chakraborty *et al.*, 2014). The respiratory diseases represent 5.6 per cent of all these diseases in sheep and goats (Hindson and Winter, 2002). Small ruminants are especially sensitive to respiratory infections, namely, viruses, bacteria, and fungi, mostly as a result of deficient management practices that make these animals more susceptible to infectious agents. The tendency of these animals to huddle and group rearing practices further predispose small ruminants to infectious and contagious diseases (Soni and Sharma, 1990). In both sheep and goat flocks, respiratory diseases may be encountered affecting individuals or groups, resulting in poor live weight gain and high rate of mortality (Kumar *et al.*, 2000). Among the mycoplasma organisms that are causing respiratory tract infection in sheep, *M. ovipneumoniae*, *M. capricolum* subsp. *capricolum*, *M. mycoides* subsp. *mycoides* LC and *M. arginini* are the most commonly isolated mycoplasmas from the upper respiratory tract of sheep with *M. ovipneumoniae* being predominant isolate (Azizi *et al.*, 2011). Many tests for biochemical characterization have been applied to mycoplasmas and recommendations relating to the characterization of species incorporate many of these tests. The tests most commonly used are glucose breakdown, arginine hydrolysis, reduction of tetrazolium chloride, 'film and spots' formation, phosphatase activity, serum digestion and digitonin sensitivity (Lefevre *et al.*, 1987).

MATERIALS AND METHODS

In the present study, a total of 180 nasal swabs were collected from 24 flocks with the history of respiratory tract infection. The swabs were inoculated into tubes containing mycoplasma PRM medium as described by OIE manual 2008. The tubes were incubated at 37°C for 72 hours. The tubes which showed change in colour and turbidity were further sub-cultured in liquid medium and inoculated to PPLO agar which was further incubated at 37°C for another 72 hours. The plates were examined for the presence of colonies and the colonies were purified as described by Awan *et al.*, 2004. The purified isolates were subjected to biochemical tests like digitonin sensitivity, arginine hydrolysis, glucose fermentation and phenolphthalein tests as described by Kumar *et al.*, 2011, Carmichael *et al.*, 1972 and Mona *et al.*, 2015 and species were identified as described by Poveda, 1998.

RESULTS AND DISCUSSION

A total of 180 nasal swabs were processed, 43 swabs revealed colonies suggestive of Mycoplasma species. Biochemical tests carried out to classify the different species of mycoplasma in the study were digitonin sensitivity, glucose fermentation, arginine hydrolysis and phenolphthalein tests. All the 43 isolates were sensitive to digitonin, six isolates hydrolysed arginine, 34 isolates utilised glucose and five isolates were positive for phenolphthalein test (Table 1). Based on the biochemical characters, isolates were classified into different species. The most frequently isolated mycoplasma species was *M. ovipneumoniae* followed by *M. arginini*, *M. agalactiae* and *M. capricolum* sp. *capricolum* with the percentage of isolation 74.11, 13.95 and 6.97 respectively (Table 2). Hence, classical biochemical and serological tests can be used for the identification of mycoplasma species in sheep (Awan *et al.*, 2009). Poveda (1998) and Tilaye *et al.* (2014) identified and classified Mycoplasma spp. based on their sensitivity to digitonin. Mollicutes may be identified based on sensitivity to digitonin which differentiates sterol requiring mollicutes from the non-sterol requiring mollicutes. A total of 43 isolates in the present study showed sensitivity to digitonin indicating that they belonged to the genus *Mycoplasma* and concur with the findings of Kumar *et al.* (2011). A total of 34 isolate fermented glucose resulting in pH change towards acidic scale. The change in pH resulted in colour of the media to change from port wine to brown or yellow. Of the 34 isolates 32 were confirmed as *M. ovipneumoniae* and two as *Mycoplasma capricolum*. The fermenting species of mycoplasma catabolise glucose and other carbohydrates yielding acid products, which results in a decrease pH (Poveda, 1998). Three isolates which were identified as *M. agalactiae* and six isolates as *M. arginini* did not ferment glucose. The results of the study are in agreement with the reports of Shmuel and Freundt (1967).



**Shivakumar et al.**

Lefevre *et al.* (1987) reported that approximately one third of all recognised mycoplasmas can hydrolyze arginine. Increase in pH of the medium above 6.5-6.7 indicated the presence of arginine-hydrolyzing mycoplasmas in a culture. The non-fermenting mycoplasmas and a small group of fermenting species hydrolyse arginine producing ammonia with an increase in pH (Poveda.,1998). Similar results have been noted in the present study where six isolates hydrolysed arginine. One isolate showed weak reaction which was confirmed as *M. capricolum* by PCR. The results are in line with the biochemical characterization of mycoplasma by Shmuel and Freundt (1967). The test is based on the liberation of phenolphthalein in the liquid medium and its reaction with sodium hydroxide which produces a red colour (Poveda, 1998). Three of the isolates of *M. agalactiae* and two *M. capricolum* gave a positive reaction to phenolphthalein tests in the present study. The results of the present study are similar to findings reported by Lefevre *et al.* (1987).

In this study, *M. ovipneumoniae* was the predominant isolate and it concurs with the findings of Azizi *et al.*, 2011 who reported that mycoplasmal pneumonia has been associated with *M. ovipneumoniae*, *M. capricolum* subsp. *capricolum*, *M. mycoides* subsp. *mycoides* LC and *M. arginini*. *M. ovipneumoniae* is the most commonly isolated mycoplasma from the upper respiratory tract of normal sheep, and can be a cause of significant respiratory disease in both sheep and goats. During times of stress, subclinical infection may predispose sheep to atypical pneumonia with paroxysmal coughing.

CONCLUSION

A number of useful biochemical reaction tests can be performed in a diagnostic laboratory as a preliminary screening system. They serve to narrow down the likely identity of an isolate, thus saving time and reagents in the final, serological phase of identification. The tests most commonly used are glucose breakdown, arginine hydrolysis, reduction of tetrazolium chloride, 'film and spots' formation and phosphatase activity.

Conflict of Interest: None Declared

REFERENCES

1. Chakraborty Sandip, Amit Kumar, Ruchi Tiwari, Anu Rahal, Yash Malik, Kuldeep Dhama, Amar Pal, and Minakshi Prasad. Advances in Diagnosis of Respiratory Diseases of Small Ruminants. *Veterinary Medicine International*. 2014. pp. 1-16.
2. Hindson J. C. and A. C. Winter, "Respiratory disease," in Manual of Sheep Diseases, pp. 196–209, Blackwell Science, Oxford, UK, 2nd edition, 2002.
3. Soni S. S. and K. N. Sharma, "Descendence of natural bacterial flora as causative agent of pneumonia in sheep," *Indian Journal of Comparative Microbiology Immunology and Infectious Diseases*. 1990. 11, pp. 79–84.
4. Kumar R., R. C. Katoch, and P. Dhar, "Bacteriological studies on pneumonic gaddi sheep of Himachal Pradesh," *Indian Veterinary Journal*. 2000. 77(10), 846–848.
5. Shmuel, R. and Freundt, E.A. The mycoplasmas. In: *Bergey's manual of systematic bacteriology*. Williams and Wilkins publication, London. 1967.
6. Carmichael, L.E., ST. George, T.D., Sullivan, N.D. and Horsfall, N., Isolation, propagation and characterization studies of an ovine mycoplasma responsible for proliferative interstitial pneumonia. *Cornell. Vet.*, 1972. 62: 634-679.
7. Lefevre, P.C., Jones, G.E. and Ojo, M.O. Pulmonary mycoplasmoses of small ruminants. *Rev. sci. tech. Off. int. Epiz.* 1987. 6(3): 759-799.
8. Poveda, J.B., Biochemical characteristics in mycoplasma identification. *Methods in molecular biology*. 1998. 104: 69-78.





Shivakumar et al.

9. Awan, M.A., Siddique, M., Abbas, F., Babar, S., Mahmood, I and Samad, A., Isolation and identification of mycoplasmas from pneumonic lungs of goats. *App.Em.Sc.*2004. 1(1): 45-50.
10. OIE.Chapter 2.7.5. Contagious agalactia. *Terrestrial manual*: 2008992-999.
11. Awan, M.A., Abbas, F., Yasinzai, M., Nicholas, R.A.J., Babar, S., Ayling, R. D., Attique, M.A. and Ahmed, Z., Prevalence of *Mycoplasma capricolum* subspecies *capricolum* and *mycoplasma putrefaciens* in goats in Pishin district of Balochistan. *Pakistan Vet. J.*, 2009. 29(4): 179-185.
12. Azizi, S. Tajbakhsh, E. Rezaii, A. Nekouei, S.H and Namjoo, A.R., The role of *Mycoplasma ovipneumoniae* and *Mycoplasma arginini* in pneumonic lungs of slaughtered sheep. *Revue Méd. Vet.*,2011.162 (6) 310-315.
13. Kumar, P., Roy, A., Bhanderi, B.B. and Pal, B.C., Isolation, identification and molecular characterization of *Mycoplasma* isolates from goats of Gujarat State, India. *Vet. archiv.* 2011.81: 443-458.
14. Tilaye, D., Fufa, D. and Tesfaye, S., Biochemical and Antigenic Characterization of *Mannheimia*, *pasteurella* and *Mycoplasma* Species from Naturally Infected Pneumonic Sheep and Goats, Bishoftu, Ethiopia. *African Journal of Basic & Applied Sciences.*, 2014. 6(6): 198-204.
15. Mona, M., Walaa, M., Zeinab, R., Manalabo, E.M., Kamelia, O and Ahmed, O., *Mycoplasma* as major pathogen of respiratory disease in cattle. *Journal of Global Biosciences.* 2015. 4(7): 2630-2635.

Table1: Biochemical characterization of Mycoplasma isolates

No.of isolate	Biochemical characteristics			
	Digitonin sensitivity	Arginine hydrolysis	Glucose fermentation	Phenolphthalein test
32	+	-	+	-
06	+	+	-	-
03	+	-	-	+
02	+	-	+	+
43	43	6	34	05

Table 2: Number of different isolates and their percentage

Sl.no.	Species	No. Isolated	Percentage
1	<i>M. ovipneumoniae</i>	32	74.11
2	<i>M. argini</i>	06	13.95
3	<i>M. agalactiae</i>	03	6.97
4	<i>M. capricolum</i> ssp. <i>Capricolum</i>	02	4.65





Effects of Fennel Seeds on Biochemical and Haematological Parameters of Wistar Albino Male Rats Fed on High Fat-Diet

Jasmine Rani K*, Shyama K., Chithrma Seethal C.R. and Ally K.

Department of Animal Nutrition, College of Veterinary and Animal Sciences, Mannuthy, Thrissur, Kerala, India

Received: 12 Dec 2017

Revised: 24 Dec 2017

Accepted: 28 Jan 2018

* Address for correspondence

Dr. Jasmine Rani K.

Assistant Professor, Department of Animal Nutrition,
College of Veterinary and Animal Sciences, Mannuthy,
Thrissur, Kerala-680651, India.

E mail: jasminerani@kvasu.ac.in



This is an Open Access Journal / article distributed under the terms of the **Creative Commons Attribution License** (CC BY-NC-ND 3.0) which permits unrestricted use, distribution, and reproduction in any medium, provided the original work is properly cited. All rights reserved.

ABSTRACT

Fennel (*Foeniculum vulgare*) is one of the important medicinal plants, the seeds of which are used widely in pharmaceutical industry. It is an aromatic medicinal herb commonly used for various medicinal purposes in households. The present study was aimed to investigate the medicinal health effects of feeding fennel seeds in rat on high fat diet. Twenty four male Wistar albino rats weighing $180 \pm 5g$ were used as experimental animals. Animals were divided into four groups of six rats each. Rats of group (1) were fed on basal diet and kept as negative control group; group (2) animals were fed on high fat-diet and kept as positive control group. Animals of groups (3), and (4) were fed on high fat diets supplemented with two different levels of fennel seeds (3% and 6%) respectively for a period of 1 month. The results revealed that rats fed on high fat-diet (positive control group) had significant ($p < 0.05$) increase in serum TG, TC, LDL-C, AST and ALT concentrations, and significant decrease ($p < 0.05$) in serum HDL-C level as compared to rats fed on basal diet (negative control group). High fat-diet supplemented rats with two different levels of fennel seeds recorded improved serum levels of TG, TC, LDL-C, AST and ALT and significant increase in serum HDL-C level compared to the positive control group. The hematological parameters were similar in all the treatment groups. ($P > 0.05$).

Keywords: Fennel seeds, *Foeniculum vulgare*, Rat, Blood, Hyperlipidimia,



Jasmine Rani *et al.*

INTRODUCTION

Medicinal plants have been well used for maintenance of health from very ancient times. Hyperlipidemia caused by many etiological factors, characterized by elevated serum parameters such as free fatty acids, triglycerides, total cholesterol, low-density lipoprotein-cholesterol (LDL-C). (Jain *et al* 2007). Fennel (*Foeniculum vulgare*) is one of the important spice plants, the seeds of which are used widely in pharmaceutical industry and found to have hypotensive effect, antispasmodic, hepatoprotective and anti-inflammatory activities (Rezq., 2012). Phenolic compounds present in this herb are caffeoylquinic acid, rosmarinic acid, eriodictyol-7-orutinoside, quercetin- 3-Ogalactoside, kaempferol-3-O-glucoside and has antioxidant activity. (Parejo *et al* 2004). The current study was aimed to investigate the beneficial health effects of fennel seeds (*Foeniculum vulgare*) administration to rats fed on high fat-diet.

MATERIALS AND METHODS

Twenty four male Wistar albino rats weighing $180 \pm 5g$ selected from Small Animal Breeding Station, College of Veterinary and Animal Sciences, Mannuthy, formed the experimental subjects for the study and were allotted randomly into four groups of six rats each. Rats of group 1 (T_1) were fed on basal diet, group 2 (T_2) animals were fed on high fat-diet. Animals of third (T_3) and fourth (T_4) were fed on high fat diets supplemented with 3% and 6% fennel seed powder, respectively. All the rations were made isonitrogenous and isocaloric. Weighed quantity of feed was given in the morning. Clean, fresh drinking water was provided *ad libitum* to all the animals. Animals were maintained under normal ambient conditions.

Blood samples were collected after 30 day in tubes with EDTA was used for the count of RBC, WBC, haemoglobin, MCV, MCH and MCHC by standard procedures described by Sanderson and Philips (1981). Serum TC, TG and HDL-C were determined by enzymatic colorimetric methods using commercial kits from Agappe diagnostics Ltd, Ernakulam, India., while LDL-C was calculated using Friedewald's equation, which is (in mg/dL): $[LDL-cho] = [TC]-[HDL-cho]-[TG/5]$. Alanine-aminotransferase (ALT) and aspartate-aminotransferase (AST) activities were measured according to the method described by Reitman and Frankel (1957).

Feed samples were analyzed for proximate principles (AOAC, 2005). Data were analyzed statistically using Analysis of Variance (Snedecor and Cochran, 1994).

RESULTS AND DISCUSSION

Data on haematological studies have been given in Table 1. The values of various hematological parameters (haemoglobin, MCV, MCH, MCHC, RBC count and WBC count) were similar in all the groups indicating that dietary incorporation of fennel seed powder did not affect these parameters to any significant effect. The results revealed that rats fed on high fat-diet (positive control group) recorded ($p < 0.05$) increased serum TG, TC, LDL-C, AST and ALT concentrations and significant decrease ($p < 0.05$) in serum HDL-C level as compared to rats fed on basal diet (negative control group). High fat-diet supplemented rats with two different levels of fennel seeds recorded improved serum levels of TG, TC, LDL-C, AST and ALT and increased serum HDL-C level compared to the positive control group. The present results are in agreement with Fatiha *et al.* (2011) who reported that hyperlipidemic rats treated with fennel extract had significant decrease in plasma levels of TL, TG, TC, LDL-C and VLDL, and significant increase in HDL-C level. Eman *et al* (2011) and Singh and Kale (2008) also reported that oral administration of *Foeniculum vulgare* in hyperlipidemic rats resulted significant increase in AST and ALT levels in treatment groups compared to control.





Jasmine Rani et al.

Fennel is an excellent source of natural antioxidants and this plant can inhibit free radicals due to the high content of polyphenols and flavonoids. (Guimaraes, 2000 and Parsaeyan, 2017). The hypo lipidemic effect of fennel could be attributed due to the presence of the polyphenolic compounds particularly tannins and flavonoids.

CONCLUSION

In conclusion, the present study revealed that supplementation of fennel seeds improves hyperlipidaemia by improving lipid profile, cholesterol and LDL-C, and by increasing level of HDL-C. Antioxidative activity of fennel seeds may be the possible mechanisms by which it improved the total lipids, cholesterol, triglycerides and LDL-C.

REFERENCES

1. Jain, K. S., Kathiravan, M. K., Somani, R. S. and Shishoo, C. J. (2007). The biology and chemistry of hyperlipidemia. *Bioorgan. Med. Chem.*, 15: 4674 – 4699.
2. Rezaq, A.A., (2012). Beneficial health effects of fennel seeds (shamar) on male rats feeding high fat-diet. *Med. J. Cairo Univ.*, V. 80: 101-113.
3. Parejo, I., Jauregui, O., Sánchez-Rabaneda, F., Viladomat, F., Bastida, J., Codina, C. (2004). Separation and characterization of phenolic compounds in fennel (*Foeniculum vulgare*) using liquid chromatography-negative electrospray ionization tandem mass spectrometry. *J. Agric. Food. Chem.* 52(12):3679-87.
4. Sanderson JH, Philips CE. New York: Oxford University Press; 1981. An atlas of laboratory animal haematology; p. 471
5. Friedewald W T, Levey R I and Fredrickson D S, (1972): Estimation of the concentration of low density lipoprotein cholesterol in plasma without use of the preparative ultracentrifuge. *Clin. Chem.* 18:499-502
6. Reitman S. and Frankel S., (1957). Colorimetric determination of SGOT and SGPT *Am. J. Clin. Path.* 28:56 - 60
7. A.O.A.C. (2005) Official methods of Analysis, 19th edition. *Association of official Analytical Chemists*, Washington, DC, 587.
8. Snedecor, G.W. and Cochran, W.G. (1994). *Statistical Methods*. 8th edn. The Iowa State University Press, Ames, USA.
9. Fatiha, O., Rachid, S., Nadia, E., Hakima, B., Mustapha, L., Souliman, A. and Noredine, G. (2011). Hypolipidemic and anti-atherogenic effect of aqueous extract of fennel (*Foeniculum Vulgare*) extract in an experimental model of atherosclerosis induced by triton WR-1339. *Euro. J. of Scie. Res.* 91-99.
10. Eman G.E. Helal, F. A. E. and Amira M. S. A.W. (2011). Effect of fennel (*Foeniculum vulgare*) on hyperlipidemic rats. *The Egy. J. of Hosp. Med.* Vol., 43: 212 – 225
11. Singh, B. and Kale, R. K. (2008). Chemomodulatory action of *Foeniculum vulgare* on skin and forestomach papillomagenesis enzymes associated with xenobiotic metabolism and antioxidant status in murine model system. *Food Chem. Toxicol.*, 46(12): 3842-3850
12. Guimaraes, P. R., Galvao, A. M., Batista, C. M., Azevedo, G. S., Oliveira, R. D., Lamounier, R. P., Freire, N., Barros, A. M., Sakurai, E., Oliveira, J. P., Vieira, E. C. And Alvarez-Leite, J. I. (2000). Egg plant (*Solanum Melangena*) infusion has a modest and transitory effect on hypercholesterolemic subjects. *Braz. J. Med. Bio. Res.*, 33: 1027-1036.
13. Parsaeyan, N. (2017). The effect of *Foeniculum Vulgare* (Fennel) extract on lipid profile, lipid peroxidation and liver enzymes of diabetic rat. *Ira. J. of diabetes and obesity*, V. 8: 25-29.





Jasmine Rani et al.

Table 1. Haematological parameters of experimental rats

Parameters	T ₁	T ₂	T ₃	T ₄
Haemoglobin (mg/dl)	14.78 ± 2.60	14.52 ± 0.34	14.48 ± 2.20	14.58 ± 0.24
MCV (fL)	58.04 ± 0.56	58.29 ± 1.20	58.24 ± 0.36	58.79 ± 1.21
MCH (pg)	18.20 ± 0.43	18.85 ± 0.39	18.60 ± 0.63	18.35 ± 0.32
MCHC (g/dl)	34.15 ± 0.39	33.28 ± 0.57	34.52 ± 0.33	33.58 ± 0.27
RBC count (× 10 ⁶ /μl)	8.84 ± 0.51	8.08 ± 0.32	8.04 ± 0.56	8.21 ± 0.31
WBC count (× 10 ³ /μl)	10.32 ± 0.14	10.44 ± 0.37	10.42 ± 0.24	10.64 ± 0.27

T₁, T₂, T₃ and T₄- mean of six values. (P > 0. 05).

Table 2. Blood biochemical parameters of experimental rats

Parameters	T ₁	T ₂	T ₃	T ₄
Total Cholesterol	73.52 ± 1.14 ^a	90.58 ± 2.34 ^b	85.67 ± 2.36 ^c	78.45 ± 2.13 ^d
Triglycerides	82.42 ± 2.62 ^a	162.42 ± 3.42 ^b	120.24 ± 2.14 ^c	118.16 ± 2.13 ^d
LDL-C	26.48 ± 0.30 ^a	29.94 ± 0.16 ^b	25.36 ± 0.23 ^c	16.48 ± 0.22 ^d
HDL-C	30.56 ± 0.48 ^a	28.16 ± 0.28 ^b	36.26 ± 0.43 ^c	38.34 ± 0.28 ^c
ALT	21.56 ± 0.22 ^a	49.82 ± 0.36 ^b	28.66 ± 0.68 ^c	26.50 ± 0.45 ^c
AST	82.85 ± 2.20 ^a	141.62 ± 3.20 ^b	108.88 ± 2.40 ^c	102.64 ± 2.26 ^c

T₁, T₂, T₃ and T₄- mean of six values, Means with different superscript letters are significantly different at p<0.05.





Influence of Laser Pulse Energies on the Structure and Optical Properties of SnO₂ Films Prepared by Laser Induce Plasma

Ramiz A.Alansari ^{1*}, Hussain Kazaal ², Kadhim A.Aadim ² and Wassan Dhia¹

¹Department of Physics, College of Science for Women, University of Baghdad, Baghdad, Iraq.

²Department of Physics, College of Science, University of Baghdad, Baghdad, Iraq.

Received: 15 Dec 2017

Revised: 20 Dec 2017

Accepted: 29 Jan 2018

*Address for correspondence

Ramiz A.Alansari

Department of Physics, College of Science for Women,
University of Baghdad, Baghdad, Iraq.

E mail: dr_wassan_kadhim@yahoo.com



This is an Open Access Journal / article distributed under the terms of the **Creative Commons Attribution License** (CC BY-NC-ND 3.0) which permits unrestricted use, distribution, and reproduction in any medium, provided the original work is properly cited. All rights reserved.

ABSTRACT

(SnO₂) films were prepared by pulsed laser deposition (PLD) technique. The Pulsed Nd:YAG laser was used for prepared SnO₂ thin films under O₂ gas environment with varying pulse energies. X-ray diffraction patterns and intensity curves for the SnO₂ films on glass substrates obtained by PLD technique show that the SnO₂ polycrystalline films with all energies. The optical properties of as-grown film such as optical transmittance spectrum, refractive index and energy gap have been measured experimentally and the effects of laser pulse energy on it were studied.

Keywords: pulsed laser deposition, SnO₂, optical transmittance spectrum, polycrystalline.

INTRODUCTION

Tin oxide films (SnO₂) have been studied with a focus on application to sensors, transparent electrodes in displays, heat mirrors and transparent conducting oxide (TCO) coatings for solar cells [1-5]. SnO₂ films have been prepared by several deposition techniques, such as pulsed laser deposition (PLD), photo-MOCVD, reactive evaporation, spray pyrolysis, sol-gel process, and dc / rf sputtering [6-8]. PLD is the plasma produced by the interaction of high-energy laser pulses with matter in any state of aggregation [9,10]. Laser induced plasmas of metals and alloys are of great interest since they have different attractive and important applications, e.g. material processing, thin film deposition, the synthesis of nanoparticles, the elemental analysis of multi component materials, precision machining, laser induced breakdown spectroscopy (LIBS), surgery, and laser micro-probe mass spectroscopy [11-13].





Ramiz A. Alansari et al.

MATERIALS AND METHODS

Typical Experimental Set-ups

PLD experiment was carried out under vacuum pressure (6×10^{-2} mbar by using Varian DS219 Rotary pump). The beam of Nd:YAG laser with second harmonic frequency ($\lambda = 532$ nm, 10 ns, 6 Hz) was focused onto target. The target of the deposition was SnO₂ bulk with purity 99.999%, shaped like a disc with a diameter of 1 cm. The target was kept onto a rotating holder (speed 4 rev/min) to prevent fast drilling. The substrate distance from the target was fixed to 2 cm. The PLD experiment was performed at room temperature and the as-grown samples were not annealed after deposition. The PLD setup scheme has been shown in figure 1. The crystalline structure was examined using X-ray diffraction (XRD). Optical properties (UV/VIS absorption spectrum) of the SnO₂ films were performed using a UV-Visible spectrometer. The laser pulse energy was varied from (400-800) mJ with an increment.

RESULTS AND DISCUSSION

X-Ray Diffraction Spectra

Fig (1-a,b,c) shows the X-ray diffraction patterns for undoped SnO₂ films grown on glass substrates. We can be seen that the degree of crystalline and grain size variation with laser energy. This can be interpreted in terms of the improvement in the crystal structure of these films with increasing laser energy. It seems that all the films are polycrystalline [18]. The grain size (D) of the material, which plays an important role in the material properties, can be estimated easily from the X-ray spectrum by means of the full width at half maximum (FWHM) method that is often calculated by Scherrer's relation [9],

$$D = \frac{k \cdot \lambda}{\beta \cdot \cos \theta}$$

Where λ is the wavelength of X-ray used (1.54 Å), β is the full width half maximum (FWHM) of the peak and θ is the glancing angle. The calculated crystalline size (D) of Tin oxide is tabulated in table 1.

UV-Visible Spectroscopy

The optical properties of SnO₂ have been determined by using a spectrophotometer in the wavelength range (200-1100) nm. SnO₂ thin films were successfully deposited on to glass substrate and the films were very transparent. Transmittance spectra recorded for SnO₂ films as a function of wavelength range (200-1100 nm) at different energies 400, 600, and 800 mJ show in figure 3. This figure shows that the transmittance decreases with increasing energies due to increasing thicknesses.

The absorption coefficient (α) is calculated using the equation, [14]

$$\alpha = \ln(1/T) / d \dots\dots\dots (1)$$

Where T is transmittance and d is film thickness. The absorption coefficient (α) and the incident photon energy ($h\nu$) are related by the following equation [15]:

$$(\alpha h\nu)^2 = A (h\nu - E_g) \dots\dots\dots (2)$$

The typical plots of $(\alpha h\nu)^2$ versus $h\nu$ for SnO₂ thin films with (400, 600, and 800) mJ energies deposited on glass substrate is shown in figure (6). It is observed that an increase in laser energies leads to an increase in optical band gap from 2.756 eV to 2.9 eV. This may be associated with the variation in crystal structure with laser energies.





Ramiz A.Alansari et al.

CONCLUSION

In this work we have reported the influence of energies of laser in the structural and optical characteristics of SnO₂ thin films.

We describe below summarization of our work:

- 1.The deposition films are having the polycrystalline structure of Tin oxide with cubic structure.
- 2.The intensity of x-ray diffraction was proportional with laser energies
- 3.The optical properties was proportional with laser energies.
- 4.The band gap increase with increasing of laser energies.

REFERENCES

- [1] I. Stambolova, K. Konstantinov, S. Vassilev, P. Peshev and Ts. Tsacheva, Mater. Ce Phys. 63, 104 (2000).
- [2] M. Chen, Z. L. Pei, C. Sun, J. Gong, R. F. Huang and L. S. Wen, Mater. Sci. Eng. B 85, 212 (2001).
- [3] Y. R. Rye, S. Zhe, D. C. Look, J. M. Wrobel, Amjeony and H. W. White, J. Cryst. Growth. 216, 330 (2000).
- [4] M. A. Martinez, J. Herero and M. T. Gutierrez, Solar Energy Materials and Solar Cells 45, 75 (1997).
- [5] K. T. R. Reddy, H. Gopaldaswamy, P. J. Reddy and R. W. Miles, J. Cryst. Growth 210, 516 (2000).
- [6] M. Ginting and J. D. Leslie, Canadian J. Phys. 12, 436 (1998).
- [7] Jinsoo Song, I-Jun Park, Kyung-Hoon Yoon, Woo-Yeong, Cho and Koeng-Su Lim, J. Korean Phys. Soc. 29, 219 (1996).
- [8] J. H. Lee, K. H. Ko and B. O. Park, J. Cryst. Growth 247, 119 (2003).
- [9]. H. M. Smith and A. F. Turner, Appl. Opt. 4, 147 (1965).
- [10] D. Dijkkamp, T. Venkatesan, X. D. Wu, S. A. Shareen, N. Jiswari, Y. H. Min- Lee, W. L. McLean, and M. Croft, Appl. Phys. Lett. 51, 619 (1987).
- [11] D. B. Chrisey and G. K. Hubler: Pulsed laser deposition of thin films, (Wiley, New York 1994).
- [12]. C. Scarfone, M. G. Norton, C. B. Carter, J. Li, and H. W. Mayer, Mat. Res. Soc. Symp. Proc. 191, 183 (1991).
- [13] S. F. Ahler, M. St. ormer, and H. U. Krebs, Appl. Surf. Sci. 109/110, 433 (1997).
- [14] D.S., Burukhin, A.A., Churagulov, B.R., Rummyantseva, M.N., Maksimov, V.D. (2003). Vol. 39, № 11, pp. 1158-1162.
- [15] Xu, Ch., Jun, T., Norio, M., Nobory, Y. (1991). Vol. 3, pp. 147–155.

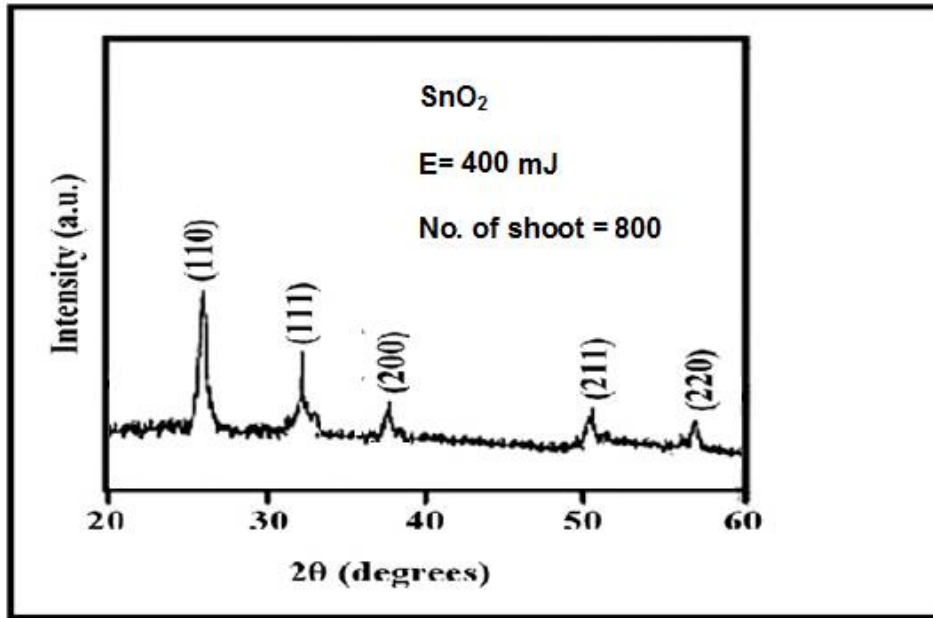


Fig.(1): Pulsed laser deposition (PLD) system.

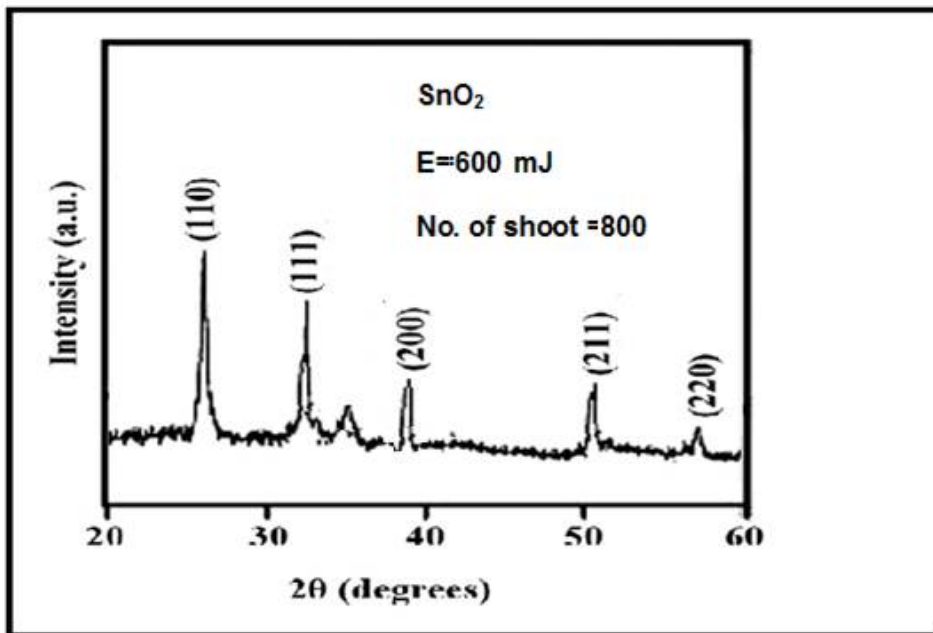




Ramiz A.Alansari et al.



(a)

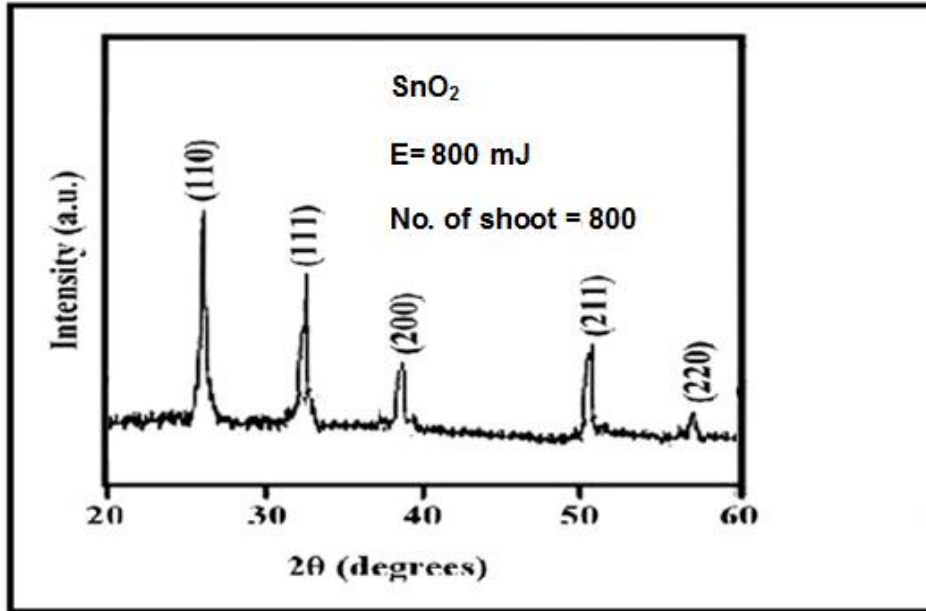


(b)



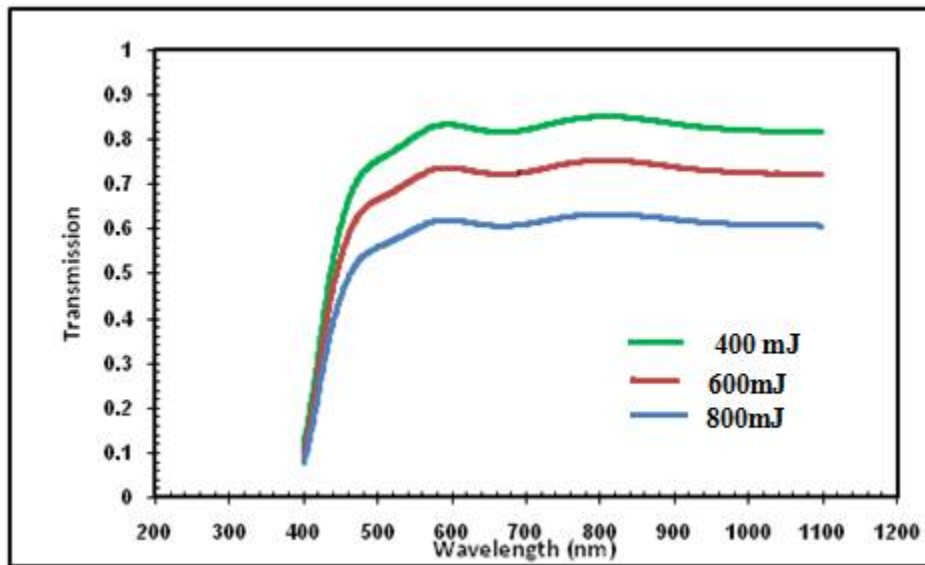


Ramiz A.Alansari et al.



(c)

Fig (2).XRD of SnO₂ thin film with Number of shoot =800 and different energies [(a)400, (b)600], (c)800]mJ

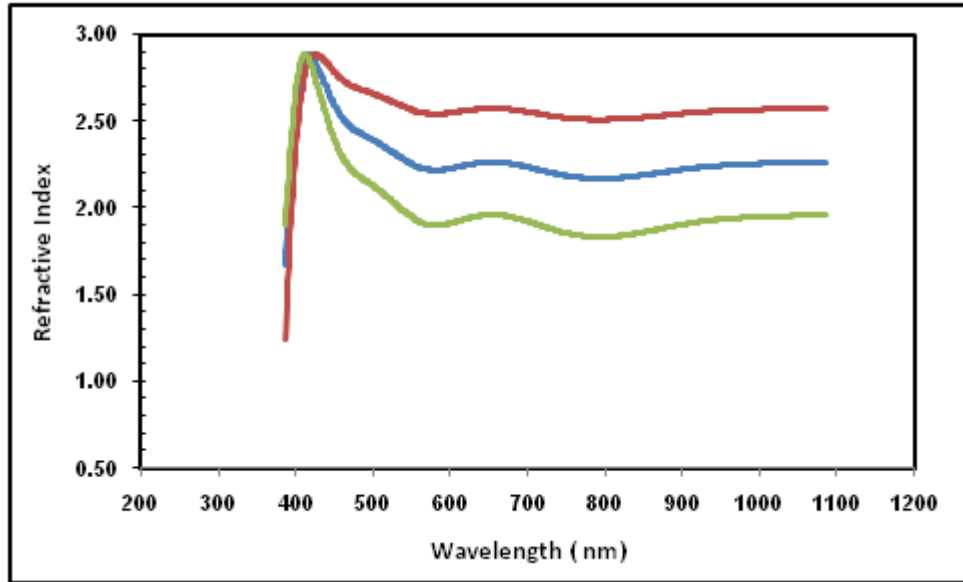


Fig(3).shows the Transition of SnO₂ thin films as a function of wavelength

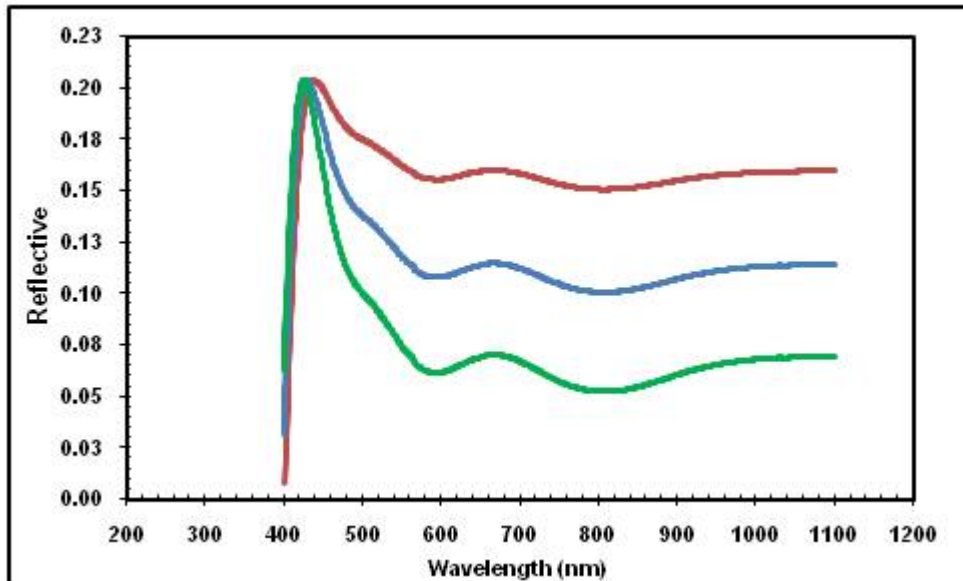




Ramiz A.Alansari et al.



Fig(4).shows the Refractive index of SnO₂ thin films as a function of wavelength

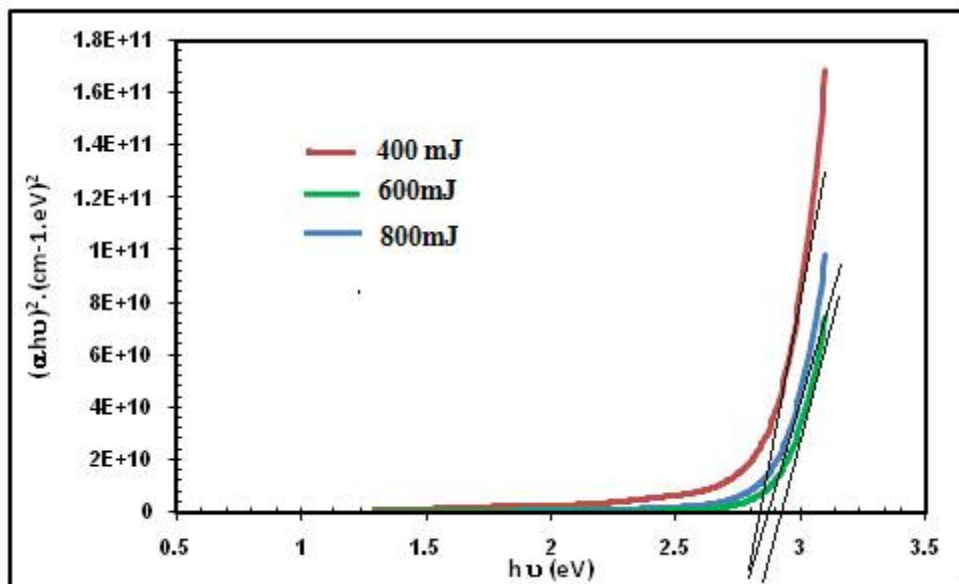


Fig(5).shows the Reflective of SnO₂ thin films as a function of wavelength





Ramiz A.Alansari et al.



Fig(6).shows the direct electronic transition for nanostructure SnO2 thin films

Table.1.The FWHM and the grain size of the samples.

Energies	2θ (Deg.)	FWHM (Deg.)	d _{hkl} Exp.(Å)	G.S (nm)	hkl
400	26.22	0.219	3.3961	371	(110)
	32.47	0.247	2.7551	338	(111)
	38.27	0.243	2.3499	301	(200)
	50.78	0.250	1.7965	278	(211)
	58.01	0.257	1.5880	246	(220)
600	26.27	0.244	3.3879	321	(110)
	32.75	0.219	2.7323	316	(111)
	38.89	0.205	2.3100	298	(200)
	50.31	0.149	1.8122	286	(211)
	58.27	0.114	1.5822	269	(220)
800	26.40	0.190	3.3733	327	(110)
	33.1	0.183	2.7040	319	(111)
	83.92	0.162	2.3100	267	(200)
	50.49	0.144	1.8000	298	(211)
	58.60	0.165	1.5740	243	(220)





Phenotypic and Pathological Variability among the Isolates of *Sclerotium rolfsii* Inciting Stem Rot Disease in Groundnut

Daniel Jebaraj, M*, Eraivan Arutkani Aiyathan, K. and S. Nakkeeran

Department of Plant Pathology, Centre for Plant Protection Studies (CPPS), Tamil Nadu Agricultural University, Coimbatore-641003, Tamil Nadu, India.

Received: 12 Dec 2017

Revised: 23 Dec 2017

Accepted: 25 Jan 2018

*Address for correspondence

Daniel Jebaraj, M

Department of Plant Pathology, Centre for Plant Protection Studies (CPPS),

Tamil Nadu Agricultural University,

Coimbatore-641003, Tamil Nadu, India.

E mail: daniel.jebaraj2011@gmail.com



This is an Open Access Journal / article distributed under the terms of the **Creative Commons Attribution License** (CC BY-NC-ND 3.0) which permits unrestricted use, distribution, and reproduction in any medium, provided the original work is properly cited. All rights reserved.

ABSTRACT

Totally eighteen *Sclerotium rolfsii* isolates have been isolated from infected groundnut plants collected from various groundnut growing regions of Tamilnadu, India. Characteristic white mycelial growth with numerous small tan to dark brown or black spherical sclerotia was observed in *S. rolfsii* isolates grown in PDA medium. Among the eighteen isolates studied, two isolates namely SrPLC and SrKNK have produced pure white and fluffy colonies. Isolates SrDGL, SrMDU, SrVAL, SrTVM, SrMDT and SrTRM have produced white creamy colonies, while other isolates produced white fluffy colonies. All the isolates produced regular colony margin. The maximum number of sclerotial production (619.67 per plate) was observed in isolate SrUDM and minimum number of sclerotia (105.33 per plate) was observed in SrTHN isolate. All the eighteen isolates produced sclerotial bodies and its colour was grouped in to three categories viz., light brown, dark brown and reddish brown. Sclerotial weight (100 Nos.) of different isolates showed appreciable variation. Number of sclerotia per cm² ranged from 4.80 to 19.60. The maximum number of sclerotial bodies/ cm² (19.60) was observed in isolate SrUDM and minimum number of sclerotial bodies/ cm² (4.80) was observed in SrTHN isolate. The diameter of the sclerotia exhibited variation and ranging between 913.27 µm and 1208.53 µm. The maximum diameter of sclerotia (1208.53 µm) was observed in isolate SrKGS and minimum diameter of sclerotia (913.27 µm) was observed in SrKAN isolate. Among the eighteen isolates tested, the *S. rolfsii* isolate collected from Udumalpet (SrUDM) showed higher disease incidence of 33% pre emergence and 48% post emergence mortality, whereas the samples collected from Madurai recorded low incidence of 11% pre emergence and 22% post emergence mortality.

Keywords: Groundnut, Stem rot, Sclerotia, *Sclerotium rolfsii*, Phenotypic characters.



**Daniel Jebaraj et al.**

INTRODUCTION

Groundnut (*Arachis hypogaea* L.) production is hindered by several biotic and abiotic stresses. Among the biotic stresses, the disease caused by soil borne fungal pathogen particularly stem rot disease is considered as the major concern. It is caused by *Sclerotium rolfsii* Sacc. This soil borne pathogen commonly occurs in the tropics, subtropics and other warm temperate regions of the world causing root rot, stem rot, wilt and foot rot on more than 500 plant species including almost all the agricultural and horticultural crops (Aycock, 1966; Domsch *et al.*, 1980; Farr *et al.*, 1989; Hossain, 2000) including groundnut, cotton, soybean, sunflower, wheat, legumes, tomato, chilli, potato, crucifers, cucurbits, onion and others. The loss of yield caused by the pathogen is 25%, but sometimes it reaches 80-90% (Grichar and Bosweel, 1987). Rangarani (2017) reviewed the stem rot of groundnut incited by *S. rolfsii* and reported the diverse level of yield loss ranged from 45 - 80 %. It has been demonstrated that various isolates of *S. rolfsii* isolated from infected plants varied in their cultural, morphological and pathological characteristics (Gupta and Kolte, 1982; Kumar *et al.*, 2014).

Variability is the property of an organism to change its characters from one generation to the other. There are several reports of *S. rolfsii* which was showing significant variations in morphological or phenotypic behaviour (Sarma *et al.*, 2002). Punja and Grogan (1983) observed the variation in growth rate particularly the sclerotial production and frequency of clamp formation among different isolates of *S. rolfsii* collected from ten fields of California. Komathi (2002) reported that the isolates of *S. rolfsii* from groundnut exhibited variation in the mycelial growth. In a study conducted by Akram *et al.* (2007), the isolates of *S. rolfsii* were classified into three groups as very fast growing, intermediate and slow growing. The isolates SRC-1, SRC-18, SRC-19 and SRC-112 were fast growing (76.7- 90 mm dia) while the isolate SRC-2, SRC-4, SRC-5 and SRC- 11 were slow growing (16.0 – 30.6mm dia). Others were medium in growth and varied from 40.8 to 61.7 mm diameter. Mahato and Biswas (2017) studied the phenotypic characterization of *S. rolfsii* infecting tomato, three isolates were found to be very fast growing (dia. > 9 cm), three were fast growing (8-8.9 cm), three moderately fast growing (5-6 cm) and one was observed as slow growing (< 3 cm). Four isolates were white, one each of extra white and cottony white, two isolates were light white and another two were dull white. The colour of sclerotia ranged from brown to dark brown, shape ranged from spherical to oval and also irregular, sclerotial weight ranged from 3.7 to 8.6 mg. Six isolates were observed as scattered, two peripheral and two were reported as central in sclerotia arrangement. Sclerotia took a range of 9 to 15 days after inoculation for maturity. A range of 154.0 to 395.0 sclerotia production per plate was reported from the tested isolates. Banakar *et al.* (2017) studied the morphological and cultural characters of *S. rolfsii* causing foot rot disease of tomato and reported the diverse level of morphological and cultural characteristics of isolates.

MATERIALS AND METHODS

Isolation and phenotypic characterization of isolates of *S. rolfsii*

The pathogen, *Sclerotium rolfsii* was isolated from the diseased groundnut plants by tissue segment method (Rangaswami, 1996) using Potato Dextrose Agar (PDA) medium. The phenotypic characters of the isolates of *S. rolfsii* from groundnut of diverse geographic origins were studied by growing the fungus in the PDA medium. Mycelial disc (9 mm) taken from the margin of an actively growing colony (3 days old) of each isolate was placed in the centre of the Petri plate. The inoculated plates were incubated at normal room temperature $28\pm 2^{\circ}\text{C}$ and replicated thrice. The colony diameter was measured every day (growth rate) and to the maximum of four days by taking two observations at right angles. The number of sclerotia per Petri plate was counted after 20 days of incubation. The growth and morphological characters of the isolates *viz.*, colony morphology, mycelial growth rate, sclerotial number, size, colour and shape were observed. Measurement of 100 sclerotia was taken under the microscope (magnification $45\times \times 10\times$) by using ocular and stage micrometers (Sarma *et al.*, 2002).



**Daniel Jebaraj et al.**

Pathogenicity of *S. rolfsii* isolates

The pot culture experiment was conducted for the pathogenicity study. The inoculum of each isolate of *S. rolfsii* grown on sand maize medium (20 days old) was applied on top two centimeter of the soil at 5 per cent (w/w basis) level in the pot. Then groundnut seeds were sown in the inoculated pots. In each isolate three replications were maintained. The seeds sown in pots without inoculum served as control. The disease incidence was calculated as described by Kokalis-Burelle *et al.* (1992).

RESULTS AND DISCUSSION

Eighteen *S. rolfsii* isolates have been successfully isolated from infected ground nut plants collected from various groundnut growing regions of Tamilnadu, India. Characteristic white mycelial growth with numerous small tan to dark brown or black spherical sclerotia was observed in *S. rolfsii* isolates grown in PDA medium. The isolate SrUDM collected from Udumalpet showed fastest growth on first day after inoculation compared to other isolates. On the third day, this isolate attained full radial growth on PDA medium (Table 1; Figure 1). By fourth day, all the isolates attained full radial growth. Among the eighteen isolates studied, two isolates namely SrPLC and SrKNK have produced pure white colonies. Isolates SrDGL, SrMDU, SrVAL, SrTVM, SrMDT and SrTRM have produced white creamy colonies, while other isolates produced white colonies (Table 1). All the isolates produced regular colony margin with fluffy consistency.

Sclerotial formation was first appeared on 7 days after inoculation in SrUDM isolate and 15 days in SrTHN isolate. All other isolates produced sclerotia in 9 to 14 days after inoculation. All the eighteen isolates produced sclerotial bodies and its colour was grouped under three categories *viz.*, light brown, dark brown and reddish brown. The isolates SrBTG and SrMDT produced reddish brown colour sclerotia. The isolates SrPLC, SrKGS, SrDGL, SrMDU, SrANP, SrVLR, SrTRM, SrUDM and SrKAN produced dark brown colour sclerotia and the other isolates produced light brown sclerotial bodies. The sclerotia showed spherical shape and smooth in all isolates except SrPLC, SrKNK, SrMDU and SrUSP isolates in which ellipsoidal and semi ellipsoidal smooth and rough shape sclerotial bodies were observed. Semi spherical rough sclerotia were observed in SrUDM isolate. The number of sclerotia produced in PDA by each isolates per Petri plate was observed. The maximum number of sclerotial production (619.67 per plate) was observed in isolate SrUDM and minimum number of sclerotia (105.33 per plate) was observed in SrTHN isolate (Table 2).

Sclerotial weight (100 Nos.) of different isolates showed appreciable variation. Among the 18 isolates, SrVLR showed maximum sclerotial weight of 86.33 mg and minimum weight of 40.33 mg was weighed in SrKNK isolate. Number of sclerotia per cm² ranged from 4.80 to 19.60. The maximum number of sclerotial bodies/ cm² (19.60) was observed in isolate SrUDM and minimum number of sclerotial bodies/ cm² (4.80) was observed in SrTHN isolate. The diameter of the sclerotia exhibited variation and ranging between 913.27 µm and 1208.53 µm. The maximum diameter of sclerotia (1208.53 µm) was observed in isolate SrKGS and minimum diameter of sclerotia (913.27 µm) was observed in SrKAN isolate (Table 2). Gupta and Kolte (1982) and Kumar *et al.* (2014) observed considerable variation of morphological characteristics in diverse isolates of *S. rolfsii* collected from groundnut. The variations of phenotypic characterization have also been reported in *S. rolfsii* isolated from chickpea and rice (Dhingra and Sinclair, 1978; Ansari and Agnihotri, 2000). Similar observations of the variability in cultural morphology, mycelial growth rate, sclerotial formation, sclerotial size and colour were reported by Okereke and Wokocho (2007) and Akram *et al.* (2008). Banakar *et al.* (2017) studied the morphological and cultural characteristics of *S. rolfsii* causing foot rot disease of tomato and reported significant variations in the colony colour, colony diameter, shape and number of the sclerotial bodies and weight of the sclerotial bodies on potato dextrose agar medium.





Daniel Jebaraj *et al.*

The pathogenicity of field collected isolates of *S. rolfsii* showed varied level of pathogenicity across the isolates and the incidence of pre emergence and post emergence mortality was ranged from 11 to 33 and 22 to 48 per cent, respectively. Among the eighteen isolates tested, the *S. rolfsii* isolate collected from Udumalpet (SrUDM) showed higher disease incidence of 33% pre emergence and 48% post emergence mortality and it was followed by K.G. Savadi (SrKGS) and Tindivanam (SrTVM) isolates, whereas the samples collected from Madurai recorded low incidence of 11% pre emergence and 22% post emergence mortality (Table 3). The result was in accordance with the earlier report of Palaiah and Adiver (2004) and Prasad *et al.* (2010). They observed diverse level of pathogenicity in *S. rolfsii* isolates collected from groundnut. Similarly, variations in the pathogenicity of *S. rolfsii* isolates causing collar rot of soybean, chilli, potato, and pepper mint has been reported by Vinod (2006), Praveenkumar (2009), Bhuiyan *et al.* (2012) and Muthukumar and Venkatesh (2013), respectively. The pathogenicity study was in accordance with the work of above researchers and explaining that the *S. rolfsii* isolate SrUDM is highly virulent in causing stem rot disease in groundnut. In addition, the effect of *S. rolfsii* on the germination of groundnut seed was also assessed in the present study and the results indicated that the same isolates SrUDM (38 %) and SrKGS (48 %) reduced the germination of groundnut seeds. This was in agreement with the report of Yamunarani (2009), who also recorded the significant reduction in groundnut seed germination and post emergence mortality. The findings of the study enunciated that the variations existed among the *S. rolfsii* isolates of groundnut and its relationship with the incidence of disease.

ACKNOWLEDGEMENTS

The authors thank the Department of Plant Pathology, Centre for Plant Protection Studies, Tamil Nadu Agricultural University, Coimbatore, India for the support of this research. The University Grant Commission, India is also acknowledged and thanked for providing the prestigious Maulana Azad National Fellowship (MANF) for the doctoral program to the first author.

REFERENCES

1. Akram, A., Iqbal, M., Qureshi, R.L. and Chaudhay, A.R. 2008. Variability among isolates of *Sclerotium rolfsii* associated with collar rot disease of chickpea in Pakistan. *Pakistan Journal of Botany*, 40(1): 453-460.
2. Akram, S.H.A., Iqbal, M., Qureshi, R.A and Rauf, C.H.A. 2007. Variability among the isolates of *Sclerotium rolfsii* associated with collar rot disease of chickpea in Pakistan. *Mycopathology*, 5(1): 23-28.
3. Ansari, M.M. and Agnihotri, S.K. 2000. Morphological, physiological and pathogenic variation among *Sclerotium rolfsii* isolates of soybean. *Indian Phytopathology*. 53(1): 65-67.
4. Aycok, R. 1966. Stem rot and other diseases caused by *Sclerotium rolfsii*. A North Carolina State University Agricultural Experiment Station. Technical Bulletin., 174:202.
5. Banakar, S. N., Sanathkumar, V.B. and Thejesha, A.G. 2017. Morphological and cultural studies of *Sclerotium rolfsii* Sacc. causing foot rot disease of tomato. *International Journal of Current Microbiology and Applied Sciences*, 6(3) : 1146-1153.
6. Bhuiyan, M.A.H.B., Rahman, M.T and Bhuiyan, K.A. 2012. *In vitro* screening of fungicides and antagonists against *Sclerotium rolfsii*. *African Journal of Biotechnology*, 11(82): 14822-14827.
7. Dhingra, O.D. and Sinclair, J.B. 1972. Variation among isolates of *Macrophomina phaseolina* (*Rhizoctonia bataticola*) from the same soybean plant. *Phytopathology*. 62: S1108.
8. Domsch, K.H., Gams, W and Anderson, T.H. 1980. *Compendium of soil fungi*. Vol-1. Academic Press (London) LTD 24/28 Oval Road London NW1. 859.



**Daniel Jebaraj et al.**

9. Farr, D.F., Bills, G.F., Chamuris, G. P and Rossman, A.Y. 1989. Fungi on plants and plant products in the United States. *American Phytopathology Society*. 1252.
10. Grichar, W.J and Boswell, T.E. 1987. Comparison of no-tillage, minimum, and full tillage cultural practices on peanuts. *Peanut Science*. 14: 101-103.
11. Gupta, S.C and Kolte, S.J. 1982. A comparative study of isolates of *Macrophomina phaseolina* from leaf and root of groundnut. *Indian Phytopathology*. 35: 619-623.
12. Hossain, I. 2000. Biocontrol of *Fusarium oxysporum* and *Sclerotium rolfsii* infection in lentil, chickpea and mungbean. *BAU Research Programme*, 11:61-65.
13. Kokalis-Burelle, N., Backman, P.A., Rodriguez-Kabana, R. and Ploper, L.D. 1992. Potential for biological control of early leafspot of peanut using *Bacillus cereus* and chitin as foliar amendments. *Biological Control* , 2:321-328.
14. Komathi, K. 2002. Studies on biological management of root rot of groundnut (*Arachis hypogaea* L.) caused by *Sclerotium rolfsii* Sacc. M.Sc. (Ag.) Thesis, Agricultural College and Research Institute, Tamil Nadu Agricultural University, Madurai. Pp.171.
15. Kumar, R.M., Madhavi Santhosi, M.V., Giridhara Krishna, T. and Raja Reddy, K. 2014. Cultural and morphological variability *Sclerotium rolfsii* isolates infecting groundnut and its reaction to some fungicidal. *International Journal of Current Microbiology and Applied Sciences*, 3(10): 553-561.
16. Mahato, A. and Biswas, M.K.2017. Cultural, morphological and pathogenic variability of different isolates of *Sclerotium rolfsii* obtained from rice-tomato-rice cropping system of undulating red and lateritic zone of West Bengal, India. *International Journal of Current Microbiology and Applied Sciences*, 6 (3) : 1843-1851.
17. Okereke, V.C. and Wokocho, R.C. 2007. *In vitro* growth of four isolates of *Sclerotium rolfsii* in the humid tropics. *African Journal of Biotechnology*. 6(16): 1879-1881.
18. Palaiah, P and Adiver, S.S. 2004. Biochemical and pathogenic variation in the isolates of *Sclerotium rolfsii* causing stem rot of groundnut. *Karnataka Journal of Agricultural Sciences*. 17(4): 843-845.
19. Prasad, S.D., Basha, S.T. and Reddy, N.P.E. 2010. Molecular variability among the isolates of *Sclerotium rolfsii* causing stem rot of groundnut by RAPD, ITS-PCR and RFLP. *Eurasian Journal of BioSciences*, 4: 80-87.
20. Praveenkumar, N. 2009. Studies on biological management of collar rot of sesame caused by *Sclerotium rolfsii* Sacc. Thesis, University of Agricultural Sciences, Dharwad. Pp.67.
21. Punja, Z.K. and Grogan, R.G. 1983. Basidiocarp induction, nuclear condition, variability, and heterokaryon incompatibility in *Athelia (Sclerotium) rolfsii*. *Phytopathology*, 73: 1273-1278.
22. Rangarani, A. 2017. Stem rot of groundnut incited by *Sclerotium rolfsii* Sacc. and it's management - a review. *International Journal of Agricultural Science and Research*. 7(3): 327-338.
23. Rangaswamy, G. 1996. Diseases of crop plants in India. Prentice Hall of India Pvt. Ltd. New Delhi.
24. Sarma, B. K., Singh, U.P and Singh, K.P. 2002. Variability in Indian isolates of *Sclerotium rolfsii*. *Mycologia*, 94 (6): 1051-1058.
25. Vinod, D. 2006. Studies on root rot of chilli caused by *Sclerotium rolfsii* sacc. Thesis . University of Agricultural Sciences, Dharwad. Pp.55.
26. Yamunarani. K. 2009. Management of stem rot caused by *Sclerotium rolfsii* Sacc. in groundnut (*Arachis hypogaea* L.). Ph.D. Thesis, Department of Plant Pathology, TNAU, Madurai. Pp. 237.





Daniel Jebaraj et al.

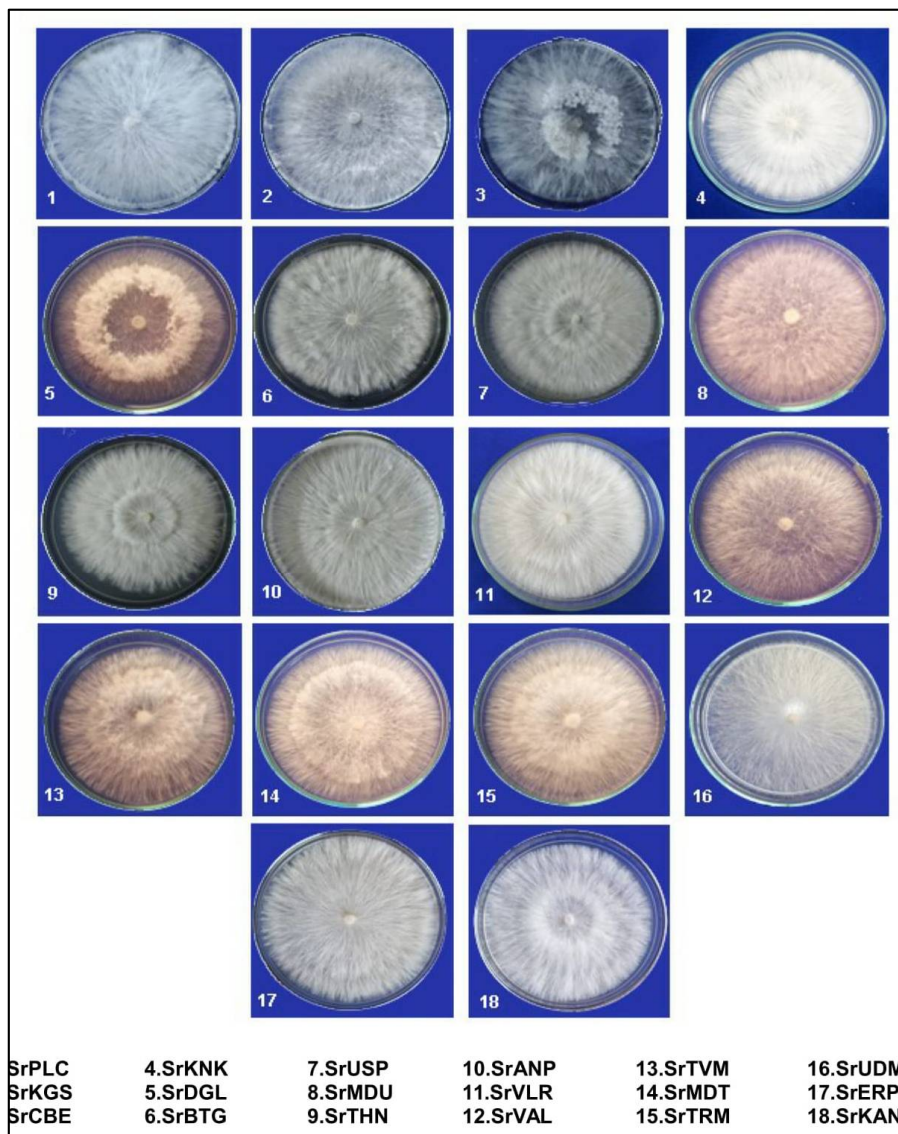


Figure 1.Mycelial growth of various *S.rolfsii* isolates on PDA medium





Daniel Jebaraj et al.

Table1. Radial growth of mycelium and colony characters of *S.rolfsii* isolates on PDA medium

S. No.	Isolate Name	Isolate Code	Radial growth of mycelium (cm)*			Colony colour
			Day 1	Day 2	Day 3	
1	Pollachi	SrPLC	2.80 ^{bcd}	5.26 ^{c-f}	8.23	Pure white
2	K.G.Savadi	SrKGS	2.72 ^{cde}	4.89 ^{fgh}	8.32	White
3	Coimbatore	SrCBE	3.00 ^b	5.56 ^{bcd}	8.76	White
4	Kinathukadavu	SrKNK	2.53 ^{ef}	4.36 ⁱ	8.60	Pure white
5	Dindigul	SrDGL	2.86 ^{bc}	5.03 ^{e-h}	8.73	White creamy
6	Batlagundu	SrBTG	2.93 ^{bc}	5.70 ^{bc}	8.76	White
7	Usilampatti	SrUSP	2.00 ^g	5.46 ^{b-e}	8.43	White
8	Madurai	SrMDU	2.93 ^{bc}	5.10 ^{d-g}	8.86	White creamy
9	Theni	SrTHN	2.40 ^f	5.90 ^b	8.80	White
10	Andipatti	SrANP	2.80 ^{bcd}	5.43 ^{b-e}	8.86	White
11	Vellore	SrVLR	2.80 ^{bcd}	4.66 ^{ghi}	8.40	White
12	Vallanadu	SrVAL	3.00 ^b	5.66 ^{bc}	8.73	White creamy
13	Tindivanam	SrTVM	2.86 ^{bc}	5.13 ^{d-g}	8.70	White creamy
14	Maduranthagam	SrMDT	2.53 ^{ef}	5.53 ^{b-e}	8.80	White creamy
15	Thiruvannamalai	SrTRM	2.60 ^{def}	5.30 ^{c-f}	8.73	White creamy
16	Udumalaipettai	SrUDM	3.400 ^a	6.42 ^a	9.00	White
17	Erisanampatti	SrERP	2.50 ^{ef}	4.56 ^{hi}	8.30	White
18	Kaniyur	SrKAN	2.53 ^{ef}	4.73 ^{ghi}	8.70	White

*Mean of three replications

Values in a column followed by same superscript letters are not significantly different according to DMRT at $P \leq 0.05$ Table 2 . Sclerotial variations among the isolates of *S. rolfsii*

S.No.	Isolate code	Sclerotial formation (No. of days)	Sclerotia colour	Sclerotia shape	Total sclerotia per plate*	Weight of 100 sclerotia (mg)*	No. of sclerotia /cm ² **	Sclerotia diameter (µm)**
1	SrPLC	10	Dark brown	Ellipsoidal, smooth	298.33 ^e	52.33 ^g	9.20 ^{fg}	1141.13 ^{abc}
2	SrKGS	12	Dark brown	Spherical, smooth	246.67 ^g	69.33 ^{bc}	7.00 ^h	1208.53 ^a
3	SrCBE	9	Light brown	Spherical, smooth	194.33 ⁱ	51.33 ^g	5.93 ⁱ	996.00 ^{ef}
4	SrKNK	11	Light brown	Ellipsoidal, smooth	333.33 ^d	40.33 ⁱ	9.80 ^{ef}	1051.87 ^{cde}
5	SrDGL	10	Dark brown	Spherical, rough	253.67 ^{fg}	67.67 ^{bcd}	8.80 ^g	1158.87 ^{ab}





Daniel Jebaraj et al.

6	SrBTG	12	Reddish brown	Spherical, rough	263.67 ^{fg}	64.67 ^d	10.33 ^e	1206.20 ^a
7	SrUSP	11	Light brown	Ellipsoidal, smooth	218.33 ^h	57.33 ^e	10.07 ^{ef}	1060.13 ^{b-e}
8	SrMDU	13	Dark brown	Semi Ellipsoidal, rough	171.67 ^j	67.33 ^{bcd}	6.20 ^{hi}	1135.87 ^{a-d}
9	SrTHN	15	Light brown	Spherical, smooth	105.33 ^k	58.33 ^e	4.80 ^j	1182.67 ^a
10	SrANP	11	Dark brown	Spherical, rough	328.67 ^d	64.67 ^d	14.33 ^c	1105.40 ^{a-d}
11	SrVLR	13	Dark brown	Spherical, rough	291.33 ^e	86.33 ^a	10.20 ^{ef}	1173.13 ^a
12	SrVAL	10	Light brown	Spherical, rough	409.33 ^c	42.67 ^{hi}	16.80 ^b	926.93 ^f
13	SrTVM	9	Light brown	Spherical, rough	222.67 ^h	53.67 ^{fg}	6.80 ^{hi}	1004.67 ^{ef}
14	SrMDT	11	Reddish brown	Spherical, smooth	185.33 ^{ij}	66.67 ^{cd}	5.80 ⁱ	1140.27 ^{abc}
15	SrTRM	13	Dark brown	Spherical, smooth	416.33 ^c	56.67 ^{ef}	10.20 ^{ef}	983.33 ^{ef}
16	SrUDM	7	Dark brown	Semi Spherical, rough	619.67 ^a	70.67 ^b	19.60 ^a	1037.00 ^{de}
17	SrERP	12	Light brown	Spherical, smooth	272.67 ^f	51.33 ^g	13.40 ^d	971.87 ^{ef}
18	SrKAN	14	Dark brown	Spherical, smooth	452.67 ^b	45.33 ^h	17.53 ^b	913.27 ^f

*Mean of three replications

**Mean of five replications

Values in a column followed by same superscript letters are not significantly different according to DMRT at $P \leq 0.05$

Table 3. Pathogenicity of *S. rolfsii* isolates in groundnut

S. No.	Isolate code	Germination (%)	Disease Incidence (%)*	
			Pre emergence (5 DAS)	Post emergence (30 DAS)
1	SrPLC	57.0 ^{cd}	14.0	33.0
2	SrKGS	48.0 ^b	28.0	33.0
3	SrCBE	71.0 ^f	13.0	30.0
4	SrKNK	57.0 ^{cd}	18.0	34.0
5	SrDGL	67.0 ^{ef}	13.0	30.0



**Daniel Jebaraj et al.**

6	SrBTG	71.0 ^f	12.0	26.0
7	SrUSP	62.0 ^{de}	13.0	25.0
8	SrMDU	67.0 ^{ef}	11.0	22.0
9	SrTHN	62.0 ^{de}	14.0	33.0
10	SrANP	62.0 ^{de}	18.0	35.0
11	SrVLR	67.0 ^{ef}	13.0	29.0
12	SrVAL	52.0 ^{bc}	12.0	26.0
13	SrTVM	57.0 ^{cd}	28.0	34.0
14	SrMDT	52.0 ^{bc}	26.0	31.0
15	SrTRM	57.0 ^{cd}	18.0	35.0
16	SrUDM	38.0 ^a	33.0	48.0
17	SrERP	57.0 ^{cd}	17.0	35.0
18	SrKAN	52.0 ^{bc}	15.0	32.0
19	Control	95.0 ^g	0.00	0.00

DAS: Days after Sowing

*Values are mean of three replications

Values in a column followed by same superscript letters are not significantly different according to DMRT at $P \leq 0.05$ 